Electromagnetic Compatibility of Power Line Communication Systems

THÈSE N^{O} 4094 (2008)

PRÉSENTÉE LE 6 JUIN 2008

À LA FACULTE SCIENCES ET TECHNIQUES DE L'INGÉNIEUR
LABORATOIRE DE RÉSEAUX ÉLECTRIQUES
PROGRAMME DOCTORAL EN ENERGIE

ÉCOLE POLYTECHNIQUE FÉDÉRALE DE LAUSANNE

POUR L'OBTENTION DU GRADE DE DOCTEUR ÈS SCIENCES

PAR

Ana VUKICEVIC

Graduate Electrical Engineer, University of Belgrade, Serbie
et de nationalité serbe

acceptée sur proposition du jury:

acceptée sur proposition du jury :
Prof. J. R. Mosig, président du jury
Dr F. Rachidi-Haeri, directeur de thèse
Prof. M. Rubinstein, rapporteur
Prof. A. Skrivervik Favre, rapporteur
Prof. R. Thottappillil, rapporteur

ÉCOLE POLYTECHNIQUE
FÉDÉRALE DE LAUSANNE
Suisse
2008

Mom zrncetu kukuruza

Résumé

Depuis des décennies, les réseaux électriques sont utilisés comme un moyen de communication, principalement par les compagnies électriques pour le contrôle de leurs propres réseaux. Toutefois, l'ouverture des marchés ces 10 dernières années a permis d'envisager d'utiliser les réseaux électriques pour toute une gamme de nouvelles applications de communication et de services. Le concept a été développé puis implémenté sur deux catégories de plages de fréquences, la large-bande (broadband) et la bande-étroite (narrowband) :

- Bande-étroite : entre 3 et 148,5 kHz en Europe (CENELEC Standard EN 50065), et jusqu'à 500 kHz au Japon et aux USA.
- Large-bande : entre 1 et 30 MHz. Soit 1 à 15 MHz en externe (réseau basse tension) et 15 à 30 MHz en interne (intérieur des bâtiments). Il n'existe à ce jour aucune réglementation claire dans cette gamme de fréquence.

Les systèmes et applications développés utilisent plusieurs secteurs du réseau électrique, soit les câbles moyenne et basse tensions (MT et BT) en extérieur, et le câblage électrique interne dans les bâtiments. Ces câbles sont conçus et optimisés pour la transmission de puissance aux fréquences de 50/60 Hz et représentent un moyen inadapté pour les transmissions à des fréquences plus élevées.

Cette thèse se concentre sur les problèmes de compatibilité électromagnétique (CEM) et certains aspects d'optimisation des systèmes à large bande, actuellement connus sous le nom de Courants Porteurs en Ligne ou plus communément en anglais 'Powerline Communications' (PLC) ou 'Broadband over Power Line' (BPL).

Ce travail de thèse a été effectué dans le cadre du projet européen OPERA (http://www.ist-opera.org/). Une brève description du projet OPERA est donnée au chapitre 1.

Le deuxième chapitre présente une description des sujets abordés dans cette thèse et présente l'état de l'art des travaux effectués. Ce chapitre est divisé en trois parties dont chacune commence par une courte introduction destinée à ceux qui ne sont pas familiers avec le sujet en question.

La première partie du chapitre 2 donne une vue d'ensemble et introduit les aspects de télécommunications pertinents à la thèse, ainsi que les spécifications techniques générales du projet OPERA. La deuxième partie traite du milieu de transmission qui, pour le cas du PLC, est le réseau électrique. Les différentes composantes du système PLC y sont décrites et l'état de l'art sur la caractérisation du canal de transmission y est présenté. La troisième partie traite du problème de la compatibilité et les questions de normalisation liés à la technologie PLC.

Les principales contributions originales de cette thèse sont présentées dans les chapitres 3 à 7.

La technologie PLC se distingue des autres technologies par l'utilisation de réseaux préexistant non dédiés à la transmission de données. Ce milieu (le réseau électrique) n'est, par conséquent, pas optimisé pour les fréquences et les applications pour la transmission à large bande. Pour que la technologie PLC soit compétitive, ces

problèmes doivent être correctement identifiés et résolus, afin de pouvoir optimiser le système en tenant compte des contraintes dues au réseau existant.

Bien que le système PLC soit en voie d'amélioration continue, il reste toujours des problèmes d'émissions, d'immunité et de standardisation qui restent à résoudre. Ces points sont d'autant plus importants que le système PLC utilise les mêmes fréquences utilisées par d'autres services, requérant une indispensable coexistence entre les systèmes. De plus, les modems PLC ont un port unique pour l'alimentation et les télécommunications. Par conséquent, les normes d'émissions conduites pour ces deux types de ports ne sont pas directement applicables. D'autre part, étant donné la très faible symétrie des câbles utilisés, les émissions sont plus élevées que celles des paires torsadées utilisées dans les systèmes xDSL. Une bonne compréhension de l'émission et de l'immunité des systèmes PLC est donc d'une grande importance pour que l'optimisation et la standardisation CEM soient basées sur des critères techniques objectifs.

Même si les phénomènes de base sont très semblables que pour tout autre système de transmission filaire, la complexité et la variabilité de la topologie des réseaux existants sont telles que des solutions simples ne sont souvent pas applicables.

Les émissions provenant du câblage sont principalement dues aux signaux en mode commun. Une partie de l'énergie dans ce mode est directement injecté par les étages de sortie des modems PLC, dû à leur asymétrie. En outre, une conversion en mode commun intervient également lors de discontinuités et d'asymétries réparties le long du réseau PLC.

Le chapitre 3 présente une étude théorique et expérimentale dont le but est d'améliorer notre compréhension sur les mécanismes de conversion du mode différentiel en mode commun. Un modèle d'habitation a été construit sur le site de l'EPFL. Différents types de câblages ont été utilisé afin d'étudier l'influence de différents paramètres sur le comportement des courants en mode commun. Ces courants sont la source principale des émissions rayonnées et conduites. Les mesures expérimentales sont également utilisées pour tester deux méthodes adoptées pour simuler la conversion mode différentiel – mode commun, à savoir la théorie des lignes de transmission et la théorie des antennes.

Le chapitre 4 traite des problèmes liés au test d'immunité des modems PLC. Nous démontrons que la conversion du mode différentiel en mode commun est associée à la conversion inverse par une relation de réciprocité. En raison de la faible symétrie du câblage PLC, une partie du signal en mode commun injecté est convertie en mode différentiel qui interfère avec le signal PLC à l'entrée du modem sous test. En fonction de la symétrie du réseau de couplage-découplage (Coupling-Decoupling Network, CDN), non spécifiée dans les normes, l'essai d'immunité peut donner lieu à des résultats erronés en raison de l'effet de cette composante en mode différentiel. En supposant que le CDN est conçu pour présenter une symétrie semblable à celle des réseaux PLC, le niveau de perturbation au niveau du modem PLC a été estimé. Le taux d'erreur binaire induit par la présence du signal perturbateur en mode différentiel a aussi été estimé à $1x10^{-5}$ to $5x10^{-5}$, ce pour un débit total de 200 Mbps. Ces taux d'erreur peuvent être facilement corrigés par des procédures MAC ARQ. Par conséquent, les modems ne risquent pas de voir leur performance dégrader sérieusement à cause des tests d'immunité, pour autant que le niveau de symétrie du CDN soit du même ordre de grandeur que celui du réseau PLC.

La simulation de la totalité ou d'une partie d'un réseau PLC à l'aide de techniques numériques comme la méthode des moments ne s'est pas avérée pertinente car ces réseaux s'étendent sur plusieurs, voire plusieurs dizaines de longueurs d'onde. De plus, l'approximation des lignes de transmission, même si elle convient parfaitement pour des calculs en mode différentiel, n'est pas directement applicable à la simulation EMC du câblage électrique interne, car elle ne tient pas compte des courants en mode d'antenne qui contribuent de manière significative aux émissions rayonnées. Le chapitre 5 présente une nouvelle approche basée sur la théorie des lignes de transmission, mais qui considère également les courants en mode antenne. Une équation intégrale décrivant les courants en mode d'antenne a été développée. Nous avons démontré que cette équation intégrale se réduit, pour le cas d'une ligne avec des dimensions transversales électriquement petites, à une paire d'équations de même forme que les équations des télégraphistes avec des paramètres linéiques équivalents. Les équations obtenues permettent d'évaluer les courants en mode d'antenne en faisant usage des codes basés sur la théorie des lignes de transmission, avec des paramètres linéiques appropriés. Les équations développées sont validées en utilisant les résultats numériques obtenus à l'aide du logiciel NEC (Numerical Electromagnetics Code).

L'atténuation des émissions représente une autre préoccupation importante en vue de la compatibilité électromagnétique des systèmes PLC. Le chapitre 6 présente une technique basée sur l'injection d'un signal de compensation sur la ligne neutre-terre, ainsi que des propositions pour son implémentation dans les modems PLC. La méthode proposée permet de réduire sensiblement le rayonnement électromagnétique des signaux PLC par un choix judicieux de l'amplitude et de la phase du signal de compensation.

Dans ce même chapitre 6, nous abordons la question plus générale de l'application de techniques d'atténuation des émissions pour augmenter le débit global de systèmes PLC. Nous montrons qu'une augmentation de la puissance du signal (rendue possible par l'application de techniques d'atténuation) conduit à une augmentation considérable de la capacité du canal PLC. En utilisant un certain nombre de simplifications, nous montrons qu'une atténuation de 10 dB des émissions permet d'augmenter la capacité du canal jusqu'à 66 Mbit/s.

Nous présentons également les résultats de mesures en laboratoire visant à étudier, dans des conditions contrôlées, des caractéristiques de la technique dite de 'Notching' dans les modems PLC du projet OPERA, particulièrement leur largeur (totale et effective) et leur profondeur. Ces mesures montrent qu'il est possible d'obtenir des atténuations de l'ordre de 45 dB dans toutes les bandes de fréquences, à savoir 10 MHz, 20 MHz et 30 MHz.

Un déploiement massif des systèmes PLC nécessite une augmentation sensible du débit. Pour atteindre les débits plus élevés, la technique dite de 'frequency reuse' peut être envisagée. Dans le chapitre 7, nous présentons l'idée d'utiliser des filtres de blocage (blocking filters) comme une solution possible pour implémenter la technique de 'frequency reuse'. Les données expérimentales obtenues lors d'une campagne de mesures sur un réseau de distribution montrent que l'utilisation de filtres de blocage peut, sous certaines conditions, garantir un niveau de séparation RF des câbles basse tension appartenant au même sous station. Dans certains cas, cependant, même avec la possibilité de conception des filtres de blocage efficaces, des mécanismes de synchronisation seront nécessaires pour rendre la technique de 'frequency reuse' applicable.

Mots-clés

Courants Porteurs en Ligne (Power Line Communications), compatibilité électromagnétique, émissions conduites et rayonnées, immunité conduite et rayonnée, conversion mode différentiel-mode commun, conversion mode commun-mode différentiel, réduction des champs électromagnétiques, coexistence

Abstract

The power system has been used for communication purposes for many decades, although it was mainly the power utility companies that used low bit rates for control and monitoring purposes. In the last ten years, however, the deregulation of the power and telecommunication markets has spurred the idea of using and commercializing the power networks for a range of new communication applications and services. The idea has been developed and implemented into both, narrowband and broadband systems, which are defined in terms of the operation frequency band.

Depending on the frequency band, the systems over powerlines can be:

- Narrow-band. They use frequencies ranging from 3-148.5 kHz in Europe, with the upper frequency extending up to 500 kHz in the United States and Japan. In Europe, this frequency range is standardized by CENELEC Standard EN 50065.
- Broadband. The used frequency range is 1-30MHz; 1-15MHz for outdoor systems and 15-30MHz for indoor systems. In this frequency range, the standardization situation is still unclear and there exist no regulations.

The developed applications and systems use different parts of the power network: medium voltage (MV) and low voltage (LV) cabling for outdoor applications and building cabling for indoor applications. These cables are designed and optimized for power transmission at frequencies of 50/60Hz and represent a hostile medium for transmissions at higher frequencies.

This thesis concentrates on electromagnetic compatibility (EMC) aspects and some optimization issues of the broadband systems, currently known as Powerline Communications (PLC) or Broadband Power Line (BPL).

The work presented here was preformed in the framework of the European project OPERA (http://www.ist-opera.org/). A short description of the project is given in Chapter 1.

The second chapter presents the basis, introduction, description and state of the art of the topics of interest for this thesis. That chapter is divided into three parts. Each of these parts starts with a short introduction to the topic to be addressed. The introductions are intended for those not familiar with the topic at hand and they can be skipped by those already knowledgeable of it.

The first part of Chapter 2 gives an overview and introduction to telecommunication issues relevant to the thesis, as well as the general technical specifications of the OPERA system. The second part deals with the transmission medium which, for the case of PLC, is the power system. The fundamentals and the different components of the PLC system are given there and the state of the art regarding the transmission channel is presented. The third part deals with the EMC and standardization issues related to the technology.

The main contributions of the thesis are presented in chapters 3 to 7.

The PLC technology distinguishes itself from other technologies in that it uses already existing, ubiquitous wiring, so that no new infrastructure is needed. On the other hand, using a channel designed originally for other purposes means that it is not optimized for

the frequencies and applications of interest for broadband transmission. If PLC is to compete with other technologies, these problems have to be well understood and solved, so that the system can be optimized by taking into account the parameters and constrains of the already existing medium.

Although the PLC system is being improved continuously, there are still concerns about emissions, immunity and standardization. These issues are important since PLC operates in an environment already populated by other services at the same frequencies, so that fair co-existence is needed. Moreover, the PLC modem has a combined mains and telecom port and, as a consequence, the standards for conducted emissions from those two types of ports are not directly applicable. In addition, the symmetry of the cables used is low and, therefore, emissions are higher than, for example, emissions from twisted pair cables used in xDSL. A good understanding of emissions and immunity in PLC systems is therefore of great importance for the optimization of the system and for EMC standardization to be based on objective technical criteria.

Even if the basic phenomena are essentially the same as for any other wire transmission system, the complexity and variability of the topologies of existing structures is so large that simple, straightforward solutions are often not applicable.

Emissions from the cabling are primarily due to the common mode signals. Part of the energy in this mode is injected by the imperfectly balanced output stages of the PLC modems themselves. In addition, the common mode appears at punctual imbalanced discontinuities and distributed asymmetry along the PLC signal path in the power cables.

Chapter 3 presents the work performed to improve our understanding of the sources of the common-mode current and the parameters that influence its behavior, including related measurements and simulations. For the purpose of this study, a model house was built at the EPFL's test site. Different cablings were used to study the influence of different parameters on the behavior of the common-mode current since it is the main source for both types of emissions, conducted and radiated ones. The influence of different parameters such as the cable terminations, the symmetry of the termination, the height of the conductors above the ground, the presence of power outlets, switches, empty and occupied sockets and the topology, are analyzed. The data are also used to test two methods used to simulate the differential-to-common-mode conversion and the conducted emissions, namely the transmission line model and the full wave approach provided by the Method of Moments through the Numerical Electromagnetic Code (NEC).

In Chapter 4, problems related to PLC immunity testing are treated. We show that the conversion of the differential mode to the common mode is coupled with the reverse conversion by reciprocity. Due to the low symmetry of PLC cabling, part of the injected common mode test signal is converted into a differential mode signal that interferes with the wanted signal at the input of the modem being tested. Depending on the actual symmetry of the Coupling-Decoupling Network (CDN), not specified in the standards, the immunity test may yield erroneous results due to the effect of this differential mode component. Working under the assumption that the CDN is built to exhibit a symmetry similar to that of PLC networks as inferred from its longitudinal conversion loss, we estimate the differential mode disturbance level that the modems should withstand from a narrowband interferer.

The bit error rate induced by the presence of the disturbing differential mode current from the CDN is also estimated, for a total physical channel transmission rate of 200

Mbps, to be of the order of $1x10^{-5}$ to $5x10^{-5}$. Since these rates can be handled by error correcting coding and MAC ARQ procedures, it is concluded that the modems are not likely to suffer any severe performance degradation due to immunity testing if the CDN exhibits a symmetry similar to that of PLC networks.

Simulating the complete PLC network or any significant part of it using numerical techniques such as the method of moments proves to be of limited practical use due to the fact that PLC networks extend over many wavelengths. The transmission line approximation, on the other hand, although more efficient and sufficiently accurate for differential mode calculations, is not directly applicable to simulate the EMC behavior since it neglects the antenna-mode currents that are significant contributors to the radiated emissions. Chapter 5 presents a novel approach to evaluate the antenna-mode currents using a modified transmission line theory, thus making this numerically efficient technique applicable to the estimation of emissions in PLC. An integral equation describing the antenna-mode currents along a two-wire transmission line is derived. It is further shown that, when the line cross-sectional dimensions are electrically small, the integral equation reduces to a pair of transmission line-like equations with equivalent line parameters (per-unit-length inductance and capacitance). The derived equations make it possible to compute the antenna mode currents using a traditional transmission line code with appropriate parameters. The derived equations are tested versus numerical results obtained using NEC and reasonably good agreement is found.

Another important EMC issue related to PLC is the mitigation of emissions.

Chapter 6 describes a technique that has been proposed to achieve a reduction of emissions associated with indoor PLC networks through the introduction of a 180^{o} out-of-phase replica of the PLC signal into the unused neutral-ground circuit. A modification to this technique is proposed based on the selection of the appropriate amplitude and phase of the auxiliary signal, allowing a higher degree of field attenuation.

A way of implementing this technique is proposed and studied, namely the integration of a required antenna into the PLC modems themselves. The measured fields very close to the modem allow the determination of the magnitude and phase of the compensation voltage. The proposed implementation should be used only to handle customer complaints, when emissions should be lowered at locations where PLC signals might cause unwanted interference or when additional capacity is required and it can be obtained through the gained signal to noise margin.

Although, in principle, due to nonalignment of the wanted and the compensation field directions, minimizing one component of the field may result in an increase of the other components, we show that the application of the technique results in an overall average reduction of 10-20 dB of all the field components in the region of interest.

In the same Chapter 6, we address the more general issue of the application of mitigation techniques' gained emissions margin to increase the overall throughput of PLC systems. We show that an increase in the signal power (made possible by the inclusion of mitigation techniques) leads to a considerable increase in the PLC channel capacity. Using a number of simplifications, we show that the capacity of the channel can indeed be increased by up to 66 Mbps for mitigation efficiencies of only 10 dB.

We also present the results of laboratory measurements aimed at studying, under controlled conditions, different characteristics of notching in OPERA PLC modems, such as total and effective notch width, notch depth, maximum notch depth, etc. These measurements show that it is possible to obtain attenuations of up to about 45 dB for

notches in all frequency bands, 10MHz, 20MHz and 30MHz. What differs for these three bands is the minimum number of carriers that need to be notched to obtain that maximum attenuation. This is an important point, since, to implement notches that have the required depth and width, one must know how many subcarriers to suppress and how deep these need to be reduced.

High density PLC deployment requires the increase of overall system data rate. To achieve the higher data rates, frequency reuse in these systems is needed. In Chapter 7, we present the idea for using so-called blocking filters as a possible solution for a frequency reuse. Experimental data obtained on a real distribution network show that the use of blocking filters can, in certain cases, ensure high enough RF separation of the LV feeders belonging to the same substation. In some cases, even with the possibility to design and integrate effective blocking filters, the system needs to provide additional synchronization mechanisms for frequency reuse.

Keywords

Powerline Communications, Broadband over Powerline, Electromagnetic Compatibility, Conducted and radiated emissions, conducted and radiated immunity, differential to common mode conversion, common to differential-mode conversion, EM mitigation, Co-existence

Acknowledgements

After years of hard work on the technical and logistic aspects of this thesis, I find myself confronted with an even bigger challenge today: How can I express all the gratitude I feel for the kindness of those who provided me all these years with their thoughtful support? I have given this question a lot of thought and I have come to the conclusion that, whatever I write, it will not reflect the true depth of my appreciation. I will, however, do my best in these paragraphs, to address my profound, heartfelt gratitude to all those who were there for me when I needed them.

First and foremost, I want to thank my advisor, Professor Farhad Rachidi. It has been a real privilege to work under the guidance of a person of his stature. He always found time to answer my very many questions with great patience and, through the difficult vicissitudes that my life dealt me in recent years, he showed a kindness I will never forget.

Without you Marcos I never would have made it! You are the constant of my thesis. Thanx for all the time that you spent working with me, time that you didn't always have. For your jokes, your intelligence, your ideas, your friendship. You are the spark of my brain.

Many thanks to Professor Alain Germond, who accepted me among the staff of the Power System Laboratory of the EPFL.

I also wish to thank my dear colleague Abby who, besides his uncanny ability to make a computer process massive amounts of data with a couple of lines of code, is a wonderful friend. He and his wife Virginia were there for me to rely upon and they have won a very special place in my heart.

Davide Pavanello was always there to listen to all I had to say, some times successes, some times complaints, but always sharing one of the apples he always had on his desk.

It was always a great pleasure to work with José Luis, whose serene demeanor and invariably competent advice made him a long time ago my engineering idol.

A big thank you goes to Dr. Pierre Zweiacker, who taught me all I know about experimental techniques, without which more than half of the work in this thesis would have not been possible. He could not, however, make me role up the coaxial cables after the experimental work was done.

Andrée Moinat was the pillar I leaned against for all sorts of administrative matters. But more than that, she had a way of letting you know she is there for you even without uttering a single word. Thank you!

Do not think, Rachid, that the fact that I have not mentioned you until now means that I do not recognize how indebted I am towards you. You kindly opened all the doors for me at the lab and you introduced me to all the wonderful people I had the chance to work and to interact with during my work and studies here. I want you to know that I am aware of all you have done for me and that I thank you very much for it.

My sincere gratitude goes also to my colleagues a the LRE, Elvira, Elena, Emanuel, Keyhan, Pooyan, Abbas, Michael, Isabel, Emmanuel, Anne-Claude, and many others who gave me their friendship day-to-day, during the much-appreciated coffee breaks at the canteen or in the corridor.

Special thanks to my colleagues from Ascom, Markus Bittner, Hanspeter Widmer and Werner Bäschlin, I had the opportunity to discuss and work with throughout the last four years. Thank you for your continuous support and valuable comments.

I am eternally grateful to my parents for the love and support that I received.

My sister Maja is my best friend and the only person in this world that gives me the hope that words like never, always and forever might have a meaning.

Glossary

ADSL	Asymmetric DSL
AE	Associated (Auxiliary) Equipment
AMN	Artificial Mains Network
ASK	Amplitude Shift Keying
BER	Bit Error Rate
BPL	Broadband over Power Line
CATV	Cable TV
CISPR	Comité International Spécial des Perturbations Radioélectriques
CD	Committee Draft
CDMA	Code Division Multiple Access
CM	Common Mode
CPE	Customer Premises Equipment
CTI	Current Technologies
DECT	Digital Enhanced Cordless Telecommunication
DM	Differential Mode
DSL	Digital Subscriber Loop
EMC	Electromagnetic Compatibility
EUT	Equipment Under Test
FD	Frequency Division
FSK	Frequency Shift Keying
HAP	House Access Point
HEU	Head End Unit
HG	Home Getaway
HPNA	Home Phoneline Networking Alliance
ISI	Inter-Symbol Interference
ISN	Impedance Stabilization Network
ISO	International Organization for Standardization
LAN	Local Area Network
LLC layer	Link Layer Control Layer
LV	Low Voltage
MAC layer	Medium Access Control Layer
MIB	Management Information Base

MV	Medium Voltage
NMS	Netvwork Management Station
NQAM	N Quadrature Amplitude Modulation
NR	Network Repeater
OFDM	Orthogonal Frequency Division Multiplexing
OOK	On-Off Keying
OPERA	Open PLC European Research Alliance
OSI model	Open Systems Interconnection Model
PHY layer	Physical Layer
PLC	Power line communications
PSD	Power Spectral Density
PSK	Phase Shift Keying
QAM	Quadrature Amplitude Modulation
QoS	Quality of Service
QPSK	Quadrature Phase Shift Keying
SNR	Signal to Noise ratio
TD	Time Division
TF	Task Force
TL	Transmission Line
VDSL	Very high speed DSL
VLAN	Virtual Local Area Network
VoIP	Voice over IP

Table of Content

Chapter 1

1 Introduction

1.1 Background

The idea of using the power network for communication purposes is almost a century old. It is the power utility companies that developed and used this capability for many decades, transmitting data at low rates, essentially for control and monitoring purposes.

With the start of the deregulation of the electricity and telecom markets in the early 90's, and motivated by the persisting monopoles of large telecom companies, the old idea of using the existing power network wiring for broadband data transmission got a new chance to be explored as a potential medium for providing telecom services to end users [7][10][18].

The power network is a large infrastructure covering most inhabited areas. It comprises three stages [5]:

- Generation: The production of electricity in the power plants
- Transport: The transmission of the high voltage electricity towards transformer substations
- Distribution: The transmission of the medium and low voltage electricity including its delivery to the final customers

The power network is typically divided into three sections, with different voltage levels:

- High voltage (HV): (110-380kV)
- Medium voltage (MV): (10-30kV)
- Low voltage (LV): (0.4kV)

From a communications point of view, not all parts of the network are of equal interest. The PLC system uses different parts of power network, MV and LV cablings for outdoor applications and building cabling for indoor applications.

Depending on the frequency band, the systems over powerlines can be narrowband or broadband.

Narrowband systems use a frequency band limited to a fraction of a megahertz and their potential as interferers is low. Although the operating frequencies employed by these systems are specific to each country, they are in general in the CENELEC bands, ranging from 3-148.5 kHz in Europe and going up to 500 kHz in United States and Japan. Some narrowband systems use proprietary, patented modulation schemes but many of them use plain frequency shift keying (FSK).

Broadband systems use the frequency band of 1-30MHz, dividing the 1 to 30 MHz used frequency band into outdoor, for which the lower half of frequency band is used and indoor, for which the rest of the spectrum is used. Broadband systems are still not standardised, although the HomePlug vendor alliance has advanced its own specifications mostly in the United States.

The frequency range between 1 and 30 MHz appears to be of practical interest for broadband services using the low voltage (LV) distribution network as a transmission

channel. The frequencies below 1 MHz cannot be used due to a high noise level produced by electrical appliances and frequencies above 30 MHz have relatively low capacity for data transmission over long distances due to high channel attenuation. For home networking, which involves small distances, however, higher frequencies e.g. up to 60MHz or even 80 MHz may be considered [7][10].

The work of this thesis concentrates on broadband systems.

The medium voltage (MV) network has been considered as a medium for the backbone connection. Indeed, the backbone connection is of vital importance for the competitiveness of data-over-powerline systems since most medium voltage to low voltage (MV/LV) substations are not connected to existing telecom infrastructure [5][6][11].

Numerous studies and field tests have shown that the channel capacity of typical distribution networks on the medium voltage and low voltage levels allows data rates up to several hundred Mbits/s for an operation frequency bandwidth of about 20 MHz.

PLC (Power Line Communications) or BPL (Broadband over Power Line) are two names given to a telecommunication technology that uses the power grid for data transmission. The technology's aim is that, in each domestic electrical socket, the customer has, in addition to the electrical energy, availability of Broadband Internet services, a telephone connection, and advanced video and high definition TV services without a need for additional connections, antennas or new cables in the house [10][11][17][18] .

The PLC technology can be used as a cost-effective "last mile" solution. An example of the topology of the PLC system is given in Figure 1-1 [15][16].

The PLC technology operates by coupling an additional, modulated signal onto the power lines transporting the 50/60 Hz electricity signal [10][11].

The PLC system uses for the outdoor (access) part the installations of the medium and low voltage (public) network and, for the indoor (in-home) part, the installations inside the buildings (private network) [5].

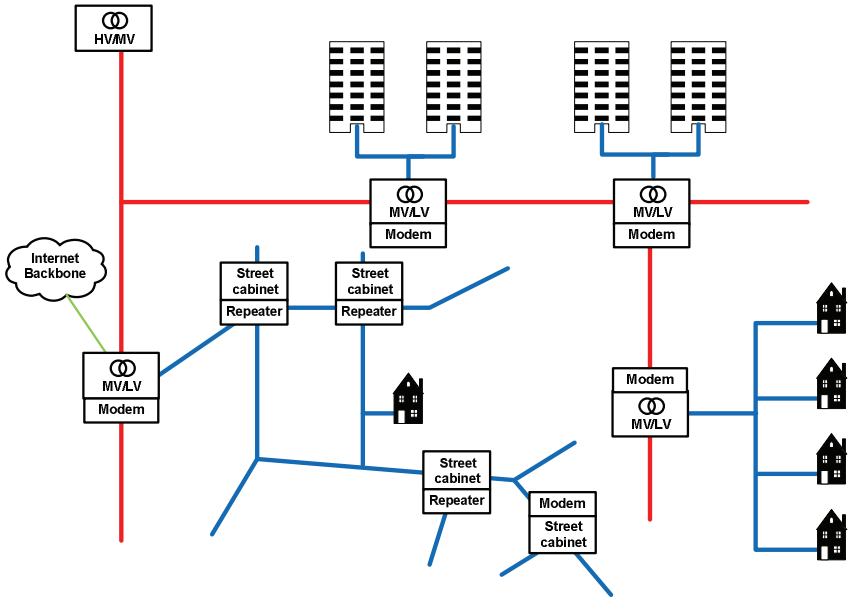

Figure 1-1: Example of the topology of the PLC system

Although the PLC technology is promising and is potentially easy to install and inexpensive, it is still not fully developed and standardized.

Competition in the current telecom market demands high-speed Internet access for voice and video applications. There is therefore a need for the highest possible performance, which can only be achieved through optimization. This is all the more important for data over the powerline grid since due to the hostility of the medium [7].

Due to asymmetries in the power network and the equipment connected to it, PLC signals are not confined to the network's guiding conductors but part is also radiated. Depending on the level of the radiated PLC signals, these may interfere with the reception of radio signals or other services in nearby receivers. Tradeoff solutions will have to be worked out for frequency allocation and the determination of level limits. [8][9] [10].

The mentioned lack of standardization in PLC concerns both the technology specification itself and the electromagnetic compatibility (EMC) aspects.

1.2 OPERA project

The research work presented in this thesis was carried out in the framework of the OPERA project. OPERA stands for Open PLC European Research Alliance [4].

OPERA is a European integrated project covered by the FP6 framework, in the Information Society Technologies (IST) thematic area. It found an important place in the scope "broadband for all" since the objective of this part is to develop network technologies and architectures allowing a generalized and affordable availability to broadband access for European users, including those in less developed regions, peripheral and rural areas [14].

OPERA is a four-year R&D project, divided into two phases. The project started on the 1st of January 2004 and the first phase ended in January 2006. The second phase started on January 1st, 2007 and will last until the end of 2008.

The project gathers over 30 partners active in PLC technology research, development and deployment from 11 countries. The partners of the project are [12][13]:

- Universities, among which the EMC Group of the EPFL
- Power utilities
- Developers and manufacturers
- Engineering and consultancy companies
- Technology providers
- Telecom operators

The PLC technology is still under development. The main objective of the project is to perform the necessary research, demonstration and dissemination to develop an improved and standardized PLC system, suitable for commercialization and where the interconnection to the most important existing technologies is feasible in order to reach users wherever they are [12][13].

The scientific and technological objectives of the project are [12][13][14][15][16]:

- Improve current Power Line Communication (PLC) systems - covering low voltage (LV) as well as medium voltage (MV) PLC systems and looking at bandwidth, reach,

ease of operation, EMC, network management and channel modeling. These objectives relate to conditioning the power grid (using couplers and filters) and improving PLC equipment.

- Develop optimal solutions for the connection of the PLC access networks to backbone networks. The objective in this area is to create well-adapted backbone solutions (satellite, MV PLC, etc.). The main aim is to reach all end users regardless of where they are.
- Develop “ready to sell services” over PLC technology and design or improve low cost user terminals.

Besides development of an improved PLC system, the project is oriented towards standardization issues, such as:

- Functional requirements: topologies of PLC networks and system requirements (performance, QoS, network management, electric safety specifications, dimensions).
- Access system specification: PHY layer, MAC layer, indoor-access coexistence, MIB for NMS, PLC network/services interfaces.
- PLC equipment specification: specification of requirements of PLC equipment.
- Electromagnetic compatibility.
- Interface with narrowband PLC systems.

1.3 Thesis objectives and dissertation overview

This thesis is mainly oriented towards the EMC problems of the PLC technology, although other aspects such as characterization and optimization of the transmission channel are also considered. The principal objectives of this thesis are:

- To understand and characterize the PLC channel from the point of view of EMC issues.
- To perform measurements aimed at helping the PLC standardization, principally in the domain of the EMC, but also from the system and components point of view. Results of some of the numerous measurement campaigns are presented here. The other results, gathered in measurement campaigns not presented, helped us to gain experience and knowledge and were used by other partners of the project.
- To understand the conversion mechanisms between differential-mode (DM) and common-mode (CM) currents, since they are the principal sources of emissions and immunity problems.
- To propose methods to evaluate conducted and radiated emissions associated with PLC signals.
- To propose and evaluate possible methods and techniques to mitigate the radiated emissions of PLC systems.
- To propose and evaluate possible methods to improve the PLC system throughput.

The dissertation is organized as follows. Chapter 2 presents the fundamentals of PLC technology, EMC aspects of the technology and its regulation. This chapter also comprises some contributions as the discussion on a definition of the delay spread, very

important parameter for prevention against intersymbol interference in OFDM signals. This topic is nowadays much discussed one since the system standardization is ongoing and there is not well defined the formulation of a delay spread which could be done in different ways. The discussion on potential interferers has been given and their possible influence on the PLC system presented.

Chapters 3 to 7 represent the core of the thesis, in which the main results and achievements are contained.

Chapter 3 deals with conducted and radiated emissions. It treats principally the source of emissions, differential and common mode currents, and their mutual conversion. Chapter 4 deals with standard immunity testing based on the use of Coupling-Decoupling Networks (CDN). The undefined symmetry of CDN and their impact on PLC test results are investigated in this part.

The method generally adopted to evaluate PLC signal propagation along power networks is the transmission line (TL) theory. One of the basic assumptions of the TL theory is that the sum of the line currents at any cross section of the line is zero. By assuming that the sum of all the currents is equal to zero, we are considering only 'transmission line mode' currents and neglecting the so-called 'antenna-mode' currents. We propose and validate in Chapter 5 a new method allowing the inclusion of antenna-mode currents in the analysis based on traditional transmission-line theory.

PLC transmission systems in the frequency band extending from 1 to 30 MHz present a number of EMC problems, the most critical of which being the emission of electromagnetic noise, which can interfere with services such as public and amateur radio. This is the subject of Chapter 6, in which two methods to mitigate the radiated emissions are described and analyzed: (1) an active cancellation technique which has been improved and tested, and, (2) the notching technique.

In Chapter 7, we propose and evaluate a multimaster deployment scheme along with blocking filters to increase the PLC throughput in low voltage networks.

Finally, Chapter 8 presents general conclusions of this thesis, as well as perspectives for future work.

REFERENCES

[1] OPERA Project, OPERA technology White Paper, IST Integrated Project No 507667. Funded by EC , February 2006

[2] OPERA Project, OPERA Technology Specification, part 1, IST Integrated Project No 507667. Funded by EC , January 2006

[3] OPERA Project, OPERA Technology Specification, part 2, IST Integrated Project No 507667. Funded by EC ,January 2006

[4] OPERA project website, http://www.ist-opera.org/

[5] Deliverable 44: "Report on presenting the architecture of PLC system, the electricity network topologies, the operating modes and the equipment over which PLC access system will be installed", IST Integrated Project No 507667. Funded by EC , December 2005

[6] Deliverable 45: "Specification of PLC System Requirements", IST Integrated Project No 507667. Funded by EC , May 2004

[7] Deliverable D46: "General specification of PLC PHY layer", IST Integrated Project No 507667. Funded by EC, August 2004

[8] Deliverable 53 "Report on disturbance voltage measurement method", IST Integrated Project No 507667. Funded by EC, 2005.

[9] Deliverable 54 "Report on Radiation", IST Integrated Project No 507667. Funded by EC, 2005.

[10] K. Dostert, Powerline communications, Prentice Hall, 2001

[11] H. Hrasnica, A. Haidine, R. Lehnert, Broadband Powerline Communications, Chichester ; Hoboken, N.J. : Wiley, 2004.

[12] OPERA Phase 1 Annex1 – Description of the Work, IST Integrated Project No 507667. Funded by EC ,October 2003

[13] OPERA Phase 2 Annex1 – Description of the Work, IST Integrated Project No 026920. Funded by EC, November 2006

[14] A. Vukicevic, COST Workshop on Powerline Communications, A 6th Framework Integrated Project on Power Line Communication Systems, March 2004, Liège

[15] Romano Napolitano, OPERA project presentation, PUA Workshop, 10th May 2005, Barcelona, Spain

[16] OPERA project presentation, 14th October 2004, Brussels, Belgium

[17] International Powerline Communication Forum: www.ipcf.org

[18] E. Marthe, Thèse No 3165, Powerline communications: Analyse des Problèmes de Compatibilité Electromagnétique dans le domaine des Courants Porteurs en Ligne, EPFL, 2005

Chapter 2

2 PLC Technology and related EMC aspects

2.1 Introduction

Since such cabling is present in most households, PLC might appear as an advantageous solution compared to conventional technologies such as DSL. This is particularly true in many underdeveloped countries, in which large sections of the population are still without telephone lines. Even in countries where twisted pair lines provide telephone service to most or all households, the number of telephone outlets per household is as low as one or two per home, making the power outlet, of which there is usually at least one in every room, more attractive. In addition, the vast majority of home appliances and entertainment systems are permanently connected to the power outlet. If a connection to a local network or to the Internet can be provided through their power cable, a host of new services involving connectivity of appliances and other objects can begin to be realized. Although wireless technologies are a potential competitor to PLC, we are likely to see the two technologies coexist and complement each other in the future since neither of the technologies is universally applicable. The fraction of the market that PLC will be able to grab will depend on how fast the remaining technical and standardization problems are resolved, on the ability of the different parties to achieve agreement so that EMC and specification standards can be produced, and, finally, on the adopted marketing strategies.

PLC technology works by coupling to the existing electrical wiring a modulated signal occupying the frequency band from 1-30MHz. The PLC signals are coupled onto the electrical wiring using inductive or capacitive couplers, specifically designed for this purpose.

Power lines were originally designed for 50 or 60 Hz power signals. They neither present ideal channel characteristics for data transmission at frequencies up to few tens of MHz, nor are they well suited from the point of view of EMC.

At the time of the writing of this thesis, manufacturers of PLC equipment apply either the current HomePlug specification or their own protocol solutions, which are different from one another and, therefore, incompatible. One of the first aims of OPERA (see Chapter 1) is to propose optimized solutions for the PHY and MAC layers that should be supported by a large number of manufacturers, thus encouraging high penetration of the PLC technology in the communications world. A consensus on the basic specification has been reached within the project and OPERA system specifications exist as candidates to be standardized ([1][2][3]). Although the manufacturers and technology providers participating in the OPERA project base their product lines on the proposed OPERA specification, there are still no standardized specifications or standards for the PHY and MAC layers and protocols for PLC network. The same applies to EMC standards, which are still under development, despite some progress in the last few years.

This chapter is divided into three parts. In the first part, the telecommunication systems issues are discussed and the general specification of a PLC system, as proposed in the OPERA project will also be summarized.

The second part deals with the physical transmission medium used by the technology at hand. First a description of the support medium - the power system - is given. Then, an overview of the fundamentals of the PLC technology is presented. The overview includes a description of a PLC network configuration and related elements, and a discussion on different coupling methods.

Finally, the third part includes a review of the EMC aspects of the PLC technology with special reference to standardization. The discussion includes the co-existence between PLC and DSL, potential interferers to the PLC system and radiated fields' mitigation techniques.

Each of the three parts starts with a general introduction of the relevant aspects of the presented topic. The aim of these introductions is to ease the reading of the thesis for readers not familiar with the topic. Those familiar with the subjects presented can go directly to the PLC related issues.

2.2 Telecom related issues

2.2.1 Introduction to relevant aspects of modern telecommunications

2.2.1.1 The OSI reference model

The early network architectures developed by various computer vendors were not compatible with each other. This situation had the effect of locking in customers with a single vendor. The desire to prevent that, led to an effort in the International Organization for Standardization (ISO) first to develop a reference model for Open System Interconnection (OSI) and later to develop the associated standard protocols. [29][30].

The OSI reference model divides the basic communication functions required for computers A and B to communicate into seven layers as shown in Figure 2-1. The principles that were applied to arrive at the seven layers can be briefly summarized as follows [32]:

- A layer should be created where a different abstraction is needed.
- Each layer should perform a well-defined function.
- The function of each layer should be chosen with an eye toward defining internationally standardized protocols.
- The layer boundaries should be chosen to minimise the information flow across the interfaces.
- The number of layers should be large enough that distinct functions need not to be thrown together in the same layer out of necessity and small enough that the architecture does not become unwieldy.

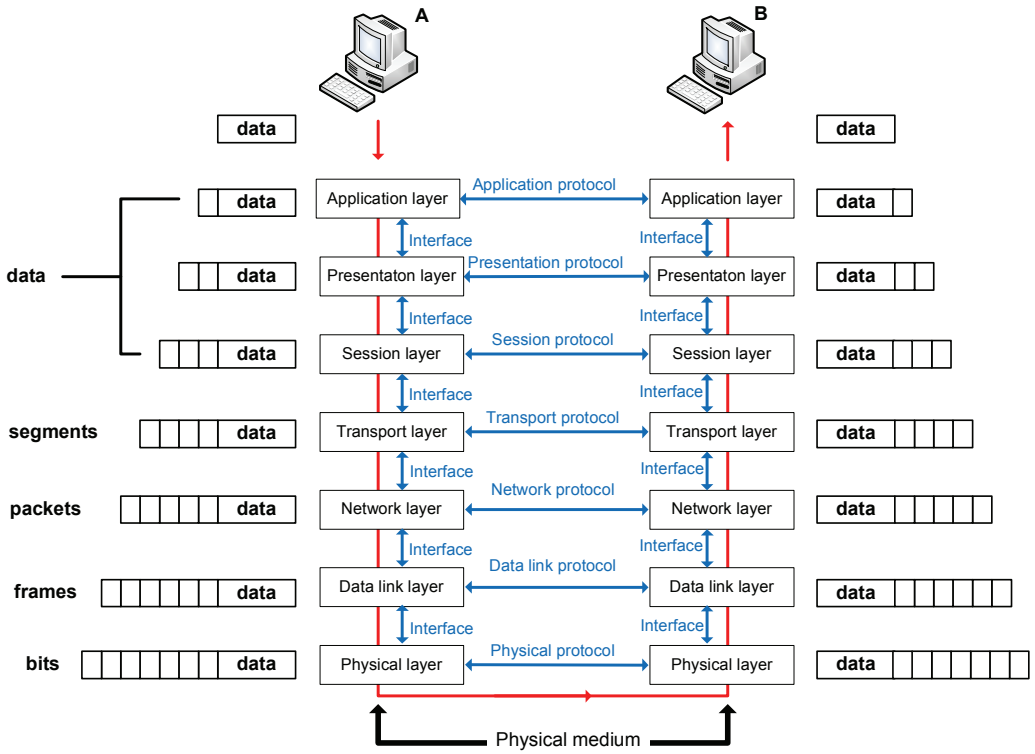

Figure 2-1: The 7 layers of OSI

Layer n of one machine carries on a conversation with layer n on another machine. The rules and conventions used in this conversation are collectively known as the layer n protocol. Basically, a protocol is an agreement between the communicating parties on how communication is to proceed. Violating the protocol will make communication more difficult, if not completely impossible [32].

The entities comprising the corresponding layers on different machines are called peers. The peers may be processes, hardware devices, or even human beings. It is the peers that communicate by using the protocol [32].

In reality, no data are directly transferred from layer n on one machine to layer n on other machine. Instead, each layer passes data and control information to the layer immediately below it, until the lowest layer is reached. Below layer 1 (physical layer) is the physical medium through which actual communication occurs. The protocols represent a virtual communication between entities of the same layer residing in general (although not necessarily) in two separate systems. The physical communication occurs by means of the physical medium [32].

Between each pair of adjacent layers is an interface. The interface defines which primitive operations and services the lower layer makes available to the upper one [32].

A set of layers and protocols is called network architecture. A list of protocols used by a certain system, one protocol per layer, is called a protocol stack.

The seven layers of the OSI model are, from top to bottom:

- Layer 7: Application - This is the layer that actually interacts with the operating system or application whenever the user chooses to transfer files, read messages or performs other network-related activities.

- Layer 6: Presentation - Layer 6 takes the data provided by the Application layer and converts it into a standard format that the other layers can understand.
- Layer 5: Session - Layer 5 establishes, maintains and ends communication with the receiving device.
- Layer 4: Transport - This layer maintains flow control of data and provides for error checking and recovery of data between the end devices.
- Layer 3: Network - The way that the data will be sent to the recipient device is determined in this layer. Logical protocols, routing and addressing are handled here.
- Layer 2: Data Link Layer – the main task of data link layer is to transform a raw transmission facility into a line that appears free of undetected transmission errors to the network layer. It accomplishes this task by having the sender break up the input data into data frames (typically a few hundred or a few thousand bytes) and transmitting the frames sequentially. If the service is reliable, the receiver typically confirms correct reception of each frame by sending back an acknowledgement frame.

  Another issue that arises in the data link layer (and most of the higher layers as well) is how to keep a fast transmitter from drowning a slow receiver in data. A traffic regulation mechanism is often needed to let the transmitter know how much buffer space the receiver has at the moment. Frequently, this flow regulation and the error handling are integrated.

  Broadcast networks have additional issues in the data link layer such as, for example, how to control access to the shared channel [32].

  This layer has two IEEE sub-layers:

  - LLC (Logical Link Control): Manage Communications
  - MAC (Media Access Control): Manages Device Addressing and access to the physical layer.
- Layer 1: Physical – is concerned with transmitting raw bits over a communication channel. The design issues have to do with making sure that when one side sends a bit 1, it is received by the other side as a bit 1, not as a bit 0. typical questions are what amplitude shape, phase or other should be used to represent a bit (1 or 0), how long a bit or symbol lasts, weather transmission may proceed simultaneously in both directions, how the initial connection is established and how it is torn down when both sides are finished, and how many pins the network connector has and what each pin is used for. The design issues here largely deal with mechanical, electrical and timing interfaces and the physical transmission medium, which lies below the physical layer [32].

Systems may implement a subset of the seven layers only. When network designers decide how many layers to include in a network and what each one should do, one of the most important considerations is defining clean interfaces between the layers. Doing so, in turn, requires that each layer perform a specific collection of well-understood functions [32].

In general, the information associated with an application is generated above the application layer. The blocks or streams of information generated by the application must be handled by all the lower layers in the protocol stack. Ultimately, the physical layer must carry out the transfer of all the bits generated by the application and the layers

below. In a sense, the application generates flows of information that need to be carried across the network; the digital transmission systems at the physical layer provide the pipes that actually carry the information flows across the network.

2.2.1.2 Digital transmission fundamentals [29]

This section deals with the physical transmission of data, which corresponds to layer 1 of the OSI model presented in the previous section.

A transmission system makes use of a physical transmission medium or channel that allows the propagation of energy in the form of pulses or variations in voltage, current or light intensity as shown in Figure 2-2. In digital transmission the objective is to transmit a given symbol that is selected from some finite set of possibilities. The task of the receiver is to determine the input signal that might have suffered from a certain level of attenuation and distortion during transmission. To transmit over long distances, it is necessary to introduce repeaters periodically to compensate for the attenuation and distortion of the signal.

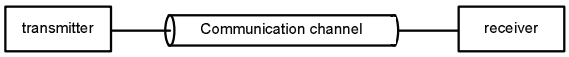

Figure 2-2: General transmission system

The throughput $R\left[bits/s\right]$, or how fast bits can be transmitted reliably over the given medium is affected by several factors:

- The amount of energy put into transmitting each signal
- The distance across which the signal has to travel
- The amount of noise that the receiver needs to contend with
- The bandwidth of the transmission channel, W

A signal or function is band-limited if it contains no energy at frequencies higher than some band limit or bandwidth W. A signal that is band limited is constrained in how rapidly it changes in time and, therefore, how much detail it can convey in an interval of time. The sampling or Nyquist theorem asserts that uniformly spaced discrete samples are a complete representation of the signal if its bandwidth is less than half the sampling rate.

If the channel has a bandwidth W, then the narrowest pulse or symbol that can be transmitted over the channel without inter-symbol interference (ISI) has a duration of $\tau = 1/2W \ seconds$, according to Nyquist's theorem. Thus, the maximum rate at which pulses can be transmitted through the channel with no ISI is given by $\tau_{max} = 2W \ \ pulses/second$. In one of the simplest schemes, we can transmit the binary information by sending positive or negative pulses, with each pulse transmitting one bit of information. The system would therefore have a rate of $2W \ \ pulses/second \times 1 \, bit/pulse = 2Wbps$. We can increase the bit rate by sending pulses with more than just two levels. If we use multilevel transmission with $M = 2^m$ amplitude levels, we can transmit at a bit rate of

2-1 $$R = 2W \ \ pulses/second \times m \, bit/pulse = 2Wm \, bits/s$$

In the absence of noise, the bit rate can be increased without limit by increasing the number of signal levels M. However, the noise is an impairment encountered in all communication channels.

Suppose we increase the number of levels while keeping the maximum signal levels $\pm A$ fixed. Each increase in the number of signal levels requires the reduction in the spacing between levels. At some point, these reductions will imply significant increase in the probability of detection errors, as the noise will be more likely to convert the transmitted signal level into other signal levels. Thus, the presence of noise limits the reliability with which the receiver can correctly determine the information that was transmitted.

The channel capacity of a transmission system is the maximum rate at which bits can be transferred reliably. The Shannon channel capacity formula is given by:

2-2 $$C = 2W \log_2(1 + SNR) bits/s$$

The SNR in the formula represents the Signal to Noise ratio and is usually stated in dB (although it is the linear SNR that needs to be used in the formula). The SNR is defined as:

2-3 $$SNR = \frac{average\ signal\ power}{average\ noise\ power} \text{ or } SNR[dB] = 10 \log_{10} SNR$$

2.2.1.2.1 Digital modulation

We assume that the bandwidth of the channel is $W = f_2 - f_1$. The basic function of the modulation is to produce a signal that contains the information sequence and that occupies frequencies in the pass-band of the channel. A modem is a device that carries out this basic function.

Let $f_c = \frac{f_1 + f_2}{2}$ be the center frequency of the band-pass channel (see Figure 2-3). The sinusoidal signal $\cos(2\pi f_c t)$ has all of its power located precisely at frequency f_c. The various types of modulation schemes involve imbedding the binary information sequence into the transmitted signal by varying or modulating some attribute of the sinusoidal signal. A scheme that uses the amplitude of the sinusoid to convey digital information is called Amplitude Shift Keying (ASK). In one form of Amplitude Shift Keying termed On-Off Keying (OOK), the sinusoidal signal is turned on and off according to the information sequence. The demodulator for an OOK signal needs only to determine the presence or absence of a sinusoid at a given time interval.

In frequency shift keying (FSK), the frequency of the sinusoid is varied according to the information. If the information bit is a 0, the sinusoid is set to frequency $f_s = f_c - \varepsilon$ and if it is a 1, the sinusoid is set to frequency $f_s = f_c + \varepsilon$. The demodulator for an FSK system must be able to determine which of two possible frequencies is present at a given time.

In phase shift keying (PSK), the phase of the sinusoid is altered according to the information sequence. If only two phases are used, a binary 1 could be transmitted using, for instance, $\cos(2\pi f_c t)$ and a binary 0 would be carried by

$cos(2\pi f_c t + \pi) = -cos(2\pi f_c t)$. The demodulator for a PSK system must be able to determine the phase of the received sinusoid with respect to some reference phase.

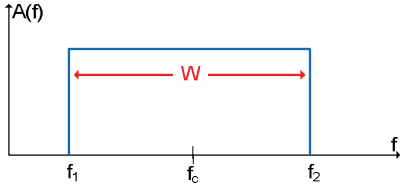

Figure 2-3: Band pass channel passes frequencies in the range f_1 to f_2

In Quadrature Amplitude modulation (QAM) the original information stream is split into two sequences that consist of odd and even symbols, B_k and A_k, respectively. Suppose that we take the even sequence A_k and produce a binary ASK-modulated signal by multiplying it by $cos(2\pi f_c t)$ for a T-second interval by either +A or -A. This modulated signal will be located within the band of the band-pass channel. Suppose now that we take the odd sequence B_k and produce a second ASK-modulated signal by multiplying it by $sin(2\pi f_c t)$ for a T-second interval also by +A or -A. This modulated signal has also its power located within the band of the band-pass channel. The composite modulated signal is obtained as the sum of two modulated sequences out of phase, occupying the same frequency band (see Figure 2-4).

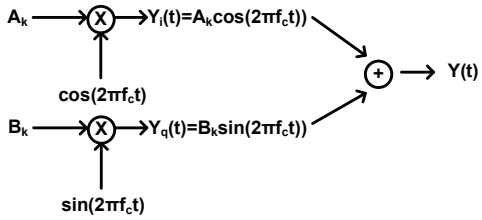

Figure 2-4: QAM modulator

In the case considered so far, the number of different symbols, corresponding to all possible combinations of the amplitudes of the sine and cosine signals is four. This corresponds to all possible combinations of two bits. We can increase the number of bits that can be transmitted in a T-second interval by increasing the number of amplitude levels that are used.

Another way of viewing QAM is as the simultaneous modulation of the amplitude and phase of a carrier signal. Indeed, each signal constellation can then be seen as determining a specific amplitude and phase (see Figure 2-5).

(a) (b)

Figure 2-5: (a) 4-point and (b) 16-points signal constellation

The number of points in the constellation equals the number of different symbols that can be transmitted in a single T-second interval. QAM constellations having a number N of points are usually called NQAM. Figure 2-5(b), for instance, is called 16QAM. Constellations consisting of 4 points or less have special names. The constellation in Figure 2-5(a), for instance, is called QPSK (quadrature phase shift keying). QAM is the basis for Orthogonal Frequency-Division Multiplexing (OFDM), which is the modulation method selected for the OPERA system and it is the same used in the HomePlug specification. OFDM is introduced in the next sub-section.

Orthogonal Frequency-Division Multiplexing (OFDM) [33]

As already mentioned, modulation is a mapping of the information to be transmitted onto changes in the carrier phase, frequency or amplitude or a combination of these.

Multiplexing is a method of sharing a bandwidth among independent data channels.

OFDM can be viewed as a combination of modulation and multiplexing. In OFDM the signal itself is first split into independent channels, modulated by data and then re-multiplexed to create the OFDM signal.

OFDM is a special case of FDM (Frequency Division Multiplexing). Frequency division multiplexing is a technology that transmits multiple signals simultaneously over a single transmission channel, such as a cable or the air. Each signal travels within its own unique frequency range (carrier), which is modulated by the data.

The Orthogonal FDM's spread spectrum technique distributes the data over a large number of carriers that are spaced apart at precise frequencies. This spacing provides the "orthogonality" in this technique, which prevents the demodulators from seeing frequencies other than their own.

If we have a bandwidth that goes from f_1 to f_2, in a single carrier system, the signal representing each bit uses the entire available spectrum (as shown in Figure 2-6(a)). In a multicarrier system such as OFDM, the available spectrum is divided into many narrow bands, the data is divided into parallel data streams, and each data stream is transmitted on a separate band (see Figure 2-6(b)).

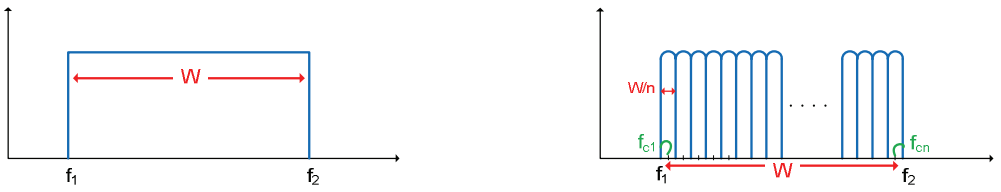

Figure 2-6: (a) single carrier system, (b) multicarrier system

OFDM uses a large number of closely-spaced orthogonal sub-carriers to carry data. These sub-carriers typically overlap in frequency, but are designed not to interfere with each other and may be efficiently separated using a Fast Fourier Transform (FFT) algorithm. Each sub-carrier is modulated with a conventional modulation scheme (such as quadrature amplitude modulation described earlier) at a low symbol rate, maintaining data rates similar to conventional single-carrier modulation schemes in the same bandwidth. An OFDM carrier signal is the sum of a number of orthogonal sub-carriers, with baseband data on each sub-carrier being independently modulated.

The primary advantage of OFDM over single-carrier schemes is its ability to cope with severe channel conditions - for example, attenuation of high frequencies in a long copper wire, narrowband interference and frequency-selective fading due to multipath- without complex equalization filters. Channel equalization is simplified because OFDM may be viewed as using many slowly-modulated narrowband signals rather than one rapidly-modulated wideband signal. The low symbol rate makes use of a guard interval between symbols affordable, making it possible to handle time-spreading and eliminate intersymbol interference (ISI) [31].

- **Orthogonality**

  In OFDM, the sub-carrier frequencies are chosen so that the sub-carriers are orthogonal to each other, meaning that cross-talk between the sub-channels is eliminated and inter-carrier guard bands are not required. This greatly simplifies the design of both the transmitter and the receiver.

  The orthogonality also allows high spectral efficiency, near the Nyquist rate. Almost the whole available frequency band can be utilized. OFDM generally has a nearly 'white' spectrum, giving it benign electromagnetic interference properties with respect to other co-channel users.

  The orthogonality allows for efficient modulator and demodulator implementation using FFT algorithms.

  OFDM requires very accurate frequency synchronization between the receiver and the transmitter; with frequency deviation, the sub-carriers are no longer orthogonal, causing inter-carrier interference (ICI), i.e. cross-talk between the sub-carriers. Frequency offsets are typically caused by mismatched transmitter and receiver oscillators. The situation is worsened when combined with multipath, as reflections will appear at various frequency offsets, which are much harder to correct. This effect typically worsens as speed increases.

- **Guard interval for elimination of inter-symbol interference**

  One key principle of OFDM is that, since low symbol rate modulation schemes (i.e. where the symbols are relatively long compared to the channel time characteristics) suffer less from intersymbol interference caused by multipath, it is advantageous to transmit a number of low-rate streams in parallel instead of a single high-rate stream. Since the duration of each symbol is long, it is feasible to insert a guard interval between the OFDM symbols, thus eliminating the intersymbol interference.

  The cyclic prefix, which is transmitted during the guard interval, consists of the end of the OFDM symbol copied into the guard interval, and the guard interval is transmitted followed by the OFDM symbol. The reason that the guard interval consists of a copy of the end of the OFDM symbol is so that the receiver will integrate over an integer number of sinusoid cycles for each of the multipaths when it performs OFDM demodulation with the FFT.

- **Adaptive transmission**

  The resilience to severe channel conditions can be enhanced if information about the channel is sent over a return-channel. Based on this feedback information, adaptive modulation, channel coding and power allocation may be applied across all sub-carriers, or individually to each sub-carrier. In the latter case, if a particular range of frequencies suffers from interference or attenuation, the carriers within that range

can be disabled or made to run slower by applying more robust modulation or error coding to those sub-carriers.

The OFDM based communication systems can adapt the transmission to the channel conditions individually for each sub-carrier, by means of so called bit-loading.

2.2.2 Some telecom issues related to PLC

2.2.2.1 Discussion on delay spread definition

The PL transmission medium is highly branched giving rise to numerous reflections. The paths travelled by the reflected signals are all of different lengths, so that the reflected signals arriving at the receiver will arrive at different times. The definition of the delay spread is commonly used as a simple measure to characterise such multi-path channels and for the dimensioning of the time that systems should have as a guard interval to avoid intersymbol interference problems [19].

The duration of the impulse response, given by the delay spread, is important for the system design since it directly gives the estimation of the guard interval necessary to prevent the inter-symbol interference (see section 2.2.1.2.1). As the discussions on the standardisation of PHY and MAC layers are currently ongoing and that the definition and duration of delay spread are one of the “hot” topics, we present and discuss in this section two different definitions and give a proposal for a correct delay spread calculation in a case of n-ary communication system [17].

One of the commonly used definitions of the delay spread is that the delay spread is the second moment of the power delay profile that may be considered as the squared magnitude of the impulse response of the network. In that case the process to calculate the delay spread would be the following:

1. Inject the test signal
2. Measure the system response
3. Calculate the impulse response of the network as shown in Figure 2-7

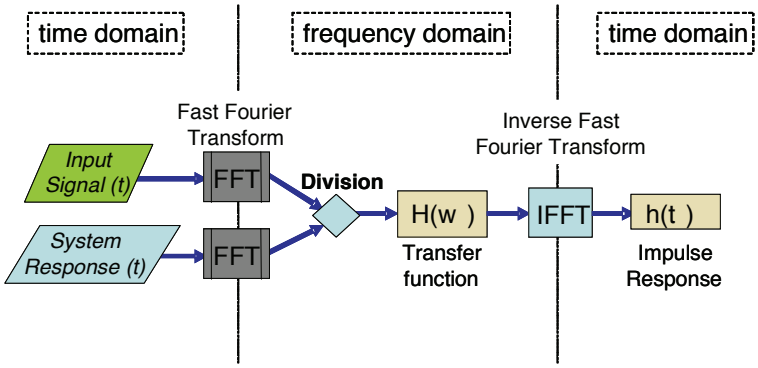

Figure 2-7: Schematic diagram for the response of a network transfer function to a given input signal

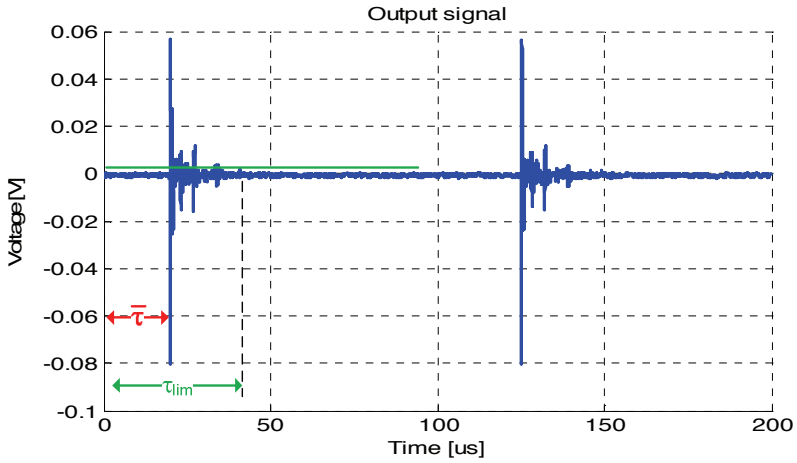

Figure 2-8: Example of a measured impulse response

4. Find the first moment of the impulse response to identify the center of gravity of the delay profile which may be considered as the mean delay. (t_{lim} denotes the integration limit defined by the time where $|h(t)|$ has decayed below a certain threshold e.g. noise floor)

2-4
$$\bar{\tau} = \frac{\int_0^{t_{lim}} t \cdot |h(t)|^2 \, dt}{\int_0^{t_{lim}} \left| h(t)^2 \right| dt}$$

5. An alternative method to the first moment may be to set $\bar{\tau}$ equal to the time where the power delay profile reaches its maximum value (peak) and then calculate the delay spread as a second moment of the power delay profile relative to $\bar{\tau}$.

2-5
$$DS = \sqrt{\frac{\int_0^{t_{\lim}} \left(t - \bar{\tau}\right)^2 \cdot |h(t)|^2 \, dt}{\int_0^{t_{\lim}} |h(t)|^2 dt}}$$

The definitions given by equations 2-4 and 2-5 are the theoretical definitions, making reference to a noiseless environment. In practice estimation of the noise level and its integration into the mentioned formulas should be taken into account.

Equation 2-5 has shown to be an appropriate measure to characterise time disperse channels with respect to binary systems. For higher order modulation (n-ary systems) requiring higher signal-to-noise/interference ratios this definition, however, needs to be reconsidered.

For the systems that use the OFDM modulation scheme with higher order QAM, a more appropriate definition of the delay spread may be the time *DS* where the energy in the tail of the power delay profile ($t > DS$) is below a certain percentage of the total energy. This percentage depends on modulation order and the required signal-to-noise/interference ratio. E.g. for 1024 QAM used in OPERA system, the required SNR is about 36 dB. It may be argued that reflected signal energy originated from the preceding symbol and received within the following OFDM symbol interval would not cause noticeable intersymbol interference if this energy was at least 36 dB lower than the total

energy in the power delay profile. For the power, 36dB represents the factor of 4000 ($10^{\frac{36dB}{10}} = 4000$), so the percentage of power is defined by:

2-6 $$\left(1 - \frac{1}{4000}\right) \times 100 = 99.975\%$$

For this particular case we may define the delay spread as the time where the cumulated energy of the power delay profile reaches 99.975% of the total energy.

For a system requiring 13 dB SNR the delay spread may be defined as the time when the cumulated energy reaches 95% of its energy.

Unfortunately, typical measured impulse responses show a signal-to-noise ratio that is lower than 36 dB due to transmit power limitations of the channel sounding system. If this is the case, measured impulse responses cannot be used to accurately compute the delay spread relevant for a 1024 QAM system. A way to circumvent this problem is to estimate the delay spread using the 95% percentile as energy threshold and to simply add some margin depending on the particular shape or decay rate of the power delay profile.

Why the delay spread statistic is important for the design of a communication system?

Knowledge of delay spread statistics of typical PL channels allow the dimensioning of the guard interval or cycle prefix such that there will be no significant intersymbol interference in a high percentage of communication links.

The OPERA-standard OFDM uses a cyclic prefix to mitigate intersymbol interference effects. Appending a cyclic prefix to an OFDM symbol means that a time portion (the end of an OFDM symbol) is added at the beginning of the OFDM symbol. This may be considered as a cyclic extension of an OFDM symbol as shown in the figure below:

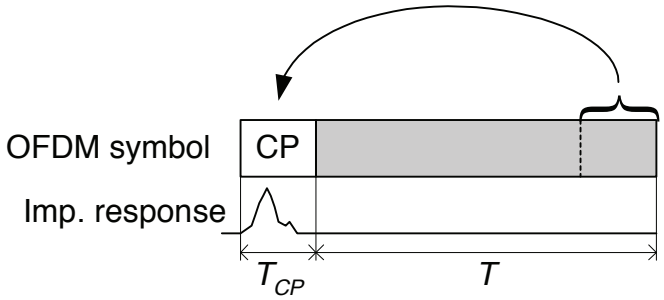

Figure 2-9: Cyclic prefix within an OFDM symbol

If the cyclic prefix is larger than the channel delay spread, no significant intersymbol interference is expected.

To avoid the intersymbol interference, the following procedure for the determination of the delay spread for n-ary systems should be performed:

1. Inject signal
2. Measure system response
3. Calculate the impulse response and the power delay profile
4. Estimate the noise floor (the noise threshold)

5. Determine the integration limits by setting the time when the power delay profile crosses the noise threshold the first time to zero delay ($t = 0$) and the time when the profile crosses the noise threshold the last time to $t_{\lim}$.

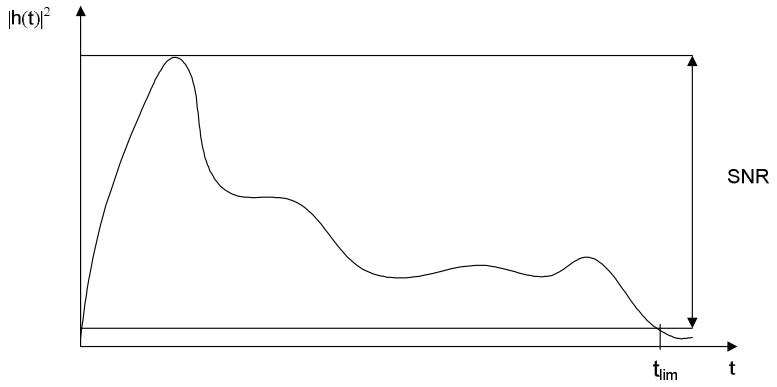

Figure 2-10: Impulse response

For a 1024 QAM OFDM system, the minimum SNR ideally required is about 36dB.

6. Calculate the function of the normalised cumulated energy:

2-7
$$W(T) = \frac{\int_0^T |h(t)|^2 \, dt}{\int_0^{t_{\lim}} |h(t)|^2 \, dt}$$

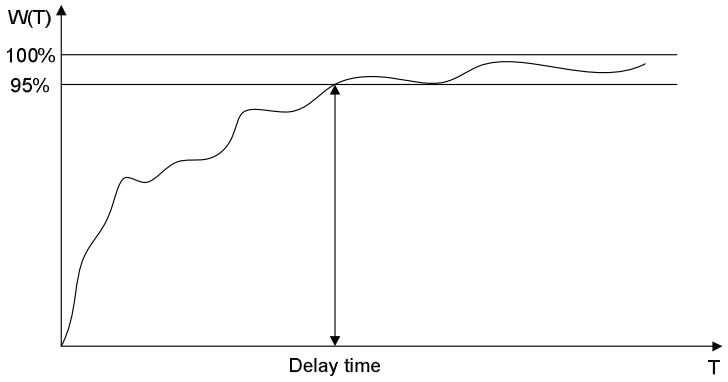

Figure 2-11: Normalised cumulated energy function with 95% percentile (valid for 13 dB SNR).

7. Calculate the cumulated energy threshold (percentile) based on the required SNR (given by the modulation scheme).
8. Determine the delay spread as the time when the cumulated energy function crosses this percentile. Add a margin to the delay spread for uncertainty, if the systems SNR requirement is higher than the SNR in the measured channel impulse response.

Depending on the SNR, some measurements may only be used for a low modulation order if a precise determination of the delay spread is targeted. To reach a higher SNR not the ordinary signal generator should be used but the pseudo-noise generator (PN generator) like usual for the wireless systems.

2.2.2.2 OPERA system specification

The OPERA system uses a Layered Reference Model based on the OSI model (Open Systems Interconnection Model) described in Section 2.2.1.1. The OPERA reference model is shown in Figure 2-12.

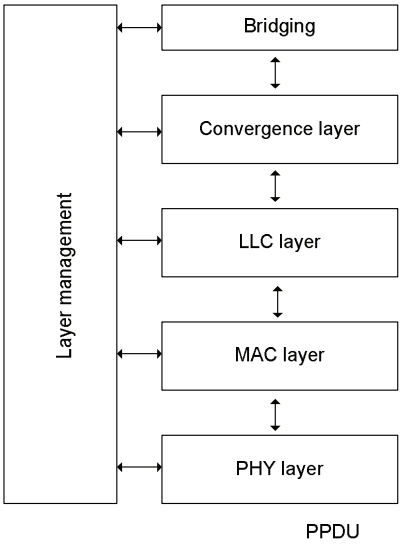

Figure 2-12: OPERA Layered Reference Model

The Physical layer in Figure 2-12 is meant to correspond closely to its homonym layer in the OSI model. The MAC (Medium Access Control), LLC (Logical Link Control), Convergence and Bridging layers, on the other hand, are meant to correspond collectively to the Data Link Layer of the OSI model (see Figure 2-1 presented in Section 2.2.1.1). The bridging sub-layer provides the necessary services to ensure seamless communication between OPERA's PLC technology and other IEEE technologies such as Ethernet. The specific issues related to OPERA system are given in what follows.

Physical (PHY) layer

The OPERA system uses Orthogonal Frequency Division Multiplexing (OFDM) as the modulation technique at the physical layer (for more details about OFDM see Section 2.2.1.2.1). OFDM has been chosen because of its inherent adaptability in the presence of frequency selective channels, its resilience to jamming signals, its robustness to impulsive noise and its capacity of achieving high spectral efficiencies [2].

OPERA's OFDM physical layer allows configurable frequency bands with bandwidths of 10, 20 and 30 MHz, supporting the frequency repeating based on frequency division and coexistence mechanisms. In 30 MHz mode, the system provides a maximum physical layer throughput of 204.94 Mbps [1][2].

The modulation parameters for each transmitter/receiver pair are adapted in real-time depending on the channel quality of each subcarrier. The Signal-to-Noise Ratio (SNR) is measured for each subcarrier and the optimum modulation is chosen with the objective of achieving the maximum transmission speed while maintaining a given Bit Error Rate (BER).

The OFDM symbol uses 1536 sub carriers, with modulation densities from 2 (corresponding to a SNR of 13dB, 4 QAM) to 10 (corresponding to a SNR of 36dB, 1024

QAM) bits per sub carrier applied independently to each of the sub carriers. The reasons for choosing this high number of sub carriers are:

- Achieving high accuracy when estimating channel Signal-to-Noise Ratio and adapting the modulation of each sub carrier accordingly.
- Achieving very narrow notches, with small impact on neighboring sub carriers.

The OFDM symbol uses always the same number of sub carriers independent of the frequency bandwidth used. That makes carrier spacing dependent on the used frequency bandwidth.

All carriers are always evenly spread over the used bandwidth and the n^{th} carrier's central frequency can be calculated as [1][2]:

2-8 $$f_{cn} = f_s + n \cdot \frac{BW}{1536}$$

where:

- n is the number of a specific carrier
- f_{cn} is the central frequency of the n^{th} carrier
- f_s is the start frequency of the used band
- BW is the used bandwidth

The Power Spectral Density at the emission point must be compliant with regulations in the country where the system is implemented. In the current OPERA specification, the used PSD mask has a maximum of $-50\,dBm/Hz$ but this value may need to be changed during the standardization process. The transmit spectrum mask may also depend on the regulation of each country or area.

Legal regulations in different countries may also impose limitations on the frequencies that can be used by powerline communications and those that must be avoided (exclusion bands).

Spectral notching is a technique commonly used to avoid exclusion bands ([20],[21]). Notches are created by turning-off those OFDM subcarriers that fall into exclusion bands, thus eliminating the energy transmitted in those bands.

The system specification claims that OPERA uses windowed-OFDM modulation that allows programmable notches with a depth of up to 30dB. However, as it will be shown in chapter 6 devoted to mitigation techniques, attenuations of up to 45 dB are achievable with actual systems.

Medium Access Control (MAC) Layer

The OPERA system is a hierarchically organised system, as opposed to self-organising systems [3].

Many applications for the transmission of data, video and audio have specific requirements in terms of bandwidth, latency, jitter and packet loss [32]. The OPERA specification's MAC layer with QoS support contains the required functionality to comply with the different services.

Because of intense competition in the telecommunications markets, network providers using PLC technology will have to be able to offer attractive telecommunications services to their customers. To compete effectively with incumbent access technologies xDSL and cable), they have to be able offer a satisfactory Quality of Service (QoS) while being, at the same time, economically efficient. For PLC access systems to provide an efficient utilization of the shared transmission medium and a satisfactory QoS, an efficient Medium Access Control (MAC) layer protocol had to be implemented. The main task of the MAC layer is to manage medium access between multiple subscribers using various telecommunications services.

Logical Link Control Layer (LLC) Layer

The LLC layer in OPERA ensures the error free transmission of data between pairs of PLC nodes.

Convergence Layer

The function of the Convergence Layer is to encapsulate packets coming from external applications before passing them to the LLC layer for transmission.

2.3 Physical medium

2.3.1 Description of the support medium

PLC technology uses the power network as a support medium. We distinguish three levels in power systems: the high voltage level (110-380kV), the medium voltage level (10-30kV) and the low voltage level (0.4kV), each adapted to the bridging of certain distances [18].

The general structure of power systems is given in Figure 2-13. The voltage levels are interconnected by transformers, designed in such a way that the energy loss is as low as possible at the power frequency (50 or 60Hz). For the higher carrier frequencies used for data communication, the transformers are “natural” obstacles, which cause a perfect separation [18].

As stated in Chapter 1, not all the parts of the power system are of the same interest from the point of view of PLC. In Figure 2-13, the part used by the PLC system is marked in red.

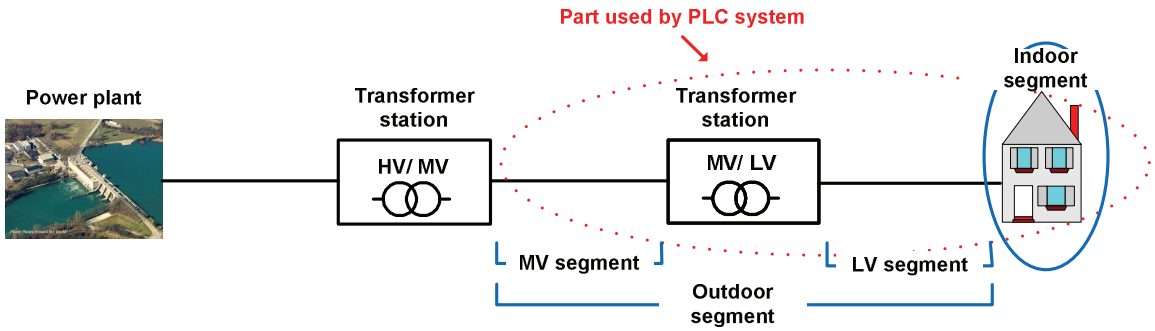

Figure 2-13: general structure of power system

Medium and low voltage networks are built from overhead lines and cables, where the cables are generally laid underground. Due to the wide range of different network topologies, which use different line or cable types, a general theoretical description is difficult, if it is at all possible [18].

The PLC system configuration will be discussed further in 2.3.2.1. We now present basic MV and LV topologies as well as building types. The different topologies, building types and the cabling are key to the study of EMC since they influence de differential to common-mode current conversion and they determine the radiation pattern of the network.

2.3.1.1 Indoor segment: Building types

The different building types are [4]:

- Multi-flat buildings with riser
- Multi-flat buildings with common distribution
- Single family houses
- High-rise buildings

Each one of these types differs in cabling and can have several subtypes. The differences in cabling are important for the study of the EMC phenomena since cabling has an influence on current mode conversion and radiation patterns. Also, the type of environment, e.g. residential or industrial, has an influence on the system deployment scheme and, therefore, on emission and immunity.

Multi-flat building with riser [22]

In multi-flat buildings with riser, the meters and the power distribution are located at the floors. Different subtypes exist characterized by different numbers of risers supporting the floors. The different subtypes are shown in Figure 2-14.

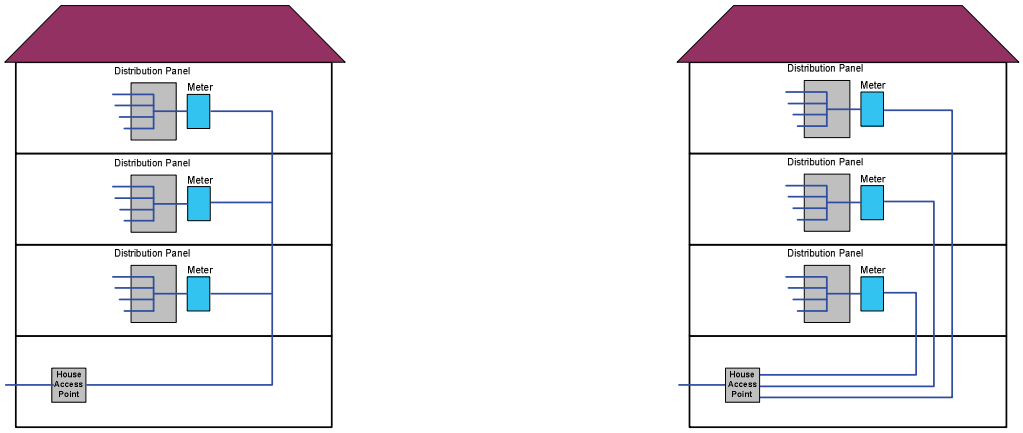

(a) (b)

Figure 2-14: Multi-flat building with riser: (a) building subtype 1- the single riser supports all the floors and (b) building subtype 2- the separate risers are going from the Hous Access Point (HAP) to each floor.

Multi-flat building with common meter room [22]

This building type is characterized by the fact that the meters and the distribution for all the flats are located at the same place. The different subtypes are shown in Figure 2-15.

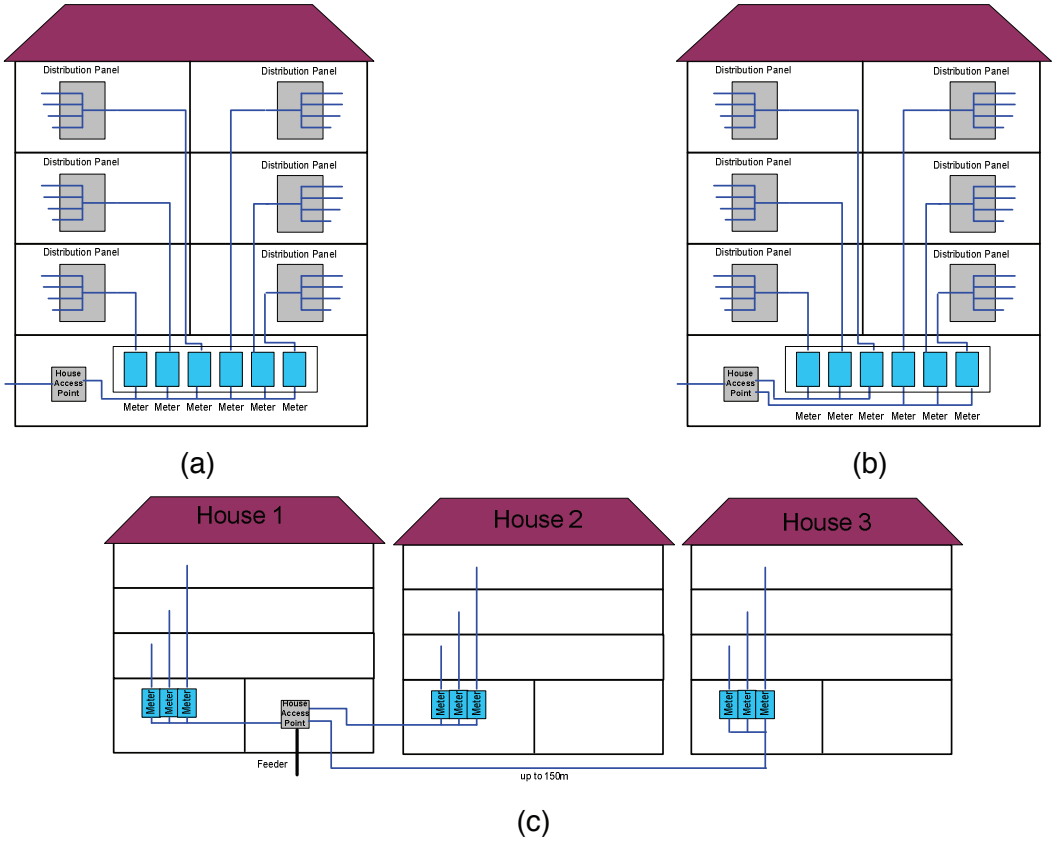

Figure 2-15: Multi-flat building with common meter room: (a) building subtype 1-the single service line goes from the HAP to the power distribution point, (b) building subtype 2-several service lines go from the HAP to the power distribution point and (c) building subtype 3-several service lines go from the House Access point (HAP) to the power distribution point (meter room) of several buildings

Single family houses [22]

Three subtypes can be identified in this category. The different subtypes are shown in Figure 2-16.

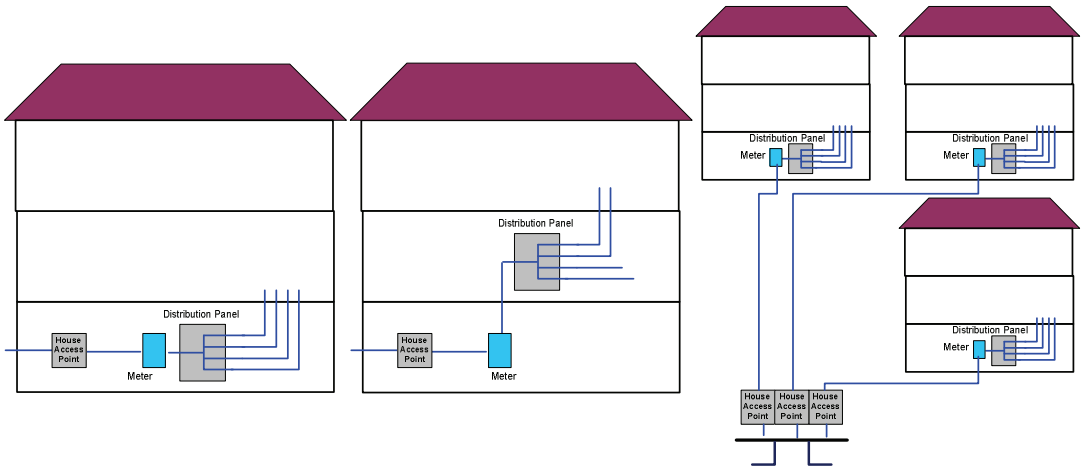

Figure 2-16: Single family houses: (a) building subtype 1-the HAP, meter and power distribution are located at the same place, (b) building subtype 2-the HAP and the meter are located at the same place and the power distribution is located on the different floor and (c) building subtype 3-the HAP with main fuses is located in a street cabinet and the meter and power distribution are located inside of the house

High-rise buildings [22]

Here, one or more risers run from the bus bar to each floor. The meters and the power distribution are located in a meter room on each floor.

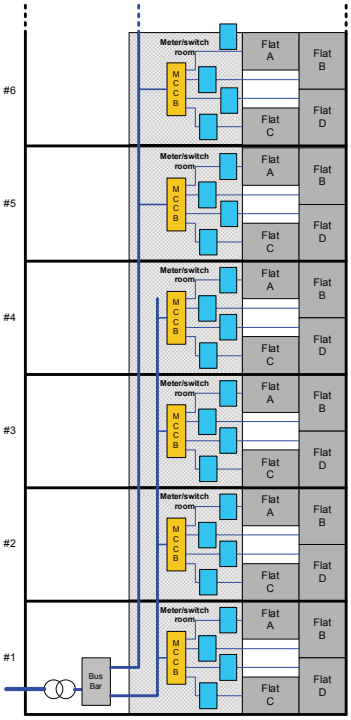

Figure 2-17: High-rise building

2.3.1.2 Outdoor segment: Network topologies

This part of the network covers the MV and LV power networks. The PLC signal is coupled in a transformer station and travels to the point where the indoor segment starts [8][9].

The lines can be:

- Underground cables
- Overhead cables
- Bare overhead lines

There exist different network topologies for LV and MV networks:

MV networks

Basically, there are three topologies to deliver electricity: radial, ring or networked [8][9].

- Radial topologies join the electrical substations (HV/MV) with the transformer substations (MV/LV) by means of radial lines. These feeders can be exclusive for

one transformer substation or cross several transformer substations (see Figure 2-18).

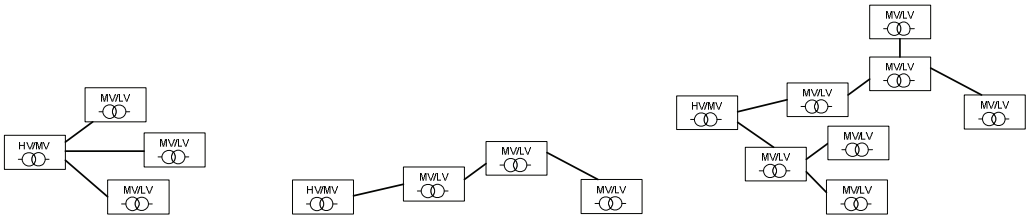

(a) (b) (c)

Figure 2-18: Radial topology: (a) exclusive MV lines, (b) single MV line and (c) tree-shaped line

- Ring topologies appear to overcome a weakness of the radial topologies, interrupting the energy after the fault point, not feeding its correspondent transformer substations. Therefore, the ring topology can be seen as an improved radial topology providing open tie points to other MV lines, that is to say, creating a redundancy. These lines are still operated radially, but if a fault occurs on one of the stretches, the tie switches allow some portion of the faulted line to be restored quickly. An example of the ring topology is given in Figure 2-19

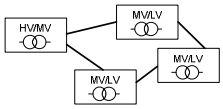

Figure 2-19: Ring topology

- Networked topology is a network in which the electrical substations and the transformer substations are joined through many MV lines in a mesh. Therefore, the power can be delivered by several routes. If a line is removed from the service, power can be rerouted.

LV networks

The net topologies for the LV network case are [22]:

- **Star connection:** The service lines go directly from the street cabinet to the buildings. The main fuses for the buildings can be located inside the street cabinet.

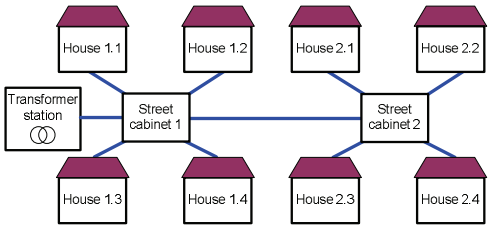

Figure 2-20: Star connection topology

- **T-off connection:** Service lines are connected directly to the feeder cable and the main fuses are always inside the buildings.

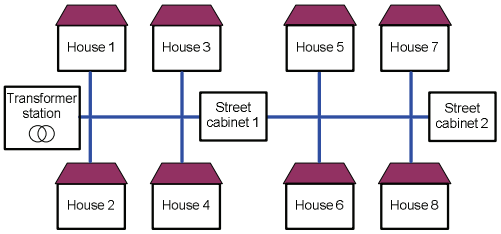

Figure 2-21: T-off connection

- **Direct connection:** Service lines are connected directly to the bus bar of the transformer station and the main fuses are always inside the buildings.

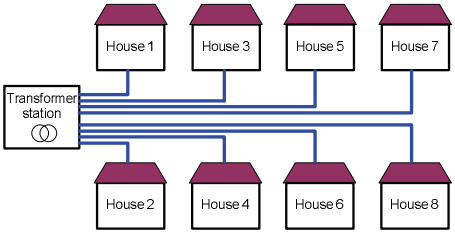

Figure 2-22: Direct connection

2.3.2 Fundamentals of PLC technology

2.3.2.1 PLC network configuration

The reference topology of the PLC system is shown in Figure 2-23. As it can be seen from the figure, the PLC system can be broken down into the following segments with reference to section 2.3.1:

- **Outdoor segment**

  The **Outdoor MV segment** extends from the connection to the backbone network (the Internet, for example) to the MV/LV transformer at the substation. As presented in section 2.3.1.2, there exist three different topologies of this part of the network: radial, ring and networked [8].

  The **Outdoor LV segment** extends from the Head End Unit (HEU) located at the substation to the outdoor port of a Home Gateway (HG) located inside a building. The HG is a time or frequency division repeater making the interface between the indoor and outdoor segments. The different possible topologies for the outdoor LV segment are star connection, T-off connection and direct connection [8] were also described in section 2.3.1.2.

- **Indoor segment**

  The **Indoor LV segment** extends from the indoor port of a Home Gateway (HG) to the Customer Premises Equipment (CPE) inside a building or, in other words, from the House Access Point (HAP) or the distribution panel to the customer.

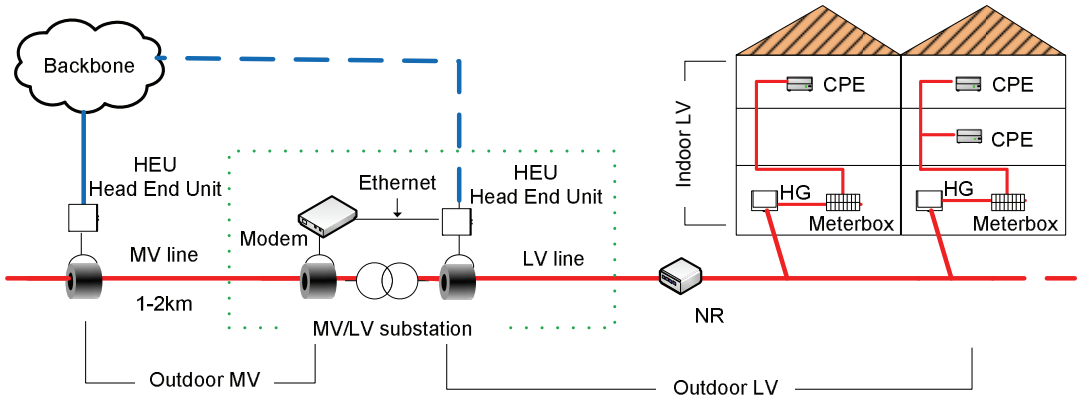

Figure 2-23: Reference topology showing the indoor and outdoor segments

In Figure 2-23, the acronyms are for:

- **LV HEU, MV HEU:** The Low/Medium Voltage Head End Unit is the unit that represents the interface between the LV or MV powerline network and the backbone (e.g. Internet).
- **HG:** The Home Gateway is a gateway between the outdoor and the indoor segments.
- **CPE:** Customer Premises Equipment is the interface between the LV network and customer's devices.
- **NR:** The Network Repeater is used to extend the coverage of the network.

The part of the power network from a MV/LV transformer to the customers fed by that transformer is known as a LV cell. The PLC connectivity within a LV cell is provided in a tree topology by a HEU which usually connects the LV cell to the MV network. CPE might be connected to the HEU either directly or through a series of repeaters. The repeaters increase the range of the PLC signal either by retransmitting the received signal at a different frequency (Frequency division FD) or in different time slots (Time Division TD) [1].

The PLC system components are:

- Modems, of which there exist three types, the central unit (head end or master device), repeaters (time division and frequency division) and customer premises equipment (slave or PLC modem).
- Signal couplers, which can be capacitive or inductive.
- Net conditioning components, such as RF-short circuits for the inductive coupling, bypass, etc.

The OPERA Powerline Access Topology Model breaks the network down into a number of levels [1]. Centrally, a core network provides core switching and management functions and storage of the network configuration data. To provide very wide area networking links, an optical fiber network is used to connect to remote medium-to-low voltage transformer sub-stations. As a low cost alternative to optical fiber, the data link can be channeled onto medium voltage (MV) power-lines allowing the connection of all the sub-stations [1].

2.3.2.2 Coupling methods [22]

Two coupling methods are used in PLC systems: capacitive and inductive coupling. When capacitive coupling is used, the modem is physically connected to the powerline. In inductive coupling, ferrites are used to realize the coupling between the modem and the powerline (see Figure 2-24).

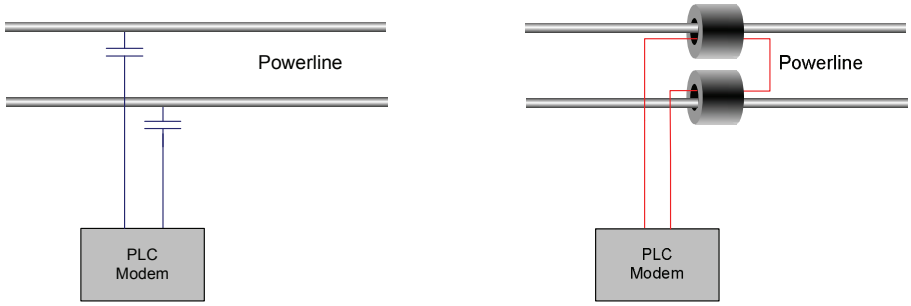

(a) (b)

Figure 2-24: Connection in a case of (a) capacitive coupling and (b) inductive coupling

Capacitive coupling introduces voltage onto the line and is the preferred method of coupling at the coupling points with relatively high impedance (>20Ω). Typically, these points are at the end of a powerline (socket) and house access point with one incoming and only one outgoing cable. Capacitive coupling is also used when inductive coupling is not possible due to the geometry of the couplers (e.g., too small inner diameter of the ferrites), due to too high current ratings, etc. In the case of LV networks, capacitive coupling is always used since inductive couplers with suitable dimensions and saturation currents are not yet available.

Inductive coupling is used at coupling points with relatively low impedance (<20Ω), such as bus bars with many feeders or service lines and House Access Points (HAP) with more than two outgoing cables. Inductive coupling is also used wherever capacitive coupling is not possible due to safety reasons.

The schematic of the connection and the equivalent circuits are given in Figure 2-25 for the case of the capacitive coupling and in Figure 2-26 for the case of inductive coupling.

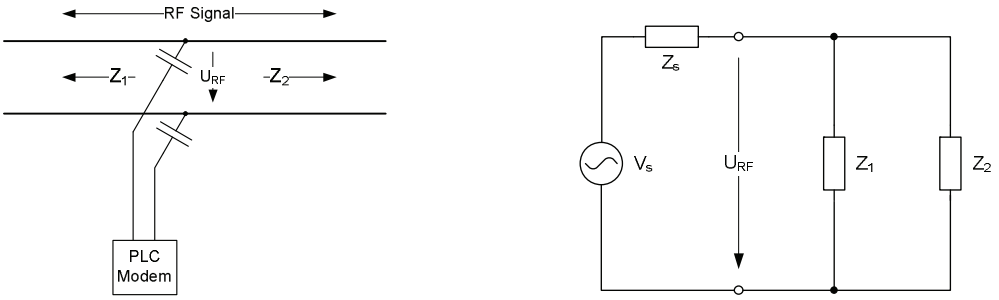

(a) (b)

Figure 2-25: Capacitive coupling: (a) principle and (b) equivalent circuit

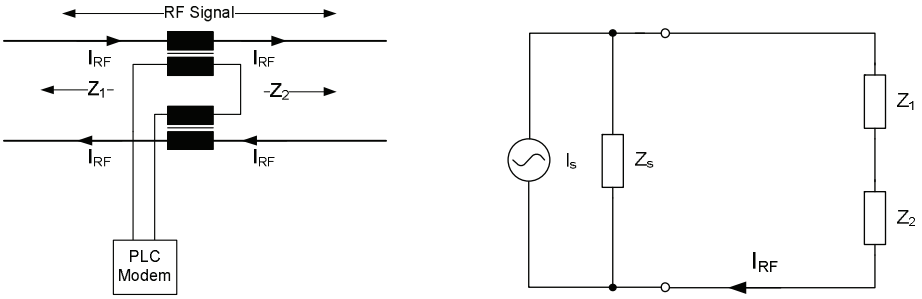

(a) (b)

Figure 2-26: Inductive coupling: (a) principle and (b) equivalent circuit

In Figure 2-25 and Figure 2-26, the impedances are:

- Z_s , impedance of the coupler
- Z_1 and Z_2 , equivalent impedances that coupler sees at both sides

Since capacitive coupling requires direct connections to conductors, the electrical power is switched off whenever possible for installation. For the cases when the power cannot be switched off, the installation is dangerous.

Unlike capacitive coupling, when inductive coupling is used there is no need to switch off the electrical power since no galvanic connection is involved. Inductive coupling is suitable for the coupling points with low impedance; the lower the impedance, the lower the coupling loss. It is also easy to realize multiple coupling points.

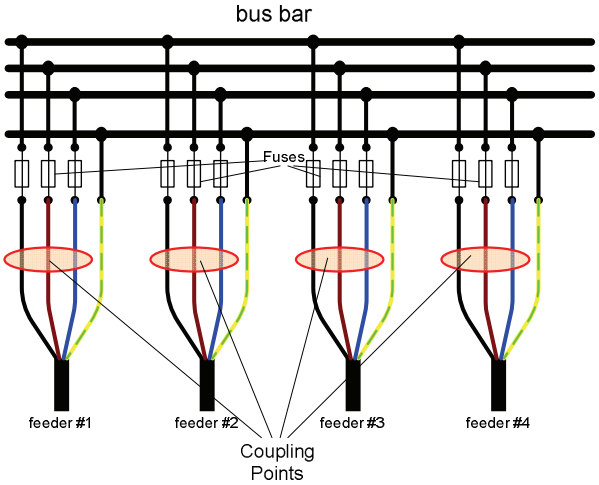

Figure 2-27: Coupling points in the transformer station

The coupling points in the transformer station for both types of coupling are presented in Figure 2-27. The coupling is not performed directly on the bus bar since, at that point, we have low impedance produced by the feeders' connecting points' impedances in parallel.

2.3.2.3 Channel characterisation and modelling

The PHY layer is the layer concerned with the properties of the transmission channel.

Studies on the characterization of propagation characteristics and performance of the LV and MV networks for the use of PLC technology started in the mid 90's ([37],[38]). Four

parameters are of major importance for the design of wire-bounded transmission systems, namely,

- Impedance
- Attenuation
- Delay dispersion
- Noise level and noise statistical parameters

There are two main effects of the propagation of the PLC signal along the power cables [5]:

- Low pass characteristics: cables have a strong low pass characteristic depending on the type of cable, the length of the cable and the frequencies of the signal.

  The low pass behavior is essentially caused by dielectric losses in the insulation of the cable and is not present in overhead lines.

  The low pass characteristic of access networks limits the maximum distance over which PLC signals can be transmitted.

- Frequency selective fading: Due to branches and multiple reflection points, the signal not only propagates on the direct connection between transmitter and receiver, but additional propagation paths have to be considered. Those usually have longer lengths and cause time-delayed echoes. The result is a multi-path signal propagation with frequency selective fading ([5],[45]). In some extreme cases, a set of frequencies may be wiped out completely. Another result of multi-path signal propagation is an extension of the impulse response of the channel, which might impair the functionality of PLC systems with high data rates, as generally the duration of the impulse response of the channel is greater than the duration of the transmitted symbol.

In power networks, there exist four different types of noise which additively and independently overlay each other [5],[18]:

- Colored background noise.
- Narrow-band noise is sometimes considered as a part of background noise.
- Periodic impulsive noise
  - Net-synchronous
  - Net-asynchronous is considered a part of colored background noise.
- Aperiodic impulsive noise

More details about noise type and its influence on PLC signal will be given in section 2.4.3.2.

Theoretical models for propagation patterns and noise are extensively discussed in [5] and [6].

Medium and low voltage electrical cabling does not represent a perfect data transmission medium. Indeed, being designed for frequencies of 50 or 60 Hz, its impedance and attenuation characteristics in the MHz region used for broadband PLC display high variability, not only when networks from different countries are considered, but also when two different, even neighboring networks are considered. Besides a

relatively high attenuation, multiple reflections from different branches make the modeling of the channel characteristics especially difficult [45]. Perhaps the most difficult problem that remains to be solved is the fact that the network characteristics can vary strongly as a function of time, since new appliances can be plugged in and out or turned on and off at any time and they present, in the general case, nonlinear impedances to the network.

A number of studies on the transmission channel characteristics and noise scenarios have been published ([4],[6],[37],[38],[46]). A better understanding of these characteristics allows for better modeling of the channel and for the optimization of the PLC PHY layer.

Sophisticated channel models have been proposed and programmed into simulators (see, for instance, [39],[40],[41],[42],[43],[44],[45],[46],[47],[48],[49]). Due to the inherent unpredictability of the channel, average parameters are used in the design of the systems, leading to suboptimal utilization of the channel's capacity potential. Adaptive, predictive models are therefore desirable.

Measurements performed during the first phase of the OPERA ([4],[6],[7]) project helped to define a unified solution for the OPERA system's PHY layer ([1],[2],[3]).

The understanding and modeling of propagation, noise and interference characteristics is also important for the EMC modeling and channel capacity.

2.4 EMC issues

2.4.1 Introduction to relevant EMC aspects

Electromagnetic compatibility refers to emissions and immunity of different systems that use the same frequency band ([51],[53],[54]). For any piece of equipment to be widely deployed, it is necessary to ensure that the emissions produced by it do not significantly disturb other services and systems using the same frequency band, and that it is can function properly in the presence of a given measure of electromagnetic pollution. The levels of immunity and emissions are regulated by EMC standards.

As shown in Figure 2-28, emissions and immunity can be either conducted or radiated.

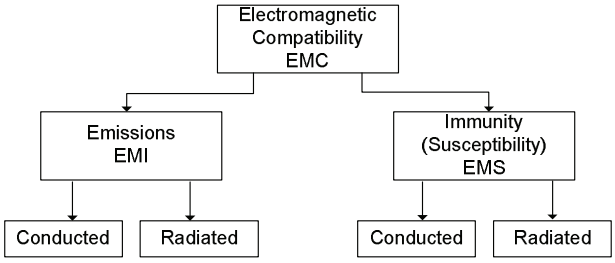

Figure 2-28: Electromagnetic Compatibility.

Several forms of electromagnetic coupling between a transmitter and a receiver are possible as illustrated in Figure 2-29. Depending on the frequency of the electromagnetic interference (EMI), various models describing the field coupling are used, ranging from low-frequency capacitive and inductive coupling to the higher frequency radiative coupling. Below, a description of conducted and radiated coupling mechanisms is given [23].

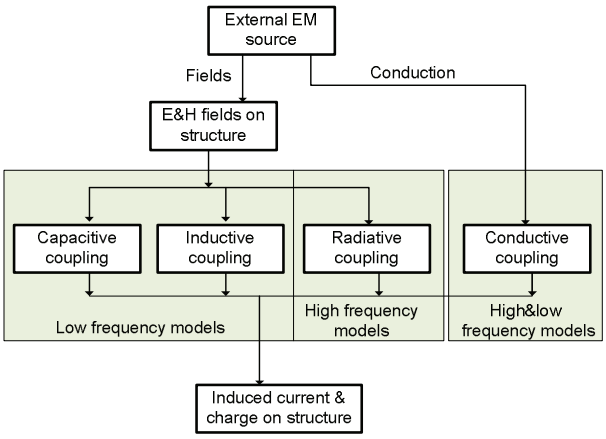

Figure 2-29: EM coupling process (figure adapted from [23])

Radiated coupling – field coupling

Radiated coupling between transmitter and receiver takes place by the transfer of electromagnetic energy through a radiation path, usually the air. Very often there is an element that behaves as an undesired transmitter or receiver antenna. At low frequencies, radiated coupling can be classified in terms of:

- Capacitive coupling, due to parasitic capacitances between nearby conductors. Its origin is the existence of an electric field.
- Inductive coupling, due to currents induced by time-varying magnetic field. All conductors generate a magnetic field and its variations can have an effect on nearby conductors.

Conducted coupling

Conducted coupling between a source and a victim takes place via a direct path between transmitter and receiver, this path being different from the air. This coupling can take place because of the existence of direct conduction or a common impedance:

- Direct conduction takes place when there is a physical connection between transmitter and receiver through the power supply cables, signal cables or control cables. The interference propagates among the different devices via these connections.
- There exists a common impedance when there are common wires among the various devices, typically power supply and ground wires. The interference propagates over these common lines to all and among all devices.

Combination of radiated and conducted coupling

The most common form of coupling of electromagnetic interference or interference coupling in many circuits and systems takes place as a combination of the two aforementioned mechanisms, radiation and conduction. Some examples of this interference coupling are:

- Coupling of electric and magnetic fields in cables and transmission lines with many conductors.

- Radiation of a transmitter connected to another device through the power supply cables and/or signal lines (this interference enters the receiver as a conducted interference over these power supply and signal lines).
- Radiation of the mains line, especially transients and voltage spikes, and from signal or control cables coupled to the mains or signal cables connected to other equipment (this interference enters the receiver as conducted interference).

2.4.2 EMC Standardisation

The EUT, or Equipment Under Test, represents the apparatus generating the emissions or suffering from disturbing signals (immunity).

Figure 2-30 illustrates the definition of the common mode and differential-mode currents that are commonly used in EMC standards for the case of two conductor ports.

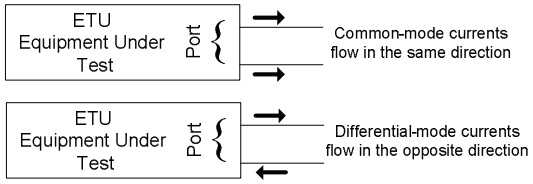

Figure 2-30: Definition of the common-mode and differential-mode currents for two-conductor ports

The meaning of “flowing in the same direction” and “flowing in opposite directions” in the figure should be understood as “being in phase” and “being $180°$ out of phase”, respectively. For common mode currents, the return path is either a ground plane or a third conductor, not shown in the figure.

Although two conductors are used in Figure 2-30, it is not uncommon to find, both in telecommunication lines and in the mains port more than two conductors. In the case of the mains port, one frequently finds three conductors, the phase, the neutral and the ground. In that case, the common-mode current can be defined in two ways:

- As the fraction of the current that flows in the same direction (in phase) in the phase and neutral and
- As the fraction of the total current that flows in phase in all three conductors and returns through a ground plane.

The differential mode current is defined as the part of the current in the phase and the neutral that are $180°$ out of phase.

The common mode and the differential mode currents are the sources of the radiated and conducted emissions as well as immunity problems.

2.4.2.1 Conducted and radiated emissions

The term “conducted emissions” refers to the signals injected by an apparatus out of its mains and telecommunication ports. Conducted emissions are, in general, composed of common mode currents, and differential mode currents.

The reference to conducted emissions as currents or voltages supposes that they are linked through a known impedance.

The CISPR 22 standard [56] has been elaborated by CISPR (Comité International Spécial des Perturbations Radioélectriques) and was created to protect radio services

from disturbances caused by information technology equipment (ITE). At frequencies below 30 MHz, this standard specifies limits for emissions conducted via the mains port of an ITE into the mains supply network. For frequencies above 30MHz, the standard requires radiated emissions testing and sets limits for radiated disturbances.

The specifications of apparatus and methods for measuring radio disturbance characteristics are provided in a separate document, CISPR 16 [57], describing an Artificial Mains Network (AMN), which is a 'V'-shaped impedance stabilisation network (V-ISN). The V-ISN is used today to test all sorts of mains supplied ITE in standardised and precisely reproducible conditions (see Figure 2-31(a)).

With the emergence of broadband telecommunications using unshielded cables (e.g. xDSL over twisted pair telephone wires, 10Base-T and 100Base-TX Ethernet, etc.), the CISPR 22 norm was extended by adding the so-called telecom port of an ITE. CISPR 16 telecom port measurements define a 'T'-shaped impedance stabilisation network (T-ISN) reproducing the impedance asymmetry being responsible for the so-called longitudinal conversion typically observed in line networks (see Figure 2-31(b)).

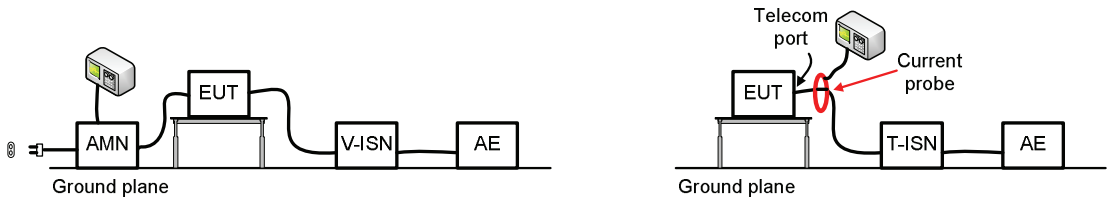

(a) (b)

Figure 2-31: Illustration of conducted emission measurements from (a) mains port, (b) telecommunication port of equipment under test. EUT: Equipment Under Test. ISN: Impedance Stabilization Network. AMN: Artificial Mains Network. AE: Associated (called also Auxiliary) Equipment

The procedures for mains and for telecommunication ports differ in a number of aspects.

The Artificial Mains Network presents an impedance of 50Ω in parallel with $50\mu H$ to the mains terminals both, between the phase and the ground and between the neutral and the ground. It is those two voltages, phase-ground and neutral-ground, that are measured and compared to emissions limits in conducted emissions tests on the mains port. Unlike the measurement on the telecommunication port, in which only the common mode signal is measured, the voltages in the mains port test include a combination of the common mode and differential mode currents. For the measurement of conducted emissions on the mains port, the situation is illustrated in Figure 2-31(a).

For telecommunication ports, only the common mode is measured. The EUT is connected to a T-ISN that presents both, a stable 150Ω common mode impedance to the port (with respect to ground) and an appropriate differential mode impedance which depends on the type of cable being used. Any associated equipment that would normally be directly connected to the telecom port is connected through the Impedance stabilisation Network (ISN) instead, as illustrated in Figure 2-31 (b). The current measurement can be made using a current probe. The current probe ensures that only the common mode current is measured. Although not given in the figure, distances between the different apparatus and the ground, lengths of cables and other aspects of the setup are specified in the applicable standard, CISPR 22.

Twisted pairs and other types of lines used for voice and data transmission partially convert the differential (symmetric) propagation mode launched at the signal injection point into a common (asymmetric) mode, which is the primary source of radiation. This effect is usually measured and quantified with relative success using the definition of the Longitudinal Conversion Loss (LCL). The T-ISN for telecom port testing can be adjusted to reproduce an LCL that is typically measured in a given network type (e.g. twisted pair telephone) at a given frequency.

The LCL is defined as [58]:

2-9 $$LCL = 20\,log_{10}\left(\frac{E_L}{V_T}\right)$$

where E_L is the injected asymmetrical voltage (or longitudinal voltage) and V_T is the measured symmetrical voltage (or transversal voltage).

ITEs are subdivided into two categories denoted class A ITEs and class B ITEs, depending on the limits that the information technology equipment in question satisfies. Class B ITEs are intended primarily for use at home, where broadcast radio and television receivers could be used within a radius of 10 m of the apparatus concerned.

Class A ITE equipment, on the other hand, concerns all other ITEs. These satisfy different, less stringent limits called class A ITE limits. Class A ITE equipment can be sold legally if it contains a warning stating that the equipment may cause radio interference and that the responsibility for solving such problems falls on the user.

Table 2-1, 2-2, 2-3 and 2-4 present the conducted emission limits for telecom and mains ports and for class A and class B equipment [56].

Table 2-1 Conducted disturbance limits on telecommunication ports for class A equipment

Frequency range	Voltage limits in dB(μV)		Current limits on dB(μA)	
	Quasi-peak	Average	Quasi-peak	Average
0.5 to 30 MHz	87	74	43	30

Table 2-2 Conducted disturbance limits on telecommunication ports for class B equipment

Frequency range	Voltage limits in dB(μV)		Current limits on dB(μA)	
	Quasi-peak	Average	Quasi-peak	Average
0.5 to 30 MHz	74	64	30	20

Table 2-3 Conducted disturbance limits at the mains ports for class A equipment

Frequency range	Voltage limits in dB(μV)	
	Quasi-peak	Average
0.5 to 30 MHz	73	60

Table 2-4 Conducted disturbance limits at the mains ports for class B equipment

Frequency range	Voltage limits in dB(μV)	
	Quasi-peak	Average
0.5 to 5 MHz	56	46
5 to 30 MHz	60	50

The limits for the radiated disturbances, not reported her, are also specified in the standards.

2.4.2.2 Immunity

The standards dealing with the conducted immunity testing of electronic and electrical equipment to electromagnetic disturbances coming from RF transmitters in the frequency range of 9 KHz to 80 MHz are IEC (EN) 61000-4-6 and CISPR 16-1. EN 61000-4-6 is the EMC basis test method for RF conducted immunity as per the last edition of the harmonized product standards or generic immunity tests.

Conducted RF immunity tests imply injecting RF in each of the cables out of the EUT. The goal of the test is to simulate the proximity of the EUT and its associated cables connected to the transmitter to devices working at low frequencies. These frequencies are difficult to test using radiated RF immunity techniques. It is indeed often difficult to generate uniform fields at frequencies lower than 80 MHz, so the test of conducted immunity is a reasonable alternative to radiated immunity at these frequencies. The tests of conducted immunity are also much cheaper than those of radiated immunity.

Equipment that does not have even a conductor cable (such as power supply, signal transmission lines or ground connections) which may couple the equipment with the high frequency disturbing fields is excluded.

This norm does not deal with the specification of the tests to be performed on particular equipment or systems. Its main goal is to give a general basic reference for all IEC product committees implied. Product committees and equipment manufacturers are responsible for an appropriate selection of the tests and severity levels to be applied to the equipment.

Alternative test methods should follow as closely as possible the methodology described in EN 61000-4-6 to test product conformity. For small devices EN 61000-4-6 considers the use of conducted tests in the range 150 KHz to 230 MHz acceptable, but for bigger devices the range is 150 KHz to 80 MHz. Small devices with short cables may not need to be tested at such low frequencies as 150 KHz.

A limitation of EN 61000-4-6 is that it injects RF in the common mode only and does not test the differential RF mode, though these disturbances may exist in the power supply network and other cables.

Another limitation of this standard is that, in practice, the sources of the interference affect all cables simultaneously, while the standard specifies that one cable at a time should be tested. When all cables are interfered simultaneously, intermodulation effects could appear that are impossible to test in a single frequency test. This limitation appears in all standards related to conducted immunity.

The simplified block diagram of conducted immunity test using a coupling-decoupling network (CDN) is given in Figure 2-32.

The coupling-decoupling network used to test conducted immunity compliance (see the simplified block diagram in Figure 2-32) is specified in terms of the common mode impedance presented to the equipment under test.

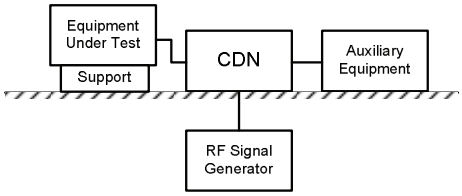

Figure 2-32: Simplified block diagram of conducted immunity test using CDN

Table 2-5: Common mode impedance of the CDN

	Frequency band	
	0,15 MHz – 26 MHz	26 MHz – 80 MHz
Impedance	150 Ω ± 20 Ω	150 Ω + 60 Ω - 45 Ω

The magnitude of this impedance is specified by the IEC 61000-4-6 standard to remain between 130 and 170 Ohm from 0.15 MHz to 26 MHz, and between 105 and 210 Ohm from 26 MHz to 80 MHz (these values are also given in Table 2-5). Since the cable at the EUT's port can be coaxial, single twisted pair or other, different CDNs are specified for different cable types so that the differential mode impedance presented to the EUT's port is close to that of the cable. This is done to minimize the effect of the CDN on the normal operation of the EUT during the test. The test signal is injected by the CDN as a common-mode, continuous, AM-modulated sinusoid with a peak amplitude that depends on the intended environment in which the device will be used. Due to the imperfect symmetry of the CDN, some amount of differential mode signal is also injected. In the case of modem ports, the differential mode signal appears at the modem's input circuitry and, depending on a number of factors, it may interfere with the proper performance of the modem. As this loss of performance is caused by a differential mode signal and not by the common mode conducted immunity test signal directly, it may lead to erroneous immunity test results. The effect will be a function of the symmetry of the CDN, which is not specified in the standards. This effect is not exclusive to PLC modems. Indeed, during immunity testing, communications ports in other types of information technology equipment (ITE) will be affected by a differential mode signal. The issue is discussed in chapter 4 of this thesis.

2.4.3 EMC issues related to PLC

PLC systems can produce non-negligible emissions in the environment already used by different services (amateur radio, broadcasting services, etc.). Depending on the level of the radiated PLC signals, these may interfere with the reception of radio signals in nearby receivers [50].

The common mode currents in PLC networks have three different sources:

- The asymmetries in the modems themselves that inject a common mode signal directly.

- The asymmetries along the network due either to the tortuosity of each of the conductors along the network or to abrupt punctual discontinuities that effectively convert part of the differential mode signals into the common mode.
- The coupling of external electromagnetic fields from intentional or unintentional radiators.

One of the most important potential EMC problems in PLC networks is the emission from the poorly symmetrical cables in low voltage (LV) and medium voltage (MV) networks. This includes radiated as well as conducted emissions.

The sources of the emissions are the differential and the common mode currents. The data signals injected by PLC modems are differential mode signals (DM). The differential mode is a poor radiator since the fields from the current in one of the conductors are nearly cancelled by the opposite-phase radiation from the current in the other conductor. The common mode (CM), on the other hand, is characterized by currents in each of the conductors being in phase, and it leads to appreciable radiation. Thus, although the differential mode is responsible for part of the radiation, the common mode is the dominant mode in most cases [86].

Presently, the most heavily discussed issue related to EMC of PLC deals with maximum limits for unintentionally radiated electromagnetic fields coming from PLC conducted signals. Power lines are not normally shielded and they are generally less symmetric compared to other wire-guided transmission media such as twisted pairs. Thus, higher radiation levels are expected from power lines if high frequency signals are injected with the same spectral power density.

Radiated and conducted emissions are linked to the mode conversion phenomena between the common and the differential modes in the lines. A good understanding of the conversion between common and differential mode currents is of great importance in PLC networks.

Due to the importance of the subject, and thanks to the availability of powerful electromagnetic simulation tools and experimental installations, some progress has been made in the past years (see, for instance, [72], [73],[74],[78],[79],[80]).

2.4.3.1 EMC standardisation issues related to PLC

2.4.3.1.1 Emissions

As PLC equipment uses the mains wiring for communication by definition, it appears logical to use CISPR 22 (EN 55022) for EMC compliance testing at product/equipment level.

Intentional use of high frequencies in power lines, in particular for broadband telecommunications, is likely to involve a significantly higher interference potential than unintentional conducted emissions of ITEs. Typically, unintentional emissions are narrow-band and spectral peak levels show certain randomness both in terms of amplitude and frequency. Emission standards normally refer to a defined narrow measurement bandwidth, thus essentially limiting the power spectral density that may be used by a broadband PLC transmitter but not its total output power. Today, EMC standards define flat emission limits over defined frequency bands.

In conclusion, it may be stated that the CISPR 22 mains port test method is not applicable to PLC. This conclusion has been commonly accepted by the different parties of both industrial and regulatory organisations.

Apart from applicability, it can be stated that CISPR 22 mains port certification would not permit to operate PLC with transmit levels as required for commercially attractive solutions. The power spectral density levels would be 30 – 40 dB below those levels typically used in present PLC deployments. So, in the case of PLC the adaptation of CISPR 22 standard is needed.

How can one go about estimating this maximum conducted level? The relationship between the power level of the PLC signal injected in a line and the electromagnetic field strength generated in the surrounding space is linear: for a given installation, a 10 dB increment in the injected power level will translate into a 10 dB increment in field strength or radiated power. What is still not well known is the absolute value for the relation between input power level and the magnetic or electric field strength (known as coupling factor).

Presently, there is no harmonised European standard on unintentionally radiated emission limits applicable for compliance testing of PLC networks at frequencies below 30 MHz. There are not also harmonised standard based on unintentional conducted emissions.

Regulatory authorities of Germany and the United Kingdom have set forth radiated emission limits (NB 30 and MPT 1570) based on magnetic field strength at a defined distance from wires or equipment of a telecom network. So far, these national regulations have not been legally enforced due to a number of technical and political problems.

The lack of a corresponding European standard put PLC technology into an unclear legal position in all European countries. In such cases, EMC of a product can be assessed by a so-called competent body, e.g. an accredited EMC certification lab. It was in 2002 that broadband PLC equipment was first certified and CE labelled by an accredited test lab in Germany. The norm and the basic test setup used for this EMC certification procedure was basically adopted from CISPR 22 telecom port based on the T-ISN and the LCL.

The standards pertaining to emissions should concern both the network in which a PLC signal is injected and the product (modem) connected to the network.

The standardization work is distributed as follows between different standardization bodies:

- Network standard: The ETSI-CENELEC Joint Working Group received a mandate from the European Commission to prepare and adopt a harmonised European standard applicable to all sorts of wire-line telecommunications networks (Mandate M313).The network standard for PLC should be developed under this mandate .
- Product standard: Subcommittee CISPR/I/.

Network standard

Different limits in terms of the electric field have been proposed by different countries and some limits, such as the NB30, are used as a guideline in case of conflict by the regulatory authorities of these countries (Figure 2-33).

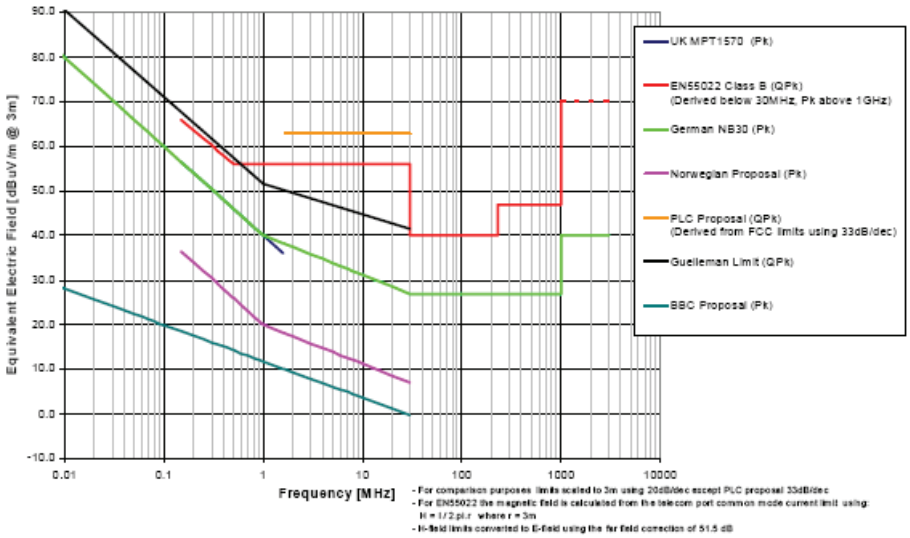

Figure 2-33: Electric field limits proposed by different Regulatory bodies for PLC emission

A Task Force (TF) of the Joint Working Group (JWG) ETSI/CENELEC produced a draft standard (Berlin 29-31 July 2002) with the aim to define:

- a proposal for radiated field limits,
- a measurement procedure.

Consensus in the TF has been reached on:

- H - field measurement and transformation into an E – field,
- Measurement of quasi-peak values,
- Measurement distance : 3 m from the source.

No consensus was reached on field limits and, in a first draft, all the limits proposed at present by different countries or bodies (Figure 2-33), were left to the appreciation of the National Committees.

Product standard

The standard for PLC products was intended to be an amendment to CISPR22 and the task of writing it was taken by CISPR/I. The first idea was to extend the concept of Longitudinal Conversion Loss (LCL) specific for symmetric telecommunication wire pairs to the non-symmetric power network.

The LCL values that are defined in CISPR 22 for type approval testing of telecom equipment using twisted pair telephone wires are relatively high. Thus, common mode currents as measured on the connection lead are mainly determined by the symmetry of the telecom port and the common mode impedance of the EUT. With a properly designed line interface, xDSL modems e.g. can pass certification tests with modest power levels.

Having recognised this fact, PLC manufacturers are pledging now for an equal treatment of PLC technology enabling solutions competitive to other access technologies. Although a telecom port of a PLC modem is always a mains port too (by definition), it has been found justified to differentiate between:

- unintentional conducted emissions
- intentional conducted emissions for telecommunications purposes

and to define the so-called Multi-purpose Port for PLC equipment. Unintentional conducted emissions are to be measured with the EUT in active transmit mode using the original CISPR 22 V-ISN-based test methods and limits, while intentional conducted emissions are to be measured with the EUT in an active transmit mode representative for real operation by means of the CISPR 22 T-ISN-based test method.

In order to adapt the CISPR 22 to the PLC it was necessary to:

- **Define an ISN**. A proposal to use a T-ISN was made because it gives the possibility to check the common mode disturbances for telecom ports. The proposed T-ISN presented an intentional imbalance representative of mains wiring. The value of this intentional unbalance should be determined on the basis of the Longitudinal Conversion Loss (LCL) of power networks.
- **Define an LCL specific for PLC in the frequency range 1.6 to 30 MHz**. LCL was a parameter used for telecommunication equipment. Its value for the equipment connected to the power network is not known.

After years of work and the development of a series of draft documents, the concept has not found until now the requested qualified majority for approval by CISPR/I, although it found majority approval within the working group ([60] - [65]).

The negotiations indicate that the PLC industry could accept the current limits, even with a reduced LCL of 24 dB, requiring the design of a new ISN. The proposal is still not accepted.

2.4.3.1.2 PLC Immunity

Immunity issues in PLC systems have not received much attention.

The mechanism through which radiation from non-PLC communications systems can disturb PLC can be divided into three phases as follows:

- The disturbing system radiates
- The radiation couples onto distribution lines or home electrical cabling in the form of a common mode current.
- Part of the common mode current converts into a differential mode current due to the asymmetry of the power line cabling. The differential mode current contributes to the noise and affects the capacity.

The coupling of radiated fields onto the distribution and the mains networks, and the conversion of the coupled currents into the differential mode depend on the propagation characteristics of the cables, on their symmetry, on the frequency and on the topology of the cabling, including the presence of the ground and objects containing conducting parts, such as furniture in the case of in-home networks and poles in the case of distribution lines. This makes it difficult to calculate the coupled currents exactly. Models exist that predict with accuracy the coupling of electromagnetic fields to lines whose per-unit-length parameters are constant ([83],[84],[85]). Models able to take into account variable parameters in a manner that makes them applicable to engineering applications are, however, lacking.

Although there exist a large number of electronic systems that are likely to be used in close proximity to PLC networks, the great majority of them will not pose a serious problem to PLC equipment and immunity against them is of low concern. Bluetooth, WLAN, and proprietary equipment, such as, for example, transmitters for the television signal and some wireless telephones do not need to be considered since they operate in the 2.4 GHz ISM band, which is well beyond PLC's allocated frequencies. Other systems also operating outside the PLC bands are DECT, ADSL, AM radio and CATV. Of the systems that function within the 1 to 30 MHz band, the ones that might affect the capacity of PLC are VDSL, HPNA and amateur radio. HPNA uses existing telephone lines. Although homes in Europe have typically only one or two telephone plugs, the latest specification, version 3.0, which offers data rates of up to 100 Mbps, may be attractive for the home networking market. VDSL is starting to be marketed as a home networking solution and it might become the successor of ADSL in some countries, although, to present, very few operators (e.g., Swisscom in Switzerland) are deploying or have announced plans to deploy that technology. Amateur radio transmitters are also a potential problem. For OFDM systems (a group to which both HomePlug and OPERA modems belongs), amateur bands can be masked out by eliminating through notching the corresponding subcarriers, thus eliminating immunity problems section 2.2.2.

The co-existence with other non-PLC telecommunication systems will be further discussed in section 2.4.3.3.1.

PLC modems, however, are different from other information technology equipment in that the mains and data ports are one and the same. For conducted immunity testing, this means that both, mains testing and telecommunication port testing, are performed using a CDN designed for electric cabling.

The common-mode immunity test signal levels are identical for both types of ports but the symmetry of the CDN's used for testing on the mains port may be worse than the CDN's specified for twisted pairs. In addition, the effect of the differential mode signal on the performance of the modems is a function of the sensitivity of the modems and their response to degraded signal-to-noise conditions. These factors are also dependent on the selected line code.

Due to the poor symmetry of electrical cabling in low voltage networks, a common mode interfering signal appearing at the mains and data ports of a PLC modem will be associated with a differential mode signal stemming from common to differential mode conversion. Realistic immunity testing should, therefore, include a differential mode component. One way to achieve this is to adjust the symmetry of the CDN in the current test specification. Determining the symmetry of the CDN that will best reproduce the conditions of a modem connected to a PLC network requires a good understanding of the conversion between common and differential modes.

Although one may think that specifying a sufficiently good symmetry for the CDN's EUT port would solve the problem and insure accurate results, this is not necessarily the case for the case of PLC networks, as we will see in Chapter 4.

2.4.3.2 Potential interferers

2.4.3.2.1 Disturbances from Electrical Appliances

The PLC channel is affected by noise that can have its origin in natural phenomena, such as lightning, or it can be caused by human activity. Human-made noise can be classified into four types: Impulsive noise, background noise, synchronized noise and

narrowband noise. Synchronized noise appears in the form of spikes at frequencies that are multiples of the 50 Hz line frequency. This noise is generally small and not a problem for PLC systems. Background noise is produced by distribution transformers and public lighting and its power spectral density decreases with frequency. Other components of background noise are cross-talk, thermal noise and cosmic noise (the latter two being actually natural).

Narrowband noise is essentially due to television screens, computer screens and amateur radio. The central frequency of narrowband interferers tends to be constant as it is defined by the frequency allocation plan at the country or at the international level. Impulsive noise is the most critical disturbance for PLC systems. Impulsive noise is of a very complex and unpredictable nature. It can appear as impulses lasting from under a microsecond to many milliseconds happening at intervals ranging from the microsecond scale to hours. The amplitudes measured range from under a volt to several kilovolts. It can be traced to a host of causes such as, for example, atmospheric discharges, the manual or automatic on-off switching of appliances at home, thermostats, bad contacts, etc.

Appliances connected to the mains network at home inject spurious signals that can have an effect on the performance of PLC equipment. Limits on the allowable voltages on the ports of appliances are set by CISPR standards in the form of conducted emissions limits. These limits are the following for the class B equipment of interest to us and in the frequency band that concerns PLC: 46dBμV (200μV on a 9 kHz bandwidth or, equivalently, 22 pV/Hz) for the range 0.5 to 5 MHz and 50dBμV (316μV on a 9 kHz bandwidth or, equivalently, 35pV/Hz) for the range from 5 MHz to 30 MHz (see

Table 2-4). Using these limits, it is possible to estimate the influence of the appliances on the capacity of coexisting PLC networks. The capacity is given by Shannon's formula [76]:

2-10
$$C = \int_W log_2(1 + \frac{S(f)}{N_r + N_2 + N_3 + \ldots N_k})df$$

where C is the capacity in bits per second, $S(f)$ is the wanted-signal spectral density at the receiver, N_r is the noise spectral density present at the receiver end in the absence of the electrical appliance disturbers, N_i are the spectral densities produced by the different appliances at the receiver being considered and W is the frequency band being utilized. The received signal's spectral density $S(f)$ can be expressed in terms of the signal's spectral density at the transmitter $S_t(f)$ and the channel's transfer function $H(f,d)$ (d is the distance between the transmitter and the receiver) as follows

2-11
$$S(f) = S_t(f)|H(f,d)|^2$$

In the last equation, we have omitted the dependence of $S(f)$ on the distance d.

In order to get estimates of the effect of appliances on the performance of PLC equipment, a scenario representing a household needs to be defined. The home will be assumed here to have nine appliances. These could be, for example, two computers, one dishwasher, one washing machine, a drying machine, one refrigerator, two

television sets and a stereo system. Appliances used infrequently or for short periods of time haven not been included in the scenario and they will not be considered.

Worst-case noise from the appliances in the scenario-based household can be estimated by using the conducted emissions limits set by CISPR standards. The different noise power spectral densities (PSD) can be added directly to the existing noise floor to estimate the effect of the appliances on the capacity of the PLC network. Using Shannon's capacity formula for the applicable CISPR limits, the capacity for the nine appliances is given by:

2-12
$$C = \int_{1.7MHz}^{5MHz} log_2(1 + \frac{S(f)}{N_r + 9x22x10^{-12}V/Hz})df + \int_{5MHz}^{30MHz} log_2(1 + \frac{S(f)}{N_r + 9x35x10^{-12}V/Hz})df$$

Assuming that the in-home frequency band is made of the upper half of the total allocated range, the capacity is given by

2-13
$$C = \int_{15MHz}^{30MHz} log_2(1 + \frac{S(f)}{N_r + 9x35x10^{-12}V/Hz})df$$

The outlined method can be used to estimate the effect of the added noise once the transmitted signal characteristics $S_t(f)$ and the transfer function $H(f,d)$ are known, and once the noise floor has been measured.

2.4.3.2.2 Disturbance Caused by non-PLC communication systems

Narrow-band Interferers

If the non-PLC system emits narrow-band signals, its effect on the PLC system will depend on the amount of power of the disturbing signal at the PLC installation site, on the central frequency of the signal, on its bandwidth, and on the line code scheme adopted for the PLC physical layer. For CDMA systems, the received narrow-band noise signal will be spread and filtered by the receiver, leading to an effective reduction of the noise by a factor equal to the squared processing gain of the CDMA spread spectrum modulator. The effect of the disturbance on the capacity of the PLC channel can be estimated by way of Shannon's capacity formula

2-14
$$C = w log_2(1 + \frac{S}{N_r + N_2/PG^2})$$

where, w is the bandwidth after dispreading (hence the absence of the integral sign), N_r is the noise floor without the disturbing signal, N_2 is the power in the noise from a narrow-band disturber, C is the capacity, S is the signal power at the receiving end after dispreading, and P_G is the processing gain. On an OFDM system, the disturbing signal will lead to the lowering of the transmitted bit rate by forcing a reduction of the number of bits loaded onto one or more affected subcarriers.

Broadband Interferers

If the non-PLC system's disturbance is a broadband signal, the effect on CDMA-like schemes will be a reduction of the signal-to-noise ratio in the same way as in the narrow-band case:

2-15
$$C = w log_2(1 + \frac{S}{N_r + N_2 / PG^2})$$

Once more, w is the bandwidth after dispreading (hence the absence of the integral sign), N_r is the noise floor without the disturbing signal, N_2 is the total power of the broadband disturber, C is the capacity, S is the signal power at the receiving end after dispreading, and P_G is the processing gain. On an OFDM system, the disturbing broadband signal may lead to the lowering of the transmitted bit rate by forcing a reduction of the number of bits loaded onto a potentially large number of subcarriers.

Moreover, measurements of radiated fields from PLC systems exhibit very high spread. For these reasons, approximate methods need to be used to obtain approximations of the induced voltages. The following approximate procedure can be used to evaluate the level of the noise coupled into the PLC system:

- For the Non-PLC system under study, obtain the maximum emission level at 3 meters from the standards and assume that this is the emission level of the system.
- Use the rate of change of the magnetic flux under the PLC cabling to estimate the induced antenna mode (also known as common mode) voltage.
- Use typical unbalance factor values to estimate the conversion from antenna to differential mode.
- The resulting differential mode signal is the noise coupled to the PLC system.

2.4.3.3 Co-existence

2.4.3.3.1 Co-existence with non-PLC communication systems

A potential disturber is a system that

- Operates in the same frequency band as PLC or has a strong enough harmonic content within the PLC band (strong out-of-band signals could also affect input amplifiers)
- Could be installed in close enough proximity to the PLC network
- Could be the source of strong enough emissions to adversely affect PLC performance.

It is important to note that some of the potential sources of interference may be confined to specific geographical areas and, therefore, the great majority of the PLC systems will never have to deal with them. Examples are systems used in airport settings.

The interferers can be classified into narrowband and broadband.

As discussed in section 2.4.3.1.2, of the systems that function within the 1 to 30 MHz band, the most likely to affect the capacity of PLC are VDSL, HPNA and amateur radio for the reasons discussed in what follows.

HPNA uses existing telephone lines. Although the appeal of HPNA could be small due to the fact that homes in Europe have typically only two telephone plugs, the latest specification, version 3.0, which offers data rates of up to 100 Mbps, may make this technology attractive for the home networking market.

ADSL, VDSL and PLC use frequency bands that overlap: the ADSL frequency band is comprised between 30kHz and 1.1MHz, the VDSL frequency band is comprised between 138kHz and 12MHz and the PLC frequency band is comprised between 1MHz (in practice more 4MHz) and 30MHz.

Recently, France Telecom published a study [91] on the co-existence between VDSL and PLC. Their study shows that, near a PLC transmission, the maximum stationary noise increase generated by coupling on the close telephone cable is 40 dB if the two transmission lines are stuck together and 25 dB if their spacing is of 10 or 30 cm. Only the stationary noise included in the second downstream VDSL band - 5.2 MHz up to 8.5 MHz - will have an impact on the performance of VDSL transmissions. Therefore, if the length of a VDSL link is such that only the first downstream band is occupied, the proximity of a PLC link will not have any impact on the VDSL transmission. Conversely, if the second VDSL frequency band is used, the reductions in terms of rate can reach 25% [91].

Finally, amateur radio transmitters are also a potential problem, although for the case of OFDM-type systems, the amateur bands are likely to be masked out by eliminating the corresponding subcarriers.

2.4.3.3.2 Co-existence between different coordinated PLC systems

The co-existence between coordinated PLC systems is based on the transmission/detection of two unmodulated OFDM signals. OPERA defines three sharing mechanisms among coexisting networks based on pure FD, pure TD and hybrid FD/TD [1][2][3].

The basic coexistence mechanism between access and in-home systems consists in FD sharing. Access systems operate in the lower frequency band while in-home systems operate in the upper frequency band. If there are several in-home systems, these systems will share the upper frequency band using TD.

2.4.3.4 Mitigation techniques

The capacity of a transmission channel (in bits per second) depends on three factors: 1) the bandwidth available, 2) the power of the signal used for the transmission of the data and 3) the power of the noise in the channel. Once all of the available bandwidth is used, the transmission speed can only be increased either by reducing the noise or by increasing the transmitted signal power. Although it is possible to reduce some of the noise in a transmission channel, one has, in general, little or no control over the noise floor and over some of the noise sources. Increasing the transmitted power is therefore the only alternative if higher bit rates are required. EMC considerations, however, place limits on the maximum power that can be transmitted. Indeed, in general, the higher the transmitted power, the higher the emissions level. This EMC-based limitation in the

maximum transmitted power could represent a major obstacle to the success of PLC technology.

A solution to this problem is to devise techniques to mitigate emissions. A number of such techniques have been proposed to reduce emissions from PLC networks without reducing the transmitted power. These techniques can be called collectively mitigation techniques. They include, for example, the reduction of the injected common mode through the use of improved couplers, the notching of sensitive frequencies, common mode suppressors and active signal injection for the cancellation of field components through deliberate induction of destructive interference ([35],[92],[93],[94],[79],[80]).

2.5 Conclusions

In this chapter, the PLC relevant telecom issues have been summarized. One of the important topics from the system design point of view, the definition of the delay spread, has been discussed and the method to calculate it of the n-ary OFDM system has been proposed. The specifications of the system recently proposed by the OPERA consortium have also been briefly presented.

The support medium for the PLC system is powerline grid. The power grid configuration and basic topologies and building types were presented. Also the fundamentals of the PLC technology have been presented, including PLC system components, coupling types, etc.

We have presented some technical issues that remain to be resolved in powerline communications technologies, concentrating mainly on those that are EMC related. We have discussed problems that still need to be solved in four areas: emissions, mitigation, channel modeling and immunity.

The main outstanding issues related to emissions are the poor current understanding of the conversion between the differential and the common mode and the absence of methodology or an appropriate set of parameters to evaluate the radiation potential of a network.

Although sophisticated PLC channel models have been proposed, the statistical variations having to do with the switching on and off of different appliances and other charges are not satisfactorily included.

Immunity appears not to be an immediate concern to PLC. If market development leads to mass deployment of technologies that share the same frequency band as PLC, such as, for example, VDSL and HPNA, the proper operation of PLC systems may be compromised.

We presented and discussed the IEC 61000-4-6 conducted immunity standard. The injection of the test common mode signal is achieved by way of the coupling-decoupling network (CDN). The CDN is specified through its common mode impedance for a range of frequencies that includes the PLC band. Different CDNs exist for the injection of test signals into different types of cables, such as coaxial and twisted pair.

The symmetry of the CDN's port is, however, not specified in standards. Due to the low symmetry of PLC cabling, part of the common mode injected test signal is converted into a differential mode signal that interferes with the wanted signal at the input of the modem being tested. Depending on the actual symmetry of the CDN, the immunity test may yield erroneous results due to the effect of this differential mode component.

Regarding mitigation of emissions, techniques such as shielding, common mode suppression and active signals to create destructive interference have been proposed. The challenges that remain have to do with the practical applicability of the already proposed techniques or the invention of new, easily applicable, economically feasible techniques.

Despite the advantages that PLC can offer, unless proper standards and regulations are developed globally, powerline risks not to live a full development and success. We presented the problems linked to standardization, regarding EMC, immunity testing and regarding the specification of the PHY and MAC layers.

REFERENCES

[1] OPERA technology White Paper, OPERA. IST Integrated Project No 507667. Funded by EC ,February 2006

[2] OPERA Technology Specification, part 1, IST Integrated Project No 507667. Funded by EC , January 2006

[3] OPERA Technology Specification, part 2, IST Integrated Project No 507667. Funded by EC , January 2006

[4] Deliverable 3: “Channel Measurements, Definitions and Procedures”, IST Integrated Project No 507667. Funded by EC , January 2005

[5] Deliverable 4: “Theoretical postulation of PLC channel model”, IST Integrated Project No 507667. Funded by EC, March 2005

[6] Deliverable 5: “Pathloss as a function of frequency, distance and network topology for various LV and MV European powerline networks”, IST Integrated Project No 507667. Funded by EC, April 2005

[7] Deliverable 8: “Report on EMC Aspects of PLC Technology”, IST Integrated Project No 507667. Funded by EC , November 2005

[8] Deliverable 44: “Report on presenting the architecture of PLC system, the electricity network topologies, the operating modes and the equipment over which PLC access system will be installed”, IST Integrated Project No 507667. Funded by EC , December 2005

[9] Deliverable 45: “Specification of PLC System Requirements”, IST Integrated Project No 507667. Funded by EC , May 2004

[10] Deliverable 46: “General specification of PLC PHY layer”, IST Integrated Project No 507667. Funded by EC, August 2004

[11] Deliverable 47: “General specification of PLC MAC layer”, IST Integrated Project No 507667. Funded by EC, July 2004

[12] Deliverable 52: “Specification for EMC measurements to be performed”, IST Integrated Project No 507667. Funded by EC, May 2004

[13] Deliverable 53 “Report on disturbance voltage measurement method”, IST Integrated Project No 507667. Funded by EC , 2005.

[14] Deliverable 54 “Report on Radiation”, IST Integrated Project No 507667. Funded by EC, 2005.

[15] D53 & D54 - Appendix 1 - EPFL MEASUREMENTS, IST Integrated Project No 507667. Funded by EC, 2005.

[16] Deliverable 55 “Report on Immunity”, IST Integrated Project No 507667. Funded by EC, 2005.

[17] Based on a discussion with Hanspeter Widmer, Ascom (Schweiz) AG

[18] K. Dostert, Powerline communications, Prentice Hall, 2001

[19] H. Hrasnica, A. Haidine, R. Lehnert, Broadband Powerline Communications, Chichester; Hoboken, N.J.: Wiley, 2004.

[20] V. Oksman, “Standard VDSL technology, overview of European (ETSI), North American (T1E1.4) and International (ITU-T) VDSL standard deployment”, July 2001

[21] S. Haas, “QAM VDSL – A tutorial”, 802.3ah EFM meeting in Seoul, S. Korea, May 2003

[22] Based on the discussions with Markus Bittner, Ascom (Schweiz) AG

[23] F. M. Tesche, M. Ianoz, and T. Karlsson, EMC Ananlysis methods and computational models. New York: Wiley Interscience, 1997.

[24] OPERA Phase 1 Annex1 – Description of the Work, IST Integrated Project No 507667. Funded by EC , October 2003

[25] OPERA Phase 2 Annex1 – Description of the Work, IST Integrated Project No 026920. Funded by EC, November 2006

[26] A. Vukicevic, COST Workshop on Powerline Communications, A 6th Framework Integrated Project on Power Line Communication Systems, March 2004, Liège

[27] Romano Napolitano, OPERA project presentation, PUA Workshop, 10th May 2005, Barcelona, Spain

[28] OPERA project presentation, 14th October 2004, Brussels, Belgium

[29] A. Leon-Garcia, I. Widjaja “Communication Networks: Fundamental Concepts and Key Architectures”, McGraw-Hill, 2004

[30] ISO/IEC 7498-1: 1994, Information technology—Open Systems Interconnection—Basic Reference Model: The Basic Model

[31] “OFDM – Orthogonal Frequency Division Multiplexing”, Dr. Jean Armstrong Department of Electronic Engineering La Trobe University, http://www.ieeevic.org/events/docs/72_armstrong_ofdm.pdf

[32] A. S. Tanenbaum, “Computer Networks”, Pearson Education International, fourth edition, 2003

[33] S. Haykin, “Communication Systems”, John Wiley & Sons, 4th Edition, 2004

[34] International Powerline Communication Forum: www.ipcf.org

[35] E. Marthe, Thèse No 3165, Powerline communications: Analyse des Problèmes de Compatibilité Electromagnétique dans le domaine des Courants Porteurs en Ligne, EPFL, 2005

[36] R. G. Olsen, "Technical Overview of Broadband Powerline (BPL) Communication Systems," presented at IEEE Symposium on Electromagnetic Compatibility, Chicago, 2005.

[37] Power-Line Communications: Channel Properties and Communication Strategies PhD thesis, Lars Selander, 1999

[38] Widmer, HP., Report of PLC Measurements from 12 to 16 April 1999 at EDF in Paris, Ascom Defense & Security, Version 0.1, April 25th, 1999.

[39] Benyoucef, D.: A New Statistical Model of the Noise Power Density Spectrum for Powerline Communication. Proceedings of the 7th International Symposium on Power-Line Communications and its Applications, Kyoto, Japan, 2003, pp. 136 – 141.

[40] M. Babic, K. Dostert: An FPGA-based High-Speed Emulation System for Powerline Channels, ISPLC 2005, Vancouver, Canada.

[41] M. Babic, T. Kistner, J. Bausch, A. Kawohl: Development of a Power Line Channel Simulator, Reports on Industrial Information Technology, Volume 8.

[42] D4: Theoretical Postulation of PLC Channel Model, http://www.ist-opera.org/project_outputs_available.html OPERA. IST Integrated Project No 507667. Funded by EC, 2005.

[43] M. Babic, J. Bausch, T. Kistner, K. Dostert: Performance Analysis of Coded OFDM Systems at Statistically Representative PLC Channels, accepted for ISPLC 2006, Orlando, USA.

[44] M. Babic, K. Dostert: Performance Analysis of OFDM Systems at Noisy, Time-Variant Power Line Channels, submitted for GLOBECOM 2006, San Francisco, USA

[45] M. Zimmermann, PhD thesis, "Energieverteilnetze als Zugangsmedium für Telekommunikationsdienste", University Karlsruhe, 2000

[46] M. Zimmermann, K. Dostert, " A Multipath Model for the Powerline Channel", IEEE Transactions on Communications, Vol. 50, No. 4, April 2002

[47] M. Zimmermann, K. Dostert, "Analysis and Modeling of Impulsive Noise in Broad-Band Powerline Communications", IEEE Transactions on Electromagnetic Compatibility, Vol. 44, No. 1, February 2002

[48] Cañete, F. J.; Díez, L.; Cortés, J. A.; Entrambasaguas, J. T: "Broadband Modeling of Indoor Power-Line Channels". IEEE Transactions on Consumer Electronics, vol. 48, no. 1, Feb. 2002, pp. 175 – 183.

[49] Cañete, F. J.; Cortés, J. A. ; Díez, L.; Entrambasaguas, J. T.: "Modeling and Evaluation of the Indoor Power-Line Transmission Medium. IEEE Communications Magazine, vol. 41, no. 4, April 2003, pp. 41 – 47.

[50] Office Fédéral de la Communication, OFCOM, Frequency allocation plan, www.ofcom.ch

[51] P.A. Brown, "PLT access products – EMC aspects", 15th International Zurich Symposium on Electromagnetic Compatibility, February 2003, Zurich, Switzerland

[52] K. Dostert, "EMC Aspects of High Speed Powerline Communications",15th International Wroclaw Symposium on Electromagnetic Compatibility, Wroclaw, 27-30 June 2006

[53] S.J. Halme, R. Kytönen, V. Nässi, L. Halme, "Transmission and EMC Aspects of Pwer Line Telecommunications", 16th International Symposium on Symposium on Electromagnetic Compatibility in Wroclaw, Wroclaw, Poland, 25 – 28 June 2002.

[54] M. Stecher, "EMC Aspects of Power Line Communications", 4th European Symposium on EMC in Brugge, 11 – 15 September 2000.

[55] HP. Widmer, "On the Global EMC Aspect of Broadband Powerline Communications using the HF Frequency Band", IEEE 2000

[56] CISPR 22/IEC, Information technology Equipment – Radio Disturbance Characteristics – Limits and methods of measurements, Third Edition, 11-97

[57] Specification for Radio Disturbance and Immunity Measuring Apparatus and Methods, Part 1, CISPR 16-1, First Edition, 08-93

[58] ITU-T Recommendation G.117, "Transmission Aspects of Unbalance About Earth (Definitions and Methods)", 1988

[59] CISPR/I, “Contribution to CISPR/I/DC”, January 2002

[60] CISPR/I/7/DC, August 2001

[61] CISPR/I/26/DC, December 2001

[62] CISPR/I/44/DC, July 2002

[63] CISPR/I/89/DC, November 2003

[64] CISPR/I/PT PLT ad-hoc ISN (Amemiya, Baeschlin, Dunker, Gonzalez, Osabe, Sisolefsky) 07-01 August, 2007 Memorandum of the ad-hoc meeting T-ISN of 31.7 / 1.8.2007 at BNetzA Berlin

[65] CISPR/I/PT PLT (Dunker/Sisolefsky)07-0y August 2007, Assessment of conducted RF disturbances at the AC mains port of PLT equipment by means of Artificial Mains Networks (AMN) or Asymmetrical Artificial Networks (AAN)

[66] Commission of the European Communities, “Standardization Mandate Addressed to CEN, CENELEC and ETSI concerning Electromagnetic Compatibility (EMC) in Telecommunication Networks” (Mandate 313), 7 August 2001.

[67] Commission of the European Communities, “Commission Recommendation of 6 April 2005 on Broadband electronic communication through power lines”, Brussels, 6 April 2005, C(2005) 1031.

[68] FCC, “Report and Order, October 14, 2004.

[69] M. Ianoz, M. Koch “Standardization and regulatory approaches related to radiated emission limits for powerline communications”,18th International Wroclaw Symposium and Exibition on Electromagnetic Compatibility, Wroclaw, Pland, 28-30 June 2006

[70] IEC 61000-4-6 standard Electromagnetic Compatibility (EMC) - Part 4-6:Testing and measurement techniques – Conducted disturbances induced by radio-frequency fields – Immunity test

[71] "Application of the LCL method to measure the unbalance of PLC equipment connected to the low voltage distribution network," IEC-CISPR, Subcommittee I, Working group 3 February 26, 2003

[72] F. Issa, M. Goldberg, E. Marthe, F. Rachidi "In Situ Characterization of Impedance Mismatch in a Medium Voltage Network", Proc. International Symposium on Power Line Communications (ISPLC 2005) in Vancouver, Canada, April 6-8, 2005

[73] F. Issa, M. Goldberg, E. Marthe "Power Line Communications using Low and Medium Voltage Networks" Proceedings of the XXVIIIth General Assembly of Internation Union of Radio Science (URSI) in New Delhi, India, October 23-29, 2005

[74] A. Rubinstein and F. Rachidi "Inclusion of an automatic adaptive sampling method in NEC", 6th International Symposium on Electromagnetic Compatibility and Electromagnetic Ecology, St. Petersburg, Russia, June 2005

[75] S. Tkachenko, F. Rachidi, J. Nitsch, "High frequency wave propagation along non-uniform transmission lines: a direct iteration approach" 28th General Assembly of International Union of Radio Science (URSI), New Delhi, India, October 23-29, 2005

[76] Shannon, C.E. (1948), "A Mathematical Theory of Communication", Bell System Technical Journal, 27, pp. 379–423 & 623–656, July & October, 1948.

[77] A. Vukicevic, M. Rubinstein, F. Rachidi, JL. Bermudez, “On the Mechanisms of differential-mode to Common-mode Conversion in the Broadband over Powerline (BPL) Frequency Band”, 17th International Zurich Symposium on Electromagnetic Compatibility, 27 February -3 March 2006, Singapore

[78] A. Vukicevic, F. Rachidi, M. Rubinstein, S. Tkachenko "An efficient method for the computation of antenna mode currents along transmission lines" 28th General Assembly of International Union of Radio Science (URSI), New Delhi, India, October 23-29, 2005

[79] M. Rubinstein, J.L. Bermudez, A. Vukicevic, F. Rachidi, M. Schneider "On the mitigation of radiation from PLC networks" 28th General Assembly of International Union of Radio Science (URSI), New Delhi, India, October 23-29, 2005

[80] M. Rubinstein, J.L. Bermudez, A. Vukicevic, F. Rachidi, M. Schneider, E. Marthe "Discussion on the assessment and mitigation of radiation from PLC networks" Proc. International Symposium on Power Line Communications (ISPLC 2005) in Vancouver, Canada, April 6-8, 2005

[81] A. Vukicevic, M. Rubinstein, F. Rachidi, JL. Bermudez, M. Schneider, P. Favre, P. Zweiacker, “Review of the Electromagnetic Compatibility PLC Work at the Swiss Federal Institute of Technology (Lausanne) and the University of Applied Sciences of Western Switzerland (Yverdon)”, 10th International Symposium on Power-Line Communications and Its Applications, 26-29 March 2007. Orlando, USA

[82] M. Rubinstein, A. Vukicevic, JL. Bermudez, F. Rachidi, P. Favre, M. Schneider, “Some Unresolved Issues Concerning EMC in Powerline Communications”, 18th International Wroclaw Symposium on Electromagnetic Compatibility, Wroclaw, 28-30 June 2006

[83] C.D. Taylor, R.S. Satterwhite and C.W. Harrison, The response of a terminated two-wire transmission line excited by a non-uniform electromagnetic field, IEEE Transactions on Antennas and Propagation, Vol. 13, No 6, November 1986

[84] A.K. Agrawal, H.J. Price and S.H. Gurbaxani, Transient response of multiconductor transmission lines excited by a nonuniform electromagnetic field, IEEE Transactions on Electromagnetic Compatibility, Vol. 22, No 2, May 1980

[85] F. Rachidi, Formulation of field to transmission line coupling equations in terms of magnetic excitation field, IEEE Transactions on Electromagnetic Compatibility, Vol. 35, No 3, August 1993

[86] C.R. Paul, “A comparison of the contributions of common-mode and differential mode currents in radiated emissions”, IEEE Trans. On EMC, Vol. 31, No. 2, pp. 189-193, May

[87] C.R. Paul and D.R. Bush, “Radiated Emissions from Common-Mode Currents”, Proc. IEEE Symposium on EMC, Atlanta, August 1987.

[88] Tudziers C. “Common-mode propagation simulations in telecommunication cables”, Cagliari EMC shop 2000, Cagliari, Italy, May 20-23, 2000.

[89] M. Rubinstein, "Effect of the wire radii tolerances on differential to common mode conversion in balanced twisted pairs," presented at 13th Zurich International Symposium on Electromagnetic Compatibility, Zurich, Switzerland, 1999.

[90] P. Favre, C. Candolfi, P. Kraehenbuehl, M. Schneider, M. Rubinstein, A. Vukicevic, “Common-mode Current and Radiation Mechanisms in PLC Networks”, 11th International Symposium on Power-Line Communications and Its Applications, 26-28 March 2007. Pisa, Italy

[91] A. Zeddam, F. Moulin, R. Tarafi, F. Gauthier, “EMC and Co-existence Issues of Broadband Communications over Copper”, 28th General Assembly of International Union of Radio Science (URSI), New Delhi, India, 2005.

[92] R.P. Rickard, Power Line Communications, Patent WO98/06188 and US6785532, 12 February 1998.

[93] R.P. Rickard, Coupling communications signals to a power line, Patent US6037678, 14 March 2003.

[94] N. Korovkin, E. Marthe, F. Rachidi, E. Selina, "Mitigation of electromagnetic field radiated by PLC systems in indoor environment", International Journal of Communication Systems, Vol. 16, pp. 417-426, May 2003.

Chapter 3

3 Conducted and radiated emissions from PLC systems

3.1 Introduction

Electronic equipment is the source of intentional or unintentional emissions in two forms: radiated electromagnetic fields, called radiated emissions, or injected currents at their mains or telecommunication ports, called conducted emissions.

In this chapter, we first describe different methods to evaluate conducted emissions and we will discuss the contribution of common mode and differential mode currents to radiated emissions. Then, we present an experimental characterization of the differential to common mode conversion. The obtained experimental data are also used to verify simulations obtained using a full-wave approach and the transmission line theory. Finally, we present and test a method to estimate the common mode current in in-house electrical wiring.

3.2 Methods to evaluate conducted emissions

In general, the calculation of conducted and radiated emissions involves the solution of Maxwell's equations. The full solution of Maxwell's equations is generally accomplished for wire-like systems by setting up integral equations and solving them using, for instance, the Method of Moments [3][42]. This method has the advantage of being accurate since very few approximations are involved. For large systems (many wavelengths long), however, this approach may prove numerically taxing in terms of the required processor power and memory requirements. In some cases, the geometry of the radiating system allows the use of simplifying approaches for the calculation of the currents and the fields. One common simplification is achieved when the radiating system exhibits some form of geometrical symmetry. A second form of simplification, which is applicable to PLC networks, is achieved when signals propagate along a system whose transverse dimensions are much smaller than the wavelengths involved. Under that condition, one can use the so-called transmission line approximation to compute the currents along the system with relative ease [4]. The transmission line approximation is used when the length of the system is comparable or larger than the wavelengths involved. For short networks, it is possible to further simplify the calculations by assuming quasi-static conditions.

The evaluation of conducted emissions can be performed using different approaches depending on the circuit configuration, its complexity, frequencies involved and the degree of approximations with respect to an exact formulation. In general, there exist three possible methods to evaluate conducted emissions associated with PLC systems:

Lumped-parameter (quasistatic) circuit models

In this approach, conducted emissions –voltages and currents– are described by means of lumped circuit elements such as resistances, inductances and capacitances. Propagation effects are not considered, meaning that the approach is applicable when the physical size of the system is much smaller than the wavelength of the signals. For a

frequency of 30 MHz, for example, a low-frequency approach can be applied for systems whose dimensions do not exceed 1 m in length (about a tenth of the wavelength). Therefore, its application to PLC appears to be inappropriate and will not be further considered. It is worth mentioning, though, that a combination of lumped parameters with the transmission line approach might prove useful since it may lead to much simpler application with acceptable loss in accuracy.

Transmission line theory

Assuming that the cross-sectional dimensions of the line are electrically small, we can consider that propagation occurs only along the line axis. This is one of the basic assumptions of the Transmission Line (TL) theory. In this way, the line can be represented by a distributed-parameter structure along its axis. For uniform transmission lines with electrically-small cross-sectional dimensions (not exceeding about one tenth of the minimum significant wavelength of the exciting electromagnetic field), the TL theory yields very accurate results. Consequently, its application to outdoor PLC networks, characterized by uniform cross sections could be envisaged[1].

Formal solutions to Maxwell's equations and the appropriate field boundary conditions

As the frequency of the conducted emissions increases to the point where the wavelength becomes comparable to the dimensions of the circuit, a more general approach based on solutions to Maxwell's equations is required. There are numerous electromagnetic modelling techniques. Methods such as the Finite Element Method (FEM), Finite Difference Time Domain (FDTD), Method of Moments (MoM), Transmission Line Matrix Method (TLM), Generalized Multipole Technique (GMT), and others have each their own set of advantages for particular applications [42]. In this work, we will make reference to the Numerical Electromagnetics Code [3], which is a well-known, widely used computer code based on the MoM and developed for the analysis of antennas and other metal structures. In general, MoM techniques do an excellent job of analyzing wire-like structures, such as an indoor PLC network.

3.2.1 Introduction to the different approaches

3.2.1.1 Transmission Line Approach

The basic assumptions of the TL theory are [5]:

- The cross-sectional dimensions of the line are electrically small
- The response of the line is quasi-transverse electromagnetic (quasi-TEM). In other words, the electromagnetic fields produced by the electric charges and currents along uniform cross-section line are confined to the transverse plane and perpendicular to the line axis.
- The sum of the line currents at any cross section of the line is zero. In other words, the ground – the reference conductor – is the return path for the currents in the n conductors forming the multiconductor line.

By assuming that the sum of all the currents is equal to zero, we are considering only 'transmission line mode' currents[2] and neglecting the so-called 'antenna-mode' currents.

[1] Especially for frequencies below 10 MHz corresponding to wavelengths of 30 m and above.
[2] Note that TL mode currents include both differential- and common-mode currents.

If we wish to compute the load responses of the line, this assumption is adequate, because the antenna mode current response is small near the ends of the line. Along the line, however, and even for an electrically small cross section of the line, the presence of antenna-mode currents implies that the sum of the currents at a cross section is not necessarily equal to zero [4]. For outdoor PLC networks, the quasi-symmetry due to the presence of the ground plane results in a very small contribution of antenna mode currents and, consequently, the predominant mode on the line will be the transmission line mode. For indoor networks, however, the antenna-mode currents could play an important role and they need to be, in principle, taken into account. This problem will be thoroughly dealt with in the next chapter.

Figure 3-1 illustrates an infinitesimal section of a three-conductor line, having a length of dx [4]. If the line is uniform along its length, the electrical parameters of the line can be considered to be uniformly distributed and they are denoted by constant per-unit-length values R', L', C' and G'.

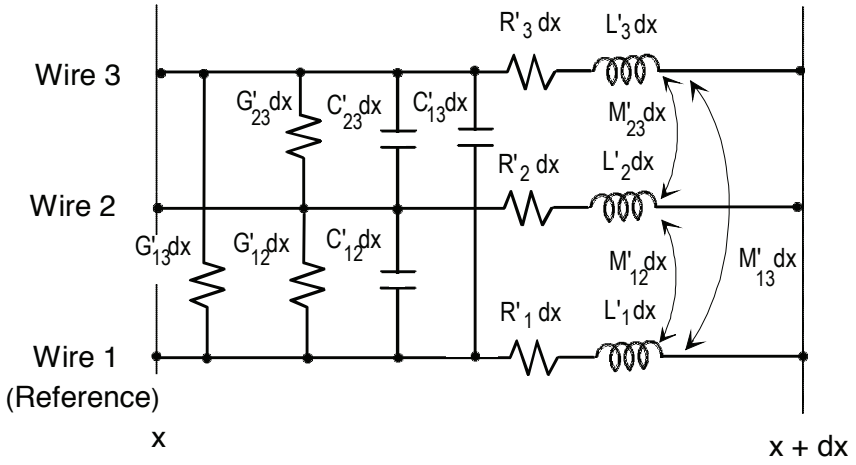

Figure 3-1: Distributed parameters of an infinitesimal section dx of a three-conductor transmission line with wire #1 serving as a reference conductor

For a general system of n conductors (plus a reference conductor), the TL telegrapher's equations can be written in matrix form as:

3-1
$$\frac{d[V(x)]}{dx} + [Z'][I(x)] = 0$$

3-2
$$\frac{d[I(x)]}{dx} + [Y'][V(x)] = 0$$

where $[V(x)]$ and $[I(x)]$ are the vectors of the n voltages and currents on the lines and $[Z']$ and $[Y']$ are the $n \times n$ matrices of the line impedances and admittances, respectively. The solution of equations 3-1 and 3-2 is complicated by the fact that these two matrices are full matrices. This is due to the mutual inductive and capacitive coupling between the n lines of the system. Note that, in equations 3-1 and 3-2, external electromagnetic field sources have been disregarded. The presence of external sources can be included by adding appropriate excitation sources in the TL telegrapher's equations [4][6].

The two coupled first-order differential equations 3-1 and 3-2 can be used to derive uncoupled, second order equations of the form

3-3 $$\frac{d^2[V(x)]}{dx^2} + [P][V(x)] = 0$$

3-4 $$\frac{d^2[I(x)]}{dx^2} + [R][I(x)] = 0$$

where the matrices [P] and [R] are full matrices defined as

3-5 $$[P] = [Z'][Y']$$

3-6 $$[R] = [Y'][Z']$$

The $n \times n$ per-unit-length impedance and admittance matrices are given by:

3-7 $$[Z'] = \begin{bmatrix} R'_1 + R'_{g11} + j\omega L'_{11} & R'_{g12} + j\omega M'_{12} & . & . & . \\ R'_{g21} + j\omega M'_{21} & R'_2 + R'_{g22} + j\omega L'_{22} & . & . & . \\ . & . & . & . & . \\ . & . & . & . & \\ . & . & . & R'_n + R'_{gnn} + j\omega L'_{nn} & \end{bmatrix}$$

and

3-8 $$[Y'] = j\omega \begin{bmatrix} C'_{11} & C'_{12} & . & . & . \\ C'_{21} & C'_{22} & . & . & . \\ . & . & . & . & . \\ . & . & . & . & . \\ . & . & . & . & . \end{bmatrix}$$

where R'_j are the resistances of each of the line conductors, R'_{gij} is the resistance of the common ground, L'_{ii} and M'_{ij} the self and mutual inductances of and between the conductors, and C'_{ij} are the capacitive coefficients for the conductors. Note that, in the expression for $[Y']$, the effects of any shunt conductance between the conductors has been neglected.

In many practical circumstances, where losses on the line can be neglected and when there is no variation in the parameters μ and ε around the line, the matrices $[P]$ and $[R]$ of equations 3-5 and 3-6 become diagonal matrices given by:

3-9 $$[P] = [Z'][Y'] = -\frac{\omega^2}{\nu^2}[U]$$

3-10 $$[R] = [Y'][Z'] = -\frac{\omega^2}{\nu^2}[U],$$

where ν is the velocity of propagation along the line and $[U]$ is the unit matrix

The diagonal form for $[P]$ and $[R]$ implies that each equation for the voltage or current in equations 3-3 and 3-4 is decoupled from the others and they may be solved independently, with solutions consisting of n forward and backward propagating modes on the line. Under the present conditions, each mode has the same propagation speed and, from equations 3-9 and 3-10, it is possible to see that the relationship between the $[L']$ and $[C']$matrices of the line is

3-11 $$[C'] = \frac{1}{\nu^2}[L']^{-1},$$

Given the fact that the $[L']$ matrix is easily computed since the self and mutual inductance terms do not depend on the presence of the other conductors, the $[C']$ matrix is in general more easily computed from equation 3-11 than by evaluating the capacitive coefficients directly.

For the case of a lossless line with no variation in the parameters μ and ε around it, the general solutions for the currents and voltages along the line read [4]

3-12 $$[V(x)] = [E^{+}(x)][a] + [E^{-}(x)][b]$$

3-13 $$[I(x)] = [Z_c]^{-1}\{[E^{+}(x)][a] - [E^{-}(x)][b]\}$$

where

3-14 $$[E^{\pm}(x)] = \begin{bmatrix} e^{\mp\gamma_1 x} & 0 & . & 0 \\ 0 & e^{\mp\gamma_2 x} & . & 0 \\ . & . & . & . \\ 0 & 0 & . & e^{\mp\gamma_n x} \end{bmatrix} \equiv e^{\mp[\gamma]x}$$

In equation 3-14, $\gamma_i = j\omega/\nu$, and $[Z_c]$ is the characteristic impedance matrix given by

3-15 $$[Z_c] = \nu[L'],$$

The n-vectors $[a]$ and $[b]$ contain the amplitudes of the forward and reverse propagating voltage modes. These constant vectors must be determined from the boundary conditions and line excitation functions.

For cases involving variable parameters μ and ε around the line (presence of dielectric jackets), the simple relationship between $[L']$ and $[C']$ is not obeyed and the $[P]$ and $[R]$ matrices are not diagonal. The implication of this is that the transmission line voltages (and currents) are coupled together and equations 3-3 and 3-4 cannot be solved in a simple manner. In this case, modal theory and matrix diagonalization have to be applied to solve the problem [4].

3.2.1.2 Full Wave Approach (MoM - NEC)

There exist several numerical techniques that can potentially be used for the analysis of signal propagation along PLC networks. These methods can be classified in terms of the

operational domain of the simulation (i.e., time or frequency) and the nature of the simulation (3D field, cable network and electrical circuit codes) [42].

Among all these numerical techniques, the Method of Moments (MoM) is perhaps the best suited for the problem of interest since it is able to handle straightforwardly wire-like structures, such as indoor PLC networks. In this work, the MoM technique and the Numerical Electromagnetics Code [3], which is a well-known, widely used computer code based on the MoM and developed for the analysis of antennas and other metal structures were used [42].

The Numerical Electromagnetics Code (NEC) is a user-oriented computer code based on the Method of Moments and written in FORTRAN for the analysis of the electromagnetic response of antennas and other metal structures [3]. It has been widely used with great success for radio communications testing as well as antenna design and EMC.

With its ability to represent models by means of wires, the code also allows the simulation of very complex 3D structures. NEC also allows the use of patches for the representation of surfaces, although constraints imposed by the code limit the application of this technique.

NEC produces an interaction matrix representing the system of integral equations needed to obtain the currents and fields. The number of elements in this matrix depends on the number of segments and patches that conform the model to be evaluated. This matrix is then reduced using LU factorization and, together with the excitation vector, the final solution to the integral equations is obtained.

3.3 Methods to evaluate radiated emissions

Although the differential mode is responsible for part of the radiation, the common mode can be designated as the main culprit when it comes to emissions from PLC networks.

Systems carrying electric currents radiate with varying degrees of efficiency which depend on the geometry, the frequency, and the types of currents that they transport. The calculation of the electromagnetic fields involves two steps:

- the estimation of the currents and
- the use of the currents for the computation of the associated electromagnetic fields.

In the sections on evaluation of radiated emissions, we will just briefly give the introduction, without entering too much into details.

3.3.1 Field calculation: General approach

In the case of low voltage PLC networks, differential signals are applied at the input of lines composed of either aerial conductors, or conductors within the walls, ceilings and possibly beneath the floor in buildings. An unintended amount of common mode is also injected by the PLC modems. Also, as the differential signals propagate along the cables, a mode conversion takes place and a common mode signal appears that adds to that already injected by the modems themselves. Among the different techniques that have been proposed and implemented to compute the currents and electromagnetic fields from complex wire structures, the one that is best suited to the problem of the computation of fields from PLC networks, as mentioned in the previous section, is the Method of Moments (MoM).

3.3.2 Field calculation: Simplified approaches

The way radiation actually occurs in PLC networks is currently poorly understood, in part due to the vast variety of network types and configurations, which has made it difficult to extract the fundamental influencing factors.

For essentially linear systems such as PLC cabling, the relationship between the power level of the PLC signal injected into a line and the electromagnetic field strength generated at any given point in the surrounding space is linear, implying that radiation between an input signal and the radiation due to it at a given point in space can be expressed as a frequency dependent, multiplicative factor with a real and an imaginary parts that determine the magnitude and the phase of the radiated field. Although this factor can, in principle, be measured for a given network and at a given location, it has been observed experimentally that the factor varies considerably from one network to the next, making it inapplicable in practice. This variation can be very high, the spread reaching 50 dB or more ([44][45]). Theoretical calculation could help reduce the spread by including the relevant influence factors in the estimation of the coupling factor. The difficulty in the estimation of the factor and thus of the fields lies in the application of the necessary equations to real power line networks, since approximations are required and the relative importance of the different intervening parameters is not yet well understood. As mentioned previously, these factors are strongly dependent on network characteristics such as the cable type, surrounding geometry, topology, building materials, etc.

3.4 DM to CM conversion

Consider a pair of parallel wires carrying currents I_1 and I_2 as shown in Figure 3-2(a). These currents can be decomposed into DM and CM mode currents as already explained in Chapter 4. The differential-mode currents in the two wires at the same cross-sectional position are equal in magnitude and phase but oppositely directed. These types of currents constitute the functional or wanted signals carried by the wires. The CM currents in the two wires at the same cross-sectional position and directed to the right are equal in magnitude and phase [9].

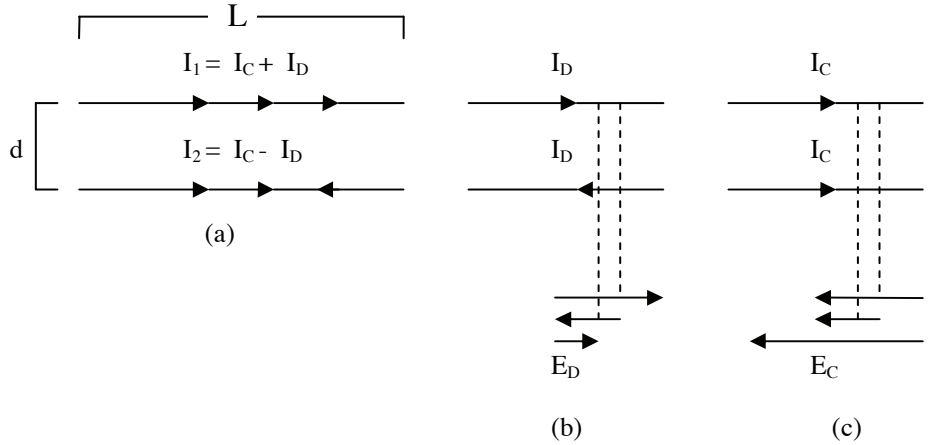

Figure 3-2: Common - mode versus differential - mode currents. (a) Decomposition of total currents. (b) Radiated emissions from differential-mode currents. (c) Radiated emissions from common-mode currents

Given the two currents I_1 and I_2, we can decompose them into their CM and DM current components as follows,

3-16
$$I_1 = I_C + I_D$$
$$I_2 = I_C - I_D$$

The CM and DM currents can be expressed as

3-17
$$I_C = \frac{I_1 + I_2}{2}$$
$$I_D = \frac{I_1 - I_2}{2}$$

The phase angles of I_1 and I_2 should be included in these computations. A current probe placed around both wires would measure $2I_C$.

A good understanding of the conversion between common and differential mode currents is of great importance in PLC networks essentially for the reasons explained in what follows. Firstly, due to the low symmetry of electric wiring, a certain amount of common mode current, that is, conducted emissions, is caused by differential to common mode conversion from the wanted signals injected by the modems. Secondly, the common mode current, of which a considerable fraction may be due to conversion from the differential mode, is the main source of radiated emissions. Thirdly, the asymmetry in the network leads also to the conversion of common mode to differential mode. This differential mode power interferes with the wanted signal and reduces the capacity of the channel. This last point is more important for immunity than emissions and will be dealt with in Chapter 4.

3.4.1 Contribution of CM and DM currents to radiated emissions

In this section, we show the relative contributions of the common and the differential mode currents to radiated emissions. In particular, we will see that radiated emissions due to CM currents in PLC networks can well exceed those due to DM currents [30].

As mentioned before, CM currents of considerably less magnitude than DM currents can have the same or even a higher level of radiated fields associated with them. To illustrate this, consider the two wires in Figure 3-2. Suppose the line length is L, the wire separation is d, and the point at which the total field is measured is at a distance R from the first wire. Also assume that this measurement point is in the plane of the two wires. If the wires are electrically short at the frequencies of interest ($L << \lambda$), then we may approximate each wire as a single Hertzian dipole and superimpose the resulting fields. Combining the fields gives, for the DM currents shown in Figure 3-2 [30][31].

3-18
$$E_{D\,max} = 1.316 \times 10^{-14} \frac{I_D f^2 L d}{R} \quad \text{in V/m}$$

Similarly, for the case of the CM currents shown in Figure 3-2, we obtain [30][31]

3-19
$$E_{C\,max} = 0.6285 \times 10^{-6} \frac{I_C f L}{R} \quad \text{in V/m}$$

Figure 3-3 shows the electric field radiated by a 4-m long line at a distance of 2 m. The separation of the wires is 1 cm. It can be seen that, for the same current amplitude, the

field due to the CM current is 3 to 4 orders of magnitudes larger than that from the DM current.

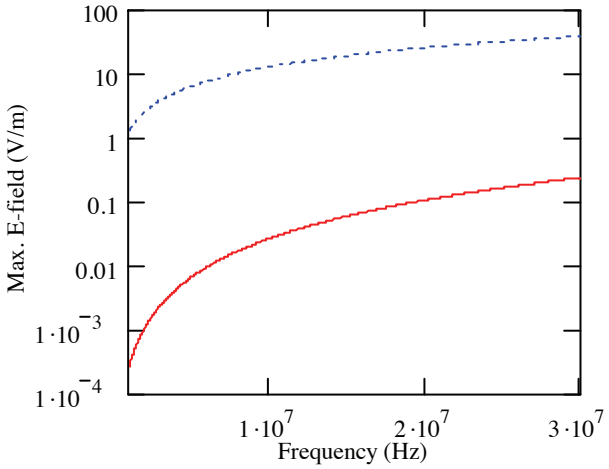

Figure 3-3: Radiated E-field as a function of frequency. L= 4 m, d=1 cm, R= 2 m. DM current and CM current amplitude are set to 1 A. Solid line: DM radiation, dotted line: CM radiation.

Figure 3-4 presents the field as a function of distance for a fixed frequency of 15 MHz. Again, it can be seen that the contribution of the CM currents is predominant regardless of the distance.

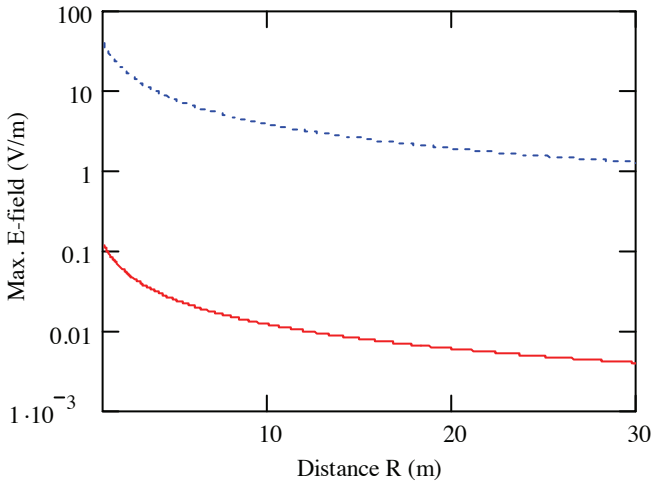

Figure 3-4: Radiated E-field as a function of distance. L= 4 m, d=1 cm, f= 15 MHz. DM current and CM current amplitude are set to 1 A. Solid line: DM radiation, dotted line: CM radiation.

The magnitude of the CM currents is in general smaller than that of the DM current [25]. Figure 3-5 presents the CM to DM E-field ratio as a function of frequency for an observation point located 2 m away from the line. It can be seen that, even for a DM-to-CM current ratio of 1000, the radiation associated with the CM currents is larger at frequencies below 10 MHz and comparable for the whole frequency range.

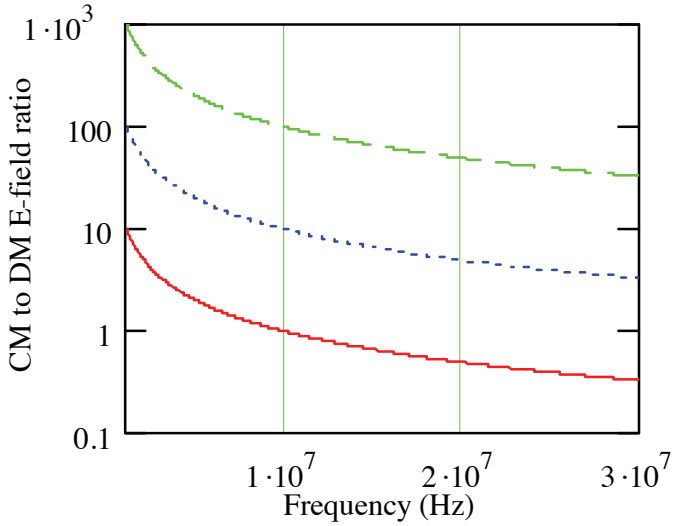

Figure 3-5: CM to DM E-field ratio as a function of frequency. L= 4 m, d=1 cm, R= 2 m. Solid line: DM current is 1000 times CM current, dotted line: The DM current is 100 times the CM current, and dashed line: The DM current is 10 times the CM current

Since the CM currents are the dominant radiation mechanism for the biggest part of the PLC frequency range (1-30 MHz), predictions of radiated emissions based solely on DM currents can underestimate actual measured emissions. Therefore, radiated emission prediction models require a good knowledge of both DM and CM current for the prediction of radiated emissions.

3.4.2 DM to CM conversion mechanisms: current state of knowledge

Unintentional common mode currents in LV electrical networks and MV cables stem from the superposition of three different sources [33]:

1. The common mode injected at the source due to asymmetries and design issues of the EUT itself.
2. The common mode that appears along the line by differential to common mode conversion, which can happen gradually, as the common mode propagates along the line, or abruptly, at punctual discontinuities.
3. The coupling of external electromagnetic fields from intentional or unintentional radiators. This last mechanism is not of interest here.

Currently, only the common mode directly injected at the source is considered in conducted emissions tests. It has been shown recently by Tudziers [32] that the conversion of the injected differential mode into the common mode can yield considerable common mode disturbance voltage. Using a multi-conductor transmission line model in which the parameters were made to vary randomly over a +/- 4% range, Tudziers showed that the common mode current is highly variable from one run to the next. Simulations showed that the balance and the common mode at the receiving end of a line are strongly dependent on the length of the line. For long lines, the imbalance can be higher at the near end than at the far end. This happens since conversion to common mode increased with cable length and, additionally, since for some types of cables, the attenuation of the common mode is smaller than that of the differential mode.

In LV cabling, punctual asymmetries, such as power outlets, switches, etc., play a role in the conversion of differential to common mode currents. Other discontinuities, such as the splicing of different cables, may also have a significant effect on the total common mode in the network.

Unbalance at the source

Any asymmetries in the circuitry in a modem or any other electronic apparatus used to produce and inject a wanted differential signal on one of its ports will lead to the injection of a common mode current. These asymmetries are typically due to differences in the stray capacitances of two otherwise symmetric circuit branches. Leakage currents are also a source of injected common mode currents.

Conversion to common mode along the line

As the differential mode signal travels down a multi-conductor line, part of it can be converted into the common mode due to small asymmetries in the line parameters. These stem from different distances to the reference conductor which generally varies as a function of the position, to differences in the dielectric material between different pairs of conductors, to the difference in the radii of the different conductors, etc.

Local asymmetries

Local asymmetries are responsible for local conversion of differential to common mode currents that manifest themselves as a leap in the common mode current around the imbalanced discontinuity. The amount of conversion depends on the magnitude of the discontinuity and the amount of imbalance in it.

Examples of local asymmetries in LV cabling are switches, power outlets, sharp corners and asymmetric cable terminations.

3.4.3 Differential Mode (DM) To Common Mode (CM) Conversion: An Experimental Characterization

In this subsection, we present the results of a measurement campaign carried out to investigate the conversion of the common to the differential mode. The measurements were performed in an outdoor test site especially set-up at the Swiss Federal Institute of Technology in Lausanne (EPFL).

The aim of the experiment was to analyze and illustrate different mechanisms responsible for the conversion of DM to CM mode signals. Particular emphasis was put on the influence of line terminations, electrical components and topology of the network.

To evaluate the influence of different electrical installations, we installed cabling and fixtures as needed on a wooden structure in the shape of a small house having dimensions comparable to those of a room.

Figure 3-6 presents an overview of the room.

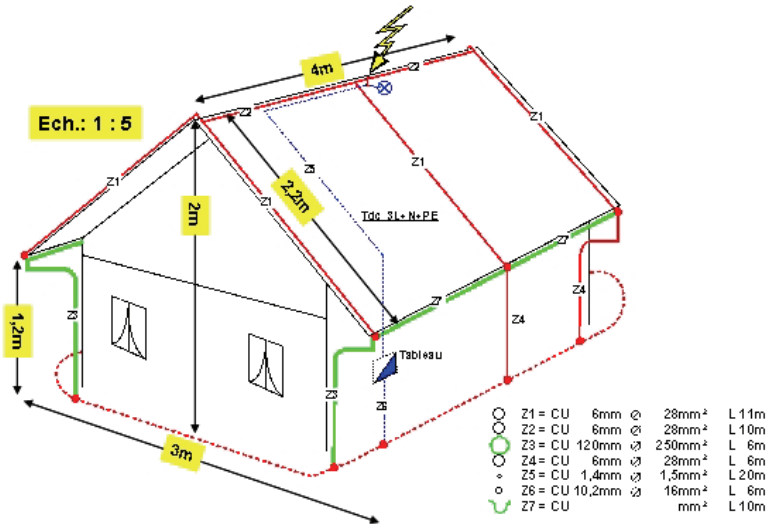

Figure 3-6: Room for the study, dimensions

Note that, although Figure 3-6 shows lightning protection cabling installed in the room, it was removed for the measurements so that only the influence of the electrical system under study would be observed.

Location of the open area test site

The system was installed outdoors, in an open green field near the Power System Laboratory (LRE) at the EPFL, as shown in Figure 3-7.

Figure 3-7 Aerial view of the location of the house-like structure at the EPFL

Ground plane installation

Following the recommendation for an open area test site (OATS) given at the CISPR 16-1, a ground plane was constructed on which the house was installed.

The space between the conductors in the ground plane should be, according to CISPR 16-1, smaller than 1/10 of the minimum wavelength used in the study. In our case, $F_{max} = 40MHz$ and, therefore,

3-20
$$\lambda_{min} = \frac{c}{F_{max}} = \frac{3 \times 10^8}{40 \times 10^6} = 7.5m$$

The ground plane was built using chicken-wire. The dimensions of the ground plane were defined to be able to measure magnetic fields at 3-m using the ground plane as a reference. Using the dimensions of the room (Figure 3-6) and adding 3-m on each side, the ground plane was defined to measure about 10 x 10 m2. Figure 3-8 presents a picture of the ground plane arrangement at the Swiss Federal Institute of Technology (EPFL).

Figure 3-8 Ground plane installation at EPFL

The canonical line

The measurements performed at the EPFL were performed on a “canonical line” model. Figure 3-9 presents a photograph of the canonical line. This line was composed of three conductors disposed together at a height of 1-m off the reference ground plane. The conductors were laid in a way representative of real installations (see Figure 3-9) and they were therefore not perfectly straight and parallel.

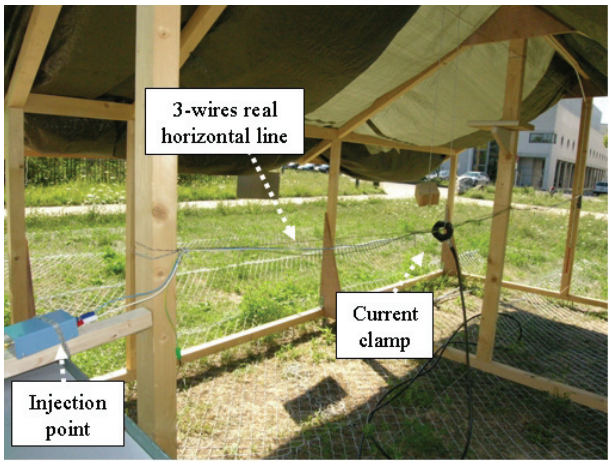

Figure 3-9 Three conductor transmission line at 1-m length

To obtain the characteristic impedance of this canonical line, the procedure described by Tesche et al. [4] was adopted. Although the approach of Tesche et al. [4] is commonly applied at low frequencies, for which the wavelength is much larger than the size of the system being considered (ten times larger is considered to be adequate), based on the measurements, the measured parameters remain applicable over the frequency range of interest..

Injected and received signal

The input signal was first generated by the internal tracking generator of a spectrum analyzer (maximum output level of 0 dBm). Then, the signal was amplified using a power

amplifier and, finally, the amplified signal was injected into the network under test through an impedance stabilizer (3 dB attenuator) (1) for the symmetrical injection, using a Home made Guanella-Balun (1:4) [41], and (2) for the asymmetrical injection, using a Macfarlane filter.

Currents or fields were measured at the receiver channel of the same spectrum analyzer, which guaranteed synchronization of the measurements between the injection and the receiver.

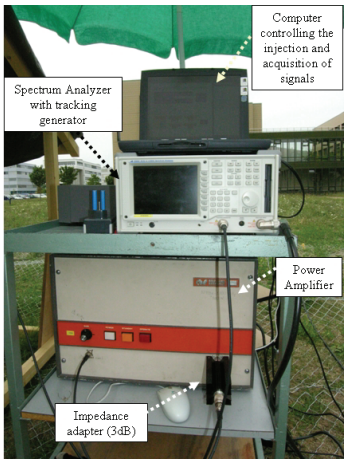

Figure 3-10: Setup for measurements injecting 40 dBm – High power

The CM and DM current measurements were performed using a current clamp. The magnetic field measurements were performed using a magnetic loop antenna. The measurement sensors were connected to the spectrum analyzer using type N connectors.

The measurements started out from a simple line geometry, which was taken as a base case (shown schematically in Figure 3-11). This base case consisted of a straight, 3-wire power line segment of length L located at a height h above the ground plane. A differential-mode voltage V_o was injected between the phase and the neutral conductors. Different line terminations, represented by general impedances $[Z_o]$ and $[Z_L]$, were considered in the study.

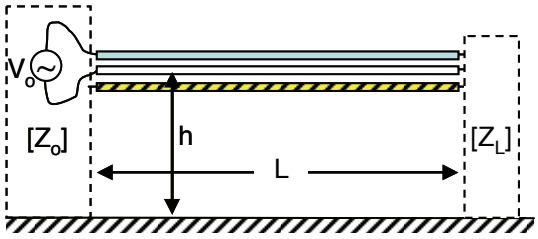

Figure 3-11: Considered base case line configuration

The measurements were performed over a 1 MHz to 32 MHz frequency range using the spectrum analyzer (tracking generator), with a resolution bandwidth of 10 kHz, and a sweep time of 781 ms. On the injection side, the signal generated by the spectrum analyzer was amplified to an amplitude of about 40 dBm and connected to the network under test through a balun.

The CM current, that is defined here as the sum of the currents in the three conductors, was measured using a high frequency (1 MHz-1 GHz) current clamp at different

positions along the line. For practical reasons, the DM current was measured only at the injection point.

3.4.3.1 Influence of terminations

To evaluate the effect of the line terminations on the CM current, different cases were considered by terminating the lines in: an open circuit, a short circuit, $3\times150\Omega$, an electrical outlet, an empty electrical socket, an electrical socket with a light bulb, an open electrical switch and a closed electrical switch (pictures of the fixtures used are shown in Figure 3-12).

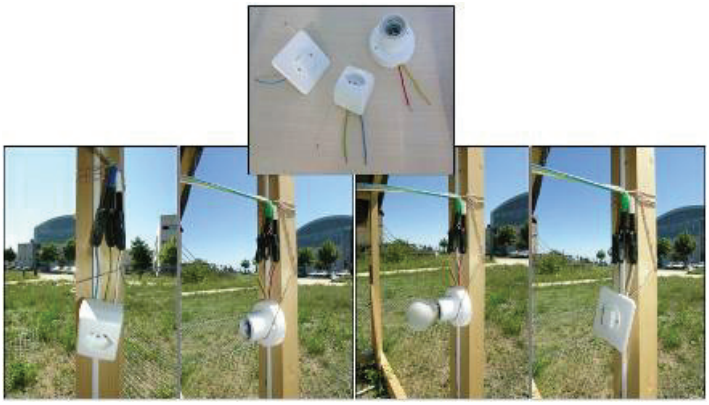

Figure 3-12: Different typical power components at the line termination

Figure 3-13 and Figure 3-14 present examples of the measured CM current as a function of frequency for a 4-m long line located 1 m above the ground plane using, as a parameter, the termination type. It can be seen that the CM current can be a strong function of the frequency, terminal conditions and the position along the line.

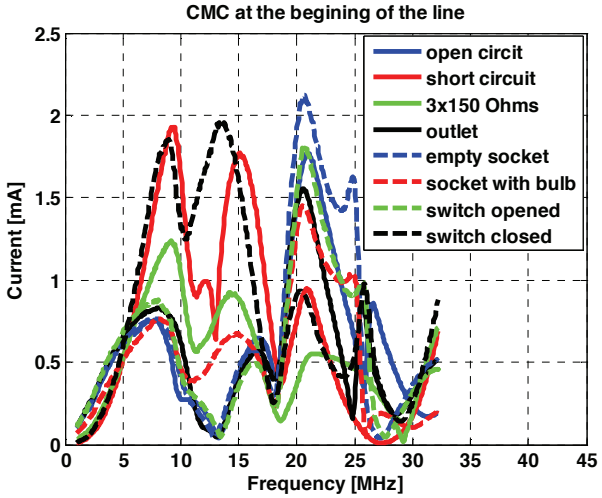

Figure 3-13: Comparison of CMC magnitudes for different termination conditions, measured at the injection point

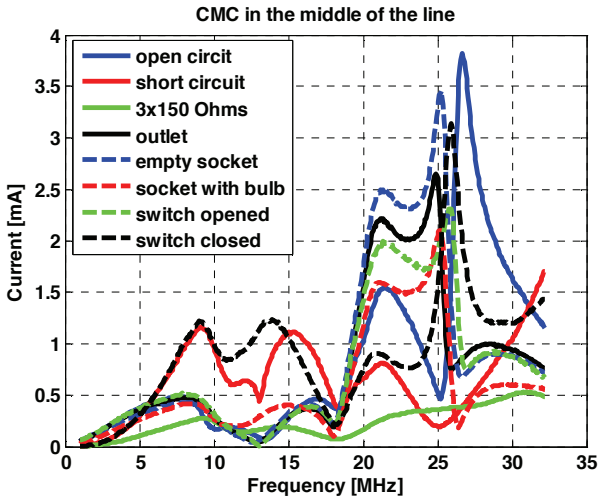

Figure 3-14: Comparison of CMC magnitudes for different termination conditions, measured at the middle of the line

3.4.3.2 Influence of the topology

To evaluate the effect of the topology on the DM to CM current conversion, the 4-m long base case was extended by adding, one at a time, (1) a 2-m long horizontal line forming an angle of $90°$ respect to the original line, and, (2) a 2-m long vertical wire. These two configurations, along with the base case, are illustrated in Figure 3-15.

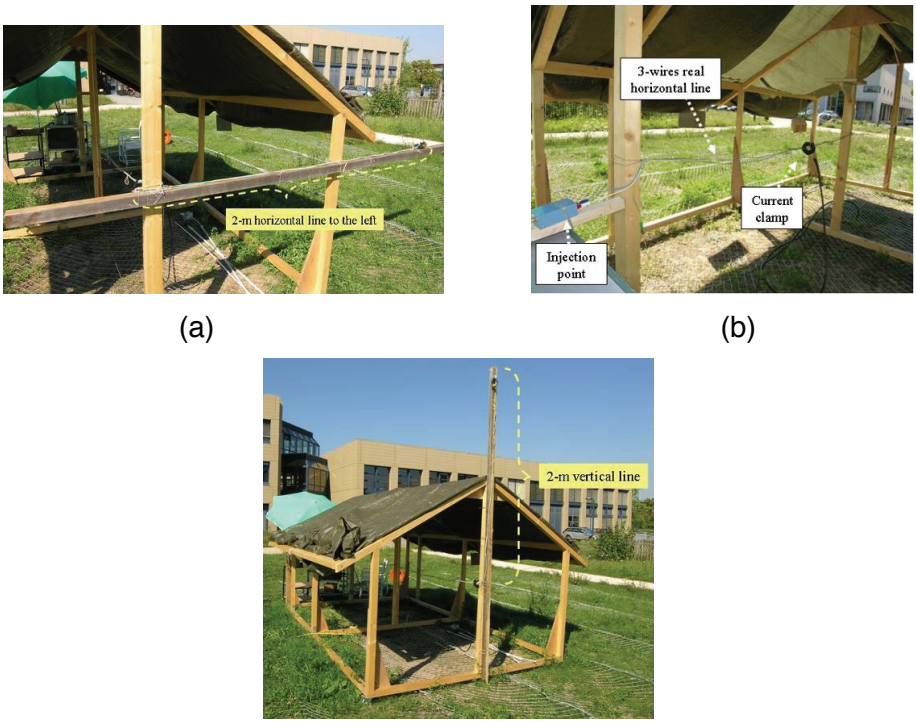

(a) (b)

(c)

Figure 3-15: Different configurations. (a) canonical line, (b) topology 1, (c) topology 2

Figure 3-16 and Figure 3-17 contain plots of the common mode current as a function of the frequency that illustrate the effect of the topology of the network on the CM current at

two positions along the line. The “canonical line” label in Figure 3-16 and Figure 3-17 refers to the base case illustrated in Figure 3-11.

It can be seen from Figure 3-16 and Figure 3-17 that the measured waveforms of the CM current for the two extended topologies of Figure 3-15b and Figure 3-15c are very similar to each other, but very different from the results associated with the base case (Figure 3-15a).

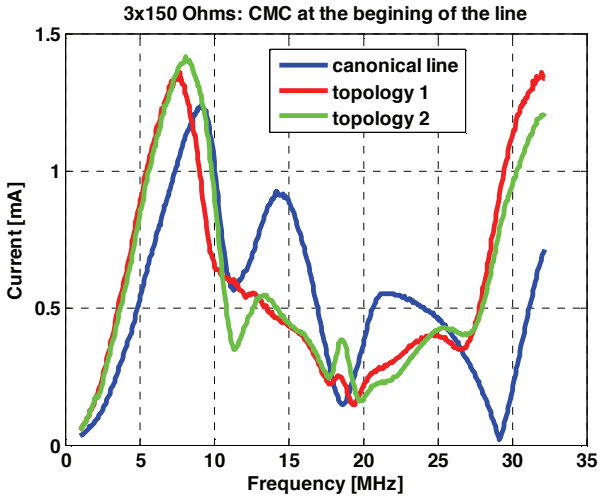

Figure 3-16: Comparison of CMC magnitudes for canonical line, topology 1 and topology 2 terminated by 3x150 Ohms at the beginning of the line

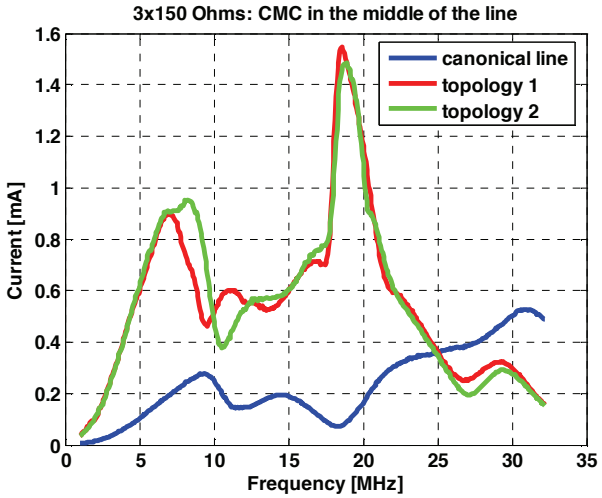

Figure 3-17: Comparison of CMC magnitudes for canonical line, topology 1 and topology 2 terminated by 3x150 Ohms in the middle of the line

Changes in the topology that include a sharp bend, which can be seen as a punctual asymmetry, increase the common mode by up to 20 dB at some frequencies. In some cases, the common mode currents on the line with a simpler topology may be higher than those on the more complex line. These, however, are few.

3.4.3.3 Influence of the height of the conductors

The measurements were performed on the base case considering two different line heights of 1 and 2 m, respectively. Measurement results for the CM current at two different locations along the line (one end and the middle) are presented in Fig. 6.

We can observe that the effect of the line height on the CM currents is small for frequencies below 10 MHz or so. Depending on the frequency, however, an increase in the line height can result in either an increase or a decrease in the CM current magnitudes. The differences between the two cases lie in general within 6 dB or so.

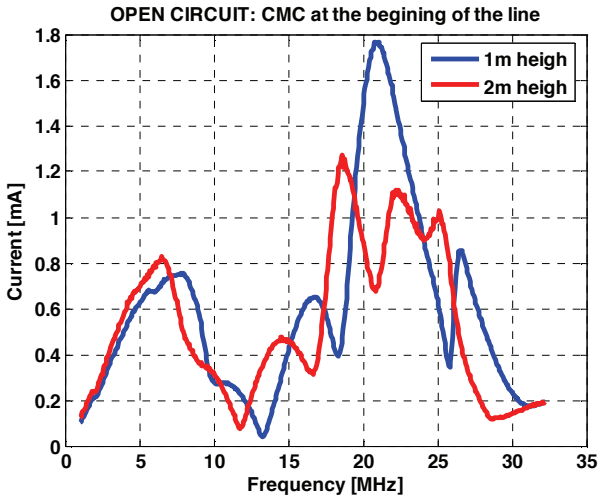

Figure 3-18: Comparison of CMC magnitudes for the base case for two different conductor heights, 1 and 2m, open circuit termination condition measured at the injection point

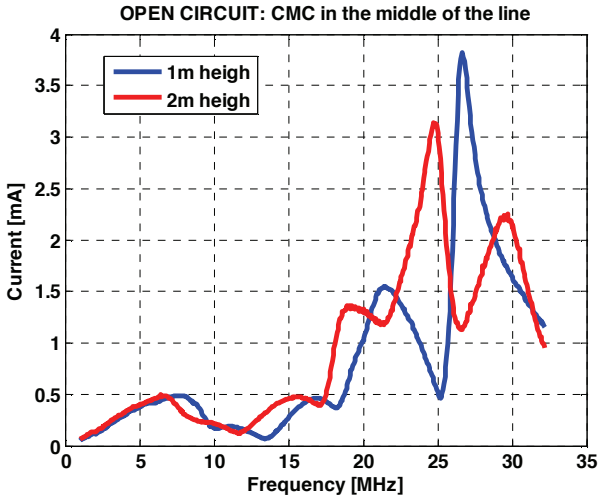

Figure 3-19: Comparison of CMC magnitudes for the base case for two different conductor heights, 1 and 2m, open circuit termination condition measured in the middle of the line

The magnitude of the common mode currents was found to be a strong function of the frequency. The common mode current is relatively small at 1 MHz, independent of the terminations used, as long as these are balanced. This includes open circuit, short circuit

and adapted to the characteristic impedance. The common mode current increases considerably at higher frequencies to a few mA at 30 MHz for a differential input of 40 dBm. In addition, the CM current distribution varies considerably along the line and as a function of the frequency. Interestingly, the highest common mode current is not observed consistently for any of the termination cases studied. For low frequencies, the common mode current was highest when the termination was open-circuited. For medium frequencies, however it was the short circuit-terminated line that produced the most common mode current.

Another interesting result coming from the measurements on the canonical line is that the common mode current tends to be higher at the beginning of the line (where the differential signal is injected) than in the middle and at the end of the line.

The results show that, with the exception of the 150 Ω termination case, the effect of the line height on the CM currents is small for frequencies below some 10 MHz. Depending on the frequency and the terminations, an increase in the line height can result in either an increase or a decrease of the CM current magnitudes. The differences between the two cases lie in general within 6 dB or so.

Changes in the topology that include a sharp bend, which can be seen as a punctual asymmetry, increase the common mode by up to 20 dB at some frequencies. Under certain conditions, the common mode current on the line with a simpler topology may be higher than those on the more complex line. These, however, are few.

Measurements to compare the open circuited-line behaviour to the behaviours of an open switch, and empty light bulb socket and a power outlet show that the behaviours are essentially identical up to about 5 MHz. The differences increase gradually but the common mode currents remain sufficiently close over the whole frequency band to merit consideration of the idea of modelling the used fixtures as simple open circuits.

When the same comparison was carried out for a closed switch, a short-circuit, a socket with a light bulb and a 3x150 Ohm termination, it was observed that the behaviour of the short-circuited case was similar to that of the closed switch whereas the light bulb in a socket behaved sufficiently similar to the 3x150 Ohm case to allow one to be modelled as the other.

3.4.4 Simulations: Model validation

As mentioned in Section 3.1, the evaluation of CM and DM conducted emissions can be performed using different approaches depending on the circuit configuration, its complexity, the frequencies involved and the degree of approximation required with respect to an exact formulation. Here, two approaches were used:

- Transmission line (TL) theory, and
- Method of Moments.

The TL theory yields accurate results as long as the cross-sectional dimensions of the line are electrically small and reasonably uniform, For complex networks such as indoor power networks the use of the TL theory could become questionable. To be able to deal with such cases, the Numerical Electromagnetics Code NEC-2 [3] was also used.

The model use for the application of the TL theory to the canonical line is presented in Figure 3-20.

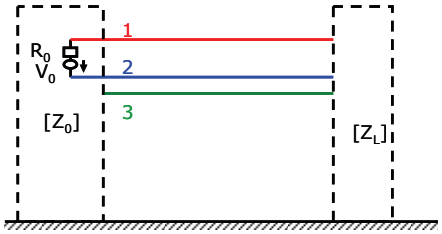

Figure 3-20: TL model of the canonical line

The differential-mode voltage source from Figure 3-20, V_0, should be transformed to the equivalent current source:

3-21
$$[I_s]=\begin{bmatrix} -V_0 Y_{01,2} \\ V_0 Y_{01,2} \\ 0 \end{bmatrix}$$

By writing the boundary conditions for the circuit from Figure 3-20, we obtain:

3-22
$$[V(0)]=[V_s]-[Z_0][I(0)], \text{ and}$$

3-23
$$[V(L)]=[Z_L][I(L)]$$

with

3-24
$$[V_s]=[Z_0][I_s].$$

By writing equations 3-12 and 3-13 at the boundaries, we obtain:

3-25
$$[V(0)]=[E^+(0)][a]+[E^-(0)][b]$$

3-26
$$[V(L)]=[E^+(L)][a]+[E^-(L)][b]$$

3-27
$$[I(0)]=[Z_c]^{-1}\{[E^+(0)][a]-[E^-(0)][b]\}$$

3-28
$$[I(L)]=[Z_c]^{-1}\{[E^+(L)][a]-[E^-(L)][b]\}$$

By putting equations 3-22, 3-23 and 3-24 into equations 3-25, 3-26, 3-27 and 3-28, we can calculate matrices $[a]$ and $[b]$ and $[I]$ and $[V]$.

This model will be used for the TL theory calculations.

Here, only the model based on TL theory is presented. This model was used further in section 3.4.4.2 for comparison with experimental data and results obtained by NEC. In the next section on contribution of different mechanisms to the total common-mode current only the results obtained by full wave approach are presented.

3.4.4.1 Contribution of Different Mechanisms to the Total Common-Mode Current

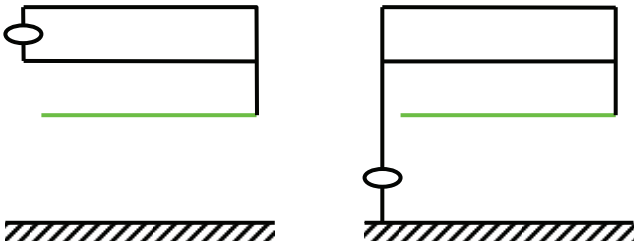

(a) (b)

Figure 3-21: Short circuit configuration: (a) NEC model for conversion along the line, (b) NEC model for simulation of unbalances at the source

Figure 3-21 shows a simple configuration used to study the different mechanisms mentioned in Section 3.4.2 and their influence of the conversion of the differential to the common mode along the line and the injection of the common mode at the source using the Method of Moments.

The input differential signal, set to 40 dBm, was injected between the phase and the neutral conductors. The earth wire was left open at the injection side (Figure 3-21a). In general, couplers used to inject the differential-mode voltage do not exhibit 100% symmetry and, therefore, a fraction of the voltage is applied directly as a CM excitation to the line, as shown schematically in Figure 3-21b.

Results of the common mode as a function of the position down the line due to along-the-line mode conversion (corresponding to Figure 3-21a) and to direct injection (corresponding to Figure 3-21b) are given in Figure 3-22 for a frequency of 30 MHz. The total common mode current is also given in that figure.

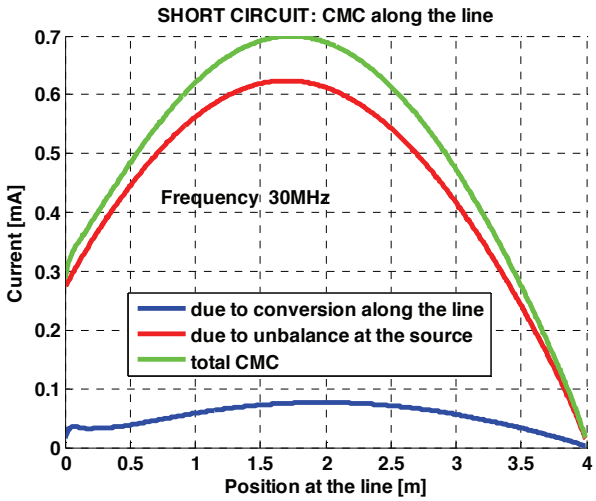

Figure 3-22: Results of simulations of the NEC models from Figure 3-21 for the frequency of 30MHz

The common mode currents separated into its components according to their source are given in Figure 3-22 as a function of the position along the line. The currents were calculated using NEC-2 for a frequency of 30MHz. A value of 40 dB was selected for the balun's asymmetry, meaning that it was assumed that the injected signal was composed

of a differential mode component with an amplitude of 40 dBm and a 40 dB lower common mode current, 0 dBm, due to the asymmetry of the coupler.

It can be seen from Figure 3-22 that, for the considered case, the dominant part of the common-mode current is due to the unbalance at the source. However, one should bear in mind that the above result depends strongly on the considered configuration.

Figure 3-23 illustrates a configuration similar to that in Figure 3-21 but with the earth wire connected to ground at both ends.

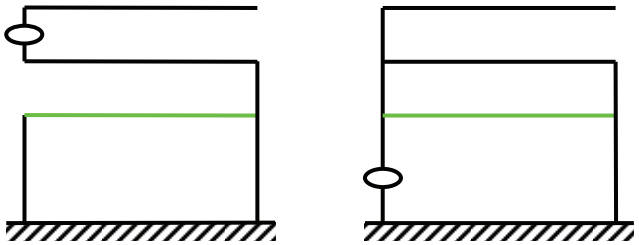

(a) (b)

Figure 3-23: 'Hybrid' configuration: (a) NEC model for conversion along the line, (b) NEC model for simulation of unbalances at the source

Figure 3-24 shows the obtained results corresponding to the configuration shown in Figure 3-23. It can be seen that, in this case, the generated common-mode current is essentially due to conversion along the line and not to the source unbalance.

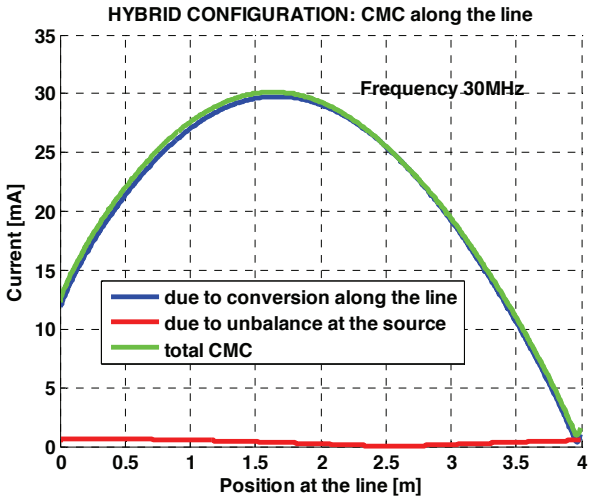

Figure 3-24: Results of simulations of the models from Figure 3-23 for the frequency of 30MHz

3.4.4.2 Comparison of Theoretical Results with Experimental Data

Figure 3-25 presents comparisons between the measured CM current along the line (Figure 3-25a), simulations obtained using the transmission line theory (Figure 3-25b) and NEC (Figure 3-25c). The configuration corresponds to that illustrated in Figure 3-21. It can be seen that the magnitude and shape of the simulated CM currents are in reasonably good agreement with the measurements.

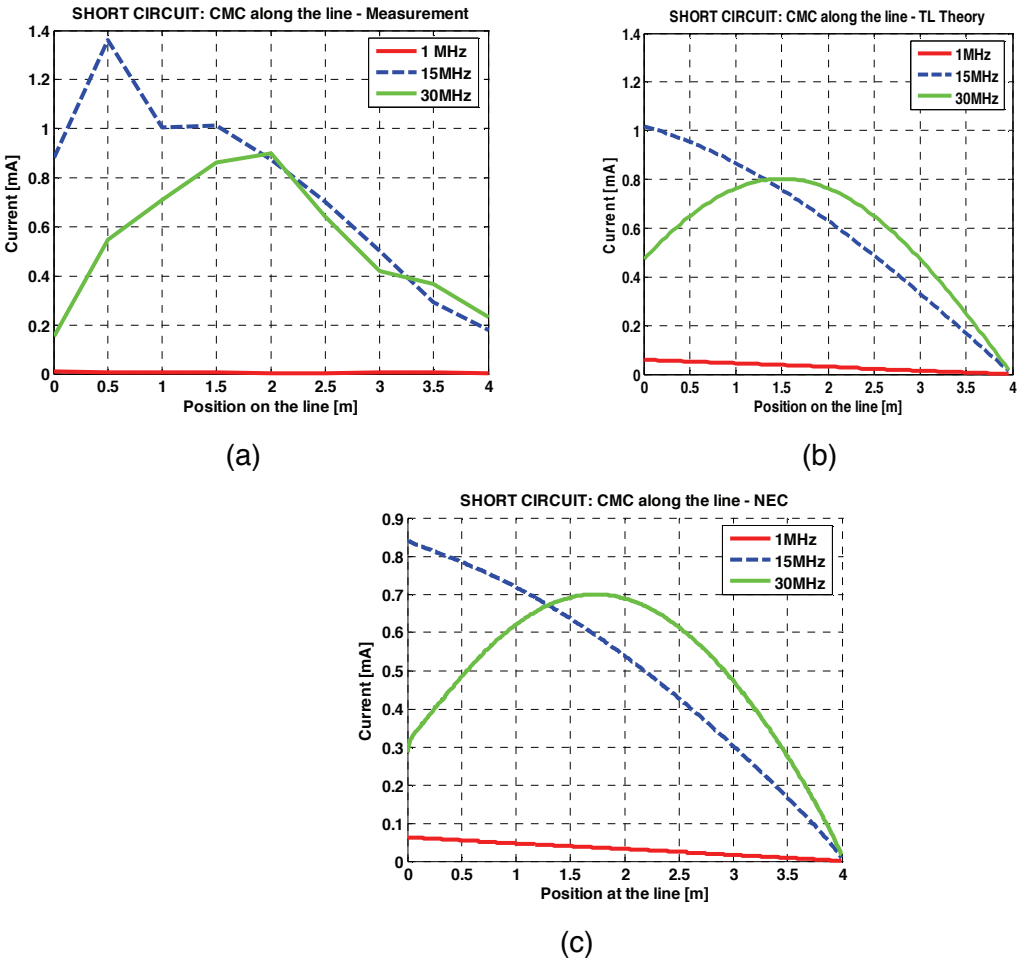

Figure 3-25: Comparison between: (a) measured waveforms and simulations obtained using (b) the transmission line approach and the (c). Method of Moment (NEC) for the short-circuit configuration.

3.4.5 Experimental verification of common-mode current generation in home electrical wiring

This section presents a test of the relation between the common mode current in the cabling inside a home and the common and differential mode signals injected into any other part of the cabling in the house. It will be shown that the results are in satisfactory agreement with the hypothesis that the common mode current at any point inside the house can be calculated by computing the linear combination of the effects of the two input modes.

As mentioned earlier, emissions from PLC transmissions inside the home are due essentially to common mode currents in the intrinsically asymmetrical electrical cabling. The common mode appears to be related to asymmetries in the home wiring, such as unequal distances of conductors to the ground, open switches [44].

We tested a simple formula that assumes that the common mode at any point along the cabling in the home can be calculated by adding the contributions to it due to the differential mode and the common mode injected elsewhere in the house. This simple approach can be extended to calculate the common mode by superposition of all of the

differential and common mode sources around the house, although the required transfer functions, which we obtained experimentally here, would need to be obtainable through theoretical modelling for the technique to become widely applicable in practice.

3.4.5.1 Experimental set-up

We installed cabling and fixtures as needed on a slightly modified wooden structure in the shape of a small house used in section 3.4.3. The difference with respect to the structure shown in Figure 3-6 is just in dimensions that are this time a bit bigger. The structure is shown in Figure 3-26a. The installed circuit, also modified for this purpose, shown in Figure 3-26b, was composed of typical electrical components, such as outlets and light sockets similar to those found in domestic and small office installations.

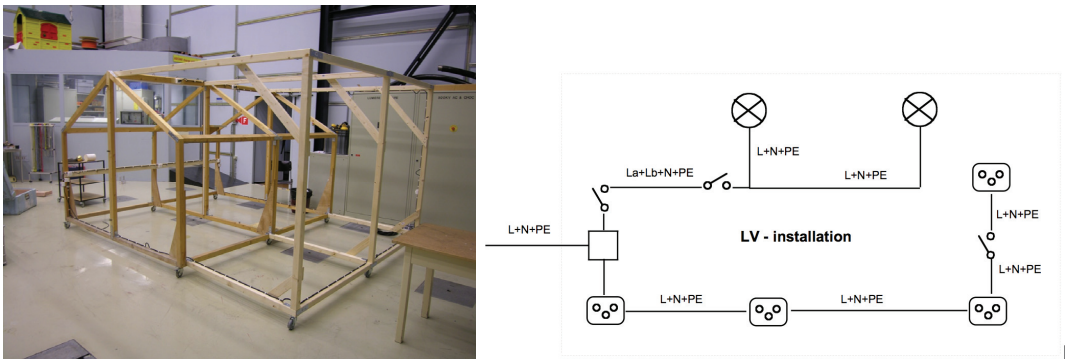

(a) (b)

Figure 3-26: (a) wooden structure and (b) Wiring used in the wooden model

The input signal was produced by a signal generator at frequencies within the PLC band. Three different baluns were used in order to inject symmetrical and asymmetrical signals (Figure 3-27).

The common mode current was measured at a point along the line, using a high frequency current clamp. The differential mode input voltage was directly measured using an oscilloscope channel in high-impedance input mode. The common mode current was also recorded at the input with a current clamp when using asymmetrical injection.

Figure 3-27: Injection and Measurement System

3.4.5.2 Theory

We analyze here the relation between the common mode current I_{CM}^{B} at an arbitrary point B in the low voltage wiring inside a house and the injected differential mode voltage

V_{DM}^{A} and common mode current I_{CM}^{A} at an injection point A in the same house wiring. We postulate that the relation between these three signals is given by

3-29 $$I_{CM}^{B} = k_{CM}^{AB} I_{CM}^{A} + k_{DM}^{AB} V_{DM}^{A}$$

where k_{CM}^{AB} and k_{DM}^{AB} are frequency-dependent, complex transfer functions.

According to this relationship, the common mode at point B stems

- from direct propagation of an injected common mode signal and
- from the conversion of a part of the injected differential mode into the common mode.

To find the complex constants k_{CM}^{AB} and k_{DM}^{AB}, one can set the inputs to zero one at a time. Setting I_{CM}^{A} to zero, we obtain

3-30 $$k_{DM}^{AB} = \frac{I_{CM}^{B}}{V_{DM}^{A}}$$

Similarly, setting V_{DM}^{A} equal to zero, we have

3-31 $$k_{CM}^{AB} = \frac{I_{CM}^{B}}{I_{CM}^{A}}$$

With the values of the two constants evaluated, we can rewrite equation 3-29 in the time domain as

3-32 $$I_{CM}^{B}(t) = \left|k_{CM}^{AB}\right| \left|I_{CM}^{A}\right| sin(\omega t + \Phi_{CM}) + \left|k_{DM}^{AB}\right| \left|V_{DM}^{A}\right| sin(\omega t + \Phi_{DM})$$

where Φ_{DM} and Φ_{CM} are the phase shifts due to each transfer function.

3.4.5.3 Measurement results

To verify equations 3-29 and 3-32, we first estimated the values of the constants k_{CM}^{AB} and k_{DM}^{AB} using different types of baluns that allowed us to apply equations (2) and (3).

Using a symmetrical balun at the input, we forced I_{CM}^{A} to be essentially zero and we measured the output common mode current I_{CM}^{B} and the input differential mode voltage V_{DM}^{A}. The results for a frequency of 20 MHz are plotted in Figure 3-28. By taking the ratio of the peak amplitudes and measuring the phase shift between the two signals, we estimated the value of the k_{DM}^{AB} constant to be

3-33 $$k_{DM}^{AB} = 2.6 \times 10^{-4} e^{-j0.33}$$

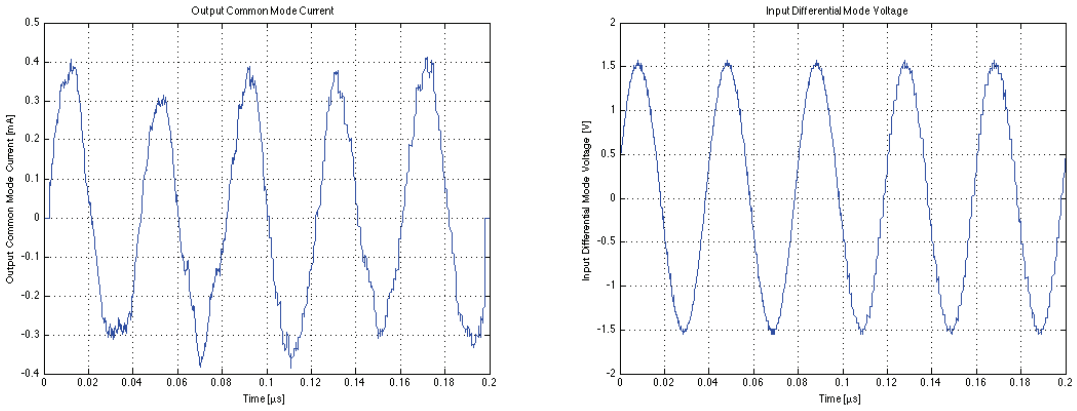

(a) (b)

Figure 3-28: (a) Output CM current for the case of a symmetrical input signal and (b) Input DM voltage that produced the CM current presented in (a)

Similarly, by using an asymmetrical balun, we injected a common mode current with negligible V_{DM}^{A} and we measured the output common mode current I_{CM}^{B} and the input common mode current I_{CM}^{A}. The results are plotted in Figure 3-29a and Figure 3-29b. We then used equation 3-31 to estimate the value of k_{CM}^{AB} to be

3-34 $$k_{DM}^{AB} = 7.5 \times 10^{-1} e^{-j}$$

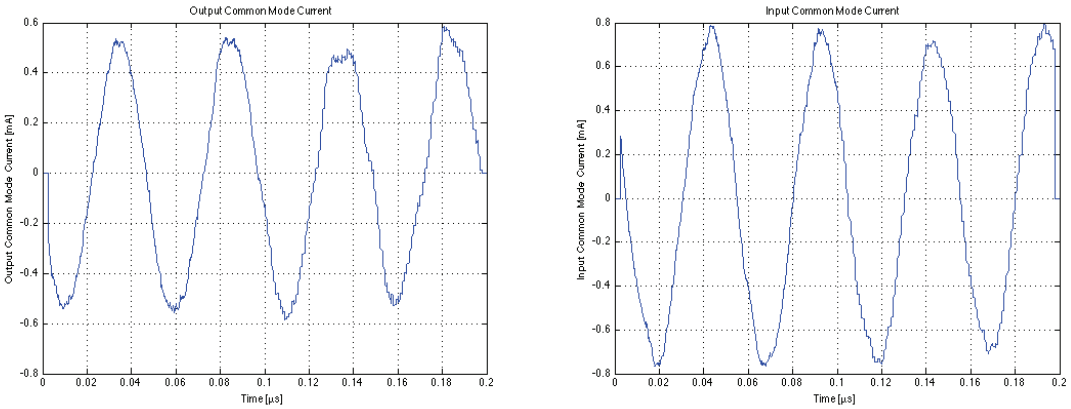

Figure 3-29: (a) Output CM current for an asymmetrical input current and (b) Input CM current that produced the output CM current presented in (a)

With the values of the two constants, we can use equation 3-32 to plot the output common mode current in the time domain and to compare it with the corresponding measured common mode current at point B. The results are plotted in Figure 3-30, from which we can observe a good agreement.

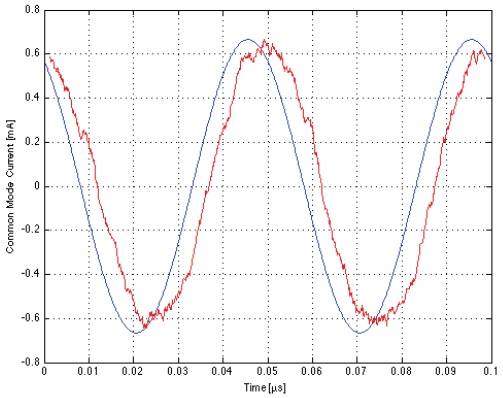

Figure 3-30: Comparison of the measured output CM current and the theoretically estimated CM current

The overall agreement between measured and calculated common mode currents was good but differences of the order of 20% or so were observed in some cases between the estimated and the measured common mode currents. It is important to make further measurements to determine whether this discrepancy was caused by measurement error or if the simple model presented here needs to be improved.

3.5 Conclusions

Transmission line theory requires uniform line structures with electrically-small cross-sectional dimensions. Therefore, it can be considered as an appropriate tool for the analysis of conducted emissions along outdoor PLC networks. As the frequency of the conducted emissions increases to the point where the wavelength becomes comparable to the dimensions of the circuit, or when the line is not uniform along its length, the use of transmission line theory could become questionable. In those cases, a more general approach based on solutions to Maxwell's equations, e.g. Method of Moment, is required.

The use of the TL model and of the method of moments in the work presented in this chapter shows that the fraction of the common mode current injected by asymmetries at the source itself, that is, at the modems' output stages, may be predominant with respect to conversion mechanisms along the lines, although these conversion mechanisms may play a more important role in radiation from PLC networks.

The data signals injected by PLC modems are differential mode signals (DM). The differential mode is a poor radiator since the fields from the current in one of the conductors are nearly cancelled by the opposite-phase radiation from the current in the other conductor. The common mode (CM), which is characterized by currents in each of the conductors being in phase, leads to appreciable radiation.

The common mode can appear due to unbalances at the source (the common mode is injected by the modem's output stages or due to imbalanced capacitances to ground), due to conversion of the wanted, differential mode along the asymmetric electric cabling, and due to the presence of local asymmetries in the cables, such as sharp bends, power outlets, sockets, switches, etc.

A measurement campaign was carried out to characterize the common mode under controlled conditions and to obtain a data set to serve as a basis for the theoretical study

of the generation of common mode in asymmetrical networks. The measurements were made on a special, house-like wooden structure on which electric cabling and electrical fixtures were installed. In addition to a characterization of the common mode on simple structures, the measurements were conducted with the aim of identifying the different parameters that influence the common mode on PLC networks. To be able to isolate the different influence factors, a canonical line consisting of a horizontal 4-m cable was used which, for some of the measurements, was extended to 6 meters. The different parameters tested were the termination of the cables (short, open and matched), the symmetry of the termination, the height of the conductors above the ground, the presence of power outlets, switches, empty and occupied sockets and the topology, including bends.

Two methods were investigated to model the common mode and conducted emissions, the transmission line model and the full wave approach provided by the Method of Moments through the Numerical Electromagnetic Code, NEC.

The transmission line theory requires uniform line structures with electrically small cross-sectional dimensions. Therefore, it can be considered as an appropriate tool for the analysis of conducted emissions along outdoor PLC networks. As the frequency of the conducted emissions increases to the point where the wavelength becomes comparable to the dimensions of the circuit, or when the line is not uniform along its length, the use of transmission line theory becomes less reliable. In those cases, a more general approach based on solutions to Maxwell's equations, e.g. Method of Moment, is required.

The estimation of the common mode current in in-house electrical wiring is important since it is this mode that produces most of the radiated emissions. We have shown that the common mode can be estimated as a linear combination of the effect of a) the injected differential mode, which converts partially to the common mode, and b) the common mode that is applied directly at the injection point and propagates through the wiring with relatively low attenuation.

Although we worked with common and differential modes injected at the same input point, the results should in principle be applicable to the case of multiple common mode sources and multiple differential mode sources spread across the low voltage network. Measurements are required to confirm this hypothesis.

REFERENCES

[1] CISPR/IEC, Information technology Equipment – Radio Disturbance Characteristics – Limits and methods of measurements, Third Edition, 11-97

[2] Specification for Radio Disturbance and Immunity Measuring Apparatus and Methods, Part 1, CISPR 16-1, First Edition, 08-93

[3] G. J. Burke, "Numerical Electromagnetics Code NEC-4 Method of Moments," Lawrence Livermore National Laboratory UCRL-MA-109338, 1992.

[4] F. M. Tesche, M. Ianoz, and T. Karlsson, EMC Ananlysis methods and computational models. New York: Wiley Interscience, 1997.

[5] F. Rachidi, S. V. Tkachenko, “Electromagnetic field interaction with transmission lines“, WIT Press, 2008

[6] C.R. Paul, Analysis of multiconductor transmission lines, John Wiley and Sons, 1994.

[7] S. Frankel, “Quasi-TEM transmission line theory”, Interaction Note 135, November 1972.

[8] K.S.H. Lee, “Two Parallel Terminated Conductors in External Fields”, IEEE Transactions on Electromagnetic compatibility, vol. EMC-20, No 2, May 1978.

[9] C.R. Paul, “A comparison of the contributions of common-mode and differential-mode currents in radiated emissions”, IEEE Trans. On Electromagnetic Compatibility, Volume 31, Issue 2 , May 1989, pp.189 – 193

[10] R. Razafferson, L. Koné, B. Demoulin, A. Zeddam, F. Gauthier, “Effects of the loads and wiring size on PLC electromagnetic pollution”, 2003 IEEE Int. Symp. on Electromagnetic Compatibility, Istanbul, May 2003.

[11] N. Korovkin, E. Marthe, F. Rachidi, E. Selina, "Mitigation of electromagnetic field radiated by PLC systems in indoor environment", International Journal of Communication Systems, Vol. 16, pp. 417-426, May 2003.

[12] U. Reggiani, A. Massarini, L. Sandrolini, M. Ciccotti, D.W.P. Thomas, C. Christopoulos, “Experimental verification of predicted electromagnetic fields radiated by straight interconnect cables carrying high-frequency currents”, 2003 IEEE Power Tech, Bologna, June 23-26, 2003.

[13] S. Tkatchenko, F. Rachidi, M. Ianoz, "Electromagnetic field coupling to a line of finite length: theory and fast iterative solutions in frequency and time domains", IEEE Trans. on Electromagnetic Compatibility, Vol. 37, no 4, pp. 509-518, November 1995.

[14] S. Tkatchenko, F. Rachidi, M. Ianoz, "High-frequency electromagnetic field coupling to long terminated lines ", IEEE Trans. on Electromagnetic Compatibility, Vol. 43, No. 2, May 2001.

[15] F. Delfino, R.Procopio, M. Rossi, P. Girdinio, "Technique for Computing the Response of a Line of Finite Length Excited by High Frequency Electromagnetic Field", IEE Proceedings - Science, Measurements and Technology, Vol. 149, No. 5, September 2002, pp.289-292.

[16] H. Haase, J.Nitsch, T. Steinmetz, “Transmission-Line Super Theory: a New Approach to an Effective Calculation of Electromagnetic Interactions”, Radio Science Bulletin No 307, December 2003, pp. 33-60.

[17] J.Nitsch, S.Tkachenko, “Complex-Valued Transmission-Line Parameters and their Relation to the Radiation Resistance”, IEEE Trans. on Electromagnetic Compatibility, Vol. EMC - 47, No. 3, Aug. 2004, pp.477-48.

[18] A. Maffucci, G. Miano, F. Villone, "An Enhanced Transmission Line Model for Conducting Wires", IEEE Trans. on Electromagnetic Compatibility, Vol. 46, No. 4, November 2004, pp.512-528.

[19] Agrawal A.K., H.J. Price, S.H. Gurbaxani, "Transient response of a multiconductor transmission line excited by a nonuniform electromagnetic field", IEEE Trans. on EMC, Vol. EMC-22, No. 2, pp. 119-129, May 1980.

[20] M.Ianoz, N.V.Korovkin, S.V. Kochetov, E.E.Selina, S.V.Tkachenko, G.V. Vodopianov, “A finite length model using the equivalent circuits for the analysis of electromagnetic radiation”, Proc. Int. Symp. on EMC,1998, Rome, Italy, pp.632-636.

[21] N.V.Korovkin, S.V. Kochetov, E.E.Selina, S.V.Tkachenko, M.Ianoz, “A model for a finite length transmission line considering skin and radiation effects”, Proc. 14th Int. Zurich Symposium on Electromagnetic compatibility, Zurich, Switzerland, Feb. 18-20, 2001, pp. 44H4.

[22] H.Haase and J.Nitsch, “Full-wave transmission line theory (FWTLT) for the analysis of three-dimensional wire-like structures,” in Proc. 14th International Zurich Symposium and Technical Exhibition on Electromagnetic Compatibility, Feb.2001, pp.235-240.

[23] H.Haase, J.Nitsch, “Investigation of nonuniform transmission line structures by a generalized transmission line theory”, in Proc.15th International Zurich Symposium and Technical Exhibition on Electromagnetic Compatibility, Feb. 2003, pp. 597-602.

[24] A. Vukicevic, F. Rachidi, M. Rubinstein, and S. Tkachenko, "An efficient method for the computation of antenna mode currents along transmission lines," presented at 28th General Assembly of International Union of Radio Science (URSI), New Delhi, India, 2005.

[25] Deliverable 53 “Report on disturbance voltage measurement method”, OPERA Project, 2005.

[26] Deliverable 54 “Report on Radiation”, OPERA Project, 2005.

[27] D53 & D54 - Appendix 1 - EPFL MEASUREMENTS, OPERA Project, 2005.

[28] M. Rubinstein, A. Vukicevic, JL. Bermudez, F. Rachidi, P. Favre, M. Schneider, “Some Unresolved Issues Concerning EMC in Powerline Communications”, 18th International Wroclaw Symposium on Electromagnetic Compatibility, Wroclaw, 28-30 June 2006

[29] A .Vukicevic, F. Rachidi, M. Rubinstein, S. Tkachenko, “On the Evaluation of Antenna-Mode Currents along Transmission Lines”, IEEE Transactions on Electromagnetic Compatibility, November 2006, Vol 48, No 4

[30] C.R. Paul, “A comparison of the contributions of common-mode and differential mode currents in radiated emissions”, IEEE Trans. On EMC, Vol. 31, No. 2, pp. 189-193, May

[31] C.R. Paul and D.R. Bush, “radiated emissions from common-mode currents, Proc. IEEE Symposium on EMC, Atlanta, August 1987.

[32] Tudziers C. “Common-mode propagation simulations in telecommunication cables”, Cagliari EMC shop 2000, Cagliary, Italy, May 20-23, 2000.

[33] A. Vukicevic, M. Rubinstein, F. Rachidi, JL. Bermudez, “On the Mechanisms of differential-mode to Common-mode Conversion in the Broadband over Powerline (BPL) Frequency Band”, 17th International Zurich Symposium on Electromagnetic Compatibility, 27 February -3 March 2006, Singapore

[34] R. G. Olsen, "Technical Overview of Broadband Powerline (BPL) Communication Systems," presented at IEEE Symposium on Electromagnetic Compatibility, Chicago, 2005.

[35] "Application of the LCL method to measure the unbalance of PLC equipment connected to the low voltage distribution network," IEC-CISPR, Subcommittee I, Working group 3 February 26, 2003

[36] M. Rubinstein, "Effect of the wire radii tolerances on differential to common mode conversion in balanced twisted pairs," presented at 13th Zurich International Symposium on Electromagnetic Compatibility, Zurich, Switzerland, 1999.

[37] A. Vukicevic, M. Rubinstein, F. Rachidi, JL. Bermudez, M. Schneider, P. Favre, P. Zweiacker, “Review of the Electromagnetic Compatibility PLC Work at the Swiss Federal Institute of Technology (Lausanne) and the University of Applied Sciences of Western Switzerland (Yverdon)”, 10th International Symposium on Power-Line Communications and Its Applications, 26-29 March 2007. Orlando, USA

[38] P. Favre, C. Candolfi, P. Kraehenbuehl, M. Schneider, M. Rubinstein, A. Vukicevic, “Common-mode Current and Radiation Mechanisms in PLC Networks”, 11th International Symposium on Power-Line Communications and Its Applications ,26-28 March 2007. Pisa, Italy

[39] IEC 61000-4-6 standard Electromagnetic Compatibility (EMC) - Part 4-6:Testing and measurement techniques – Conducted disturbances induced by radio-frequency fields – Immunity test

[40] Werner Bäschlin, Evolution of CISPR 22

[41] Schneider, M.: Internal report. University of Applied Sciences of Western Switzerland, 2004.

[42] A. Rubinstein, Thesis No 2957, Simulation of Electrically large structures in EMC studies: Application to automotive EMC, EPFL, 2004

[43] M. Ianoz, M. Koch “Standardization and regulatory approaches related to radiated emission limits for powerline communications”,18th International Wroclaw Symposium and Exibition on Electromagnetic Compatibility, Wroclaw, Pland, 28-30 June 2006

[44] K. Dostert, Powerline communications, Prentice Hall, 2001

[45] K. Dostert, “EMC Aspects of High Speed Powerline Communications”,15th International Wroclaw Symposium on Electromagnetic Compatibility, Wroclaw, 27-30 June 2006

[46] A. Rubinstein, A. Vukicevic, M. Rubinstein, F. Rachidi, “ Experimental Verification of Common-Mode Current Generation in Home Electrical Wiring in the Poweline

Communications Band, 29th General Assembly of International Union of Radio Science (URSI), Chicago, USA, 2008.

Chapter 4

4 Conducted Immunity Testing of PLC Modems

Immunity refers to the ability of a piece of equipment to operate in the presence of a given level of electromagnetic disturbance without unacceptable degradation of its performance. The disturbance can come in the form of an electromagnetic field that couples to the victim equipment either directly or through the cables that are attached to the equipment's ports.

In practice, the required level of immunity of a given piece of equipment working within a system is a function 1) of the efficiency with which exogenous electromagnetic energy couples to the system and 2) of the efficiency with which the coupled energy is carried to the piece of equipment. PLC modems are, per design, attached to network cabling. Electrical cabling can constitute an efficient antenna to ambient electromagnetic fields produced either by other systems or by natural causes. An understanding of the coupling of electromagnetic fields to lines is therefore important.

As discussed in Chapter 2, the coupling-decoupling network (CDN) is used to test conducted immunity compliance. In the same chapter some problems related to PLC immunity testing according to the existing standards [2] were examined. In the next sections, we will discuss the effect of the CDN's imperfect symmetry on the immunity test results.

4.1 CM to DM conversion mechanisms

Under current standard testing procedures, the CDN's imperfect symmetry might lead to incorrect immunity test results due to the generation of unwanted differential mode signals.

Due to the poor symmetry of electrical cabling in low voltage networks, a common mode interfering signal appearing at the mains and data ports of a PLC modem will be associated with a differential mode signal stemming from common to differential mode conversion. Realistic immunity testing should, therefore, include a differential mode component. One way to achieve this is to adjust the symmetry of the CDN in the current test specification. Determining the symmetry of the CDN that will best reproduce the conditions of a modem connected to a PLC network requires a good understanding of the conversion between common and differential modes.

The mechanisms leading to the conversion of the common mode into the differential mode are similar to the inverse problem already treated in the previous chapter for the study of emissions. It is possible to adapt those results to the present case by assuming that reciprocity applies in the CM-DM conversion.

Consider Figure 4-1 and Figure 4-2, in which we have represented the mode conversion as a two-port network.

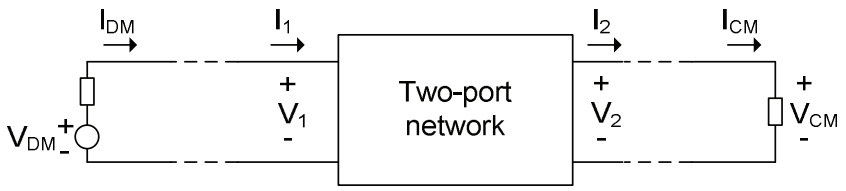

Figure 4-1: Two-port model used for the study of the differential-to-common mode conversion

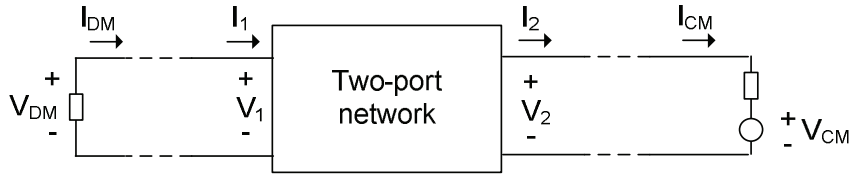

Figure 4-2: Two-port model used for the study of the common-to-differential mode conversion.

Using the chain parameters of the two-port network, we can write [4]

4-1
$$\begin{bmatrix} V_1 \\ I_1 \end{bmatrix} = \begin{bmatrix} A & B \\ C & D \end{bmatrix} \begin{bmatrix} V_2 \\ I_2 \end{bmatrix}$$

For reciprocal networks, the chain parameters satisfy the condition $AD - BC = 1$.

We can solve for the voltage and the current at port 2 using the inverse of the chain matrix as follows:

4-2
$$\begin{bmatrix} V_2 \\ I_2 \end{bmatrix} = \begin{bmatrix} D & -B \\ -C & A \end{bmatrix} \begin{bmatrix} V_1 \\ I_1 \end{bmatrix}$$

We will now use Figure 4-1, Figure 4-2 and equations 4-1 and 4-2 to derive expressions for the transfer functions between the differential and the common modes. From equation 4-1, which corresponds to Figure 4-2, we can write the following two equations:

4-3
$$V_1 = AV_2 + BI_2$$

4-4
$$I_1 = CV_2 + DI_2$$

Now, from Figure 4-2, we can write

4-5
$$V_1 = V_{DM}$$

4-6
$$V_2 = V_{CM} + I_{CM} Z_L$$

4-7
$$I_1 = -\frac{V_{DM}}{Z_s}$$

4-8
$$I_2 = I_{CM}$$

Substituting equations 4-5 through 4-8 into equations 4-3 and 4-4, we get

4-9
$$V_{DM} = AV_{CM} + AI_{CM} Z_L + BI_{CM}$$

4-10
$$-\frac{V_{DM}}{Z_s} = CV_{CM} + CI_{CM} Z_L + DI_{CM}$$

Now, solving for I_{CM} in equation 4-9, we obtain

4-11 $$I_{CM} = \frac{V_{DM} - AV_{CM}}{AZ_L + B}$$

Substituting equation 4-11 into equation 4-10, we get

4-12 $$-\frac{V_{DM}}{Z_s} = CV_{CM} + (CZ_L + D)\frac{V_{DM} - AV_{CM}}{AZ_L + B}$$

Rearranging terms, we obtain

4-13 $$-V_{DM}\left(\frac{1}{Z_s} + \frac{CZ_L + D}{AZ_L + B}\right) = V_{CM}\left(C - \frac{A(CZ_L + D)}{AZ_L + B}\right)$$

Multiplying equation 4-13 by $Z_S \cdot (AZ_L + B)$ yields

4-14 $$V_{DM}(AZ_L + B + Z_sCZ_L + Z_sD) = V_{CM}Z_S$$

where we have used the fact that $AD - BC = 1$.

Solving for V_{DM}, we get

4-15 $$V_{DM} = V_{CM}\frac{Z_S}{AZ_L + B + Z_sCZ_L + Z_sD}$$

Equation 4-15 represents the relation between the differential mode voltage and the common mode voltage when the common mode is injected. It can be used to calculate the differential to common mode conversion factor if the chain parameters are known.

We will now follow a similar derivation for Figure 4-1.

The two linear equations represented by the matrix 4-2 are,

4-16 $$V_2 = DV_1 - BI_1$$

4-17 $$I_2 = -CV_1 + AI_1$$

As in the derivation above, the relation between V_{DM} and V_{CM} are needed.

From Figure 4-1, we can write

4-18 $$V_2 = V_{CM}$$

4-19 $$V_1 = V_{DM} - I_{DM}Z_S$$

4-20 $$I_1 = I_{DM}$$

4-21 $$I_2 = \frac{V_{CM}}{Z_L}$$

Substituting equations 4-8 through 4-21 into equations 4-16 and 4-17:

4-22 $$V_{CM} = DV_{DM} - DI_{DM}Z_S - BI_{DM}$$

4-23 $$\frac{V_{CM}}{Z_L} = -CV_{DM} + CI_{DM}Z_S + AI_{DM}$$

Now, solving for I_{DM} in 4-22, one has

4-24 $$I_{DM} = \frac{DV_{DM} - V_{CM}}{DZ_S + B}$$

Substituting 4-24 into 4-23, one gets

4-25 $$\frac{V_{CM}}{Z_L} = -CV_{DM} + (CZ_S + A)\frac{DV_{DM} - V_{CM}}{DZ_S + B}$$

Rearranging terms:

4-26 $$V_{CM}\left(\frac{1}{Z_L} + \frac{CZ_S + A}{DZ_S + B}\right) = V_{DM}\left(-C + \frac{D(CZ_S + A)}{DZ_S + B}\right)$$

Multiplying 4-26 by $Z_L(DZ_S + B)$ yields

4-27 $$V_{CM}(DZ_S + B + Z_L CZ_S + Z_L A) = V_{DM} Z_L$$

Finally, solving for V_{CM} :

4-28 $$V_{CM} = V_{DM}\frac{Z_L}{Z_L A + B + Z_L CZ_S + DZ_S}$$

As already mentioned, if the $ABCD$ parameters are known, equation 4-15 can be used to calculate the amount of differential mode voltage due to the injection of a common mode voltage. Equation 4-28 can be used o calculate the common mode voltage when a given differential mode voltage is injected.

The common to differential mode conversion factor K_1 can be defined from equation 4-15 as follows

4-29 $$K_1 = \frac{V_{DM}}{V_{CM}} = \frac{Z_S}{AZ_L + B + Z_s CZ_L + DZ_s}$$

Similarly, the differential to common mode conversion factor K_2 is defined from equation 4-28 as

4-30 $$K_2 = \frac{V_{CM}}{V_{DM}} = \frac{Z_L}{AZ_L + B + Z_s CZ_L + DZ_s}$$

Notice that the only difference between the two factors is the impedance in the numerator. If the impedance of the source and the load are equal, the factors are numerically identical. This is an expected result due to reciprocity in the applied passive linear model.

4.1.1 Reciprocity

The result of dividing the equation 4-30 by equation 4-29 is:

4-31 $$\frac{K_2}{K_1} = \frac{Z_L}{Z_S} = \frac{Z_{CM}}{Z_{DM}}$$

where the fact that $Z_L = Z_{CM}$ and $Z_S = Z_{DM}$ has been used. This implies that the common-to-differential mode conversion factor and the differential-to-common mode conversion factor are related by the ratio of two impedances. These results were tested in [34].

The results presented in this and the previous sections allow the calculation of the conversion ratio of the differential to the common mode and the common to differential mode ratios.

4.2 Immunity tests and the symmetry of the coupling-decoupling network

4.2.1 LCL

It is assumed that a CDN is designed with a given symmetry that corresponds to that of typical PLC networks. The parameter that is usually employed for this characterization is the Longitudinal Conversion Loss (LCL).

The overall objective of the following derivation is to calculate the actual differential mode voltage presented to a modem when a common mode signal is injected by a CDN whose LCL (measured using the Macfarlane filter) is that of a PLC network.

The LCL measurement setup can be represented in a simplified fashion as shown in Figure 4-3, where the unlabeled square represents the equipment under test which, in the present case, is the CDN. Note that, for simplicity, the two ports are drawn on different sides of the EUT.

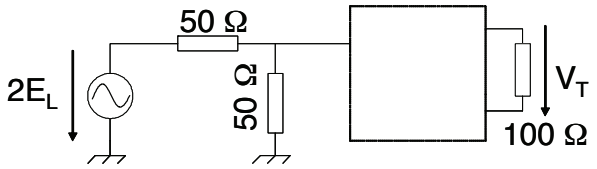

Figure 4-3: Equivalent simplified diagram for the LCL measurement

Using straightforward circuit transformations, one can redraw the input circuit as shown in Figure 4-4.

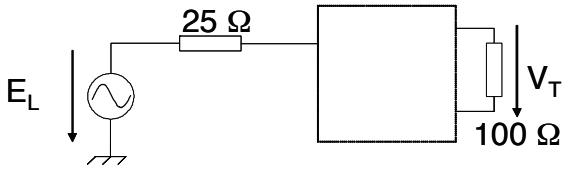

Figure 4-4: Equivalent simplified diagram for the LCL measurement with simplified common mode input circuit

If knowledge of the common mode impedance Z_{IN} presented by the CDN at its input and of the differential mode impedance Z_{OUT} presented by the CDN at its output is assumed, the model in Figure 4-4 can be redrawn as shown in Figure 4-5.

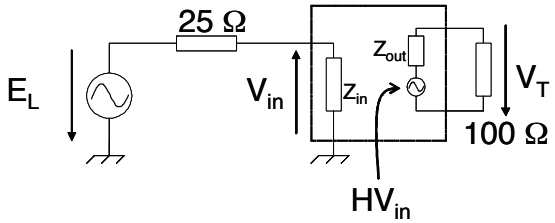

Figure 4-5: Equivalent circuit for the LCL measurement with input common mode and output differential mode impedance

H represents the ratio of the amplitude of the equivalent output source and the input voltage V_{IN}. The voltage V_{IN} can be written in terms of E_L as:

4-32
$$V_{IN} = E_L \frac{Z_{IN}}{25 + Z_{IN}}$$

On the other hand, V_T can be expressed in terms of HV_{IN} as:

4-33
$$V_T = HV_{IN} \frac{100}{100 + Z_{OUT}}$$

Now, substituting 4-32 into 4-33, V_T can be easily found to be

4-34
$$V_T = E_L \frac{HZ_{in}}{25 + Z_{in}} \frac{100}{100 + Z_{out}}$$

Since LCL in linear units is given by $LCL_{linear} = \frac{E_L}{V_T}$, solving for H in equation 4-34 yields

4-35
$$H = \frac{(25 + Z_{in})(100 + Z_{out})}{100 Z_{in} LCL_{linear}}$$

Now, as discussed, the magnitude of the CDN's common mode impedance is specified by the IEC 61000-4-6 [2] standard and is given in Table 2-5, which we rewrite here for convenience as Table 4-1. On the other hand, the differential mode impedance of the CDN must be is as close as possible to that of the cable used in the systems to minimize interference effects.

Table 4-1: Common mode impedance of the CDN

	Frequency band	
	0,15 MHz – 26 MHz	26 MHz – 80 MHz
Impedance	150 Ω ± 20 Ω	150 Ω + 60 Ω - 45 Ω

With these impedance values, the value of H can be estimated as a function of the linear value of LCL by introducing them into equation 4-35 by taking into account $Z_{OUT} = 200\Omega$ as follows:

1. For frequencies between 0.15 MHz and 26 MHz, the value of H for the minimum common mode impedance (130 Ohm) is

4-36 $$H = \frac{3.6}{LCL_{linear}}$$

and the corresponding value for the maximum impedance (170 Ohm) is

4-37 $$H = \frac{3.4}{LCL_{linear}}$$

2. For frequencies above 26 MHz, the value of H for the minimum impedance (105 Ohm) is given by

4-38 $$H = \frac{3.7}{LCL_{linear}}$$

and the corresponding value for the maximum impedance (210 Ohm) is

4-39 $$H = \frac{3.4}{LCL_{linear}}$$

With these results, we now investigate the differential mode signal V_D that is injected by the CDN when it is used to test the immunity of a PLC modem. To that end, we will refer to Figure 4-6, where the model for the CDN is connected to a PLC network under test and where we have added the source U_0 that injects the common mode test signal.

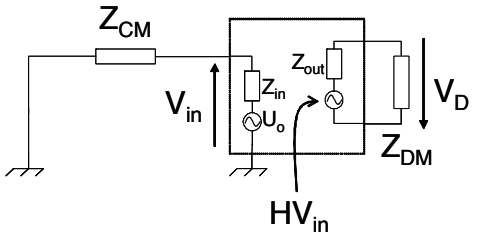

Figure 4-6: The equivalent circuit of the CDN connected to an NUT that corresponds to a PLC network

From Figure 4-6, we can calculate V_{IN} as

4-40 $$V_{in} = U_o \frac{Z_{CM}}{Z_{CM} + Z_{in}}$$

On the other hand, V_D is given by

4-41 $$V_D = HV_{in} \frac{Z_{DM}}{Z_{DM} + Z_{out}}$$

Substituting equation 4-40 into equation 4-41, we obtain the result sought,

4-42 $$V_D = HU_o \frac{Z_{CM}}{Z_{CM} + Z_{in}} \frac{Z_{DM}}{Z_{DM} + Z_{out}}$$

The case for which V_D is the highest, which is the worst case, is of interest. The value of H given in equation 4-36 is used for frequencies from 0.15 MHz to 26 MHz and that

given in equation 4-38 will be used for frequencies above 26 MHz. Making those substitutions we obtain:

4-43
$$V_D = U_o \frac{3.6}{LCL_{linear}} \frac{Z_{CM}}{Z_{CM} + Z_{in}} \frac{Z_{DM}}{Z_{DM} + Z_{out}}$$

4-44
$$V_D = U_o \frac{3.7}{LCL_{linear}} \frac{Z_{CM}}{Z_{CM} + Z_{in}} \frac{Z_{DM}}{Z_{DM} + Z_{out}}$$

In equations 4-43 and 4-44, U_0 is the perturbation signal whose level is given in the IEC 61000-4-6 conducted immunity standard, Z_{IN} is the input impedance of the CDN, also given in the IEC 61000-4-6 standard, Z_{OUT} is the differential impedance presented to the PLC network, which should be, according to the standard, similar enough not to disturb the normal performance of the system, Z_{CM} is the common mode impedance of the PLC network and Z_{DM} is the differential impedance of the PLC network.

The following Table 4-2 summarizes the values of the parameters.

Table 4-2: Summary of the parameters

U_0	1V, 3V, 10V for levels 1 to 3, respectively
Z_{IN}	130Ω -170Ω(0.15MHz to 26 MHz) 105Ω-210Ω(26MHz to 80 MHz)
Z_{OUT}	200Ω
Z_{CM}	150Ω
Z_{DM}	200Ω(from our measurements)
LCL	36±3dB (proposed by CENELEC)
LCL_{lineal}	2000 (worst case, corresponding to 33 dB)

Since equations 4-43 and 4-44 are essentially identical, only equation 4-44 will be used (since it gives a slightly higher differential voltage).

The worst-case value of V_D for frequencies from 0.15 MHz to 26 MHz is, therefore:

For level 1

4-45
$$V_D = \frac{3.7}{2000} \frac{150}{150 + 130} \frac{200}{200 + 200} = 0.5[mV]$$

For level 2

4-46
$$V_D = 3\frac{3.7}{2000} \frac{150}{150 + 130} \frac{200}{200 + 200} = 1.5[mV]$$

For level 3

4-47 $$V_D = 10\frac{3.7}{2000}\frac{150}{150+130}\frac{200}{200+200} = 5[mV]$$

The worst-case value of V_D for frequencies above 26 MHz is:

For level 1

4-48 $$V_D = \frac{3.7}{2000}\frac{150}{150+105}\frac{200}{200+200} = 0.54[mV]$$

For level 2

4-49 $$V_D = 3\frac{3.7}{2000}\frac{150}{150+105}\frac{200}{200+200} = 1.6[mV]$$

For level 3

4-50 $$V_D = 10\frac{3.7}{2000}\frac{150}{150+105}\frac{200}{200+200} = 5.4[mV]$$

4.3 Impact of the symmetry of coupling-decoupling networks on the conducted immunity testing of PLC modems

To understand the effect of the differential signals given in Section 4.2 for the testing of PLC modems, one needs to understand first the effect of different types of disturbances on current PLC systems.

Disturbance Caused by non-PLC Communication Systems

As already mentioned in Chapter 2, Section 2.4.3.3.1, a number of communications systems within the PLC frequency band are already in use at home, in offices and in industrial environments.

A potential disturber is a system that

1. operates in the same frequency band as PLC or has a strong enough harmonic content within the PLC band (strong out-of-band signals could also affect input amplifiers)
2. could be installed in close enough proximity to the PLC network
3. is the source of strong enough emissions to adversely affect PLC performance.

Narrow-band Interferers

Narrow-band interferers have already been discussed in chapter 2, section 2.4.3.2.2. Based on that discussion, we will consider now their influence on immunity measurement results.

For OPERA PLC systems using OFDM, the disturbing signal will lead to the lowering of the transmitted bit rate by forcing a reduction of the number of bits loaded onto one or more affected subcarriers. The capacity of the i^{th} subcarrier in the absence of narrowband interference, this time in bits per channel utilization, can be estimated as

4-51 $$C_{sc}^{i} = \frac{1}{2}log_2(1+\frac{PSD(f_i)|H(f_i)|^2}{IN_r(f_i)})$$

where C_{sc}^{i} is the capacity of the i[th] subcarrier which gives the number of bits that can be loaded onto that carrier, $PSD(f)$ is the transmitted power spectral density, $H(f)$ is the transfer function from the transmitter to the receiver, w_{sc} is the bandwidth of a subcarrier, $N_r(f)$ is the spectral density of the noise floor and Γ is a factor that takes into account any margin and implementation losses due to coding, impulsive noise, etc.

Due to the narrowband noise, the capacity of a subcarrier will be reduced by

4-52 $$\Delta C_{sc}^{i} = \frac{1}{2}\left(log_2(1 + \frac{PSD(f_i)|H(f_i)|^2}{\Gamma N_r(f_i)}) - log_2(1 + \frac{w_{sc}PSD(f_i)|H(f_i)|^2}{\Gamma(w_{sc}N_r(f_i) + P_{nbi})}) \right)$$

where P_{nbi} represents the power in the i[th] narrowband interferer. Equation 4-52 can be rewritten as

4-53 $$\Delta C_{sc}^{i} = \frac{1}{2} log_2 \left(\frac{(1 + \frac{PSD(f_i)|H(f_i)|^2}{\Gamma N_r(f_i)})}{(1 + \frac{w_{sc}PSD(f_i)|H(f_i)|^2}{\Gamma(w_{sc}N_r(f_i) + P_{nbi})})} \right)$$

In the case of multiple narrowband interferers, the capacity will be reduced by

4-54 $$\Delta C = \frac{1}{2}\sum_{i=1}^{m} log_2 \left(\frac{1 + \frac{PSD(f_i)|H(f_i)|^2}{\Gamma N_r(f_i)}}{1 + \frac{w_{sc}PSD(f_i)|H(f_i)|^2}{\Gamma(w_{sc}N_r(f_i) + P_{nbi})}} \right)$$

The values of the different parameters in equations 4-53 and 4-54 depend on the technology utilized, the immunity measurement conditions and the power that can be transmitted by a modem. The PSD as a function of frequency, for instance, depends on the transmission mask approved in standards. The transfer function H depends on the quality of the cabling and on the distance between the transmitting and the receiving devices. The bandwidth of the subcarriers and the margin factor Γ depend both on the details of the physical and MAC layers specified for the technology and on the conditions of the channel.

If the signal to noise ratio is comfortably high, the additive term “1” in equations 4-53 and 4-54 can be considered negligible and those two equations can be rewritten in a simplified form:

4-55 $$\Delta C_{sc}^{i} = \frac{1}{2} log_2 \left(1 + \frac{P_{nbi}}{w_{sc}N_r(f_i)} \right)$$

and

4-56 $$\Delta C = \frac{1}{2}\sum_{i=1}^{m} log_2 \left(1 + \frac{P_{nbi}}{w_{sc}N_r(f_i)} \right)$$

We can use the voltages in equations 4-45 through 4-50 to estimate the interfering power P_{nbi} and then plug these values into equation 4-55 to estimate the capacity loss in a channel.

The power associated with V_D injected by the CDN for frequencies from 0.15 MHz to 26 MHz is, from equations 4-45 to 4-47:

For level 1

4-57 $$P_{nbi} = \frac{(0.5[mV])^2}{200\Omega} = 1.25[\mu W]$$

For level 2

4-58 $$P_{nbi} = \frac{(1.5[mV])^2}{200\Omega} = 11.3[\mu W]$$

For level 3

4-59 $$P_{nbi} = \frac{(5[mV])^2}{200\Omega} = 125[\mu W]$$

The power associated with V_D injected by the CDN for frequencies above 26 MHz is, from equations 4-60 to 4-62:

For level 1

4-60 $$P_{nbi} = \frac{(0.54[mV])^2}{200\Omega} = 1.46[\mu W]$$

For level 2

4-61 $$P_{nbi} = \frac{(1.6[mV])^2}{200\Omega} = 12.8[\mu W]$$

For level 3

4-62 $$P_{nbi} = \frac{(5.4[mV])^2}{200\Omega} = 146[\mu W]$$

Plugging these values into equation 4-55 and assuming a channel $w_{sc} = 4kHz$ and a noise floor of $N_r(f_i) = -125\,dBm/Hz$ on 200Ω, we can get estimates of the loss in capacity per channel utilization from the differential voltage injected by the CDN during standard immunity testing:

For frequencies from 0.15 MHz to 26 MHz the loss of capacity for the different injection levels is,

For level 1

4-63 $$\Delta C_{nbi} = 0.5[bit / channel\ utilization]$$

For level 2

4-64 $$\Delta C_{nbi} = 1.7\left[bit / channel\ utilization\right]$$

For level 3

4-65 $$\Delta C_{nbi} = 3.3\left[bit / channel\ utilization\right]$$

The power associated with V_D injected by the CDN for frequencies above 26 MHz is, from equation 4-45 to equation 4-47:

For level 1

4-66 $$\Delta C_{nbi} = 0.6\left[bit / channel\ utilization\right]$$

For level 2

4-67 $$\Delta C_{nbi} = 1.7\left[bit / channel\ utilization\right]$$

For level 3

4-68 $$\Delta C_{nbi} = 3.4\left[bit / channel\ utilization\right]$$

Since the immunity test is performed injecting a common mode, 2-kHz bandwidth, narrowband signal whose central frequency is changed periodically over the test band, the capacity of the channel will be reduced for one or two subcarriers at a time. The bit error rate induced by the presence of the disturbing differential mode current from the CDN can be estimated by dividing the product $2w_{sc}\Delta C_{nbi}$ by the total physical channel capacity which, for current modems, is of the order of 200 Mbps.

4-69 $$Bit\ Error\ Rate = \frac{2w_{sc}\Delta C_{nbi}}{200Mbps}$$

For the values of ΔC_{nbi} given in equations 4-63 through 4-68 the bit error rate is of the order of 10^{-5} to $5x10^{-5}$. Since these rates can be handled by error correcting coding and MAC ARQ techniques, the modems are not likely to suffer any appreciable performance degradation due to immunity testing if the CDN exhibits a symmetry similar to that of PLC networks.

Another mechanism that could affect the performance of the modem during immunity testing is the overload of the input stages, even if the signal is narrowband. It is however unlikely that this effect manifests itself given the low power of the interfering differential mode signals.

Broadband Interferers

The influence of the broadband interferers was discussed in chapter 2.

4.4 Conclusions

We showed that the conversion of the differential mode to the common mode is coupled with the reverse conversion by reciprocity. The common-to-differential mode conversion ratio is related to the differential-to-common mode conversion ratio by a multiplicative factor equal to the ratio of the impedances of the common mode source and he differential mode source. This result implies that the measurement of one of the ratios is sufficient to characterize both ratios.

Due to the low symmetry of PLC cabling, part of the injected common mode test signal is converted into a differential mode signal that interferes with the wanted signal at the input of the modem being tested. Depending on the actual symmetry of the CDN, the immunity test may yield erroneous results due to the effect of this differential mode component.

Working under the assumption that the CDN is built to exhibit a symmetry similar to that of PLC networks as inferred from its longitudinal conversion loss, we estimated the differential mode disturbance level that the modems should withstand from a narrowband interferer.

Since the immunity test is performed injecting a common mode, 2-kHz bandwidth, narrowband signal whose central frequency is changed periodically over the test band, the capacity of the channel will be reduced for one or two subcarriers at a time. The bit error rate induced by the presence of the disturbing differential mode current from the CDN was estimated, for a total physical channel transmission rate of 200 Mbps, to be of the order of $1x10^{-5}$ to $5x10^{-5}$. Since these rates can be handled by error correcting coding and MAC ARQ procedures, the modems are not likely to suffer any severe performance degradation due to immunity testing if the CDN exhibits a symmetry similar to that of PLC networks.

We also discussed another mechanism that could affect the performance of the modem during immunity testing, namely the overload of the input stages by a narrowband interferer. We showed that it is unlikely that the low-level differential mode signals from the CDN's finite longitudinal conversion loss will overload the modems.

REFERENCES

[1] CISPR/IEC, Information technology Equipment – Radio Disturbance Characteristics – Limits and methods of measurements, Third Edition, 11-97

[2] Specification for Radio Disturbance and Immunity Measuring Apparatus and Methods, Part 1, CISPR 16-1, First Edition, 08-93

[3] G. J. Burke, "Numerical Electromagnetics Code NEC-4 Method of Moments," Lawrence Livermore National Laboratory UCRL-MA-109338, 1992.

[4] F. M. Tesche, M. Ianoz, and T. Karlsson, EMC Ananlysis methods and computational models. New York: Wiley Interscience, 1997.

[5] F. Rachidi, S. V. Tkachenko, “Electromagnetic field interaction with transmission lines“, WIT Press, 2008

[6] C.R. Paul, Analysis of multiconductor transmission lines, John Wiley and Sons, 1994.

[7] S. Frankel, “Quasi-TEM transmission line theory”, Interaction Note 135, November 1972.

[8] K.S.H. Lee, “Two Parallel Terminated Conductors in External Fields”, IEEE Transactions on Electromagnetic compatibility, vol. EMC-20, No 2, May 1978.

[9] C.R. Paul, “A comparison of the contributions of common-mode and differential-mode currents in radiated emissions”, IEEE Trans. On Electromagnetic Compatibility, Volume 31, Issue 2 , May 1989, pp.189 – 193

[10] S. Tkatchenko, F. Rachidi, M. Ianoz, "Electromagnetic field coupling to a line of finite length: theory and fast iterative solutions in frequency and time domains", IEEE Trans. on Electromagnetic Compatibility, Vol. 37, no 4, pp. 509-518, November 1995.

[11] S. Tkatchenko, F. Rachidi, M. Ianoz, "High-frequency electromagnetic field coupling to long terminated lines ", IEEE Trans. on Electromagnetic Compatibility, Vol. 43, No. 2, May 2001.

[12] F. Delfino, R.Procopio, M. Rossi, P. Girdinio, "Technique for Computing the Response of a Line of Finite Length Excited by High Frequency Electromagnetic Field", IEE Proceedings - Science, Measurements and Technology, Vol. 149, No. 5, September 2002, pp.289-292.

[13] H. Haase, J.Nitsch, T. Steinmetz, “Transmission-Line Super Theory: a New Approach to an Effective Calculation of Electromagnetic Interactions”, Radio Science Bulletin No 307, December 2003, pp. 33-60.

[14] J.Nitsch, S.Tkachenko, “Complex-Valued Transmission-Line Parameters and their Relation to the Radiation Resistance”, IEEE Trans. on Electromagnetic Compatibility, Vol. EMC - 47, No. 3, Aug. 2004, pp.477-48.

[15] A. Maffucci, G. Miano, F. Villone, "An Enhanced Transmission Line Model for Conducting Wires", IEEE Trans. on Electromagnetic Compatibility, Vol. 46, No. 4, November 2004, pp.512-528.

[16] Agrawal A.K., H.J. Price, S.H. Gurbaxani, "Transient response of a multiconductor transmission line excited by a nonuniform electromagnetic field", IEEE Trans. on EMC, Vol. EMC-22, No. 2, pp. 119-129, May 1980.

[17] M.Ianoz, N.V.Korovkin, S.V. Kochetov, E.E.Selina, S.V.Tkachenko, G.V. Vodopianov, “A finite length model using the equivalent circuits for the analysis of electromagnetic radiation”, Proc. Int. Symp. on EMC,1998, Rome, Italy, pp.632-636.

[18] N.V.Korovkin, S.V. Kochetov, E.E.Selina, S.V.Tkachenko, M.Ianoz, “A model for a finite length transmission line considering skin and radiation effects”, Proc. 14th Int. Zurich Symposium on Electromagnetic compatibility, Zurich, Switzerland, Feb. 18-20, 2001, pp. 44H4.

[19] H.Haase and J.Nitsch, “Full-wave transmission line theory (FWTLT) for the analysis of three-dimensional wire-like structures,” in Proc. 14th International Zurich Symposium and Technical Exhibition on Electromagnetic Compatibility, Feb.2001, pp.235-240.

[20] H.Haase, J.Nitsch, “Investigation of nonuniform transmission line structures by a generalized transmission line theory”, in Proc.15th International Zurich Symposium and Technical Exhibition on Electromagnetic Compatibility, Feb. 2003, pp. 597-602.

[21] A. Vukicevic, F. Rachidi, M. Rubinstein, and S. Tkachenko, "An efficient method for the computation of antenna mode currents along transmission lines," presented at 28th General Assembly of International Union of Radio Science (URSI), New Delhi, India, 2005.

[22] Deliverable 53 “Report on disturbance voltage measurement method”, IST Integrated Project No 507667. Funded by EC , 2005.

[23] Deliverable 54 “Report on Radiation”, IST Integrated Project No 507667. Funded by EC, 2005.

[24] D53 & D54 - Appendix 1 - EPFL MEASUREMENTS, IST Integrated Project No 507667. Funded by EC, 2005.

[25] M. Rubinstein, A. Vukicevic, JL. Bermudez, F. Rachidi, P. Favre, M. Schneider, “Some Unresolved Issues Concerning EMC in Powerline Communications”, 18th International Wroclaw Symposium on Electromagnetic Compatibility, Wroclaw, 28-30 June 2006

[26] A .Vukicevic, F. Rachidi, M. Rubinstein, S. Tkachenko, “On the Evaluation of Antenna-Mode Currents along Transmission Lines”, IEEE Transactions on Electromagnetic Compatibility, November 2006, Vol 48, No 4

[27] C.R. Paul, “A comparison of the contributions of common-mode and differential mode currents in radiated emissions”, IEEE Trans. On EMC, Vol. 31, No. 2, pp. 189-193, May

[28] C.R. Paul and D.R. Bush, “radiated emissions from common-mode currents, Proc. IEEE Symposium on EMC, Atlanta, August 1987.

[29] Tudziers C. “Common-mode propagation simulations in telecommunication cables”, Cagliari EMC shop 2000, Cagliary, Italy, May 20-23, 2000.

[30] A. Vukicevic, M. Rubinstein, F. Rachidi, JL. Bermudez, “On the Mechanisms of differential-mode to Common-mode Conversion in the Broadband over Powerline (BPL) Frequency Band”, 17th International Zurich Symposium on Electromagnetic Compatibility, 27 February -3 March 2006, Singapore

[31] R. G. Olsen, "Technical Overview of Broadband Powerline (BPL) Communication Systems," presented at IEEE Symposium on Electromagnetic Compatibility, Chicago, 2005.

[32] M. Rubinstein, "Effect of the wire radii tolerances on differential to common mode conversion in balanced wtisted pairs," presented at 13th Zurich International Symposium on Electromagnetic Compatibility, Zurich, Switzerland, 1999.

[33] A. Vukicevic, M. Rubinstein, F. Rachidi, JL. Bermudez, M. Schneider, P. Favre, P. Zweiacker, “Review of the Electromagnetic Compatibility PLC Work at the Swiss Federal Institute of Technology (Lausanne) and the University of Applied Sciences of Western Switzerland (Yverdon)”, 10th International Symposium on Power-Line Communications and Its Applications, 26-29 March 2007. Orlando, USA

[34] Deliverable 55 “Report on Immunity”, IST Integrated Project No 507667. Funded by EC, 2005.

[35] M. Rubinstein, A. Vukicevic, F. Rachidi, JL. Bermudez, “Impact of the Symmetry of Coupling – Decoupling Networks on the conducted Immunity Testing of PLC modems”, 18th International Zurich Symposium on Electromagnetic Compatibility, 24-28 September 2007, Munich, Germany

[36] P. Favre, C. Candolfi, P. Kraehenbuehl, M. Schneider, M. Rubinstein, A. Vukicevic, “Common-mode Current and Radiation Mechanisms in PLC Networks”, 11th International Symposium on Power-Line Communications and Its Applications ,26-28 March 2007. Pisa, Italy

[37] IEC 61000-4-6 standard Electromagnetic Compatibility (EMC) - Part 4-6:Testing and measurement techniques – Conducted disturbances induced by radio-frequency fields – Immunity test

[38] Werner Bäschlin, Evolution of CISPR 22

[39] Schneider, M.: Internal report. University of Applied Sciences of Western Switzerland, 2004.

[40] A. Rubinstein, Thesis No 2957, Simulation of Electrically large structures in EMC studies: Application to automotive EMC, EPFL, 2004

[41] M. Ianoz, M. Koch “Standardization and regulatory approaches related to radiated emission limits for powerline communications”,18th International Wroclaw Symposium and Exibition on Electromagnetic Compatibility, Wroclaw, Pland, 28-30 June 2006

[42] K. Dostert, Powerline communications, Prentice Hall, 2001

Chapter 5

5 Evaluation of antenna-mode currents

As mentioned previously, the Transmission Line (TL) theory is a useful tool for the analysis of surge propagation along transmission lines (e.g. [2]-[4]). The basic assumptions of the TL theory have been mentioned earlier and repeated here for the sake of clarity:

1. the cross-sectional dimensions of the line are electrically small, so that propagation occurs only along the line axis;
2. the response of the line is quasi-transverse electromagnetic (quasi-TEM), and
3. the sum of the line currents at any cross section of the line is zero; For multiconductor lines above a reference ground, the reference conductor is the return path for the currents in the n overhead conductors.

If the sum of all currents crossing a plane perpendicular to the direction of the line can be assumed to be zero, one can consider the 'transmission line mode' currents only and neglect the so-called 'antenna-mode' currents [2]-[5]. For a line consisting of a conductor above ground, the quasi-symmetry due to the presence of the ground plane results in a very small contribution of antenna-mode currents and, consequently, the predominant mode on the line will be the transmission line mode [2].

For a two- (or multi-) conductor line, however, even for electrically small line cross sections, the presence of antenna-mode currents implies that the sum of the currents in a cross section is not necessarily equal to zero [2], [3]. If we wish to compute only the load responses of the line, consideration of only the TL model current is adequate, since the antenna-mode current response is small near the ends of the line. On the other hand, if we want to evaluate the current along the line, the presence of antenna-mode currents needs to be taken into account, even for electrically small line cross sections. It has been shown in [2]-[6] that the amplitude of these antenna-mode currents may even be much larger than that of transmission line mode currents. Therefore, to compute the fields radiated by power line communication signals from indoor low-voltage power lines or radiated emissions from printed circuit boards, one must take into account the contribution of the antenna-mode currents as these are often the predominant source of radiation [6] -[9].

To evaluate the antenna-mode currents, one has to apply general scattering theory. Lee in [5] derived Telegrapher's equations for lines consisting of two parallel wires of unequal cross-sectional areas. In his development, Lee included the antenna-mode current which is the solution of the scattering problem involving two conductors excited by two symmetric incident waves [5]. This scattering problem can be approximated by that of one conductor with an equivalent radius, as in the case of a folded dipole antenna [5].

Some recent studies have proposed methods to include high frequency effects into the classical transmission line theory (e.g. [10]-[15]).

In this chapter, An integral equation describing the antenna-mode currents along a two-wire transmission line along the z-axis will be derived [21]**Error! Reference source not found.**. When the line cross-sectional dimensions are electrically small, the integral equation reduces to a pair of transmission-line-like equations with equivalent line parameters (inductance and capacitance per unit length). The derived equations make it

possible to compute the antenna mode currents using a traditional transmission-line code with appropriate parameters.

5.1 Derivation of the integral equation

Consider a two-wire line of length L in free space, as shown in Figure 5-1.

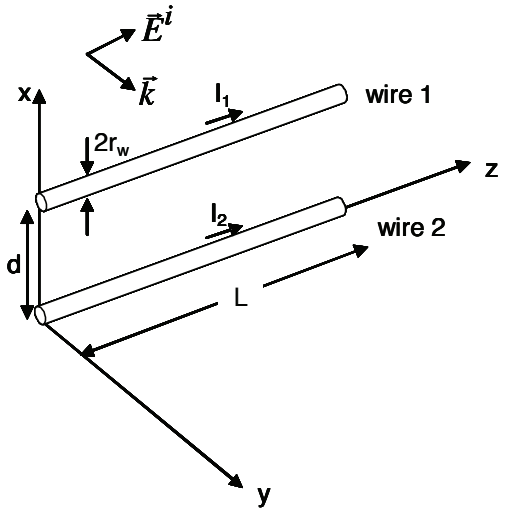

Figure 5-1: Geometry of the problem.

The two conductors are separated by a distance *d*. The line is illuminated by an external electromagnetic field. The currents along the two conductors $I_1(z)$ and $I_2(z)$ can be decomposed as follows:

5-1 $$I_1(z) = I_a(z) + I_{tl}(z)$$

5-2 $$I_2(z) = I_a(z) - I_{tl}(z)$$

where $I_a(z)$ and $I_{tl}(z)$ represent the antenna-mode and transmission-line-mode currents, respectively.

Since the wires are assumed to be perfectly conducting, on the wire's surface, the total tangential electric field should be equal to zero. In the case of the thin wire approximation, this condition can be expressed as:

5-3 $$\vec{e}_z \cdot \vec{E} = \vec{e}_z \cdot \left(\vec{E}^i + \vec{E}^s \right) = 0 \qquad \text{on the surface of the wires}$$

In 5-3, $\vec{E}^i$ is the incident electric field in the absence of the two wires and $\vec{E}^s$ is the scattered electric field which represents the reaction of the wires to the incident field.

The scattered electric field, produced by the line charge and current densities ρ and $\vec{J}$, can be expressed in terms of retarded scalar and vector potentials[1]:

5-4 $$\vec{E}^s = -j\omega\vec{A} - \nabla\Phi$$

With

[1] All quantities are time-harmonic.

5-5 $$\vec{A}\left(\vec{r}\right)=\vec{A}_1\left(\vec{r}\right)+\vec{A}_2\left(\vec{r}\right)=\frac{\mu}{4\pi}\int_0^L I_1(\vec{r}'_1)\vec{e}_z g_1(\vec{r},\vec{r}'_1)dz'+\frac{\mu}{4\pi}\int_0^L I_2(\vec{r}'_2)\vec{e}_z g_2(\vec{r},\vec{r}'_2)dz'$$

and

5-6 $$\Phi\left(\vec{r}\right)=\Phi_1\left(\vec{r}\right)+\Phi_2\left(\vec{r}\right)=\frac{1}{4\pi\varepsilon}\int_0^L \rho_1(\vec{r}'_1)g_1(\vec{r},\vec{r}'_1)dz'+\frac{1}{4\pi\varepsilon}\int_0^L \rho_2(\vec{r}'_2)g_2(\vec{r},\vec{r}'_2)dz'$$

where

- $\omega = 2\pi f$, where f is the frequency of the excitation,
- z' is the length variable along the wire axis,
- $\vec{r} = x\vec{e}_x + y\vec{e}_y + z\vec{e}_z$ is the position vector of the field point, measured from the origin to the observation point,
- $\vec{r}_{1,2}$ is the position vector of the source point from the origin to the position of the source (in the thin wire approximation we assume that currents are concentrated in the wire axis for the first as well as for the second wire), and
- $I_1(z), I_2(z), \rho_1(z)$ and $\rho_2(z)$ are currents and charge densities along the two wires.
- $g_{1,2}(\vec{r},\vec{r}')$ are Green's functions given by:

5-7 $$g_1(\vec{r},\vec{r}'_1)=\frac{e^{-jk|\vec{r}-\vec{r}'_1|}}{|\vec{r}-\vec{r}'_1|}$$

5-8 $$g_2(\vec{r},\vec{r}'_2)=\frac{e^{-jk|\vec{r}-\vec{r}'_2|}}{|\vec{r}-\vec{r}'_2|}$$

where

5-9 $$k=\frac{\omega}{c}$$

is the wave number in free space.

When the observation point is on the surface of wire 1, the expressions for the Green's functions become:

5-10 $$g_1(z,z')=\frac{e^{-jk\sqrt{(z-z')^2+r_w^2}}}{\sqrt{(z-z')^2+r_w^2}}$$

5-11 $$g_2(z,z')=\frac{e^{-jk\sqrt{(z-z')^2+d^2}}}{\sqrt{(z-z')^2+d^2}}$$

The vector potentials for a point on the surface of wire 1 become:

5-12 $$\vec{A}_1(d,0,z)=\frac{\mu}{4\pi}\int_0^L I_1(z')\vec{e}_z g_1(z,z')dz'$$

5-13 $$\vec{A}_2(d,0,z) = \frac{\mu}{4\pi}\int_0^L I_2(z')\vec{e}_z\, g_2(z,z')dz'$$

The current and the charge density along the wire are related by the continuity equation:

5-14 $$\rho_{1,2} = -\frac{1}{j\omega}\nabla\cdot\vec{J}_{1,2} = -\frac{1}{j\omega}\frac{dI_{1,2}}{dz}$$

Introducing equation 5-14 into the equations for the scalar potentials (the first and second integrals on the right hand side in equation 5-6), and still considering an observation point on the surface of wire 1, we obtain:

5-15 $$\Phi_1(d,z,0) = -\frac{1}{4\pi\varepsilon\, j\omega}\int_0^L \frac{dI_1(z')}{dz'} g_1(z,z')dz'$$

5-16 $$\Phi_2(d,0,z) - \frac{1}{4\pi\varepsilon\ j\omega}\int_0^L \frac{dI_2(z')}{dz'} g_2(z,z')dz'$$

Integrating equations 5-15 and 5-16 by parts, we obtain:

5-17 $$\Phi_1(d,0,z) = -\frac{1}{4\pi\varepsilon\, j\omega}\left[I_1(L)g_1(z,L) - I_1(0)g_1(z,0) - \int_0^L I_1(z')\frac{\partial g_1(z,z')}{\partial z'}dz'\right]$$

5-18 $$\Phi_2(d,0,z) = -\frac{1}{4\pi\varepsilon\, j\omega}\left[I_2(L)g_2(z,L) - I_2(0)g_2(z,0) - \int_0^L I_2(z')\frac{\partial g_2(z,z')}{\partial z'}dz'\right]$$

Since the line is open-circuited at both ends, we have:

5-19 $$I_{1,2}(0) = I_{1,2}(L) = 0$$

Due to the symmetry property of the Green's functions, we can derive from equations 5-10 and 5-11.

5-20 $$\frac{\partial}{\partial z} g_{1,2}(z,z') = -\frac{\partial}{\partial z} g_{1,2}(z,z')$$

Using equations 5-19 and 5-20, the expressions for the retarded scalar potential 5-17 and 5-18 become:

5-21 $$\Phi_1(d,0,z) = -\frac{1}{4\pi\varepsilon\ j\omega}\frac{d}{dz}\int_0^L I_1(z')g_1(z,z')dz'$$

5-22 $$\Phi_2(d,0,z) = -\frac{1}{4\pi\varepsilon\, j\omega}\frac{d}{dz}\int_0^L I_2(z')g_2(z,z')dz'$$

Now, following similar mathematical developments as in equations 5-15 - 5-22, we obtain the following expressions for the scalar and vector potentials for an observation point located on the surface of wire 2:

5-23 $$\Phi_1(0,0,z) = -\frac{1}{4\pi\varepsilon\, j\omega}\frac{d}{dz}\int_0^L I_1(z')\,g_2(z,z')\,dz'$$

5-24 $$\Phi_2(0,0,z) = -\frac{1}{4\pi\varepsilon\, j\omega}\frac{d}{dz}\int_0^L I_2(z')\,g_1(z,z')\,dz'$$

5-25 $$\vec{A}_1(0,0,z) = \frac{\mu}{4\pi}\int_0^L I_1(z')\,\vec{e}_z\,g_2(z,z')\,dz'$$

5-26 $$\vec{A}_2(0,0,z) = \frac{\mu}{4\pi}\int_0^L I_2(z')\,\vec{e}_z\,g_1(z,z')\,dz'$$

Introducing equation 5-4 into equation 5-3, we obtain:

5-27 $$\vec{e}_z \cdot \vec{E} = \vec{e}_z \cdot (\vec{E}^i + \vec{E}^s) = \vec{e}_z \cdot (\vec{E}^i - j\omega\vec{A} - \nabla\Phi) = 0$$

which is equivalent to:

5-28 $$E_z^i(x,y,z) - j\omega A_z(x,y,z) - \frac{d\Phi(x,y,z)}{dz} = 0$$

For an observation point on the surface of wire 1, the above expression becomes:

5-29 $$E_z^i(d,0,z) - j\omega A_z(d,0,z) - \frac{d\Phi(d,0,z)}{dz} = 0$$

And, similarly, for an observation point on wire 2, we have:

5-30 $$E_z^i(0,0,z) - j\omega A_z(0,0,z) - \frac{d\Phi(0,0,z)}{dz} = 0$$

Introducing the expressions for the scalar potentials (equations 5-21 through 5-24) and those for the vector potentials (equations 5-12, 5-13, 5-25 and 5-26) into equations 5-29 and 5-30 yields the desired integral.

5.2 Particularisation for the Transmission-Line Mode current

Taking the difference between 5-29 and 5-30 yields:

5-31 $$E_z^i(d,0,z) - E_z^i(0,0,z) - j\omega(A_z(d,0,z) - A_z(0,0,z)) - \frac{d\left(\Phi(d,0,z) - \Phi(0,0,z)\right)}{dz} = 0$$

Now, let us consider the scattered voltage as defined in the standard transmission line theory [16]:

5-32 $$V^s(z) = -\int_0^d E_x^s(x,0,z)\,dx$$

Since the vector potential $\vec{A}(\vec{r})$ has only a z-component (see equation 5-5), the x-component of the electric field can be written from 5-4 as:

5-33 $$E_x^s(x,y,z) = -\frac{\partial}{\partial x}\Phi(x,y,z)$$

Introducing equation 5-33 into equation 5-32, the scattered voltage becomes[2]

5-34 $$V^s(z) = \Phi(d,0,z) - \Phi(0,0,z)$$

Introducing equations 5-21, 5-22, 5-23 and 5-24, into equation 5-34, we obtain:

5-35 $$V^s(z) = -\frac{1}{4\pi\varepsilon\, j\omega}\frac{d}{dz}\int_0^L (I_1(z') - I_2(z'))(g_1(z,z') - g_2(z,z'))dz'$$

Introducing now equations 5-12, 5-13, 5-25 and 5-26, into equation 5-31, we obtain[3]:

5-36 $$\frac{dV^s(z)}{dz} + j\omega\frac{\mu}{4\pi}\int_0^L (I_1(z') - I_2(z'))(g_1(z,z') - g_2(z,z'))dz' = E_z^i(d,0,z) - E_z^i(0,0,z)$$

Now, we have:

5-37 $$I_1(z) - I_2(z) = 2I_{tl}(z)$$

Therefore, equations 5-35 and 5-36 become, respectively:

5-38 $$V^s(z) = -\frac{1}{2\pi\varepsilon\, j\omega}\frac{d}{dz}\int_0^L I_{tl}(z')(g_1(z,z') - g_2(z,z'))dz'$$

and

---

[2] Note that from 5-15 and 5-16

$$\Phi(d,0,z) = \Phi_1(d,0,z) + \Phi_2(d,0,z) = -\frac{1}{4\pi\varepsilon j\omega}\frac{d}{dz}\int_0^L (I_1(z')g_1(z,z') + I_2(z')g_2(z,z'))dz'$$

and from 5-23 and 5-24

$$\Phi(0,0,z) = \Phi_1(0,0,z) + \Phi_2(0,0,z) = -\frac{1}{4\pi\varepsilon j\omega}\frac{d}{dz}\int_0^L (I_1(z')g_2(z,z') + I_2(z')g_1(z,z'))dz'$$

[3] Taking into account 5-34, 5-31 reads

$$E_z^i(d,0,z) - E_z^i(0,0,z) - j\omega(A_z(d,0,z) - A_z(0,0,z)) - \frac{dV^s(z)}{dz} = 0$$

The vector potential at (d,0,z) is obtained by 5-12 and 5-13

$$A_z(d,0,z) = A_{1z}(d,0,z) + A_{2z}(d,0,z) = \frac{\mu}{4\pi}\int_0^L (I_1(z')g_1(z,z') + I_2(z')g_2(z,z'))dz'$$

And the vector potential at (0,0,z) is obtained from 5-25 and 5-26

$$A_z(0,0,z) = A_{1z}(0,0,z) + A_{2z}(0,0,z) = \frac{\mu}{4\pi}\int_0^L (I_1(z')g_2(z,z') + I_2(z')g_1(z,z'))dz'$$

5-39 $$\frac{dV^s(z)}{dz} + j\omega\frac{\mu}{2\pi}\int_0^L I_{tl}(z')\left(g_1(z,z') - g_2(z,z')\right)dz' = E_z^i(d,z) - E_z^i(0,z)$$

The above equations are indeed equivalent to the pair of equations derived by Tkatchenko et al. [10] for the case of a wire above a perfectly conducting ground.

It is shown in [10] that, under the TL approximation, the integral

5-40 $$\int_0^L I_{tl}(z')\left(g_1(z,z') - g_2(z,z')\right)dz'$$

reduces to

5-41 $$I_{tl}(z')\cdot 2\ln\left(\frac{d}{r_w}\right)$$

and, therefore, the two equations 5-38 and 5-39 reduce to the well-known Agrawal et al. [16] field-to-transmission line equations.

5.3 Particularisation for the Antenna Mode current

By using equations 5-29 and 5-30 but this time instead of finding their difference, we will sum these two equations:

5-42 $$E_z^i(d,0,z) + E_z^i(0,0,z) - j\omega\left(A_z(d,0,z) + A_z(0,0,z)\right) - \frac{d\left(\Phi(d,0,z) + \Phi(0,0,z)\right)}{dz} = 0$$

The antenna-mode scattered “voltage” is defined as follows:

5-43 $$V_a^s(z) = \frac{\Phi(d,0,z) + \Phi(0,0,z)}{2}$$

Instead of the scattered differential-mode voltage in equation 5-32, which is defined as the integral of the electric field in the plane perpendicular to the wire, and which does not depend on the path of integration, the antenna-mode “voltage” is only the averaged potential for two wires, which depends on the choice of the reference point.

Introducing equations 5-21, 5-22, 5-23 and 5-24 into equation 5-43, we obtain

5-44 $$V_a^s(z) = -\frac{1}{8\pi\varepsilon\, j\omega}\frac{d}{dz}\int_0^L \left(I_1(z') + I_2(z')\right)\left(g_1(z,z') + g_2(z,z')\right)dz'$$

Substituting equations 5-21, 5-22, 5-23, 5-24, 5-25, 5-26 and 5-43 into equation 5-42, we obtain:

5-45 $$\frac{dV_a^s(z)}{dz} + j\omega\frac{\mu}{8\pi}\int_0^L \left(I_1(z') + I_2(z')\right)\left(g_1(z,z') + g_2(z,z')\right)dz' = \frac{E_z^i(d,z) + E_z^i(0,z)}{2}$$

Taking into account the fact that

5-46 $$I_1(z) + I_2(z) = 2I_a(z)$$

equations 5-44 and 5-45 become, respectively

5-47 $$V_a^s(z) = -\frac{1}{4\pi\varepsilon\, j\omega}\frac{d}{dz}\int_0^L I_a(z')\left(g_1(z,z') + g_2(z,z')\right)dz'$$

and

5-48 $$\frac{dV_a^s(z)}{dz} + j\omega\frac{\mu}{4\pi}\int_0^L I_a(z')\left(g_1(z,z') + g_2(z,z')\right)dz' = \frac{E_z^i(d,z) + E_z^i(0,z)}{2}$$

The antenna mode current $I_a(z)$ is the solution of the pair of equations 5-47 and 5-48. These two equations are similar in their form to those describing the transmission line-mode current (equations 5-38 and 5-39). However, they differ in two points[4]:

1. the source term for the antenna-mode current is the sum of the tangential electric fields along the two conductors whereas, for the transmission line-mode current, it is given by their difference; and
2. the Green's function for the antenna-mode current is given by $g_1(z,z') + g_2(z,z')$, whereas for the transmission line-mode current, it is given by $g_1(z,z') - g_2(z,z')$.

5.4 Solution of the equations for the Antenna Mode current for lines with electrically-short cross sections

Equations 5-47 and 5-48 will be simplified for lines with electrically-short cross sections by first re-writing equation 5-47 as:

5-49
$$\begin{aligned} V_a^s(z) &= -\frac{1}{4\pi\varepsilon\, j\omega}\frac{d}{dz}\int_0^L I_a(z')\left(g_1(z,z') + g_2(z,z')\right)dz' \\ &= -\frac{1}{4\pi\varepsilon\, j\omega}\int_0^L I_a(z')\frac{\partial}{\partial z}\left(g_1(z,z') + g_2(z,z')\right)dz' \end{aligned}$$

Considering the fact that

5-50 $$\frac{\partial}{\partial z}\left(g_1(z,z') + g_2(z,z')\right) = -\frac{\partial}{\partial z'}\left(g_1(z,z') + g_2(z,z')\right)$$

Equation 5-49 can be re-written as follows:

5-51 $$V_a^s(z) = \frac{1}{4\pi\varepsilon\, j\omega}\int_0^L I_a(z')\frac{\partial}{\partial z'}\left(g_1(z,z') + g_2(z,z')\right)dz'$$

[4] Actually, a third difference between these two systems is connected with gauge dependence of the obtained equations. The initial integro-differential equations for the current and potential, which are described at the end of Section 5.1, are dependent on the used gauge. The form is different if we use the Lorenz condition, as it is usual in applied electrodynamics, from the form obtained using the Coulomb gauge [14]. In the low-frequency case (2kd<<1) the gauge-dependence for the system 5-38 and 5-39 disappears (and we come to the gauge independent classical transmission system), but this dependence remains for the system 5-47 and 5-48.

Now, integrating equation 5-51 by parts yields

5-52

$$V_a^s(z) = \frac{1}{4\pi\varepsilon\, j\omega}\left[I_a(z')\left(g_1(z,z') + g_2(z,z')\right)\right]_0^L - \frac{1}{4\pi\varepsilon\, j\omega}\int_0^L \frac{dI_a(z')}{dz'}\left(g_1(z,z') + g_2(z,z')\right)dz'$$

The antenna-mode current being zero at the line extremities, the first term of the right-hand side of equation 5-52 is simply zero. Thus, equation 5-52 becomes

5-53

$$V_a^s(z) = -\frac{1}{4\pi\varepsilon\, j\omega}\int_0^L \frac{dI_a(z')}{dz'}\left(g_1(z,z') + g_2(z,z')\right)dz'$$

Considering the expressions for the Green's functions, the integral terms in equations 5-48 and 5-53 can be respectively written as:

5-54

$$\int_0^L I_a(z')\left(g_1(z,z') + g_2(z,z')\right)dz' = \int_0^L I_a(z')\left(\frac{e^{-jk\sqrt{(z-z')^2+r_w^2}}}{\sqrt{(z-z')^2+r_w^2}} + \frac{e^{-jk\sqrt{(z-z')^2+d^2}}}{\sqrt{(z-z')^2+d^2}}\right)dz'$$

5-55

$$\int_0^L \frac{dI_a(z')}{dz'}\left(g_1(z,z') + g_2(z,z')\right)dz' = \int_0^L \frac{dI_a(z')}{dz'}\left(\frac{e^{-jk\sqrt{(z-z')^2+r_w^2}}}{\sqrt{(z-z')^2+r_w^2}} + \frac{e^{-jk\sqrt{(z-z')^2+d^2}}}{\sqrt{(z-z')^2+d^2}}\right)dz'$$

Now, when kd<<1 and L>>d, and considering that the Green's function decays rapidly[5] as a function of $|z-z'|$, equations 5-54 and 5-55 can be respectively approximated as:

5-56

$$\int_0^L I_a(z')\left(g_1(z,z') + g_2(z,z')\right)dz' \cong I_a(z)\int_0^L\left(\frac{1}{\sqrt{(z-z')^2+r_w^2}} + \frac{1}{\sqrt{(z-z')^2+d^2}}\right)dz'$$

5-57

$$\int_0^L \frac{dI_a(z')}{dz'}\left(g_1(z,z') + g_2(z,z')\right)dz' \cong \frac{dI_a(z)}{dz}\int_0^L\left(\frac{1}{\sqrt{(z-z')^2+r_w^2}} + \frac{1}{\sqrt{(z-z')^2+d^2}}\right)dz'$$

The integral in equations 5-56 and 5-57 can be solved analytically to yield:

5-58

[5] Note that the decay is not as rapid as in the case of the transmission line mode current, for which the Green's function is given by the difference of the two terms g_1-g_2 [11].

$$\int_0^L \left(\frac{1}{\sqrt{(z-z')^2 + r_w^2}} + \frac{1}{\sqrt{(z-z')^2 + d^2}} \right) dz'$$

$$= ln\left\{ \frac{\left[L - z + \sqrt{(L-z)^2 + r_w^2} \right] \left[z + \sqrt{z^2 + r_w^2} \right]}{r_w^2} \frac{\left[L - z + \sqrt{(L-z)^2 + d^2} \right] \left[z + \sqrt{z^2 + d^2} \right]}{d^2} \right\}$$

Introducing equation 5-58 into equations 5-48 and 5-57 yields

5-59
$$\frac{dV_a^s(z)}{dz} + j\omega L'_a I_a(z) = \frac{E_z^i(d,0,z) + E_z^i(0,0,z)}{2}$$

5-60
$$\frac{dI_a(z)}{dz} + j\omega C'_a V_a^s(z) = 0$$

where L_a' and C_a' are the equivalent per-unit-length inductance and capacitance for the antenna-mode current, respectively, given by:

5-61
$$L'_a = \frac{\mu_o}{4\pi} ln\left\{ \frac{\left[L - z + \sqrt{(L-z)^2 + r_w^2} \right] \left[z + \sqrt{z^2 + r_w^2} \right]}{r_w^2} \frac{\left[L - z + \sqrt{(L-z)^2 + d^2} \right] \left[z + \sqrt{z^2 + d^2} \right]}{d^2} \right\}$$

and

5-62
$$C'_a = \frac{4\pi\varepsilon_o}{ln\left\{ \frac{\left[L - z + \sqrt{(L-z)^2 + r_w^2} \right] \left[z + \sqrt{z^2 + r_w^2} \right]}{r_w^2} \frac{\left[L - z + \sqrt{(L-z)^2 + d^2} \right] \left[z + \sqrt{z^2 + d^2} \right]}{d^2} \right\}}$$

The antenna-mode current $I_a(z)$ is the solution of the pair of transmission-line-like equations 5-59 and 5-60. Note that the equivalent antenna-mode per-unit-length inductance and capacitance are dependent on z. Figure 5-2 and Figure 5-3 L_a' and C_a' as a function of z along the line for a 41-m long line (d = 20 cm and r_w = 1.5 mm). It can be seen that the inductance is minimum at the two line ends and reaches its maximum at the line center. Conversely, the capacitance reaches its maximum value at the line ends and its minimum at the center.

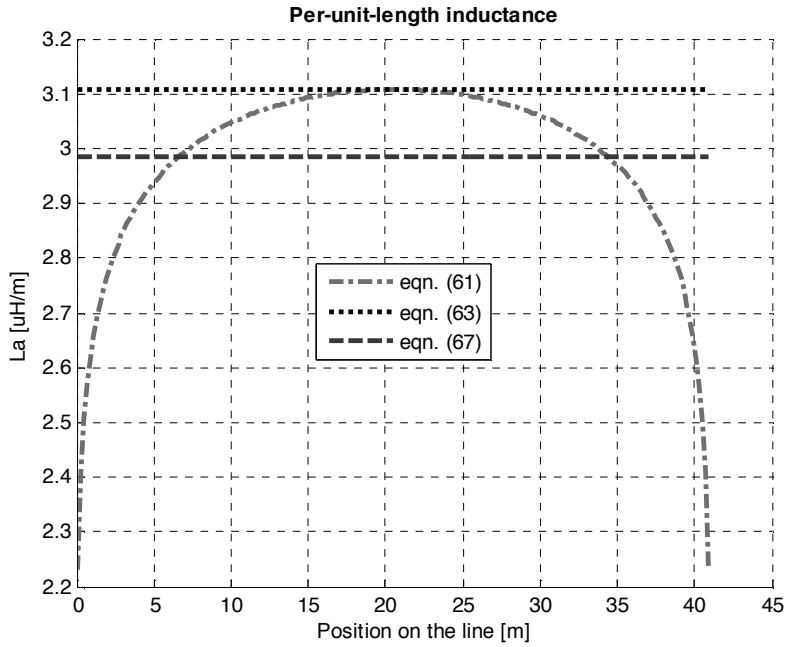

Figure 5-2: Antenna-mode line per-unit-length inductance.

Line parameters: L =41 m, d = 20 cm, r_w = 1.5 mm.

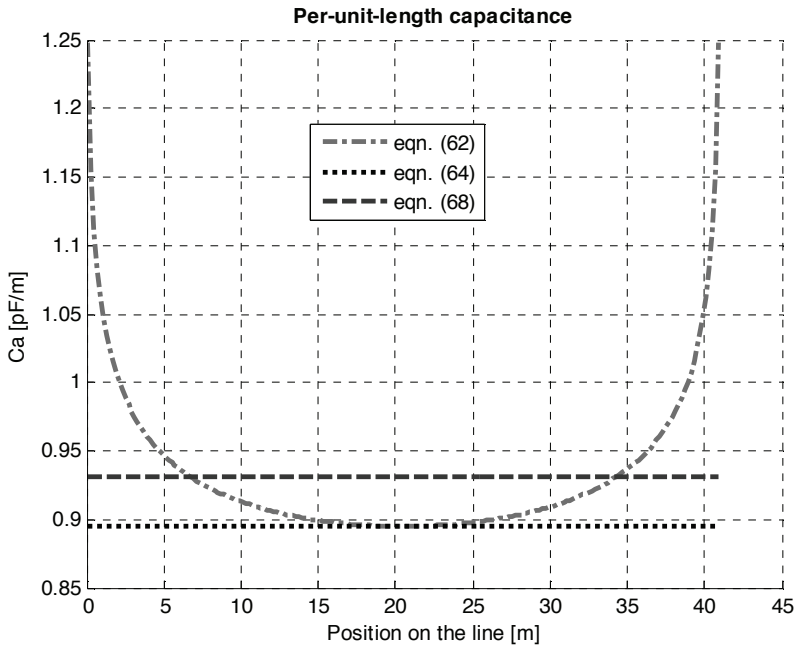

Figure 5-3: Antenna-mode line per-unit-length capacitance.

Line parameters: L =41 m, d = 20 cm, r_w = 1.5 mm.

Considering now observation points along the line far from the line extremities, it is straightforward to show that the per-unit-length inductance and capacitance expressions reduce to:

5-63 $$\hat{L}'_a = \frac{\mu_o}{2\pi} ln \frac{L^4}{r_w^2 d^2}$$

5-64 $$\hat{C}'_a = \frac{2\pi\varepsilon_o}{ln\frac{L^4}{r_w^2 d^2}}$$

The average values of the inductance and the capacitance can be obtained, respectively, by

5-65 $$\tilde{L}'_a = \frac{1}{L}\int_0^L L'_a(z)dz$$

5-66 $$\tilde{C}'_a = \frac{1}{L}\int_0^L C'_a(z)dz$$

For r<<L and d<<L, we obtain, after straightforward mathematical manipulations,

5-67 $$\tilde{L}'_a = \frac{\mu_o}{2\pi} ln \frac{0.29\ L^4}{r_w^2 d^2}$$

5-68 $$\tilde{C}'_a = \frac{2\pi\varepsilon_o}{ln\frac{0.29L^4}{r_w^2 d^2}}$$

The above values are also represented in Figure 5-2 and Figure 5-3.

5.5 Validation of the Proposed Equations: Comparison with the Numerical Electromagnetics Code (NEC)

The proposed pair of transmission-line-like equations 5-59 and 5-60 for the computation of antenna-mode currents are tested here versus numerical results obtained using the Numerical Electromagnetics Code (NEC) [1]. The derived equations 5-59 and 5-60 are solved using a conventional transmission line code (such as the frequency-domain approach presented in [2]). The per-unit-length inductance and capacitance associated with the antenna-mode currents are determined using the approximate expressions 5-67 and 5-68.

We will consider a two-conductor line (as in Figure 5-1) characterized by L = 41 m, d = 0.2 m, r_w = 1.5 mm. The wires are assumed to be perfectly conducting and the load impedances at the $z = 0$ and $z = L$ ends are taken to be $Z_1 = Z_2 = 293\ \Omega$, which is approximately equal to one-half of the characteristic impedance of the line. This structure is excited by an incident plane wave that propagates in the plane of the line and impinges on it with an angle of incidence ψ.

Figure 5-4 presents the computed results for the transmission-line mode and antenna-mode current magnitudes along the line, for a frequency f = 20 MHz and for an angle of

incidence $\psi = 45^o$. The calculations are performed using the constant average expressions for the equivalent inductance and capacitance given, respectively, by equations 5-67 and 5-68. It can be seen that the computed results using the derived equations are in reasonably good agreement with the numerical results obtained using NEC.

In the same figures, we have also represented the transmission line mode current magnitudes calculated using both NEC and the TL approximation. In this case, as expected, the two results are in excellent agreement to the point of being indistinguishable.

It is worth noting that, even for the considered low frequencies, the antenna-mode currents can reach much larger values than the transmission line mode currents.

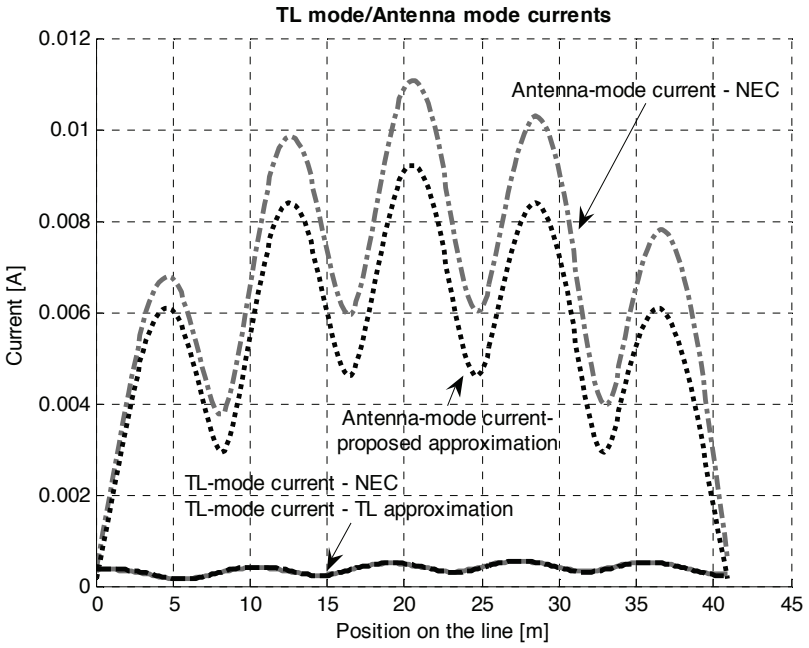

Figure 5-4: The computed results for the transmission line mode and antenna mode current magnitudes along the 41-m long line, for an angle of incidence $\psi = 45^o$ and f = 20 MHz.

In Figure 5-5 and Figure 5-6, we present similar results for different line lengths, namely 31 m (Figure 5-5) and 18 m (Figure 5-6). It can be seen that the computed results using the derived equations are again in reasonably good agreement with numerical results obtained using NEC.

The observed differences between the proposed approach and NEC results can be essentially attributed to the simplified procedure adopted for the determination of the equivalent inductance and capacitance parameters. More elaborate techniques such as those described in [13], [14], [17], [18], [19] and [20] could be used in this respect for the considered problem.

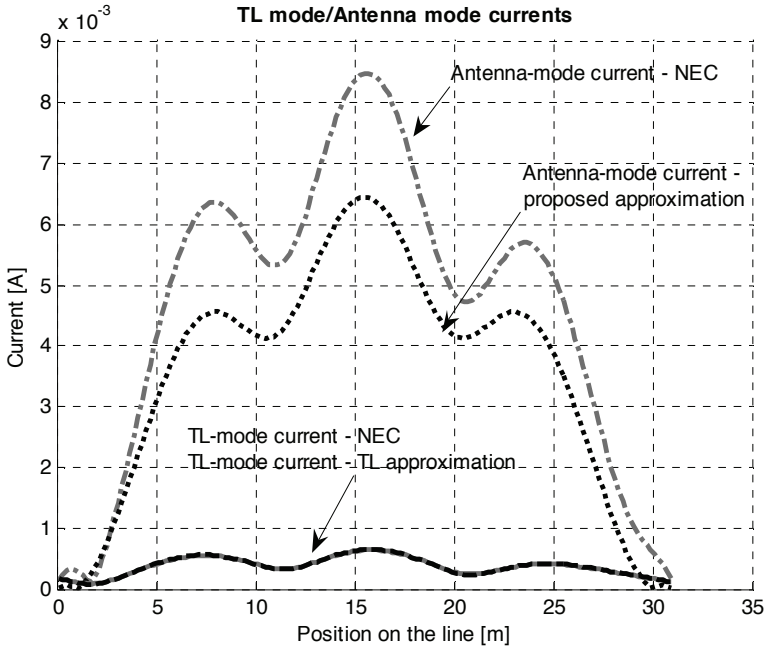

Figure 5-5: The computed results for the transmission line mode and antenna mode current magnitudes along the 31-m long line, for an angle of incidence $\psi = 60^o$ and f = 20 MHz.

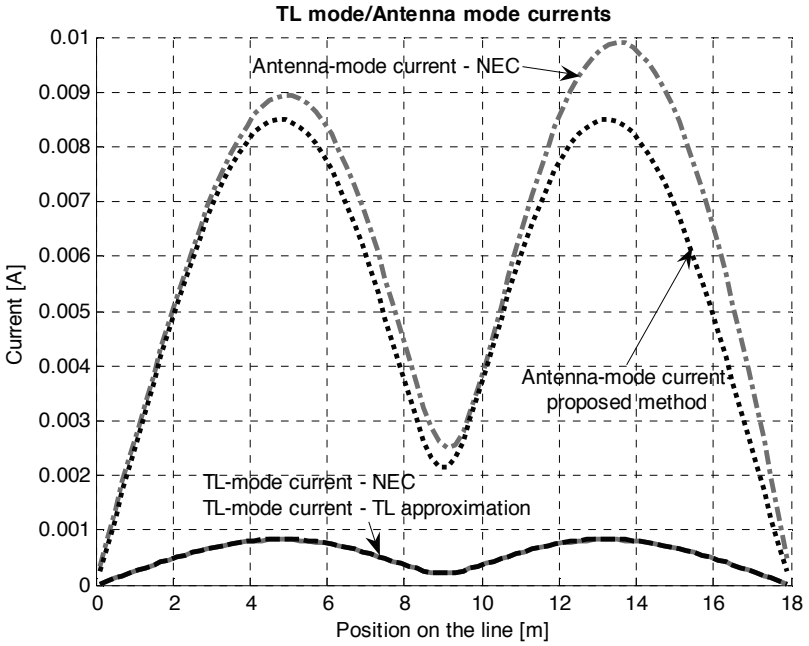

Figure 5-6: The computed results for the transmission line mode and antenna mode current magnitudes along the 18-m long line, for an angle of incidence $\psi = 60^o$ and f = 20 MHz. In this case line was left opened at both ends.

5.6 Conclusions

For a transmission line, even if the line cross section is electrically small, the presence of antenna-mode currents causes the sum of the currents at a cross section to be, in the general case, different from zero. Since the antenna mode current response is small near the ends of the line, it is appropriate to consider the TL model current only if all that is needed is the response of the line at the load. On the other hand, if we wish to evaluate the current along the line, the presence of antenna-mode currents needs to be taken into account, even for electrically small line cross sections.

We have derived an integral equation describing the antenna-mode currents along a two-wire transmission line.

We have further shown that, when the line cross-sectional dimensions are electrically small, the integral equation reduces to a pair of transmission line-like equations with equivalent line parameters (per-unit-length inductance and capacitance). The derived equations make it possible to compute the antenna mode currents using a traditional transmission line code with appropriate parameters.

The derived equations were tested versus numerical results obtained using NEC and reasonably good agreement was found.

Work is currently underway to improve the accuracy of the model, specifically with regard to the determination of the line parameters and evaluation of currents at resonant frequencies, and inclusion of multiconductor lines.

REFERENCES

[1] G. J. Burke, "Numerical Electromagnetics Code NEC-4 Method of Moments," Lawrence Livermore National Laboratory UCRL-MA-109338, 1992.

[2] F. M. Tesche, M. Ianoz, and T. Karlsson, EMC Ananlysis methods and computational models. New York: Wiley Interscience, 1997.

[3] C.R. Paul, Analysis of multiconductor transmission lines, John Wiley and Sons, 1994.

[4] S. Frankel, “Quasi-TEM transmission line theory”, Interaction Note 135, November 1972.

[5] K.S.H. Lee, “Two Parallel Terminated Conductors in External Fields”, IEEE Transactions on Electromagnetic compatibility, vol. EMC-20, No 2, May 1978.

[6] C.R. Paul, “A comparison of the contributions of common-mode and differential-mode currents in radiated emissions”, IEEE Trans. On Electromagnetic Compatibility, Volume 31, Issue 2 , May 1989, pp.189 – 193

[7] R. Razafferson, L. Koné, B. Demoulin, A. Zeddam, F. Gauthier, “Effects of the loads and wiring size on PLC electromagnetic pollution”, 2003 IEEE Int. Symp. on Electromagnetic Compatibility, Istanbul, May 2003.

[8] N. Korovkin, E. Marthe, F. Rachidi, E. Selina, "Mitigation of electromagnetic field radiated by PLC systems in indoor environment", International Journal of Communication Systems, Vol. 16, pp. 417-426, May 2003.

[9] U. Reggiani, A. Massarini, L. Sandrolini, M. Ciccotti, D.W.P. Thomas, C. Christopoulos, “Experimental verification of predicted electromagnetic fields radiated by straight interconnect cables carrying high-frequency currents”, 2003 IEEE Power Tech, Bologna, June 23-26, 2003.

[10] S. Tkatchenko, F. Rachidi, M. Ianoz, "Electromagnetic field coupling to a line of finite length: theory and fast iterative solutions in frequency and time domains", IEEE Trans. on Electromagnetic Compatibility, Vol. 37, no 4, pp. 509-518, November 1995.

[11] S. Tkatchenko, F. Rachidi, M. Ianoz, "High-frequency electromagnetic field coupling to long terminated lines ", IEEE Trans. on Electromagnetic Compatibility, Vol. 43, No. 2, May 2001.

[12] F. Delfino, R.Procopio, M. Rossi, P. Girdinio, "Technique for Computing the Response of a Line of Finite Length Excited by High Frequency Electromagnetic Field", IEE Proceedings - Science, Measurements and Technology, Vol. 149, No. 5, September 2002, pp.289-292.

[13] H. Haase, J.Nitsch, T. Steinmetz, “Transmission-Line Super Theory: a New Approach to an Effective Calculation of Electromagnetic Interactions”, Radio Science Bulletin No 307, December 2003, pp. 33-60.

[14] J.Nitsch, S.Tkachenko, “Complex-Valued Transmission-Line Parameters and their Relation to the Radiation Resistance”, IEEE Trans. on Electromagnetic Compatibility, Vol. EMC - 47, No. 3, Aug. 2004, pp.477-48.

[15] A. Maffucci, G. Miano, F. Villone, "An Enhanced Transmission Line Model for Conducting Wires", IEEE Trans. on Electromagnetic Compatibility, Vol. 46, No. 4, November 2004, pp.512-528.

[16] Agrawal A.K., H.J. Price, S.H. Gurbaxani, "Transient response of a multiconductor transmission line excited by a nonuniform electromagnetic field", IEEE Trans. on EMC, Vol. EMC-22, No. 2, pp. 119-129, May 1980.

[17] M.Ianoz, N.V.Korovkin, S.V. Kochetov, E.E.Selina, S.V.Tkachenko, G.V. Vodopianov, “A finite length model using the equivalent circuits for the analysis of electromagnetic radiation”, Proc. Int. Symp. on EMC,1998, Rome, Italy, pp.632-636.

[18] N.V.Korovkin, S.V. Kochetov, E.E.Selina, S.V.Tkachenko, M.Ianoz, “A model for a finite length transmission line considering skin and radiation effects”, Proc. 14th Int. Zurich Symposium on Electromagnetic compatibility, Zurich, Switzerland, Feb. 18-20, 2001, pp. 44H4.

[19] H.Haase and J.Nitsch, “Full-wave transmission line theory (FWTLT) for the analysis of three-dimensional wire-like structures,” in Proc. 14th International Zurich Symposium and Technical Exhibition on Electromagnetic Compatibility, Feb.2001, pp.235-240.

[20] H.Haase, J.Nitsch, “Investigation of nonuniform transmission line structures by a generalized transmission line theory”, in Proc.15th International Zurich Symposium and Technical Exhibition on Electromagnetic Compatibility, Feb. 2003, pp. 597-602.

[21] A. Vukicevic, F. Rachidi, M. Rubinstein, and S. Tkachenko, "An efficient method for the computation of antenna mode currents along transmission lines," presented at 28th General Assembly of International Union of Radio Science (URSI), New Delhi, India, 2005.

[22] A .Vukicevic, F. Rachidi, M. Rubinstein, S. Tkachenko, “On the Evaluation of Antenna-Mode Currents along Transmission Lines”, IEEE Transactions on Electromagnetic Compatibility, November 2006, Vol 48, No 4

Chapter 6

6 Mitigation of radiated electromagnetic fields emitted by PLC networks

6.1 Introduction

The expression “mitigation technique” in the PLC domain refers to any method designed to lower emissions without significantly affecting the attainable transmission throughput. Mitigation techniques can be either passive or active, depending on whether or not additional power is required for the technique to operate.

A few techniques have been proposed to mitigate electromagnetic interferences caused by PLC systems.

The patent WO98/06188 [1] proposes an apparatus for coupling PLC signals to a transmission line. The apparatus includes a first coupler to inject the wanted signal at a first position and a second coupler to inject a cancelling signal on the same line at a second position, different from the first one. The two signals combine destructively in one direction (direction of the unshielded part of an electricity substation), while enabling the wanted signal to propagate in the other direction along the line. This method is therefore not applicable to an indoor environment [5][7].

In US Patent 6,037,678 [2], a technique is proposed to couple a set of communication signals to a multiconductor line, typically a 3-phase line. The phases of the signals are chosen such that the resulting radiation is minimised. The phase adjustment is achieved using an antenna which senses the field radiation. This method, however, is not applicable to indoor environments since in indoor networks only one phase (of the 3 phases) is generally available. Additionally, all of the above-discussed mitigation methods consider a unidirectional data transmission system [5][7].

There exist at least four classes of techniques which can be used to mitigate emissions from PLC networks:

1) Those that achieve reduction of emissions at the source itself by modification of the transmitted signal. An example is the use of notches in the Power Spectral Density mask at frequencies already used by critical services or creating disturbances on other nearby systems. This technique can be classified as passive since it can be implemented in software in OFDM systems. Spectral notching is a technique commonly used for avoiding of exclusion bands (frequencies at which there exist interference problems). Notches are created by turning off those OFDM subcarriers that fall in the exclusion bands, thus eliminating the energy transmitted in those bands.
2) Those that attain a reduction by shielding at the source. This could involve, for instance, the shielding of the low voltage cables in the home or the use of a metallic grid in wallpaper, although these measures may prove expensive and impractical in most cases. This class is also passive.
3) Those that use shielding at the victim equipment. This refers to the use of measures to improve the immunity of the victim. This technique is passive as well.

4) Those that introduce a new signal to diminish emissions. The techniques in this class are generally active since additional energy is required for the extra signal.

In this chapter, we present a mitigation technique based on the method proposed previously by Korovkin et al. [5]. A practical implementation of the developed method is given and the influence of the use of the presented technique to the channel capacity is given.

We also present the results of laboratory and field measurements preformed to test the effectiveness of the spectral notching technique.

6.2 The proposed method

6.2.1 Description

A mitigation method using an auxiliary signal was recently proposed in [3]. The idea was to take advantage of the presence of the additional ground conductor in the low voltage power network to inject a $180°$ out-of-phase version of the PLC wanted signal into the ground-neutral circuit. If all three wires run parallel and in close proximity to one another, the expectation is that the radiated fields from both circuits will have similar amplitudes and that they will be approximately $180°$ out of phase. Under these conditions, destructive interference should lead to partial or total cancellation of the radiation. Numerical and experimental tests carried out on simple network geometries show that reductions in the emissions of more than 20 dB can in fact be achieved [6]. Measurements made on more realistic geometry networks, however, show less good results and even a worsening of the emissions level for certain frequencies at which the interference between the radiation from the wanted and from the compensation signals (also called auxiliary signals) is constructive [6][7].

The experimental setup used to test this technique is shown in Figure 6-1.

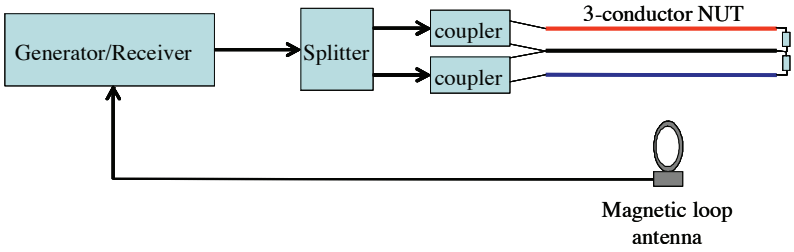

Figure 6-1: Schematic measurement setup

A simple extension cord was used as the Network Under Test (NUT). The measurements were carried out for two different cable layouts:

1) a 2-meter, straight layout (see Figure 6-3a) and,
2) a random layout (see Figure 6-3b)

In both cases, the NTU was terminated in two resistances of 150Ω, one between phase and neutral and the second between neutral and ground.

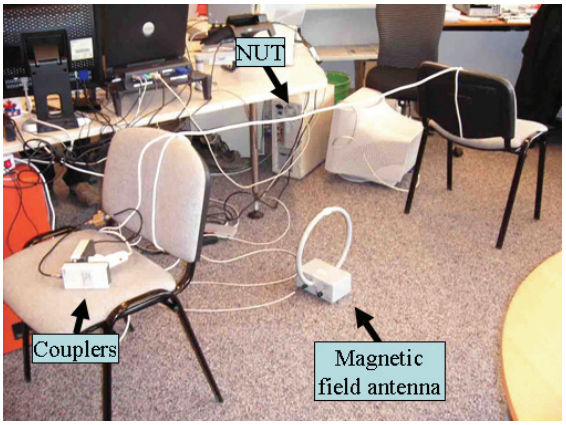

(a)

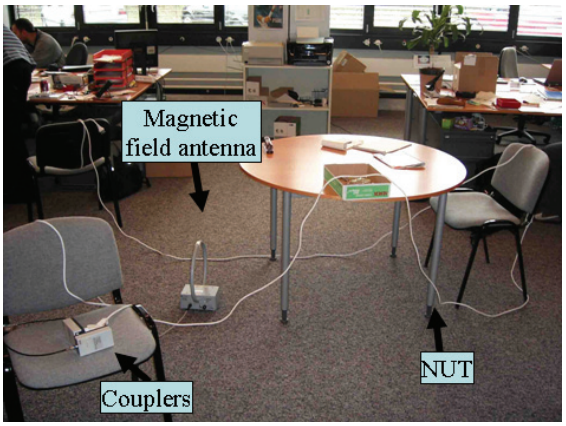

(b)

Figure 6-2: Photographs of the NUT layouts used. a) Straight 2-m cable layout. b) Random layout

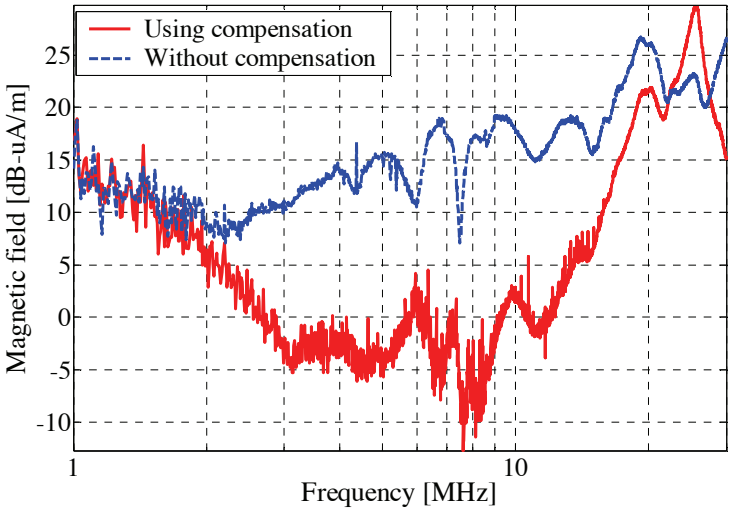

(a)

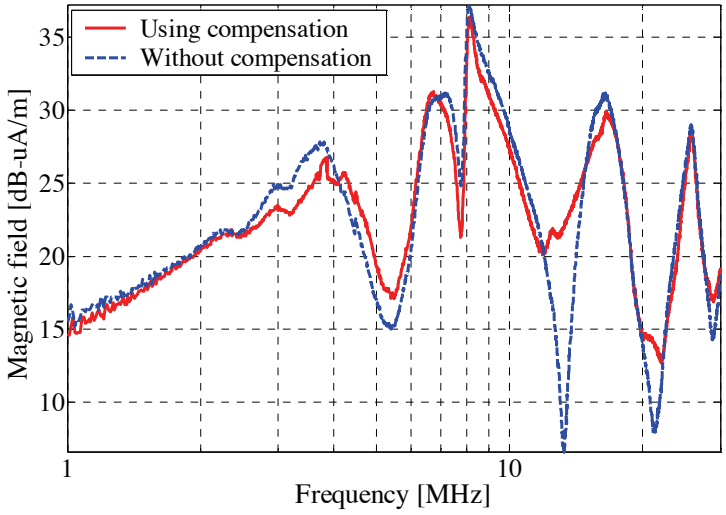

(b)

Figure 6-3: Magnetic field measured with and without the compensation signal for (a) the 2-meter straight-segment setup, and (b) the random layout

As can be seen in Figure 6-3c, the compensation signal significantly reduces the emissions from a straight cable over a wide range of frequencies. However, for the random configuration layout in Figure 6-3d, the compensation signal does not help reduce the emissions level over the whole band and, even at those frequencies at which a reduction is in fact observed, it is considerably smaller than in the straight cable case.

This was the reason to introduce an improvement to this mitigation technique to allow the reduction of emissions for complex, realistic NTUs.

A modification was proposed in [8] in which, instead of a constant $180°$ phase shift, the phase and the amplitude of the auxiliary signal are selected adaptively.

The basis for the modified mitigation method is now briefly presented by making reference to Figure 6-4, in which $h_{plc}(f)$ is a transfer function relating a component of the magnetic field at a given point in space to the injected PLC voltage as a source, and $h_{comp}(f)$ is the transfer function relating the magnetic field at the same point to the compensation signal as a source.

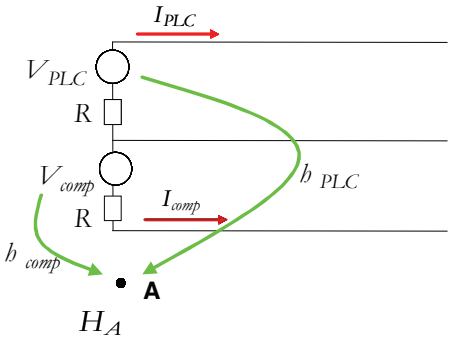

Figure 6-4: Simplified diagram of the mitigation approach proposed by Rubinstein et al [8].

Since we are dealing with a linear system, the total field at any observation point is the sum of the fields produced by the wanted PLC signal and from the compensation signal.

The total field is, therefore, given by

6-1 $$H_A = h_{plc}(f)V_{plc} + h_{comp}(f)V_{comp}$$

Making $H_A = 0$, one can readily show that the compensation signal (expressed as a voltage) is given by

6-2 $$V_{comp} = -\frac{h_{plc}(f)}{h_{comp}(f)}V_{plc}$$

The schematic representation of the proposed technique is given in Figure 6-5. The magnetic field is measured with the loop antenna under different signal injection conditions controlled by the block labelled “Logic” in Figure 6-5. If the appropriate measurements are made, it is possible to determine the compensation signal that needs to be injected into the lower circuit so as to cancel out the magnetic field due to the wanted PLC signal.

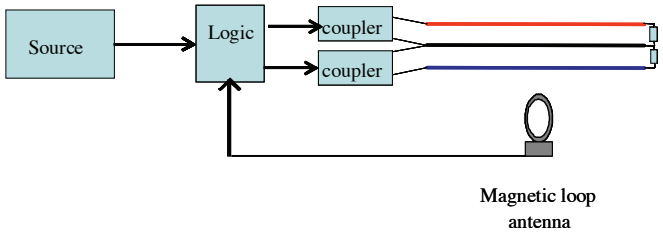

Figure 6-5: Schematic representation of the implementation of the mitigation technique.

6.2.2 Practical implementation [10]

The method requires that field measurements be made in the field mitigation area and that the information be relayed back to the PLC-signal injection point. Since this may be technologically challenging and economically costly, the technique would have to be applied only when customers file a complaint and it is determined that PLC network is to blame.

Variations in the network conditions necessitate periodic adaptation. Since this can be achieved by way of a periodic, software-controlled recalibration, it does not necessarily lead to additional implementation costs.

To reduce the cost of implementation, the possibility of using the mitigation of the fields close to the modem as an indicator of the mitigation undergone by fields further away was investigated. If mitigation can be achieved in this manner, the antenna could be integrated into the modem itself or it could be placed a short distance away from it using a shielded cable as illustrated in Figure 6-5.

The idea was tested by using the Numerical Electromagnetics Code (NEC-2) [11] on two cabling configurations with different levels of complexity. A field point was defined 10 cm away from the injection point on the modem, shown as point A in Figure 6-6 and Figure 6-10:

The vertical surfaces were added to the figures to ease the representation of the cables but they were not modelled. The ground plane is perfectly conducting.

The compensation signal was selected to minimize the z component of the magnetic field at point A.

6.2.2.1 Low complexity configuration

The simple configuration consisted of three straight parallel conductors of length L=4m, located 0.5 meters above the perfectly conducting ground as shown in Figure 6-6.

First, the dependence of the required compensating voltage on frequency was calculated. The results for all three components: x, y and z, are presented in Figure 6-7.

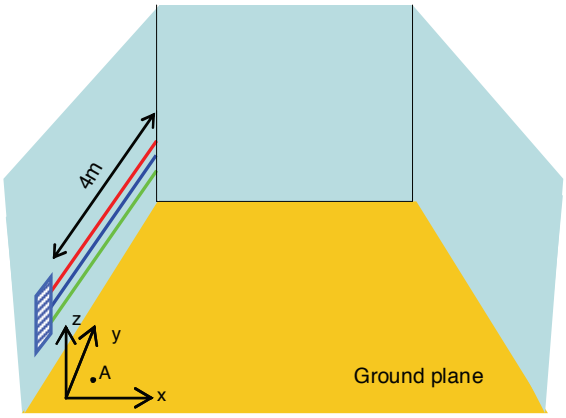

Figure 6-6: Low complexity configuration

It can be seen that the compensation voltage corresponding to any of the three components exhibits a resonance at 19 MHz, which corresponds to a wavelength $\lambda = 4L$.

Note that minimizing one component of the field could result in an increase of the other components.

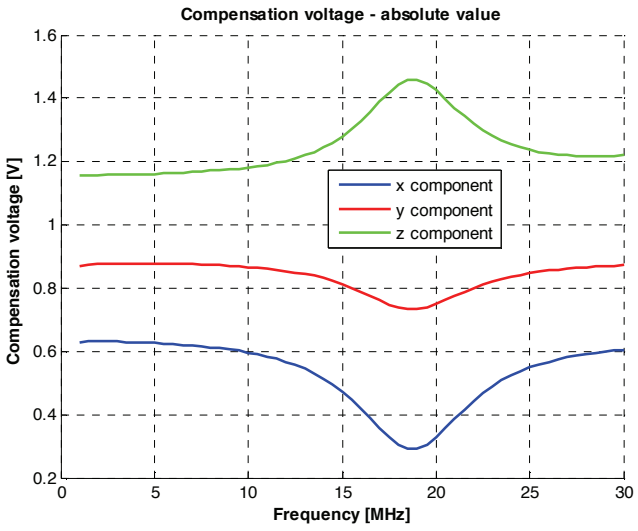

(a)

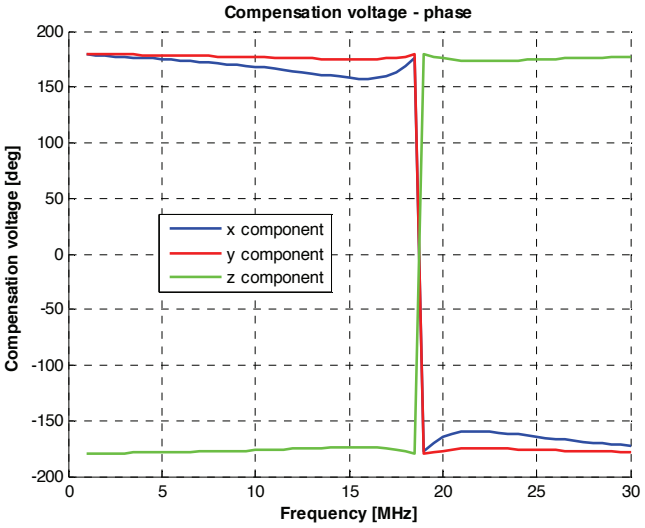

(b)

Figure 6-7: Dependence of compensation voltage as a function of frequency. (a) Magnitude and (b) Phase.

Figure 6-8 presents the attenuation of the z-component of the magnetic field in a considered surface of 4x4 m^2, at a height of 0.5 m, for two frequencies, 15 and 30 MHz.

It can be seen from Figure 6-8 that, although the compensation voltage was determined to minimize the z-component of the magnetic field at a single point near the injection point, the fields in a large region are attenuated as well. However, application of the auxiliary voltage enhances the magnetic field in a narrow region (x=0.4-0.8 m).

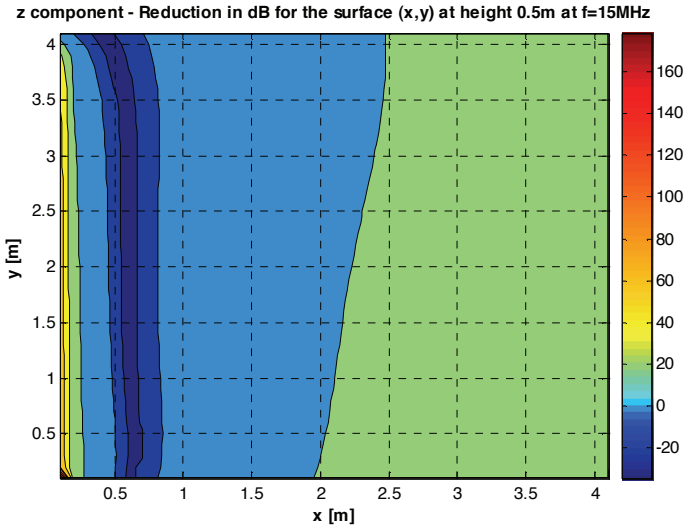

(a)

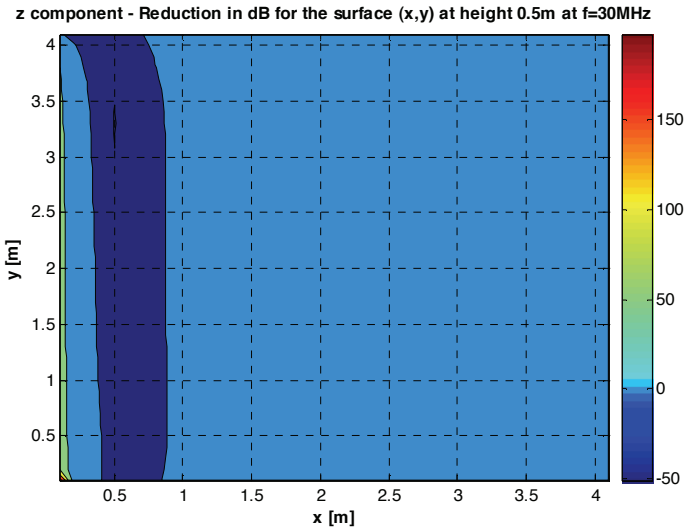

(b)

Figure 6-8: Attenuation of the z-component of magnetic field for the frequency of (a) 15MHz and (b) 30MHz. Height above ground: 0.5 m.

Figure 6-9 presents the attenuation of the y-component, which is damped over the whole surface for both frequencies.

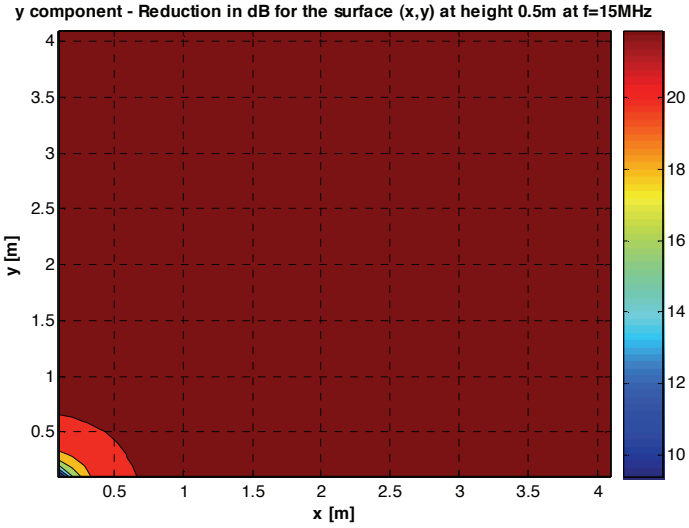

(a)

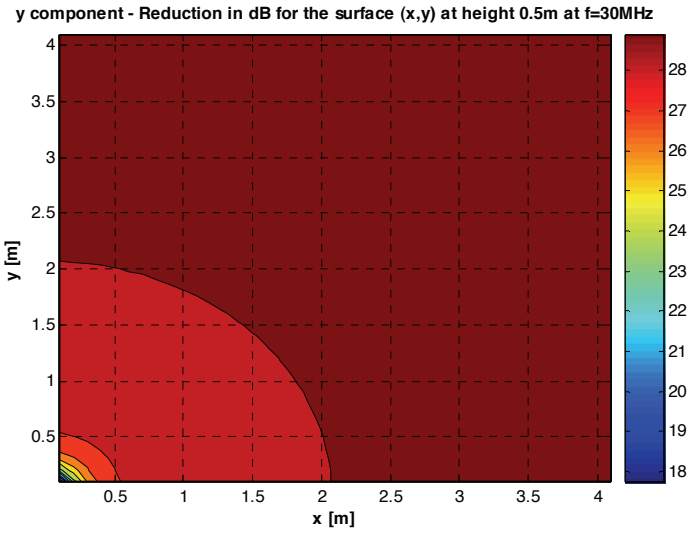

(b)

Figure 6-9: Attenuation of the y-component of the magnetic field when the compensation is applied to the z-component. (a) f=15MHz and (b) f=30MHz

Table 6-1 presents the average attenuation for the three magnetic field components in the considered surface at heights of 0.5 m and 1 m, respectively. It can be seen that the mitigation technique results in an overall average attenuation of the fields ranging from 11 to 29 dB.

Table 6-1: Average reduction over the surface at 15MHz and 30MHz

f [MHz]	Surface at height of 0.5m			Surface at height of 1m		
	x [dB]	y [dB]	z [dB]	x [dB]	y [dB]	z [dB]
15	21.01	23.17	16.65	25.54	23.85	23.81
30	18.22	29.15	11.49	20.59	29.62	17.85

6.2.2.2 Complex Configuration

The second configuration that we considered is composed of four straight, three-conductors segments disposed as shown in Figure 6-10.

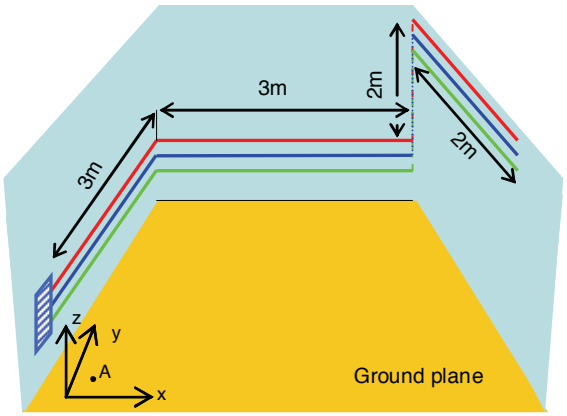

Figure 6-10: Higher complexity configuration

The compensation signal was once more selected to mitigate the z component of the magnetic field. Figure 6-11: presents the attenuation of this component in the considered 4x4 m^2 surface at a height of 0.5 m for 15 and 30 MHz.

As for the simple configuration, with the compensation voltage determined to minimize the field at a single point close to the injection point, the fields over a large region are attenuated as well. In a narrow region for y~3 m, however, the magnetic field is enhanced.

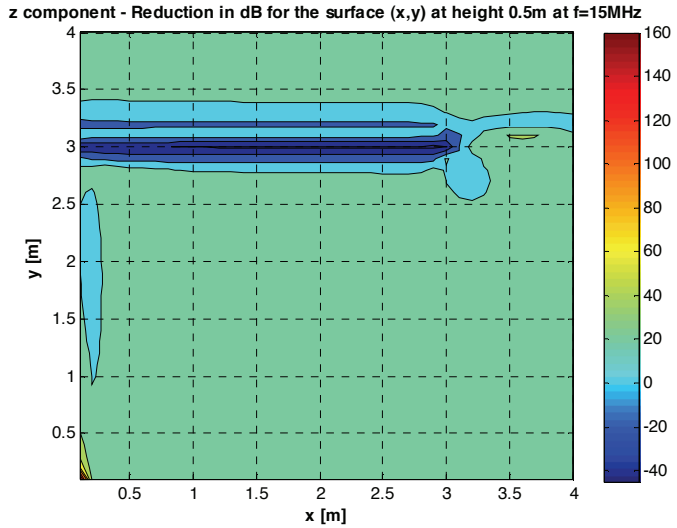

(a)

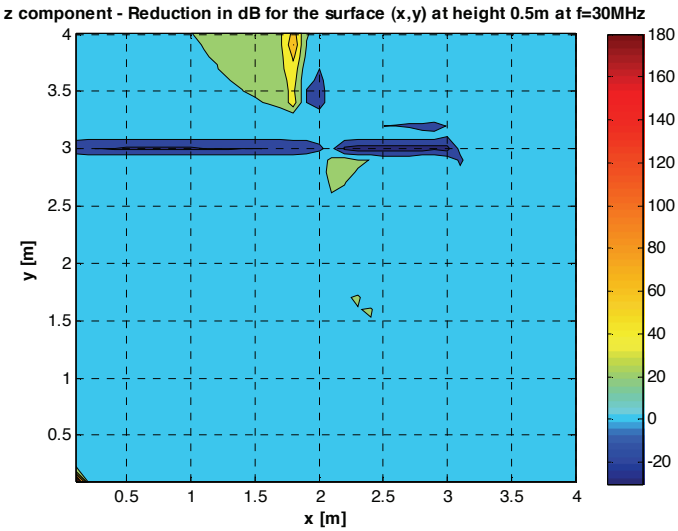

(b)

Figure 6-11: Attenuation of the z-component of the magnetic field for a frequency of (a) 15MHz and (b) 30MHz. Height above ground: 0.5 m.

Figure 6-12 presents the attenuation of the y-component of the field in the considered region. Again, the mitigation technique, although failing in some areas, is effective in a large region.

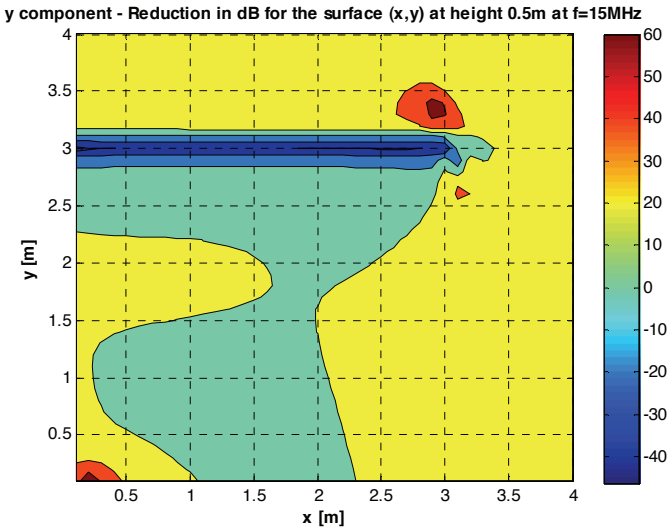

(a)

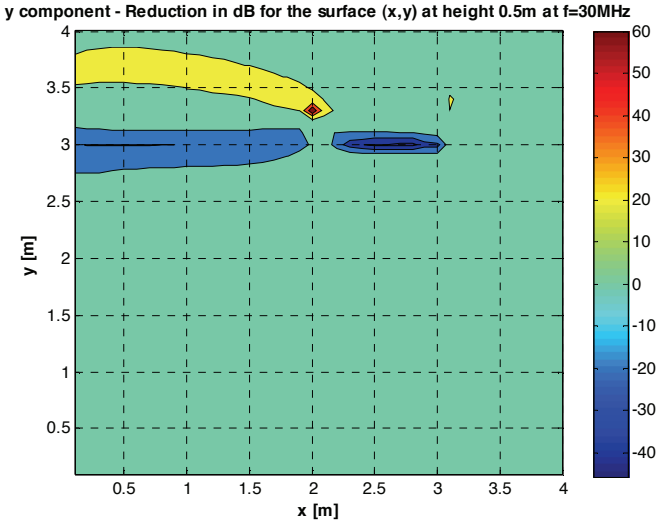

(b)

Figure 6-12 - Attenuation of the y-component of magnetic field when the compensation is applied to the z-component. (a) f=15MHz and (b) f=30MHz

Table 6-2 presents the average attenuation for the three magnetic field components in the considered surface at two different heights, 0.5 and 1 m. The overall average attenuation of the mitigation technique ranges from 12 to 24 dB.

Table 6-2 - Table with average reduction over the surface at 15MHz and 30MHz

f [MHz]	Surface at height of 0.5m			Surface at height of 1m		
	x [dB]	y [dB]	z [dB]	x [dB]	y [dB]	z [dB]
15	23.16	20.64	21.05	24.62	24.92	23.84
30	13.28	12.76	12.91	13.64	13.29	14.38

6.2.3 Influence on the channel capacity [10]

If mitigation measures are used to bring emissions to levels below EMC limits, they can be used to increase the Shannon capacity of PLC systems by making use of the gained margin to increase the signal to noise ratio.

It is possible to estimate the capacity gain if one assumes that the signal to noise ratio over the whole frequency band of interest remains much greater than zero. To see this, let us write Shannon's capacity formula [12].

6-3 $$C = \int_{BW} log_2(1 + \frac{S}{\Gamma N}) df$$

where C is the capacity in bits per second, SNR is the signal to noise ratio at the receiver end, BW is the used frequency band, and Γ is used to account for imperfect coding, added margin, impulsive noise, etc.. Interestingly, the capacity of a channel is strictly independent of the selected modulation.

In the absence of crosstalk, an increase in the signal by a factor M_g leads to an equivalent gain in the signal to noise ratio. Using this factor, the capacity can be rewritten as,

6-4 $$C' = \int_{BW} log_2(1 + \frac{M_g S}{\Gamma N}) df$$

where C' is the new capacity including mitigation.

The case where $\frac{S}{\Gamma N} >> 1$ will be considered first. Using this condition, equation 6-4 can be rewritten as

6-5 $$C' \cong \int_{BW} log_2(\frac{M_g S}{\Gamma N}) df = \int_{BW} log_2(M_g) df + \int_{BW} log_2(\frac{S}{\Gamma N}) df$$

Now, recognizing that the second term on the right hand side equals the capacity prior to mitigation (for $\frac{S}{\Gamma N} >> 1$), we can write

6-6 $$C' \cong C + \int_{BW} log_2(M_g) df$$

in which the second term allows the mitigation gain to be readily estimated as,

6-7 $$\Delta C \cong \int_{BW} log_2(M_g) df$$

If it is assumed further that M_g is constant over the range of frequencies of interest, we can estimate the capacity gain with a bandwidth of 20 MHz:

Table 6-3: Approximate capacity gain as a function of the signal to noise increase for a 20MHz bandwidth

Mg [dB]	Capacity gain [Mbits/s]
2	13
4	26

6	39
8	53
10	66

We will now apply the same procedure using power and noise models that are more representative of real PLC networks [9]. We will assume an indoor PLC network with a -50 dBm/Hz transmission PSD mask. We will further assume a residential environment and we will use the following function to model the noise [13]

6-8 $$\mu_N = a1 \cdot exp(-k \cdot f) + a2$$

where μ_N is the mean noise level in dBm, measured with 30kHz bandwidth, f is the frequency in MHz and a_1, a_2 and k are coefficients whose values, $a_1 = 502$, $a_2 = 601$ and $k = 0.001$, are based on statistical experimental measurements as illustrated in Figure 6-13.

The function used to represent the noise in [dBm/Hz] including the 30kHz measurement bandwidth is given by:

6-9 $$N[dBm/Hz] = a1 \cdot exp(-k \cdot f) + a2 - 10\log(30kHz)$$

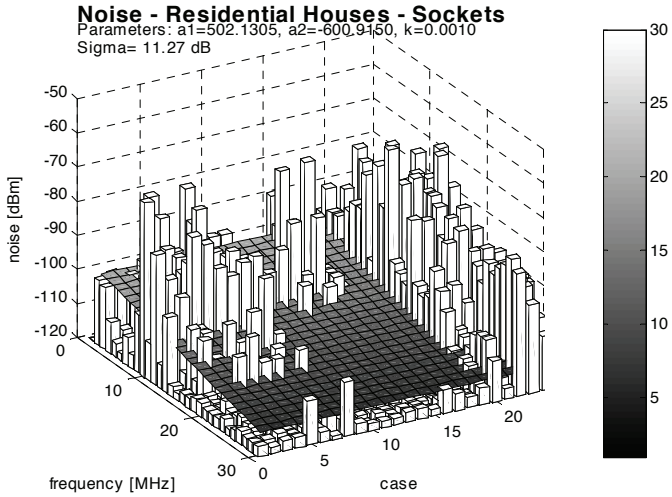

Figure 6-13: Exponential model of noise measured at the wall sockets of residential houses

The attenuation will be modelled using the function

6-10 $$\mu_A = b1 \cdot f + b_2$$

where b_1 and b_2 are coefficients with units of dB/MHz and dB, respectively. As shown in Figure 6-14, the experimentally measured mean values for the parameters are $b_1 = 0.596$ and $b_2 = 45.315$.

The signal at the receiver is therefore given by:

6-11 $$S[dBm/Hz] = -50\,dBm/Hz - b1 \cdot f - b_2$$

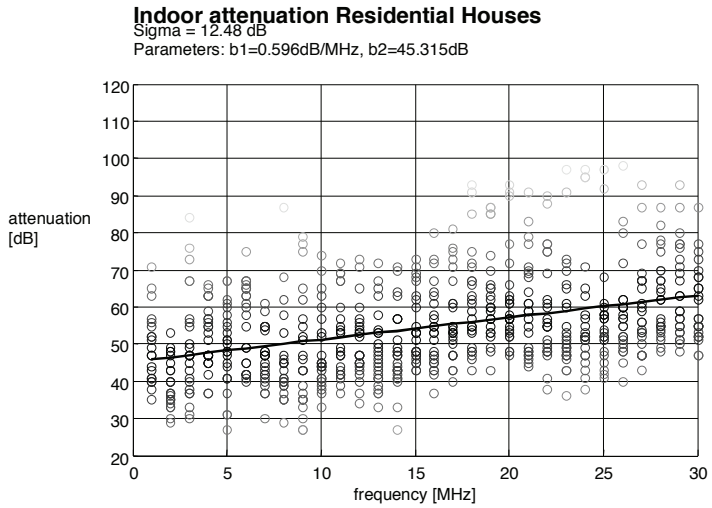

Figure 6-14: Indoor attenuation for residential houses

The capacity gain can be calculated by introducing equations **6-9** and **6-11** into equations 6-4 and 6-6 and comparing the results for different values of M_g. Using the same values of M_g as in Table 6-3, and assuming $\Gamma = 30$ in equations 6-3 and 6-4 and, we obtain the values for the capacity gain given in Table 6-4:

Table 6-4: Capacity gain as a function of the signal to noise increase for realistic attenuation and noise models

Mg [dB]	Capacity gain [Mbits/s]
2	12
4	24
6	36
8	48
10	60

From Table 6-3 it can be seen that the capacity of the channel can indeed be increased by up to 66 Mbps for mitigation efficiencies of only 10 dB.

6.3 Notching [14]

6.3.1 Description

Notches can be used to avoid interference between PLC networks and other services, such as amateur radio or broadcasting services that operate in the same frequency bands. A PLC system with sufficient notching capabilities can leave out the frequencies that are already occupied by other services, thus ensuring peaceful coexistence with those services.

Although turning off sub-carriers ensures that PLC will not interfere with services using the corresponding frequencies, it is sometimes desirable to use finite notch depths in

order to allow the use of the attenuated frequencies for data transmission while decreasing the disturbances at the given frequencies.

As mentioned before in chapter 2, the OPERA system uses OFDM with 1536 subcarriers. Notches are created by attenuating or turning off those OFDM sub-carriers that fall in the exclusion band, thus eliminating the energy transmitted in those bands.

A notch is defined by the following parameters:

- Effective width: The required notch width for a given service (e.g. 10kHz for an AM radio station)
- Total width, the width needed to realize the effective notch
- Depth, the attenuation the notch introduces in the PSD of the Powerline signal

The definition of the notch parameters is illustrated in Figure 6-15.

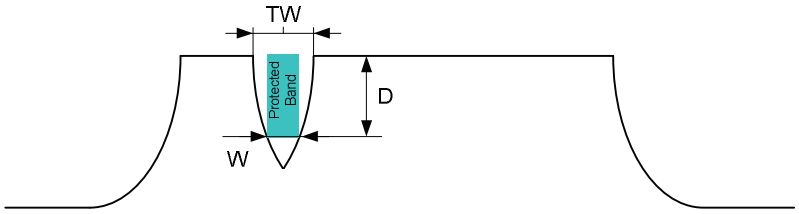

W = Required Width of Notch with a defined Depth
D = Required Depth of Notch
TW = Coresponding Total Width

Figure 6-15: Notch parameters

The number of notched frequency bands and their characteristics, such as the center frequency, width and depth, will be determined in each country by the competent regulator agencies. The center frequencies will coincide with those occupied by existing services.

Both laboratory and field measurements were performed to verify the efficiency of EMC mitigation mechanisms in radio amateur and broadcast radio bands.

6.3.2 Laboratory measurements

During the lab measurements, the PSD of the modem during data transmission was assessed. The results allow the evaluation of the active notches and relevant parameters.

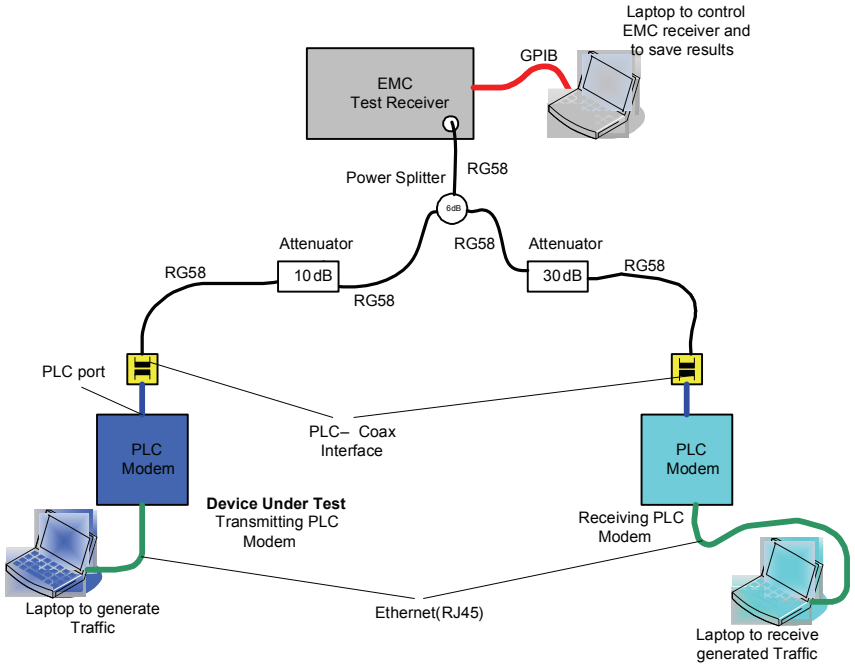

Figure 6-16 Laboratory notch measurement setup

The laboratory notch measurement setup is shown in Figure 6-16.

The measured values need to be corrected by the attenuation introduced by the power splitter and a value introduced by the attenuator (in our case 10dB) in order to get the absolute values of the PSD. Insertion losses due to the PLC-Coax interfaces and the losses in the coaxial cables should also be measured and used to obtain the transmitted PSD.

Modems manufactured by CTI (Current Technologies) were used for the lab measurements. The PLC modems under test were set to transmit at maximum signal level and at maximum traffic capacity to maximize the effect of notching on the throughput of each subcarrier. This is so since notching sub-channels that are already transmitting a small number of bits per utilization would have a negligible influence.

Three frequency bandwidths were considered, 10MHz, 20MHz and 30MHz. As mentioned before, the OFDM symbol uses 1536 subcarriers independent of the frequency bandwidth used. That makes carrier spacing dependent on the used frequency band.

All carriers are always evenly spread over the used bandwidth and the carrier central frequency can be calculated as:

6-12

$$f_{cn} = f_s + n \cdot \frac{BW}{1536}$$

where:

- f_{cn} is the central frequency of the specific carrier
- f_s is the start frequency of the used band
- BW is the used bandwidth

- n is the number of a specific carrier

The aim of the measurements was the assessment of the efficiency of notching in modems based on the OPERA specification. The system is limited in the maximum attenuation level that can be achieved by notching a certain number of carriers. The procedure that we adopted here for each frequency band was to start by notching the minimum number of carriers (4) and to notch one additional carrier at a time until we attained the maximum achievable attenuation level. The minimum number of carriers that we needed to switch off to achieve that attenuation was the parameter that sought. The procedure is schematically presented in Figure 6-17, Figure 6-18 and Figure 6-19.

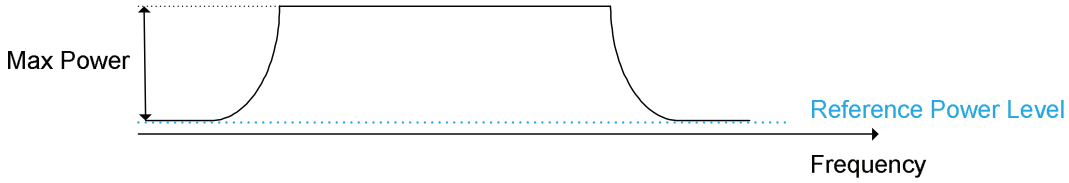

Figure 6-17: Notch parameters: Case without notches

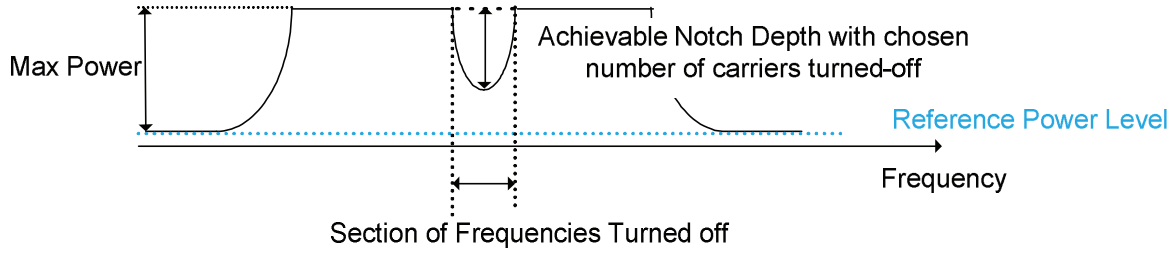

Figure 6-18 Achievable notch depth when selected number of carriers turned-off

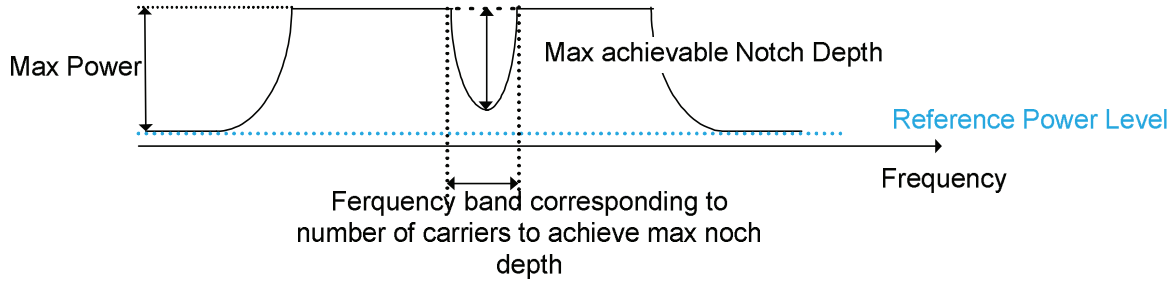

Figure 6-19 Maximum achievable notch depth

For each of the measurements for a specific frequency band we used the appropriate settings of the EMC receiver, given in general as:

- Start Frequency = Central frequency of the chosen start carrier
- Stop frequency = Central frequency of the chosen stop carrier
- Step = Carrier spacing
- Measurement Time = 100ms
- Bandwidth = 10kHz (it was not possible to change this setting)

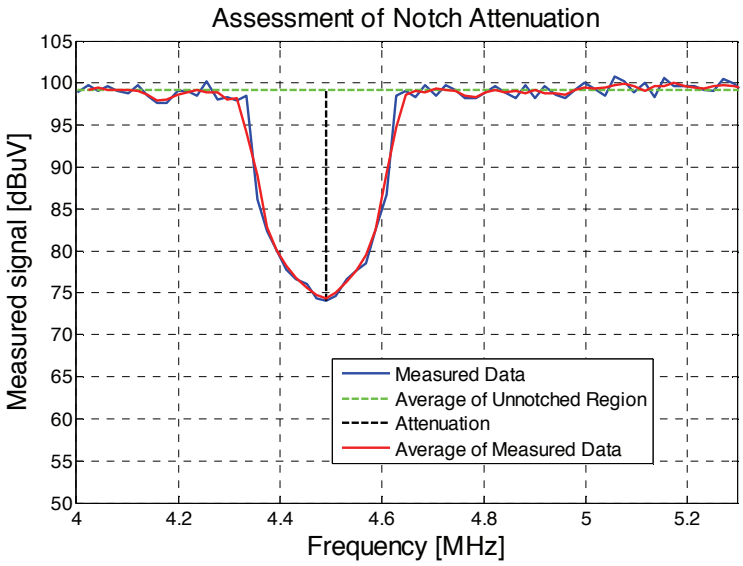

Figure 6-20 Example of the calculation of the attenuation for a given number of carriers (Remark: The 100 dBμV transmission level used as a basis for this simple evaluation is only an example)

In Figure 6-20, the blue line represents the measured PLC transmitted signal, the red line is the average of the measured data and the green line represents the average of the PLC signal level corresponding only to the unnotched carriers. The PSDs in Figure 6-20 were corrected for the attenuations due to the power splitter and the 10-dB attenuator. Our measurements showed that the coaxial cable did not introduce any appreciable attenuation.

The value at which the PLC signal hits its minimum is considered to be the maximum attenuation point. From this point up to the green average line, we calculated the notch depth for the given number of notched carriers.

By applying the same procedure systematically for the three frequency bands of interest, 10MHz, 20MHz and 30MHz, we obtained the data represented graphically in Figure 6-21, Figure 6-22 and Figure 6-23. From these figures the minimum number of carriers to be switched-off in order to achieve the maximum achievable attenuation can be measured.

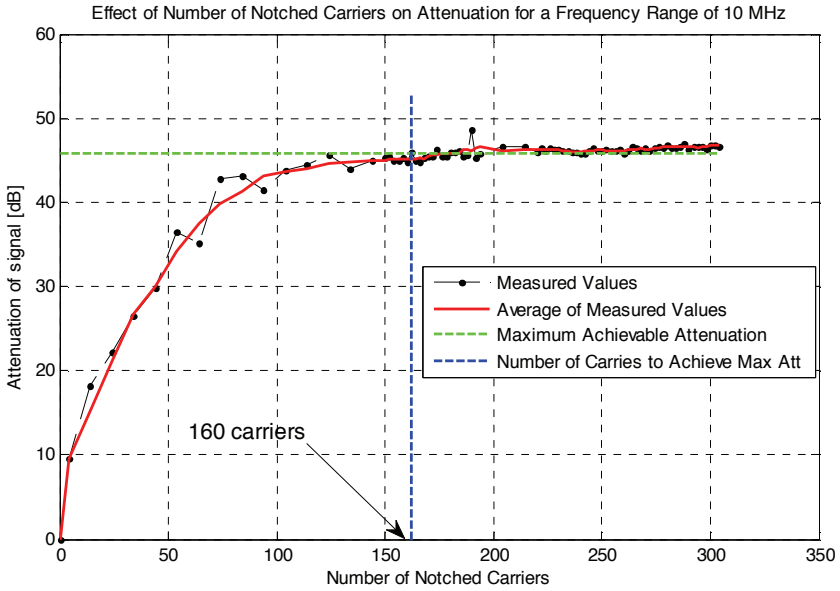

Figure 6-21 Effect of the number of notched carriers on the attenuation of the PLC signal for the frequency band of 10MHz

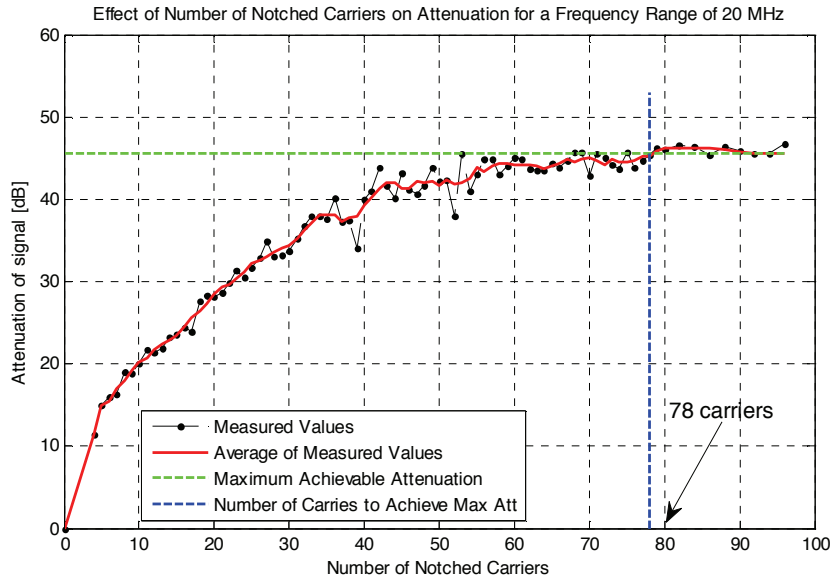

Figure 6-22 Effect of the number of notched carriers on the attenuation of the PLC signal for the frequency band of 20MHz

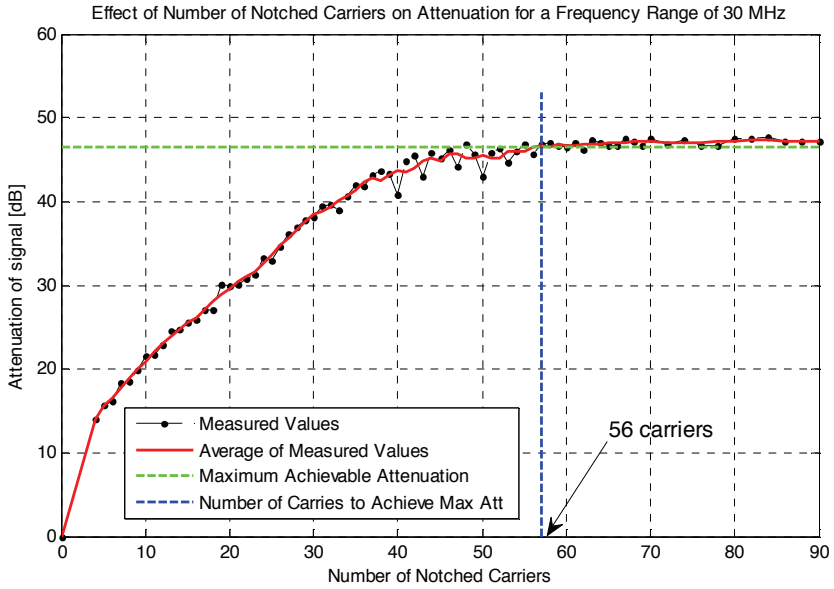

Figure 6-23 Effect of the number of notched carriers on the attenuation of the PLC signal for the frequency band of 30MHz

In Figure 6-21, Figure 6-22 and Figure 6-23, the black dotted line represents the resulting attenuation values obtained using the method described in Figure 6-20 as a function of the number of notched carriers. The moving average of these measured values is presented in red. The value of the maximum attenuation (green line) is the value at which the attenuation function stabilizes. The minimum number of carriers at which this attenuation value is obtained is represented by the blue line.

The maximum achievable attenuation for all three frequency bands was around 45 dB.

The minimum number of carriers needed to obtain this attenuation for the chosen band, times the carrier spacing for that band, gives the value that should be added to the effective notch width to obtain the total notch width (see Figure 6-15).

One can estimate the number of notched sub-carriers needed to obtain a notch with specified characteristics (effective notch width, notch depth and the selected frequency bandwidth) using the results obtained above. To this end, one begins by estimating, from Figure 6-21, Figure 6-22 and Figure 6-23, the number of notched sub-carriers needed to achieve the desired depth. This number is then added to the number of carriers that will actually constitute the effective width of the notch. The formulas to calculate the real effective and the total notch width are given by equations 6-13, 6-14 and 6-15 and the calculated values for the three frequency bands in Table 6-5 and Table 6-6.

6-13 $$W_{total} = n_{min} * CS + W_{effective}$$

where:

- W_{total} is the total notch width
- $W_{effective}$ is the effective notch width
- n_{min} is the minimum number of subcarriers that have to be notched and

- CS is the carrier spacing.

Table 6-5: Values to be added to the effective notch width to obtain the total notch width in the case of 45dB attenuation, for all three bands

	Min No of Carriers (from FIGURE 6-21, FIGURE 6-22 and FIGURE 6-23)	Carrier Spacing	Frequency band to be added
10MHz	160	6.5kHz	1.09MHz
20MHz	78	13.0kHz	1.02MHz
30MHz	56	19.5kHz	1.04MHz

6-14 $$RW_{effective} = n * CS$$

In equation 6-14 symbols represent:

- $RW_{effective}$ - real effective notch width
- n - number of carriers in effective notch width
- CS - carrier spacing.

6-15 $$W_{total} = RW_{effective} + FB$$

In equation 6-15 symbols are:

- W_{total} - total notch width
- $RW_{effective}$ - real effective notch width (see Table 6-6)
- FB - frequency band to be added

Table 6-6: Real effective notch width values

	Effective notch width	No of Carriers in Effective Notch Width - rounded	Real Effective Notch Width
10MHz	10kHz	2	13.0kHz
	100kHz	15	97.7kHz
	1MHz	153	996.1kHz
20MHz	10kHz	1	13.0kHz
	100kHz	8	104.2kHz
	1MHz	77	1002.6kHz
30MHz	10kHz	1	19.5kHz
	100kHz	5	97.7kHz
	1MHz	50	976.6kHz

6.3.3 Field measurements

6.3.3.1 Field trials - LINZ STROM (Linz, Austria)

The selected area for the trial implementation was Altenberg bei Linz, which is located in north of the city of Linz, Austria. Altenberg is a village in a rural area. The density of the housing and customers is low and the distances as well as the cabling are challenging in terms of reach and throughput.

In the area of Altenberg, the two transformers of interest are equipped with fibre optics as backbone connection. These are connected to a 100 Mbps switch port on the backbone network of LINZ STROM. In the transformer stations, a media converter provides a 100 Mbps Ethernet connection directly (see Figure 6-24).

The network is split by using different VLANs into the user part (all traffic generated by the customers) and the management part (traffic to remote-control, configure, monitor and assess the system).

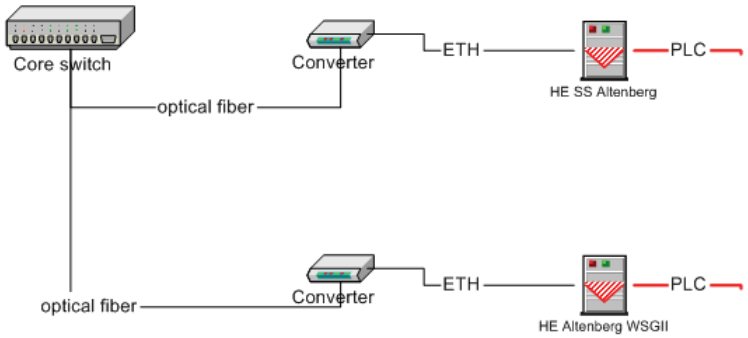

Figure 6-24 - LINZ – Backbone connection schematic – Altenberg

In the PLC system in Linz, the notches are already implemented for the chosen frequencies. The currently notched frequencies are:

- from 3.500 MHz to 3.800 MHz
- from 7.000 MHz to 7.200 MHz
- from 10.100 MHz to 10.150 MHz
- from 14.000 MHz to 14.350 MHz
- from 18.068 MHz to 18.168 MHz
- from 21.000 MHz to 21.450 MHz
- from 24.890 MHz to 24.990 MHz
- from 28.000 MHz to 29.700 MHz

The nominal depth of each notch is the maximum achievable, which is, in this case, around 30 dB, as given by the OPERA specification.

For each measurement point, the three components of the magnetic field as well as the vertical electric field were measured.

The measurements were performed for three different network states:

1) without active PLC signal;

2) with active PLC signal but no notches;

3) with active PLC signal and notches implemented.

The set-up used for the magnetic and electric field measurements is shown in Figure 6-25. A monopole antenna (EMCO, model 3301B) was used for the electric field and a loop antenna (Rhode & Schwarz, 9kHz-30MHz) for the magnetic field measurements.

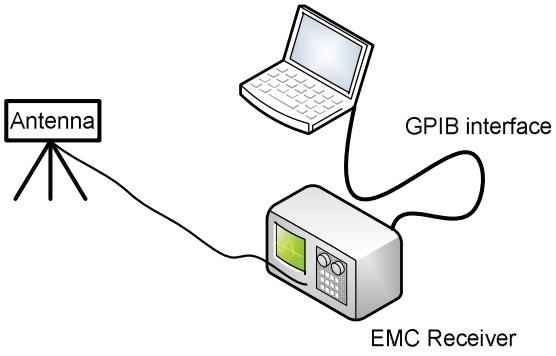

Figure 6-25 Measurement set-up for the field measurements

The EMC test receiver, a Rohde&Schwarz 9kHz-30MHz ESHS10, was operated by a laptop computer connected to it via the GPIB interface.

Here, the representative measurements of the magnetic field at a 1m distance from different injection points in a real network installed for the field trials in Linz are presented. In addition, they are compared to data reproduced in the laboratory.

To clearly show the effective notch depth, the difference between the measured magnetic field strengths with and without the power mask was determined. This difference for two measurement points, MP2 and MP9, is presented in Figure 6-28, Figure 6-32 and Figure 6-33, for the frequency band of interest. The locations of MP2 and MP9 are shown in Figure 6-26 and Figure 6-27.

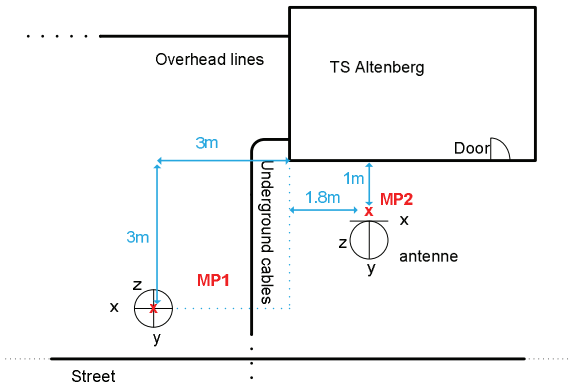

Figure 6-26: The location of MP92 near the transformer station

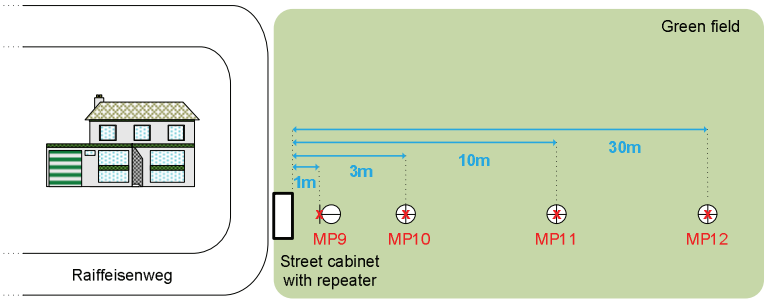

Figure 6-27: The location of MP9 near the street with integrated repeater, occupied indoor and outdoor frequencies

Figure 6-29, Figure 6-30 and Figure 6-31 present a zoom of each notch for the case of MP2 and Figure 6-32 and Figure 6-33 for the case of MP9.

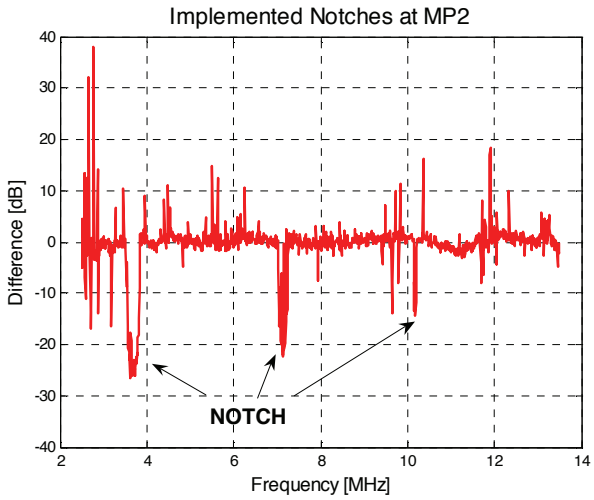

Figure 6-28 Effective notch depth obtained in the field measurements for MP2

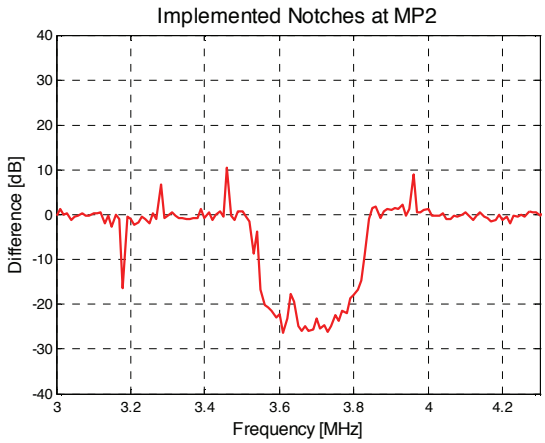

Figure 6-29 Zoom of the notch defined from 3.5MHz to 3.8MHz, measured at MP2

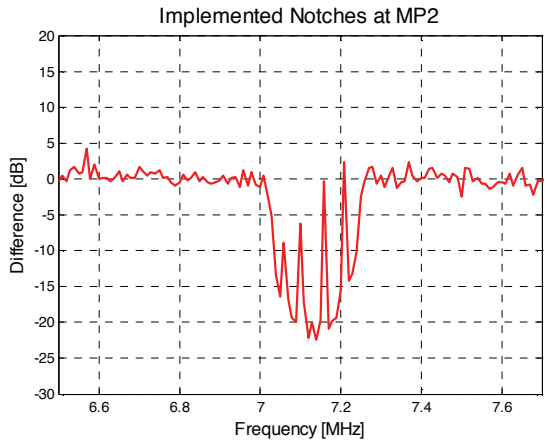

Figure 6-30 Zoom of the notch defined from 7MHz to 7.2MHz, measured at MP2

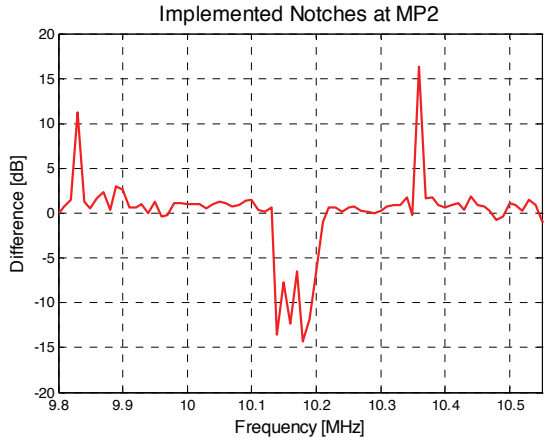

Figure 6-31 Zoom of the notch defined from 10.1MHz to 10.15MHz, measured at MP2

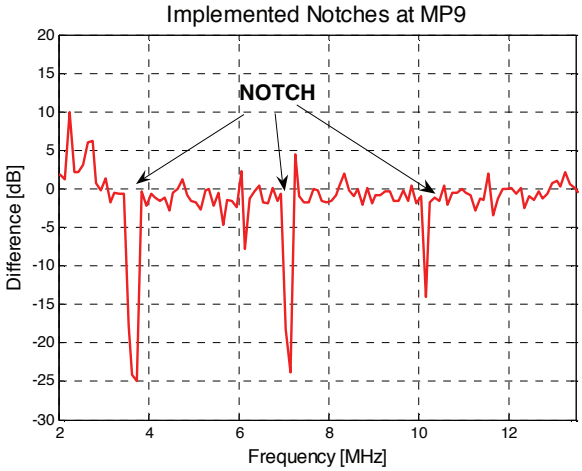

Figure 6-32 Effective notch depth obtained in the field measurements for MP9, lower frequency band (outdoor frequencies)

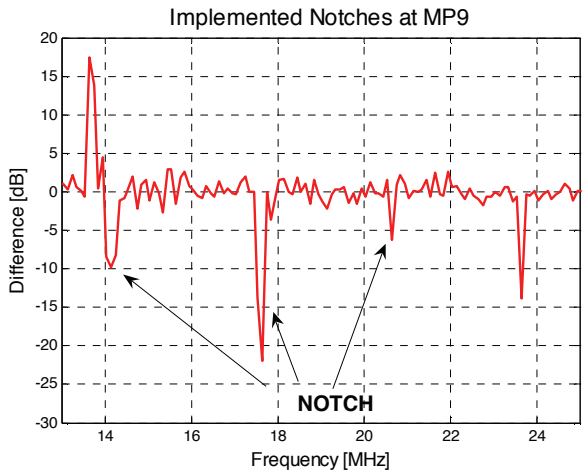

Figure 6-33 Effective notch depth obtained in the field measurements for MP9, higher frequency band (indoor frequencies)

Although all the notches have been defined for a 30-dB depth, it can be seen that the effective depth varies from one case to another. This may be explained by different facts. First, these notches are defined in frequency bands occupied by different services (among which broadcast stations). Some of these services have transmitting power levels that can be as high as, or even higher than, the gap created by the notch. Second, different notch widths may influence the effective depth of the notch.

Even the very narrow notches can be observed, as seen, for example at around 10MHz in Figure 6-31.

All the notches implemented in different parts of the system at outdoor frequencies are present in these figures. For example, in Figure 6-28 and Figure 6-32, the notches at frequencies:

- 3.5MHz-3.8MHz
- 7MHz-7.2MHz
- 10.1MHz-10.15MHz

are readily observable.

The same is true for the notches at frequencies:

- 14MHz-14.350MHz
- 18.068MHz-18.168MHz
- 21MHz-21.45MHz

for the indoor frequency band, which can be observed in Figure 6-33. The notches in the indoor frequency band, at frequencies of:

- 24.890MHz-24.990MHz
- 28.000MHz-29.700MHz

cannot be identified since the signal strength is very low around those frequencies.

In the case where the interferer is much smaller and narrower than the notch in the power mask and the total notch width corresponds to that needed to reach the desired

depth, the characteristics of the measured notch match those obtained from LINZ AG reasonably well. As an example, the notch in Figure 6-29 has a measured width of about 300 kHz and a depth of about 26 dB.

In order to evaluate a possible frequency dependence of notch depth, a set of identical, equally distanced notches over the complete 30-MHz frequency band were implemented in the lab. To clearly show the effective notch depth, the difference between the transmitted power with and without the notched power mask was calculated. This difference is presented in Figure 6-34.

As evidenced in Figure 6-34, the lab measurements did not show any frequency dependence of notch depth.

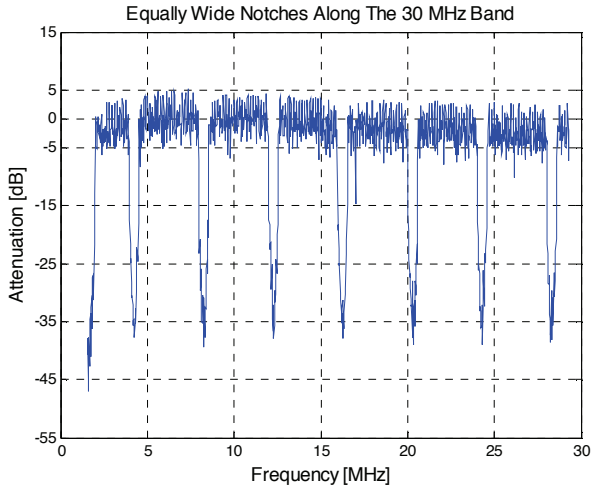

Figure 6-34 Equally distanced and equally wide 30 carrier notches implemented along the 30 MHz PLC operating band

In Figure 6-35 and Figure 6-36, the notches measured during the field trial in Linz are compared to the same notches measured in the laboratories of the EPFL.

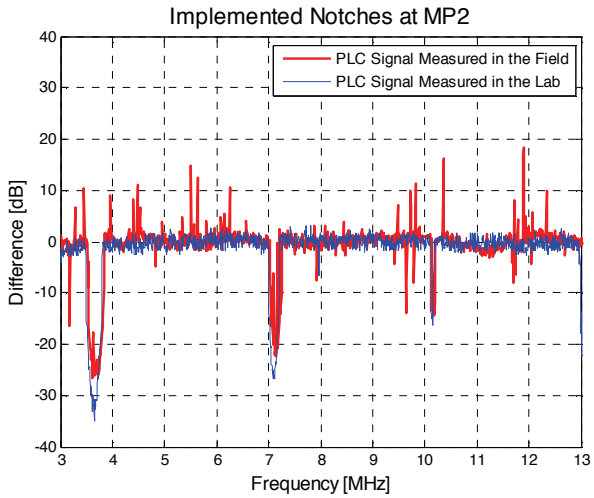

Figure 6-35 Comparison of the notches measured in the field at MP2 with those reproduced in the lab

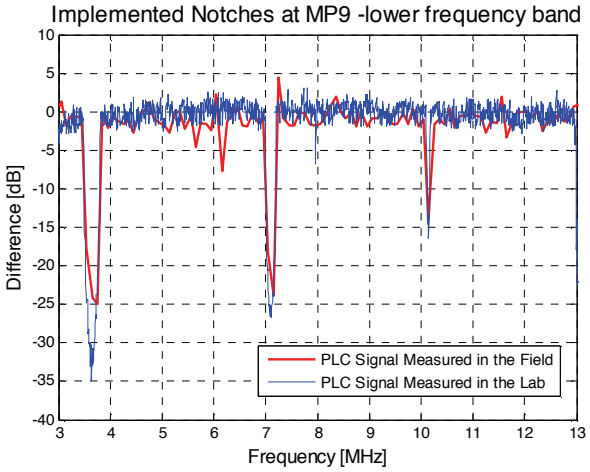

Figure 6-36 Comparison of the notches measured in the field at MP9 with those reproduced in the lab

As can be seen from Figure 6-35 and Figure 6-36, the notches measured in the field correspond well to those reproduced in the lab. The difference in depth can be explained by the fact that the notches in the field were measured in a noisy environment and that their depth could therefore be influenced by that noise, as mentioned before.

The depth of the notches measured in the lab does not always correspond to the desired value of 30 dB since, as explained before, one needs to notch a certain minimum number of carriers for a certain frequency band to achieve a specified notch depth.

6.4 Conclusions

We presented a technique [3] that has been proposed to achieve a reduction of emissions associated with indoor PLC networks through the introduction of a 180^{o} out-of-phase replica of the PLC signal into the unused neutral-ground circuit. We also proposed a modification to this technique based on the selection of the appropriate amplitude and phase of the auxiliary signal.

Theoretical considerations suggest that the improved technique can be effective in the reduction of emissions for a given observation point and considering a single field component. However, an effective strategy is needed for its application to real cases taking into account technical and economical constraints. In this chapter, we have proposed and studied a way of implementing this technique, namely the integration of a required antenna into the PLC modems themselves. The measured fields very close to the modem allow the determination of the magnitude and phase of the compensation voltage. The proposed implementation should be used only when a customer files a complaint, when emissions should be lowered at locations where PLC signals might cause unwanted interferences or when additional capacity is required and it can be obtained through the gained signal to noise margin.

Although, in principle, due to nonalignment of the wanted and the compensation field directions, minimizing one component of the field may result in an increase of the other components, we have shown here that the application of the technique results in an overall average reduction of 10-20 dB of all the field components in the region of interest.

We addressed the more general issue of the application of mitigation techniques' gained emissions margin to increase the overall throughput of PLC systems. We showed that an increase in the signal power (made possible by the inclusion of mitigation techniques) leads to a considerable increase in the PLC channel capacity. Using a number of simplifications, we showed that the capacity of the channel can indeed be increased by up to 66 Mbps for mitigation efficiencies of only 10 dB. To test the applicability of the used approximations and to explore a more realistic scenario, we also used measurement-based attenuation and noise models developed in the framework of the OPERA project [13] to recalculate the expected capacity gain. The results showed good agreement with the simplified calculations. The capacity gain in this case is 60 MHz for a 10-dB mitigation attenuation.

We also showed the results of laboratory measurements aimed at studying, under controlled conditions, different characteristics of notching in OPERA PLC modems, such as total and effective notch width, notch depth, maximum notch depth, etc. These measurements showed that it is possible to obtain attenuations of up to about 45 dB for notches in all frequency bands, 10MHz, 20MHz and 30MHz. What differs for these three bands is the minimum number of carriers that need to be notched to obtain that maximum attenuation. This is an important point, since, to implement notches that have the required depth and width, one must know how many subcarriers to suppress and how deep these need to be reduced.

In addition to the laboratory measurements, we made field measurements that showed that the expected notch characteristics are also present in real PLC systems. As can be seen from Figure 6-35 and Figure 6-36 the notches measured in the field correspond well to those reproduced in the lab. Apparent differences between the expected and the measured notch depths at some frequencies can be explained by the fact that the notches in the field are often measured in the presence of the very narrowband interferers that the notches are there to avoid. These interferers can fill the notches and make them appear shallower.

REFERENCES

[1] R.P. Rickard, Power Line Communications, Patent WO98/06188 and US6785532, 12 February 1998.

[2] R.P. Rickard, Coupling communications signals to a power line, Patent US6037678, 14 March 2003.

[3] Deliverable 8: “Report on EMC Aspects of PLC Technology”, IST Integrated Project No 507667. Funded by EC , November 2005

[4] OPERA technology White Paper, OPERA. IST Integrated Project No 507667. Funded by EC ,February 2006

[5] N. Korovkin, E. Marthe, F. Rachidi, E. Selina, "Mitigation of electromagnetic field radiated by PLC systems in indoor environment", International Journal of Communication Systems, Vol. 16, pp. 417-426, May 2003.

[6] E. Marthe, N. Korovkin, F. Rachidi, A. Vukicevic, and F. Issa, "A technique electromagnetic field radiated by indoor PLC systems", 17th International Symposium on Electromagnetic Compatibility, Wroclaw, 29 June-1 July, 2004.

[7] E. Marthe, Power line communications : analyse des problèmes de compatibilité électromagnétique dans le domaine des courants porteurs en ligne, Ph.D. Thesis, Swiss Federal Institute of Technology, Lausanne, Thesis Number 3166, 2005.

[8] M. Rubinstein, J.-L. Bermudez, A. Vukicevic, F. Rachidi, M. Schneider, and E. Marthe, "Discussion on the assessment and mitigation of radiation from PLC networks," presented at 9th International Symposium on Power-Line Communications and Its Applications (ISPLC’05), Vancouver - Canada, 2005.

[9] M. Rubinstein, J.L. Bermudez, A. Vukicevic, F. Rachidi, M. Schneider, "On the mitigation of radiation from PLC networks" 28th General Assembly of International Union of Radio Science (URSI), New Delhi, India, October 23-29, 2005.

[10] A. Vukicevic, M. Rubinstein, F. Rachidi, J.L. Bermudez, ”On the impact of mitigating radiated emissions on the capacity of PLC systems”, 11th International Symposium on Power-Line Communications and Its Applications (ISPLC’07), Pisa - Italy, 2007.

[11] G. Burke and A. Poggio, "Numerical Electromagnetics Code - method of moments", Livermore CA: Lawrence Livermore National Laboratory, Report No. UCID-18834, 1981.

[12] Shannon, C.E. (1948), "A Mathematical Theory of Communication", Bell System Technical Journal, 27, pp. 379–423 & 623–656, July & October, 1948.

[13] Deliverable 5: “Pathloss as a function of frequency, distance and network topology for various LV and MV European powerline networks”, IST Integrated Project No 507667. Funded by EC, April 2005

[14] Deliverable 8: “EMC measurement report on efficiency of EMC mitigation mechanisms”, IST Integrated Project No 026920. Funded by EC , October 2007

[15] A. Vukicevic, A. Rubinstein, M. Rubinstein, F. Rachidi, “On the efficiency of notching technique to reduce EM radiation from PLC networks”, 12th International Symposium on Power-Line Communications and Its Applications (ISPLC’08), South Korea, 2008

Chapter 7

7 Multi-master deployment

High density Power Line Communication (PLC) deployment in a competitive commercial environment requires the increase of overall system data rate. The current solution for PLC deployment in low voltage (LV) networks is illustrated in Figure 7-1.

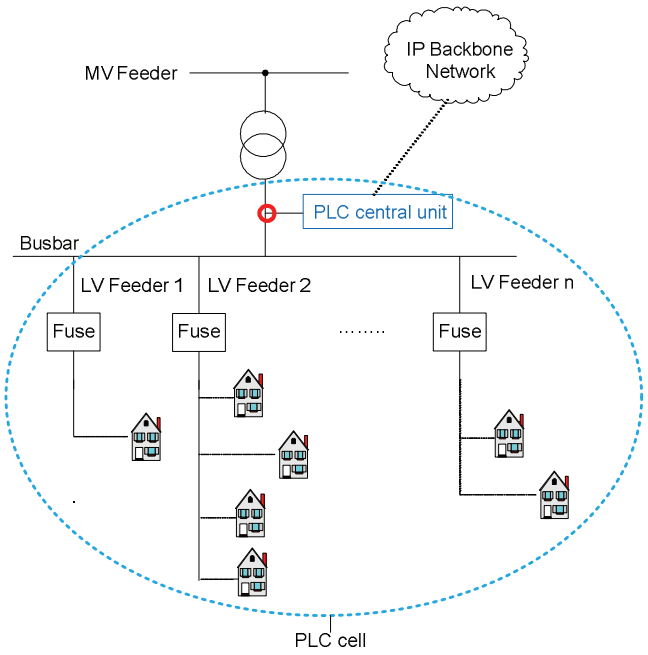

Figure 7-1: State of the art PLC access deployment network

In Figure 7-1, the IP Backbone cloud is connected directly to the single PLC central unit by way of an unspecified technology, which could be fiberoptics cable, satellite or other. With the current scheme, service is provided to all customers belonging to the same PLC cell by a single central PLC unit which is connected to the same LV busbar in the transformer station. This means that all customers share the available data bandwidth provided by the controlling unit.

An approach to increase the PLC cell's data rate is to divide the PLC cell into several PLC sub-cells in order to reuse the same frequencies in each one of them. Since each sub-cell uses its own Control Unit (CU) or master, the approach is called 'multi-master'. To avoid interference between the sub-cells, they need to be RF-isolated from each other. The separation of the LV feeders could be achieved by using RF blocking filters in each sub-cell as schematically presented in Figure 7-2. Note though that, since the feeder cables are physically close to one another, crosstalk between them is also a potential interference mechanism. The actual RF separation between the feeders depends therefore on the achievable attenuation of the cross-talk between LV feeders. The cross-talk between the feeders depends to a large extent on the separation distance between the cables and on the length of the section that these feeders run parallel to each other. The closer the cables are and the longer the section they run parallel to each other, the higher the cross-talk and the lower the possibility to use the multi-master approach on the feeders.

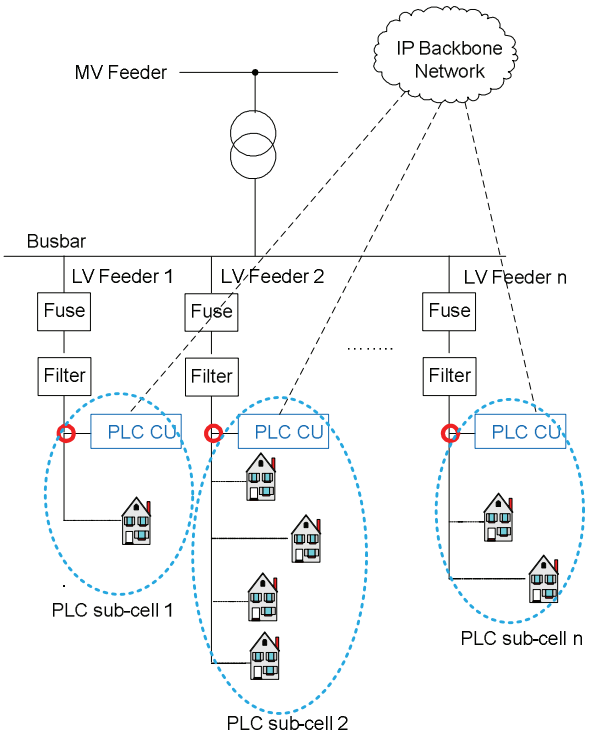

Figure 7-2: Proposed PLC access network deployment for higher data rate

To verify the general feasibility of multi-master deployment by using blocking filters, measurements on actual LV networks were performed.

7.1 Measurement configurations

The measurements were made in Saint Sulpice, a village close to the city of Lausanne, Switzerland.

In Figure 7-3, the LV feeders belonging to the same MV feeder are presented schematically.

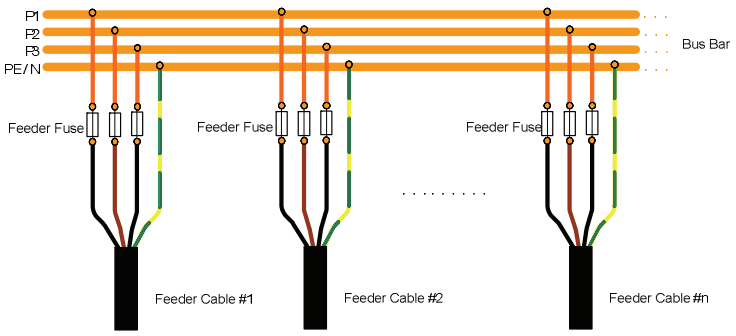

Figure 7-3: LV feeders belonging to the same MV feeder

We first made measurements aimed at assessing the minimum level of attenuation between the feeders, namely, the attenuation introduced by a busbar. The setup of these measurements is shown in Figure 7-4.

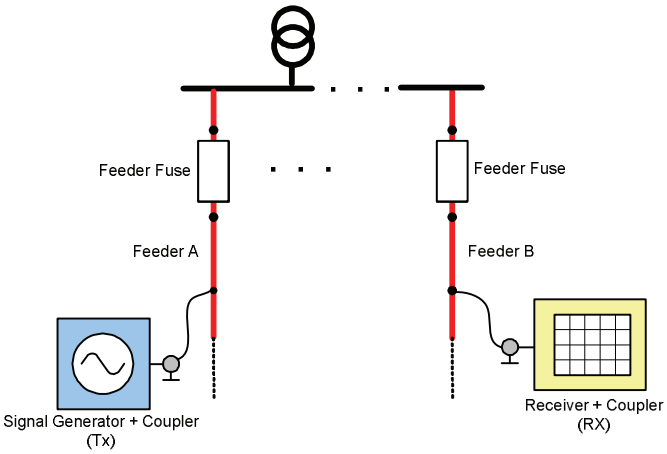

Figure 7-4: The schematic of the measurement configuration for the minimum (busbar) attenuation measurements

Crosstalk measurements were preformed between adjacent LV feeders. In this case, the feeders were separated from the busbar by disconnecting the fuses as shown in Figure 7-5. This second case with fuses disconnected corresponds to the simulation of an ideal blocking filter.

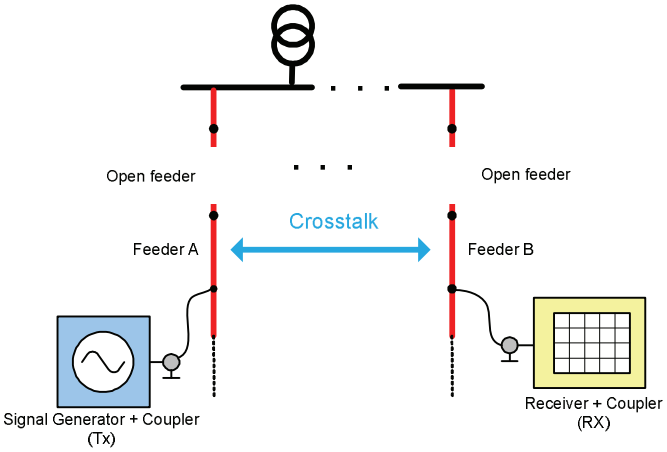

Figure 7-5: The schematic of the measurement configuration for the maximum (crosstalk) attenuation measurements

To ensure that these two measurements did not disturb existing customers, they were carried out using the configurations illustrated in Figure 7-6 and Figure 7-7. This is possible since the feeders can be supplied by two independent substations. The feeder is always supplied from only one side, but by removing or putting back the fuses, we could select the side the feeder was actually supplied from.

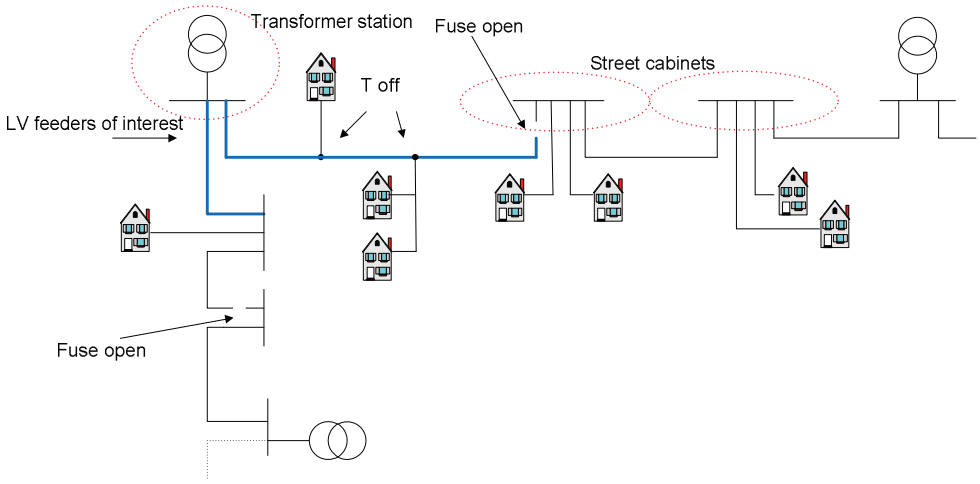

Figure 7-6: Configuration for minimum attenuation measurements

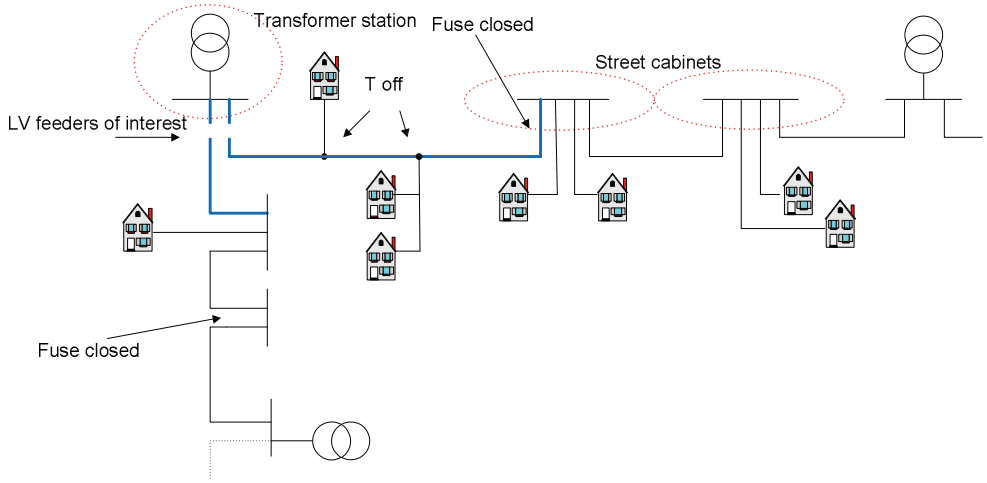

Figure 7-7: Configuration for cross talk measurements

7.2 Measurement set-up

It is convenient to define path attenuation as the insertion loss caused by the network between the standard 50 Ω reference planes 1 and 2 as shown in Figure 7-8. This definition includes the couplers into the PLC network [1]. The path attenuation is defined as:

7-1
$$A(f) = 10log_{10}\frac{P_{in}}{P_{out}} \quad [dB]$$

where $P_{in}(f)$ is the available source power at port 1 (input port) and $P_{out}(f)$ is the power at port 2 (output port) fed into the measurement receiver's nominal 50 Ω input. In general, both powers are a function of the frequency f. The available source power is the power measured by the measurement receiver directly connected to the source at reference plane 1.

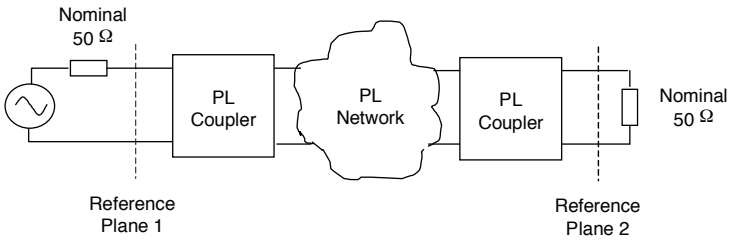

Figure 7-8: The definition of PL network attenuation

The crosstalk measurement method and the path attenuation method are identical. In both cases, we inject the signal on one of the feeders, between two phases and we measure the resulting signal between two phases (same combination of phases as well as different phase combination) for all the other feeders.

A channel sounder is used to inject the signal and a receiver is used to detect the signal. The transmitter and the receiver sides are presented in Figure 7-9 and Figure 7-10, respectively.

The measured frequency band is 1 – 30 MHz. For the crosstalk measurements, special care must be taken that no alternative signal path between the transmitter and the receiver exists.

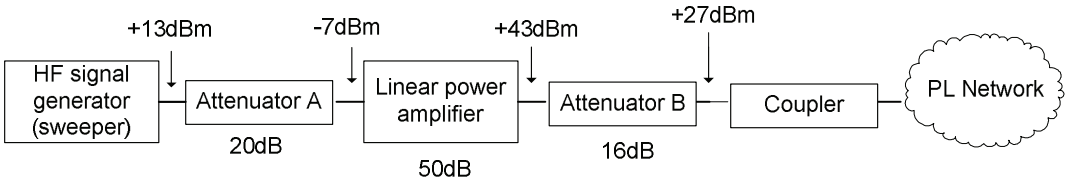

Figure 7-9: Transmitter: Measurement set-up at the injection side

The signal injected in the PLC network was a 27-dBm continuous sine wave sweeping through the frequency range of interest.

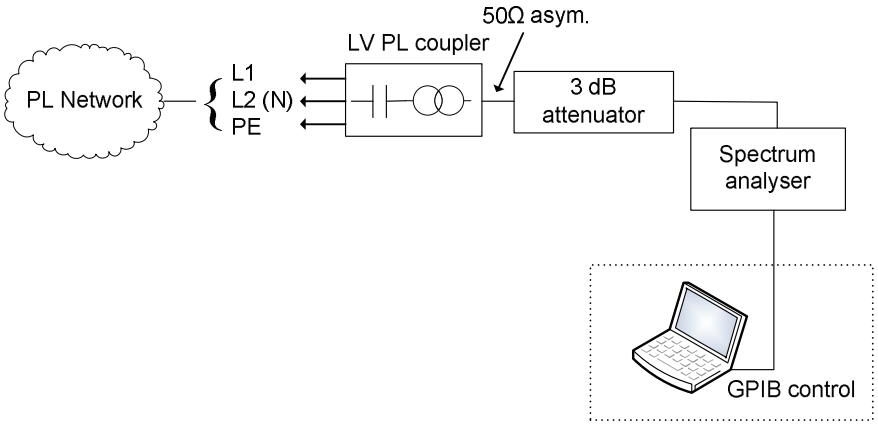

Figure 7-10: Receiver: Measurement set-up at the reception side

It is necessary to have the low voltage network topology schematics since we have to evaluate measurement results depending on topology.

7.3 Measurement results

Here, the values for three transformer stations are presented. The first transformer station had 8, the second one 6 and the third one 7 LV feeders. For technical reasons, we were only able to use some of them for our measurements. A comparison of minimum path attenuation values for these three substations is presented in Figure 7-11 and Figure 7-12. The minimum path attenuation takes into account only busbar attenuation and it was measured for a standard LV power network configuration. To inject the signal, into the input-side feeder, we used a capacitive coupler (the inductive coupler case will be presented later in this chapter).

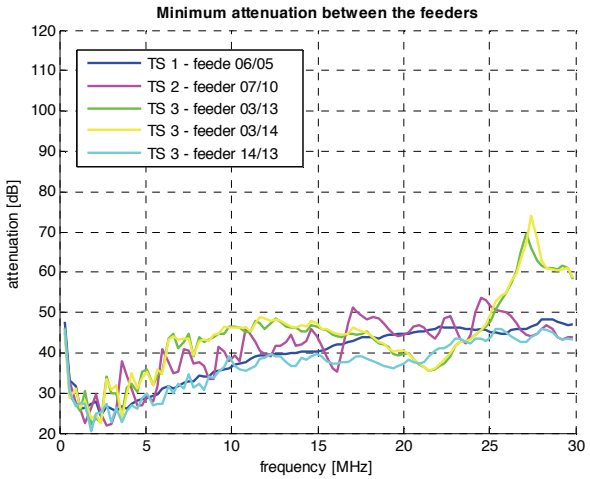

Figure 7-11: Comparison of minimum attenuation levels for different configurations in the case of capacitive coupling

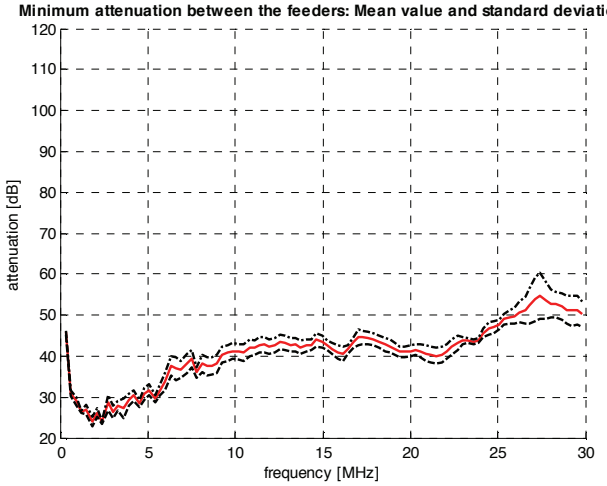

Figure 7-12: Average value and standard deviation of minimum attenuation levels for different configurations in the case of capacitive coupling

Figure 7-13 and Figure 7-14 show the crosstalk values for the same feeders. The chosen feeders were galvanically decoupled by removing the fuses that connect them to the busbar under normal operation. The signal was injected into one of them (again by using a capacitive coupler) and measured on the second one.

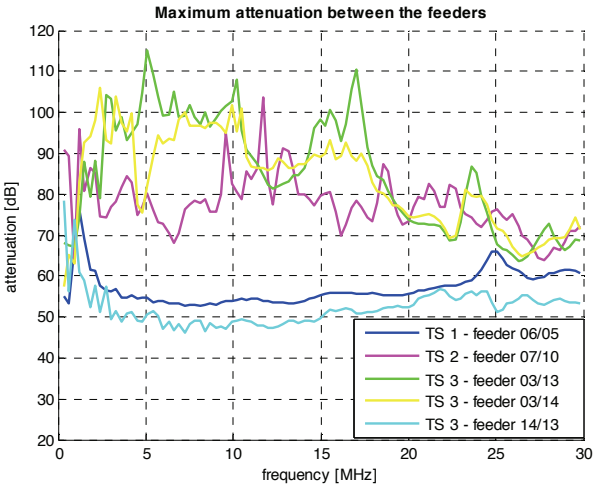

Figure 7-13: Comparison of maximum cross-talk attenuation levels for different configurations in the case of capacitive coupling

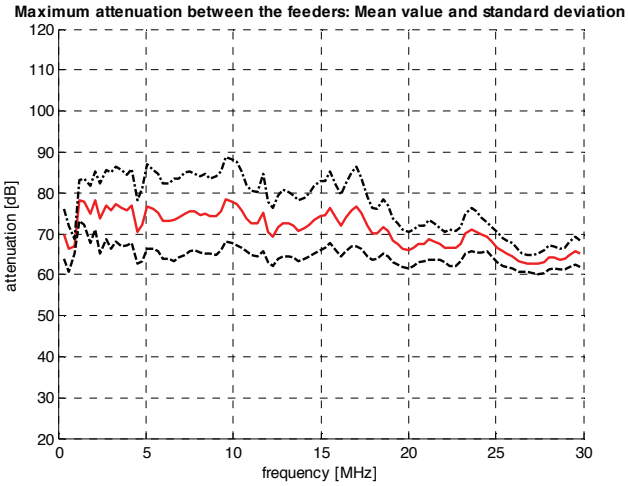

Figure 7-14: Average value and standard deviation of maximum cross-talk attenuation levels for different configurations in the case of capacitive coupling

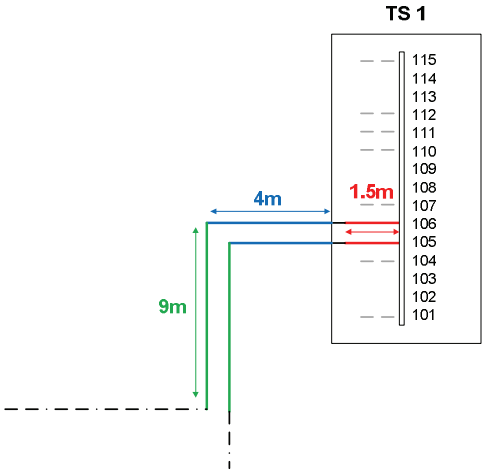

Figure 7-15: Schematics of the configuration of the TS1

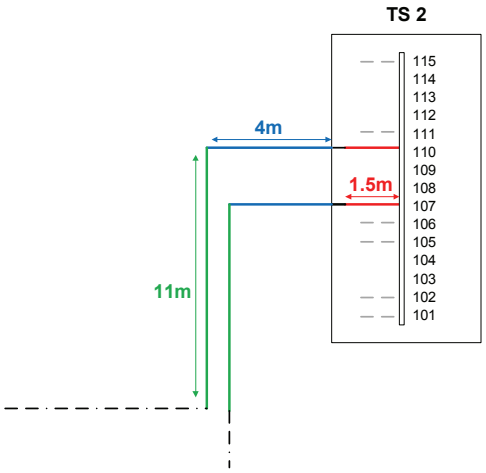

Figure 7-16: Schematics of the configuration of the TS2

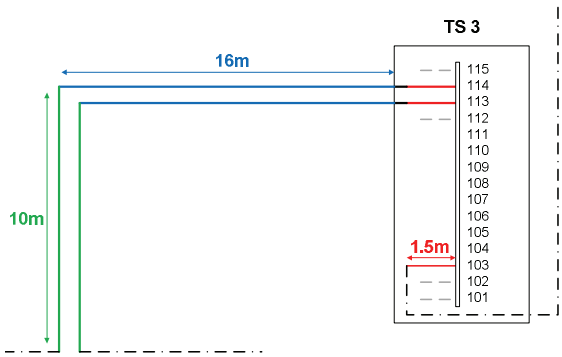

Figure 7-17: Schematics of the configuration of the TS3

The schematics of the configurations for three transformer stations of interest are presented in Figure 7-15, Figure 7-16 and Figure 7-17. It can be seen from these figures that each TS has 15 dedicated slots for feeders but not all of them are used. The unused slots are recognized by the absence of a line connected to them. The LV feeders that are connected but not used for our study are presented in gray dashed lines. The distance between adjacent slots is around 80 cm.

For all the transformer stations, the LV cables connected to the same busbar run in parallel for the first 1-1.5m. This length is represented by a red line in Figure 7-15, Figure 7-16 and Figure 7-17. Beyond this length, the feeder cables may continue in parallel or separate completely. The different sections that feeder cables run in parallel and their lengths are represented in Figure 7-15, Figure 7-16 and Figure 7-17 by blue and green lines. Other parts of the cable, not important for our study, are represented in dash-dotted lines.

A closer look at Figure 7-13 reveals a similarity between the shapes of the curves representing the maximum attenuation measured between the feeders 06 and 05 of transformer station 1 and the same curve for the feeders 14 and 13 of transformer station 3. A similarity can also be observed between the case of feeders 07 and 10 (transformer station 2), the case of feeders 03 and 13 (transformer station 3), and the case of 03 and 14 (transformer station 3).

Feeders 05 and 06 run parallel for around 15 m beyond the TS and feeders 13 and 14 for around 28 m.

For all the other cases, the feeders are not directly next to each other. As expected, the determinant factor in the crosstalk attenuation is the proximity of the cables.

If the fact that the feeders are next to each other in the TS is predominant over the fact that they run in parallel (which cannot be surely concluded from preformed measurements) than in most cases, we should consider the worst case scenario that maximum attenuation that we can have in the case of the capacitive coupling is around 50dB. This will be checked in further field measurements.

A comparison of the minimum path attenuation values for three substations for the case of inductive coupling is presented in Figure 7-18 and Figure 7-19. In Figure 7-20 and Figure 7-21, we present the maximum crosstalk attenuation for inductive coupling.

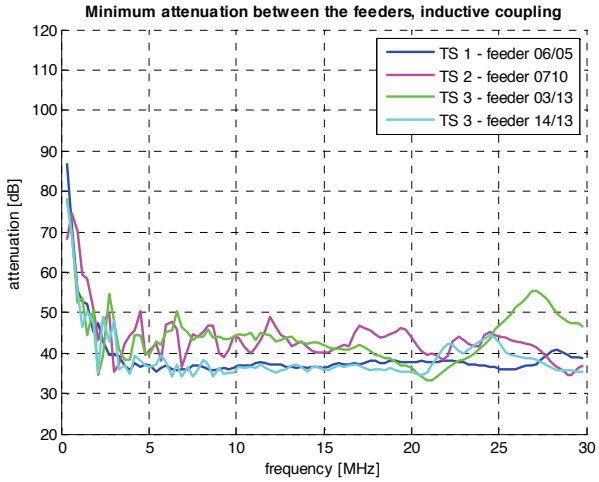

Figure 7-18: Comparison of minimum attenuation levels for different configurations in the case of inductive coupling

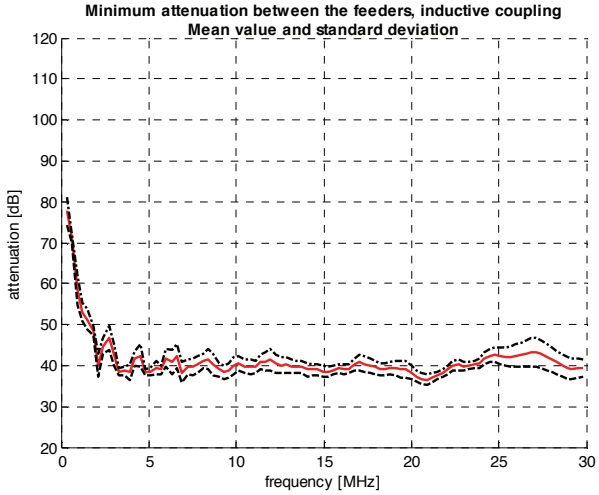

Figure 7-19: Average value and standard deviation of minimum attenuation levels for different configurations in the case of inductive coupling

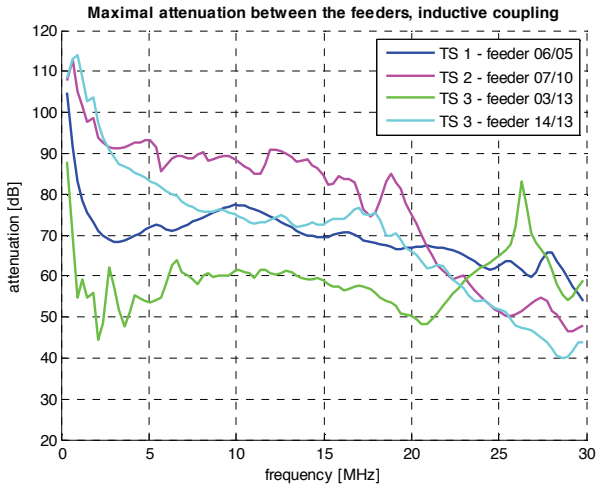

Figure 7-20: Comparison of maximum attenuation levels for different configurations in the case of inductive coupling

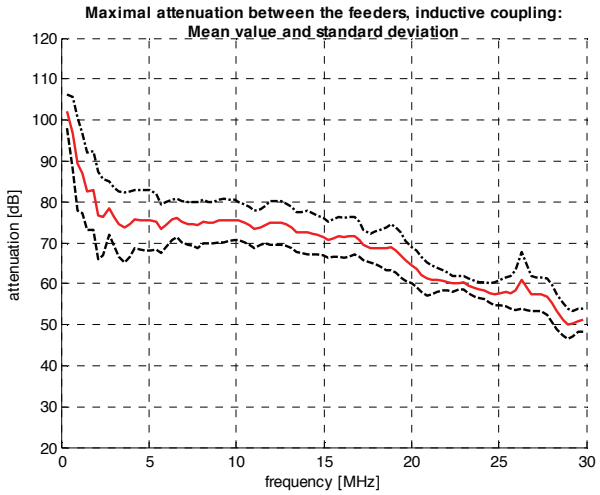

Figure 7-21: Average value and standard deviation of maximal attenuation levels for different configurations in the case of inductive coupling

Regarding crosstalk values, the correlation between the crosstalk and the separation/length the feeders run in parallel does not seem to follow a simple function as for the case of the capacitive coupling.

Here, the crosstalk is higher for cases in which the feeders are not next to each other and do not run in parallel more than the initial 1.5m (feeders 03 and 13 of the TS3).

7.4 Discussion on system mechanisms for multi-master deployment

From Figure 7-13, we can see that there is large variation in the crosstalk level for the considered cases which correspond to different LV feeder topologies, different distances between feeders of interest and different lengths of the parallel segments. Theoretically,

the crosstalk attenuation is dominated by common-mode propagation along the lines and it depends on the impedance of the reference conductor.

The measured crosstalk attenuation is in the range of 50 to 100 dB for different configurations and different frequency bands.

Assuming a state of the art PLC system, which requires an SNR of approximately 30 to 40 dB for high bit loading, the required separation between two feeders can be calculated by considering the different interference scenarios for a multimaster configuration presented in Figure 7-22.

Interference scenario 1: Both masters are transmitting simultaneously.

The transmission of Master 1 represents noise for the modems of sub-cell 2 and vice versa. To insure an SNR of 40 dB for the transmission from Master 1 to all slaves of sub-cell 1, and from Master 2 to all slaves of sub-cell 2, the attenuation between the two masters should be of at least A = 40 dB. (see Figure 7-22).

Interference scenario 2: Both masters are simultaneously receiving from their corresponding slaves.

In this case, we will consider the worst case scenario: Slave 11 with the lowest attenuation to its master in sub-cell 1, Master 1 transmitting; and, the Slave 2n with the highest attenuation to its master in the sub-cell 2, Master 2 transmitting. The signal from Slave 11 arrives to Master 2 attenuated by (B1+A) dB and represents the noise for it. The useful signal from its respective slave, Slave 2n, arrives to Master 2 attenuated for C2 dB. To insure that Master 2 receives correctly with the minimum required performance, the filter should be selected so that the attenuation (B1+A) dB is at least 20dB higher than the attenuation C2, namely, (B1+A)> C2+20dB.

Interference scenario 3: One master is transmitting to the slaves of its own sub-cell; the other is receiving from the slaves from its own sub-cell.

Let us assume that Master 1 is transmitting and Master 2 is receiving from its most distant slave, Slave 2n. The signal received from Master 1 represents noise for Master 2 and is received attenuated by A dB. The useful signal, the signal transmitted by Slave 2n, is received attenuated by C2 dB. To ensure the minimum requirements on attenuation, A should satisfy the equation:

7-2 $$A = C2 + 20\ dB$$

And in order to have the same, usual requirements for an SNR of 40 dB, as we imposed for case 1, A=C2 + 40 dB.

When comparing the three interference scenarios, it is obvious that scenario 3 is the critical one and presents the requirement for filter specification.

The attenuation A represents the initial attenuation caused by the busbar presented in Figure 7-11 plus the attenuations provided from two filters. If we take for C2 a typical value of 60 dB, a rough estimation of A would be 100 dB. If we assume a value of 40 dB for the busbar attenuation (see Figure 7-11), the estimated value for the filter attenuation would be 30 dB.

From Figure 7-13 it can be seen that, due to crosstalk, the implementation of blocking filters is not enough to guarantee the proper functioning of the multimaster deployment for all cases. For those cases, additional improvements are needed.

One mechanism that allows the lowering of the requirements for the blocking filters is the Rx/Tx synchronisation of the PLC sub-cells. All the masters of the sub-cells belonging to the same PLC cell are synchronised, or synchronise themselves in a way that they transmit and receive in the same time slots. This means that the interference scenario 3 described earlier does not exist in this configuration. Under these conditions, interference scenario 2 becomes the most critical one and can be evaluated from the equation:

7-3 $(B1+A) > C2+20\ dB$

If we consider a value of 60 dB for C2, a busbar attenuation of 40 dB as in the previous case and we assume B1=20 dB, then the required filter attenuation for this case would be 10 dB. By referring once more to Figure 7-13, we can see that this is satisfied in nearly all cases.

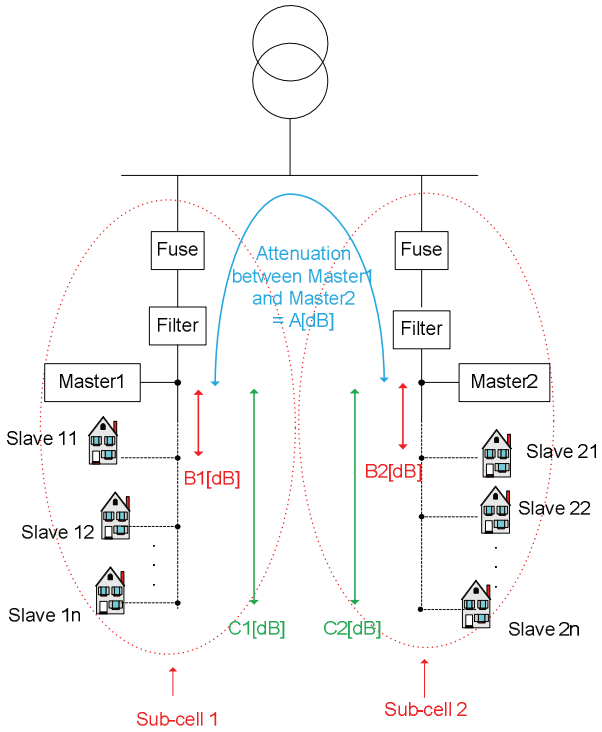

Figure 7-22: Interference scenarios

The drawback of the synchronisation mechanism is that in the case that one sub-cell requires only downlink traffic, the available downlink data rate for this sub-cell would be reduced by half in the case that the up and down link ratio is 50:50.

A second possibility to overcome the too-high requirements for the blocking filter attenuation is a frequency division concept, with dedicated frequency bands for up and down link. In this case, the previously described interference scenario 3 is not applicable since the masters never transmit and receive at the same time and at the same frequencies. Once more, scenarios 1 and 2 are applicable, but interference scenario 2 is the most critical. By applying the same calculation as for the synchronisation solution, we obtain the same requirement for the filter attenuation. Once more, this value is of 10 dB and this is feasible for nearly all cases. The disadvantage of this solution is once more the reduction of the data rate due to the lowered frequency band. The level of

reduction for the cases of uplink and downlink depends on the ratio of the frequency bands dedicated to them respectively.

7.5 Discussion on filter concepts

The design of a blocking filter capable of withstanding a steady state 50 Hz current of 400 Amps represents certainly a challenging task.

A proposal for a first blocking filter prototype is given in Figure 7-23. The idea is to put blocking capacitances between each two phases and between each phase and the ground. Special care should be taken so that, when making the capacitances, the distances are kept at minimum, to avoid parasite inductances.

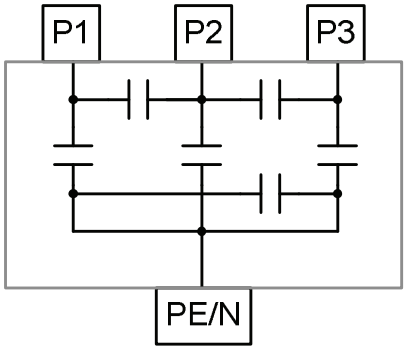

Figure 7-23: Schematics of the blocking filter prototype

Work towards the design and testing of first filter prototypes is ongoing in the framework of OPERA project. The prototypes of the blocking filters will be tested in OPERA field trials.

7.5.1 General requirement specifications for blocking filter

The filter should provide an attenuation of 30 dB in a frequency range from 2 – 15 MHz in order to meet the requirements which are given by the worst case interference scenario 3 as discussed in section 7.4.

Further requirements are:

- Easy to install without cutting off electrical power for installation
- Should fit in the standard busbar equipment
- Tested with 6kV surge voltage which is required for installations in transformer stations

7.5.2 Conceptual design of blocking filters

Taking into account a reasonable price for the blocking filters and the high 50Hz current which has to pass through the filters, standard filter concepts using L and C are not applicable.

A concept which looks very promising is based on inductive signal coupling. In combination with an RF-short circuit, the signal propagation will be blocked in the direction of the bus bar. Furthermore the RF-short circuit improves the coupling performance for the desired direction.

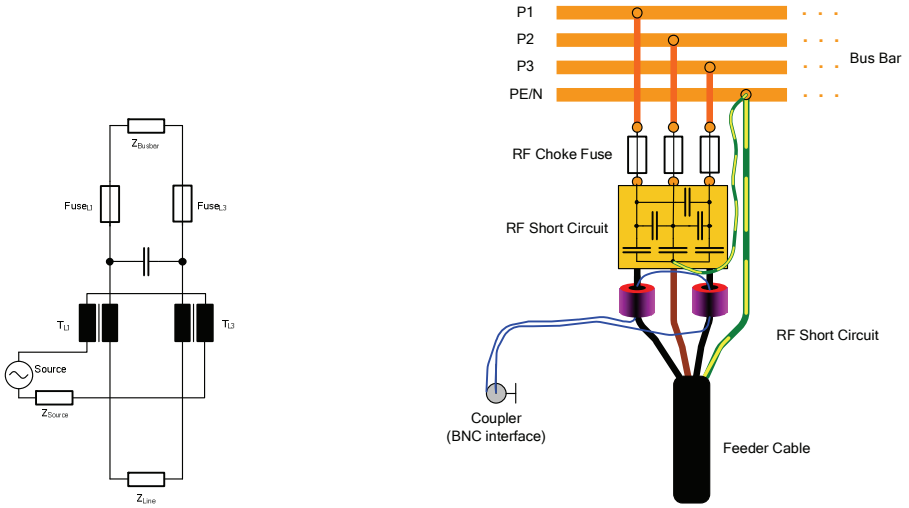

Figure 7-24: (a) Blocking filter concept and (b) blocking filter implementation

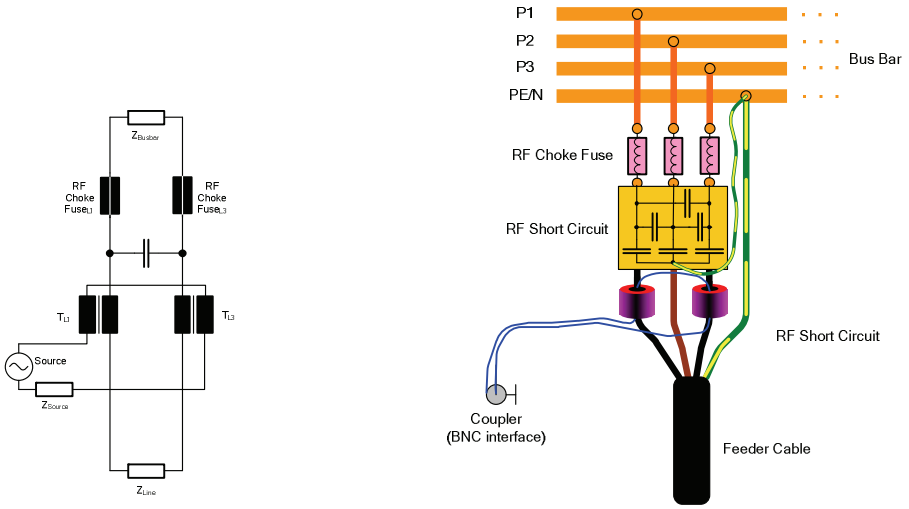

Figure 7-25:, (a) Enhanced blocking filter concept with RF-choke-fuses and (b) enhanced blocking filter implementation with additional RF-choke-fuses to reach higher attenuation

7.6 Conclusions

High density PLC deployment in a competitive market requires the increase of overall system data rate. To achieve the higher data rates, frequency reuse in these systems is needed. In this chapter, we presented an innovative idea for using so-called blocking filters as a possible solution for a frequency reuse.

We presented measurements to verify the concept of blocking filters. The measurements were made in Saint Sulpice, near Lausanne.

The results of our measurements show that the use of blocking filters can, in certain cases, ensure high enough RF separation of the LV feeders belonging to the same substation. In some cases, even with the possibility to design and integrate effective

blocking filters, the system needs to provide additional synchronisation mechanisms for frequency reuse.

Two of these additional mechanisms were discussed: Synchronised Tx/Rx for all masters and Rx/Tx frequency duplexing. In synchronised Rx/Tx, all masters are synchronised to transmit as well as to receive at the same time. In Rx/Tx frequency duplexing, different frequency bands are used for transmitting and receiving for Master and Slave.

The design of a blocking filter capable of withstanding a steady state 50 Hz current of 400 Amps represents certainly a challenging task. Work towards the design and testing of first filter prototypes is ongoing.

REFERENCES

[1] Deliverable 44: “Report on presenting the architecture of PLC system, the electricity network topologies, the operating modes and the equipment over which PLC access system will be installed”, IST Integrated Project No 507667. Funded by EC , December 2005

[2] Deliverable 4: “Theoretical postulation of PLC channel model”, IST Integrated Project No 507667. Funded by EC, March 2005

[3] Deliverable 5: “Pathloss as a function of frequency, distance and network topology for various LV and MV European powerline networks”, IST Integrated Project No 507667. Funded by EC, April 2005

[4] Deliverable 45: “Specification of PLC System Requirements”, IST Integrated Project No 507667. Funded by EC , May 2004

[5] Deliverable 46: “General specification of PLC PHY layer”, IST Integrated Project No 507667. Funded by EC, August 2004

[6] Deliverable 1: “Blocking filters to enable multi-master deployment in high density LV areas”, IST Integrated Project No 026920. Funded by EC

[7] A. Vukicevic, M. Bittner, A. Rubinstein, M. Rubinstein, F. Rachidi, “A concept to enhance system data rate for PLC access networks”, 12th International Symposium on Power-Line Communications and Its Applications (ISPLC’08), South Korea, 2008

[8] E. Marthe, Thèse No 3165, Powerline communications: Analyse des Problèmes de Compatibilité Electromagnétique dans le domaine des Courants Porteurs en Ligne, EPFL, 2005

Chapter 8

8 Conclusions and Perspectives

The principal objective of this thesis is the analysis of problems related to electromagnetic compatibility of broadband powerline communications although some non-EMC related issues have also been dealt with and original contributions related to them presented.

The study comprises both theoretical analysis and experimental characterization. The experimental work was conducted in the form of field measurements, performed in real power networks and in the laboratory, performed in a “PLC simulated” environment. For the theoretical work, simulations were performed by means of both the Transmission Line (TL) theory and a Full-Wave approach based on the Method of Moments and using the Numerical Electromagnetics Code (NEC).

The delay spread is an important parameter related to intersymbol interference in OFDM, the modulation technique used in today's HomePlug and OPERA specification compliant PLC equipment. This parameter is currently the subject of intense discussions since the system standardization is ongoing and there is, as of the writing of this thesis, no agreement on the appropriate formulation for its measurement and calculation.

Despite the advantages that PLC can offer, powerline risks not to live up to a full development and success unless proper standards and regulations are developed globally. Although work is being done to achieve standardization, problems regarding EMC, immunity testing and the specification of the PHY and MAC layers still persist.

The data signals injected by PLC modems are differential mode signals. The differential mode is a poorer radiator than the common mode since the fields from the currents in one of the conductors are nearly cancelled by the opposite-phase radiation from the current in the other conductor. The common mode, which is characterized by currents in each of the conductors being in phase, on the other hand, leads to appreciable radiation.

The common mode can appear due to unbalances at the source (the common mode is injected by the modem’s output stages or due to imbalanced capacitances to ground), due to conversion of the wanted, differential mode along the asymmetric electric cabling, and due to the presence of local asymmetries in the cables, such as sharp bends, power outlets, sockets, switches, etc.

A measurement campaign was carried out to characterize the common mode under controlled conditions and to obtain a data set to serve as a basis for the theoretical study of the generation of common mode in asymmetrical networks. The measurements were made on a special, house-like wooden structure on which electric cabling and electrical fixtures were installed. In addition to a characterization of the common mode on simple structures, the measurements were conducted with the aim of identifying the different parameters that influence the common mode on PLC networks.

Two methods were investigated to model the common mode and conducted emissions, the transmission line model and the full wave approach provided by the Method of Moments through the Numerical Electromagnetic Code, NEC.

The estimation of the common mode current in in-house electrical wiring is important since it is this mode that produces most of the radiated emissions. We have shown that

the common mode can be estimated as a linear combination of the effect of a) the injected differential mode, which converts partially to the common mode, and b) the common mode that is applied directly at the injection point and propagates through the wiring with relatively low attenuation.

Although we worked with common and differential modes injected at the same input point, the results should in principle be applicable to the case of multiple common mode sources and multiple differential mode sources spread across the low voltage network.

As part of the effort to better understand the consequences of the poor symmetry in powerline cabling on standardized immunity testing applied to PLC, we showed that the conversion of the differential mode to the common mode is coupled with the reverse conversion by reciprocity. The common-to-differential mode conversion ratio is related to the differential-to-common mode conversion ratio by a multiplicative factor equal to the ratio of the impedances of the common mode source and the differential mode source. This result implies that the measurement of one of the ratios is sufficient to characterize both ratios.

Due to the low symmetry of PLC cabling, part of the injected common mode immunity test signal is converted into a differential mode signal that interferes with the wanted signal at the input of the modem being tested. Depending on the actual symmetry of the coupling-decoupling network (CDN), the immunity test may yield erroneous results due to the effect of this differential mode component.

Working under the assumption that the CDN is built to exhibit a symmetry similar to that of PLC networks as inferred from its longitudinal conversion loss, we estimated the differential mode disturbance level that the modems should withstand from a narrowband interferer.

Since the immunity test is performed injecting a common mode, 2-kHz bandwidth, narrowband signal whose central frequency is changed periodically over the test band, the capacity of the channel will be reduced for one or two subcarriers at a time. The bit error rate induced by the presence of the disturbing differential mode current from the CDN was estimated, for a total physical channel transmission rate of 200 Mbps, which is the maximum physical rate of current modems, to be of the order of $1x10^{-5}$ to $5x10^{-5}$. Since these rates can be handled by error correcting strategies such as coding and MAC ARQ procedures, the modems are not likely to suffer any severe performance degradation due to immunity testing if the CDN exhibits a symmetry similar to that of PLC networks.

Another mechanism that could affect the performance of PLC modems during immunity testing is the overload of the input stages by a narrowband interferer. It is however unlikely that the low-level differential mode signals from the CDN's finite longitudinal conversion loss will overload the modems.

For a transmission line, even if the line cross section is electrically small, the presence of antenna-mode currents causes the sum of the currents at a cross section to be, in the general case, different from zero. Since the antenna mode current response is small near the ends of the line, it is appropriate to consider the TL model current only if all that is needed is the response of the line at the load. On the other hand, if the currents along the line are required (to calculate radiation, for instance), the presence of antenna-mode currents needs to be taken into account, even for electrically small line cross sections.

We derived an integral equation describing the antenna-mode currents along a two-wire transmission line. We also showed that, when the line's cross-sectional dimensions are

electrically small, the integral equation reduces to a pair of transmission line-like equations with equivalent line parameters (per-unit-length inductance and capacitance). The derived equations make it possible to compute the antenna mode currents using a traditional transmission line code with appropriate parameters.

The derived equations were tested versus numerical results obtained using NEC and reasonably good agreement was found.

We briefly presented a technique that has been proposed to achieve a reduction of emissions associated with indoor PLC networks through the introduction of a 180^{o} out-of-phase replica of the PLC signal into the unused neutral-ground circuit. We also proposed a modification to this technique based on the selection of the appropriate amplitude and phase of the auxiliary signal.

Theoretical considerations suggest that the improved technique can be effective in the reduction of emissions for a given observation point and considering a single field component. However, an effective strategy is needed for its application to real cases taking into account technical and economical constraints. We proposed and studied a way of implementing this technique, namely the integration of a required antenna into the PLC modems themselves. The measured fields very close to the modem allow the determination of the magnitude and phase of the compensation voltage. The proposed implementation should be used only to handle customer complaints, when emissions should be lowered at locations where PLC signals might cause unwanted interference or when additional capacity is required and it can be obtained through the gained signal to noise margin.

Although, in principle, due to nonalignment of the wanted and the compensation field directions, minimizing one component of the field may result in an increase of the other components, we have shown here that the application of the technique results in an overall average reduction of 10-20 dB of all the field components in the region of interest.

We addressed the more general issue of the application of mitigation techniques' gained emissions margin to increase the overall throughput of PLC systems. We showed that an increase in the signal power (made possible by the inclusion of mitigation techniques) leads to a considerable increase in the PLC channel capacity. Using a number of simplifications, we showed that the capacity of the channel can indeed be increased by by over 60 Mbps for mitigation efficiencies of only 10 dB. Measurement-based attenuation and noise models developed in the framework of the OPERA project confirmed the results.

We also presented the results of laboratory measurement aimed at studying, under controlled conditions, different characteristics of notching in OPERA PLC modems, such as total and effective notch width, notch depth, maximum notch depth, etc. These measurements showed that it is possible to obtain attenuations of up to about 45 dB for notches in all frequency bands, 10MHz, 20MHz and 30MHz. What differs for these three bands is the minimum number of carriers that need to be notched to obtain that maximum attenuation. This is an important point, since, to implement notches that have the required depth and width, one must know how many subcarriers to suppress and how deep these need to be reduced.

In addition to the laboratory measurements, we made field measurements that showed that the expected notch characteristics are also present in real PLC systems. The notches measured in the field correspond well to those reproduced in the lab.

High density PLC deployment requires the increase of overall system data rate. To achieve the higher rates, frequency reuse in these systems is needed. We presented the idea for using so-called blocking filters as a possible solution for a frequency reuse.

We presented measurements to verify the concept of blocking filters. The measurements were made in Saint Sulpice, near Lausanne.

The use of blocking filters can, in certain cases, ensure high enough RF separation of the LV feeders belonging to the same substation. In some cases, even with the possibility to design and integrate effective blocking filters, the system needs to provide additional synchronization mechanisms for frequency reuse.

Two of these additional mechanisms were discussed: synchronized Tx/Rx for all masters and Rx/Tx frequency duplexing. In synchronized Rx/Tx, all masters are synchronized to transmit as well as to receive at the same time. In Rx/Tx frequency duplexing, different frequency bands are used for transmitting and receiving for Master and Slave.

Future work

The work in this thesis has contributed to a better understand EMC issues in PLC systems such as the behavior of the common mode, the calculation of emissions, and the study of new and existing mitigation techniques. This work should be continued to improve further our understanding and for verification of proposed models such as the linear two-source model in which the common mode anywhere can be determined from the amount of common mode and differential mode injected.

The results of the experimental and theoretical work which were geared towards a better understanding of EMC phenomena in powerline systems should be adapted to obtain approximate, analytical and simple-to-use formulas applicable in practical cases as EMC guidelines to avoid interference and guarantee the coexistence with radio amateurs and broadcast radio services.

For the integral equation describing the antenna-mode currents along a two-wire transmission line, work is currently underway to improve the accuracy of the model, specifically with regard to the determination of the line parameters and evaluation of currents at resonant frequencies, and inclusion of multiconductor lines.

The benefits of the proposed mitigation technique merit its further development. Work should also be done on the development of other innovative mitigation techniques that would allow higher not only lower emissions but also higher data rates through the increase in the margin of the signal to noise ratio.

The design of a blocking filter capable of withstanding a steady state 50 Hz current of 400 Amps represents a challenging task. Work towards the design and testing of first filter prototypes is ongoing.

Curriculum Vitae

Ana Vukicevic
Born on June 17, 1974 in Belgrade, Serbia
Serbian
Single

Education

2004	Postgraduate course in Electrical Engineering, Swiss Federal Institute of Technology, Lausanne, Switzerland (2002 - 2004)
2001	M.S. in Electrical Engineering, orientation Electronics from Faculty of Electrical Engineering, University of Belgrade, Serbia, Department of Electronic Engineering

Professional experience

2004 – 2008	Research and teaching assistant at the Power Systems Laboratory (LRE) of the Swiss Federal Institute of Technology in Lausanne (EPFL), Switzerland
August 2003 – May 2004	Research engineer, Service de l'Electricité de la Ville de Lausanne/ Power System Laboratory, EPFL, Switzerland
June 2003 – August 2003	Electronic Engineer – Trainee, Vibro-meter, Fribourg, Switzerland
2001 – 2002	R&D Electronic engineer, Information Technology Group, Belgrade, Serbia

Distinctions

November 2005	'Young Scientist Award', URSI General Assembly (Union Radio Scientifique Internationale), New Delhi, India,

Publications

A. Rubinstein, A. Vukicevic, M. Rubinstein, F. Rachidi, " Experimental Verification of Common-Mode Current Generation in Home Electrical Wiring in the Poweline Communications Band, 29th General Assembly of International Union of Radio Science (URSI), Chicago, USA, 2008.

A. Vukicevic, M. Bittner, A. Rubinstein, M. Rubinstein, F. Rachidi, “A concept to enhance system data rate for PLC access networks”, 12th International Symposium on Power-Line Communications and Its Applications (ISPLC’08), South Korea, 2008

A. Vukicevic, A. Rubinstein, M. Rubinstein, F. Rachidi, “On the efficiency of notching technique to reduce EM radiation from PLC networks”, 12th International Symposium on Power-Line Communications and Its Applications (ISPLC’08), South Korea, 2008

M. Rubinstein, A. Vukicevic, F. Rachidi, JL. Bermudez, “Impact of the Symmetry of Coupling – Decoupling Networks on the conducted Immunity Testing of PLC modems”, 18th International Zurich Symposium on Electromagnetic Compatibility, 24-28 September 2007, Munich, Germany

P. Favre, C. Candolfi, P. Kraehenbuehl, M. Schneider, M. Rubinstein, A. Vukicevic, “Common-mode Current and Radiation Mechanisms in PLC Networks”, 11th International Symposium on Power-Line Communications and Its Applications ,26-28 March 2007. Pisa, Italy

A. Vukicevic, M. Rubinstein, F. Rachidi, JL. Bermudez, “On the Impact of Mitigating Radiated Emissions on the Capacity of, PLC”, 11th International Symposium on Power-Line Communications and Its Applications, 26-28 March 2007. Pisa, Italy

JL Bermudez, E. Marthe, F. Rachidi, M. Rubinstein, A. Vukicevic, “La Compatibilité Electromagnétique de la Technologie CPL”, Bulletin Electrosuisse, 19/2006

M. Rubinstein, A. Vukicevic, JL. Bermudez, F. Rachidi, P. Favre, M. Schneider, “Some Unresolved Issues Concerning EMC in Powerline Communications”, 18th International Wroclaw Symposium on Electromagnetic Compatibility, Wroclaw, 28-30 June 2006

A. Vukicevic, M. Rubinstein, F. Rachidi, JL. Bermudez, M. Schneider, P. Favre, P. Zweiacker, “Review of the Electromagnetic Compatibility PLC Work at the Swiss Federal Institute of Technology (Lausanne) and the University of Applied Sciences of Western Switzerland (Yverdon)”, 10th International Symposium on Power-Line Communications and Its Applications, 26-29 March 2007. Orlando, USA

A. Vukicevic, M. Rubinstein, F. Rachidi, JL. Bermudez, “On the Mechanisms of differential-mode to Common-mode Conversion in the Broadband over Powerline (BPL) Frequency Band”, 17th International Zurich Symposium on Electromagnetic Compatibility, 27 February -3 March 2006, Singapore

A .Vukicevic, F. Rachidi, M. Rubinstein, S. Tkachenko, “On the Evaluation of Antenna-Mode Currents along Transmission Lines”, IEEE Transactions on Electromagnetic Compatibility, November 2006, Vol 48, No 4

M. Rubinstein, J.L. Bermudez, A. Vukicevic, F. Rachidi, M. Schneider, E Marthe, “Assessment and Mitigation of Radiation from PLC Networks”, Submitted to IEEE Journal on Selected Areas in Communications, 2005

A. Vukicevic, F. Rachidi, M. Rubinstein, S. Tkachenko, “An Efficient Method for the Computation of Antenna-Mode Currents along Transmission Lines”, 28th General Assembly of International Union of Radio Science (URSI), 23-29 October 2005. New Delhi, India

M. Rubinstein, J.L. Bermudez, A. Vukicevic, F. Rachidi, M. Schneider, "On the mitigation of radiation from PLC networks", 28th General Assembly of International Union of Radio Science (URSI), 23-29 October 2005. New Delhi, India.

A. Vukicevic, “Analysis and Mitigation of Electromagnetic Radiation from PLC Networks”, Journée de la Recherche, 11 November 2006, EPFL, Lausanne, Switzerland

M. Rubinstein, J.L. Bermudez, A. Vukicevic, F. Rachidi, M. Schneider, E Marthe, “Discussion on the Assessment and Mitigation of Radiation from PLC Networks“, 9th International Symposium on Power-Line Communications and Its Applications, 6-8 April 2005. Vancouver, Canada

A. Vukicevic, F. Rachidi, M. Rubinstein, “A 6^{th} Framework Project on Powerline Communication Systems”, COST Workshop, March 2004, Liege, Belgium

E. Marthe, N. Korovkin, F. Rachidi, A. Vukicevic, and F. Issa, "A technique to reduce electromagnetic field radiated by indoor PLC systems", 17th International Wroclaw Symposium on Electromagnetic Compatibility, Wroclaw, 29 June-1 July 2004